SAVINA, 1985

REDWOOD COUNTRY

AMERICAN GEOMORPHOLOGICAL FIELD GROUP FIELD TRIP GUIDEBOOK

1985 Conference
Northwestern California

Co-conveners: H.M.Kelsey, T.E.Lisle, M.E.Savina

Guidebook edited by M.E.Savina

REDWOOD COUNTRY

AMERICAN GEOMORPHOLOGICAL FIELD GROUP 1985 FIELD TRIP GUIDEBOOK

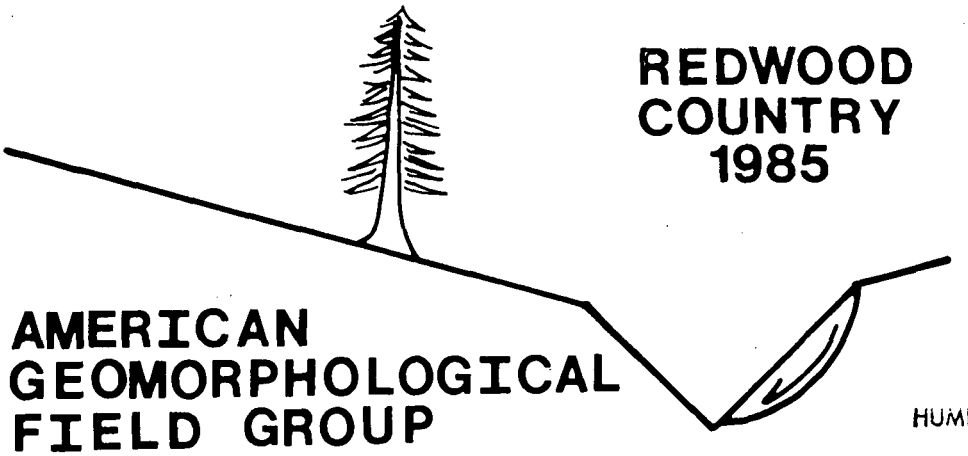

Co-conveners

Harvey M. Kelsey
Department of Geology
Western Washington University
Bellingham, Washington 98225

Thomas E. Lisle
U.S. Forest Service
Redwood Sciences Laboratory
1700 Bayview
Arcata, California 95521

Mary E. Savina [guidebook editor]
Department of Geology
Carleton College
Northfield, Minnesota 55057

ACKNOWLEDGEMENTS

The co-convenors of this field conference wish to sincerely thank the many people who assisted with logistical arrangements, guidebook preparation, and organization of the meeting.

We thank the following persons, most of whom are graduate students in the Watershed Studies or Geology programs at Humboldt State University, for their tremendous help with the organization and execution of this conference. It is not an exaggeration to say the conference could not have been organized, nor have been affordable to other graduate students, without the unselfish, dedicated, and enthusiastic help of Frank Bickner, Mark Haley, Randy Klein, Scott Lundstrom, Vicki Ozaki, John Parker, Darci Short, Dave Steenson, Nick Varnum and Judi Waite.

We also wish to thank professors Bud Burke and Sue Cashman of the Geology Department, Humboldt State University, who helped arrange many aspects of the field conference.

Art Bolli, superintendent of the Mad River Water District, granted us permission to use the Mad River campground during the meeting. Permission for access to private property was given by Mrs. Dwight May (Donaker earthflow), and by other landowners in the Minor Creek and Jacoby Creek areas.

At Carleton College, Charles Hoskins, Susan Swan, Betty Bray, Paul Wetherbee, Diane Cassidy, Sally Robinson, Elizabeth Barsness, and Sean McKenna helped to prepare and print the field trip guidebook. A grant from the Shell Foundation to the Carleton College Geology Department helped to defray some of the expenses connected with guidebook preparation.

The AGFG Secretariat (Luna Leopold, Bill Emmett, and Bill Dietrich) at Berkeley and Denver printed and mailed the meeting announcements.

Douglas Warnock, superintendent of Redwood National Park, provided field vehicles for our use.

The cover illustration, a logged redwood area, was drawn by Breuer and reprinted in Willis Linn Jepson, 1909, Trees of California: San Francisco, Cunningham, Curtis and Welch, p. 9 by permission of Mrs. Volney D. Moody of Berkeley.

TABLE OF CONTENTS

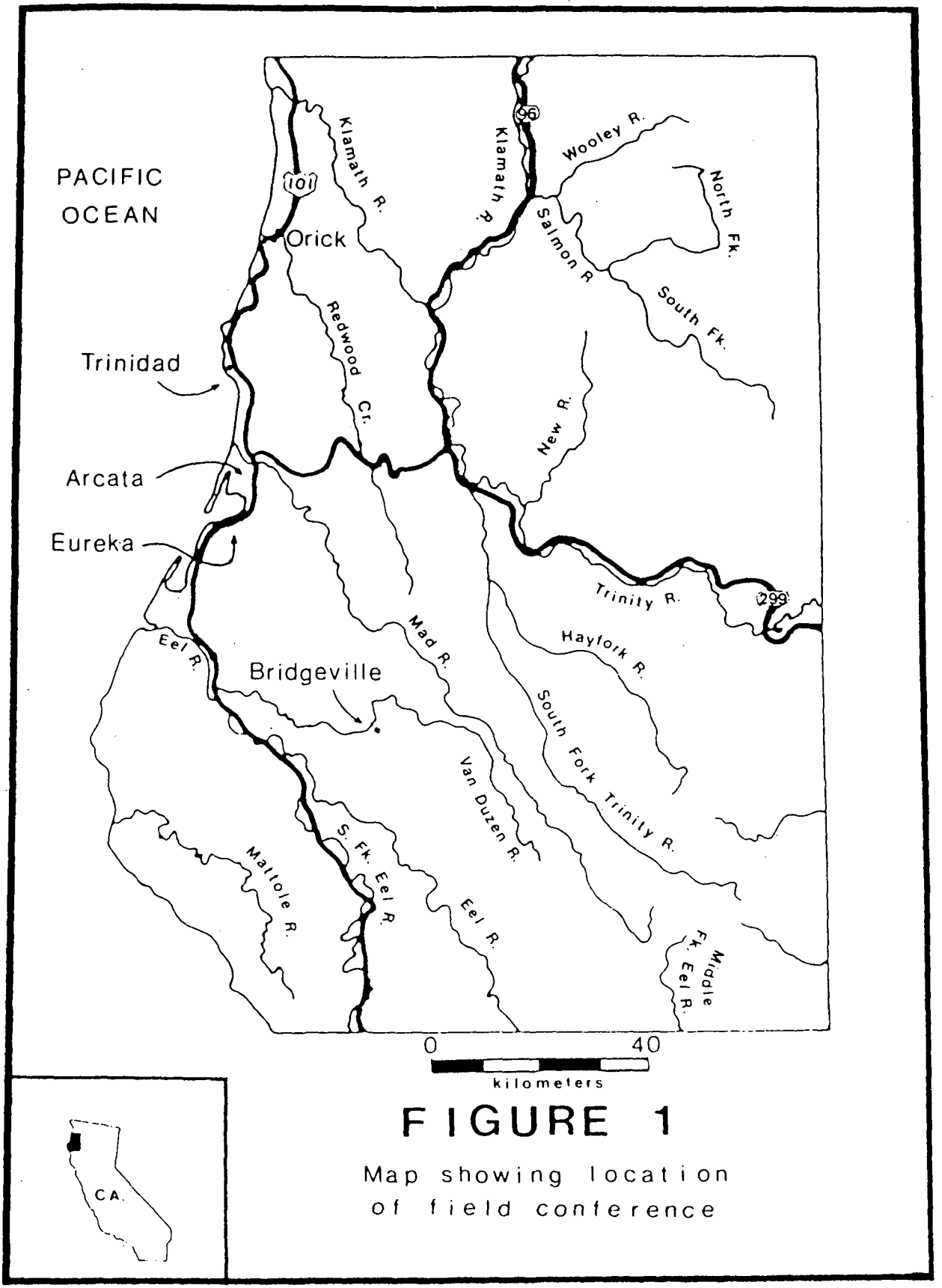

FIGURE 1

Map showing location of field conference

Field Guide Day 1: Geomorphic Processes and Landscapes, Van Duzen River basin

By Harvey Kelsey, Department of Geology, Western Washington University, Bellingham, WA and Mary Savina, Department of Geology, Carleton College, Northfield, MN

The general purpose of today's field trip is to show the variety of hillslope processes active in northern California drainage basins. We chose the Van Duzen basin for today's stops because it has been studied in detail (Kelsey, 1977, 1978, 1980) and the basin is representative in many ways of the other basins in the area. In the Van Duzen basin, Kelsey has studied landslide movement rates, sediment production, the effects of the slope movements on the stream channels, and the recovery of the channels from the effects of a major flood in December 1964. Tomorrow, we will look at some landslides in Redwood Creek basin that are similar in process to those in the Van Duzen basin. Groundwater and slope movement have been monitored on the Redwood Creek landslides.

The Van Duzen basin and other Coast Range basins of northern California are the most rapidly eroding regions of comparable size in the United States (Judson and Ritter, 1964; Brown and Ritter, 1971). Most of the coastal area has undergone recent (post-Miocene) uplift of 1 mm/yr or more. This uplift has most probably been a response to the northward migration of the Mendocino triple junction.

The Van Duzen basin, site of today's field trip, is the northernmost tributary of the Eel River and flows into the Eel at a point 480 km north of San Francisco. The two main physiographic types in the Van Duzen basin are: 1) gently rolling to hummocky grasslands and grass-oak woodlands underlain by Franciscan melange; and 2) more competent forested slopes underlain by Franciscan sandstone. These are also the main physiographic types in neighboring basins in the area. Studies in the Van Duzen have focused on the quantification of a sediment budget that summarizes major erosional and depositional processes. A major aspect of this study was the determination of the effects of the December 1964 flood, which created major landscape changes in the basin. The effects of the flood will be discussed at three of the field stops. As an indication of the magnitude of the 1964 event, during the three days of highest discharge in the Van Duzen, the 1964 flood accounted for 7% of the total suspended sediment discharge calculated for the 35 year study period, 1941-1975 (Kelsey, 1977). Suspended sediment yield for the Van Duzen basin, averaged for 1941-1975, was 2570 t/km^2 /yr.

Road Log:

Miles

0.0 Right turn from campground onto West End Rd. The campground is part of the domestic water supply system for the Humboldt Bay area. The large towers (about six of them) are set 50 to 100 feet deep in the alluvium of the lower Mad River and pump pure, clear water from these depths.

The Mad River was named in the winter of 1849 by members of the Doctor Josiah Gregg party that re-discovered Humboldt Bay a few days after crossing the Mad River. Evidently throughout the expedition, Dr. Gregg, who wanted to make scientific observations, battled with his men, who wanted to keep moving. As one member of the exploration company relates:

"The Doctor wished to ascertain the latitude of the mouth of the river, in order hereafter to know where it was. This was, of course, opposed by the rest of the company. Regardless of this opposition, he proceeded to take his observation. We were, however, equally obstinate in adhering to the determination of proceeding without delay. Thus decided, our animals were speedily crossed over, and our blankets and ourselves placed in canoes - which we had procured from the Indians for this purpose - ready to cross. As the canoes were about pushing off, the Doctor, as if convinced that we would carry our determination into effect, and he be left behind, hastily caught up his instruments and ran for the canoe, to reach which, however, he was compelled to wade several steps in the water. His cup of wrath was now filled to the brim; but he remained silent until the opposite shore was gained, when he opened upon us a perfect battery of the most withering and violent abuse. Several times during the ebullition of the old man's passion he indulged in such insulting language and comparisons that some of the party, at best not too amiable in their disposition, came very near inflicting upon him summary punishment by consigning him, instruments and all, to this beautiful river. Fortunately for the old gentleman, pacific councils prevailed, and we were soon ready and off again. This stream, in commemoration of the difficulty I have just related, we called Mad River." (quoted in Coy, Owen C., 1929, p. 41)

At all of today's field stops, we will examine the effects of the December 1964 storm and flood. At the U.S.G.S. gaging site on the Mad River at our campground, the suspended sediment load recorded for the 14 days during and after the flood was seven times the average annual sediment transport for the year 1958 through 1962.

1.1 Railroad crossing

1.45 Right onto overpass; turn left onto Rte. 299 west

2.2 Take Highway 101 south

2.8 Marine terrace deposits (Late Pleistocene) in bluffs on left. The town of Arcata is built on at least three marine terraces. However, erosion as well as landscaping has obscured most of the original treads and scarps. To the west is Arcata Bay, the northern part of Humboldt Bay. Four principal streams enter Humboldt and Arcata Bays. From north to south, these are Jacoby Creek, Freshwater Creek, Elk River and Salmon Creek. Some of the stops on Day 3 of the field conference will be in the Jacoby Creek drainage basin, which drains the southeastern part of the town of Arcata.

5.7 Crossing bottomlands of Humboldt Bay. These were all tidal flats until they were blocked off by the highway and drained for pasture and residences. Humboldt Bay is the only reasonably well-protected harbor between San Francisco and the Oregon Border. Much exploration of the northern California coast had taken place before Humboldt Bay was re-discovered in the mid-nineteenth century. An early fur trader, Capt. Jonathan Winship, may have sailed into the Bay in 1806, but the Bay

and surrounding coast were bypassed by subsequent settlers. In fact, Trinidad, about 15 km north of Arcata, is the oldest settlement in this part of Humboldt County. The Bay was named after the German naturalist, Baron Alexander von Humboldt, by the crew of a clipper ship, the Laura Virginia that crossed the bar in 1850. Humboldt never saw the bay. (Humboldt Bay Maritime Museum, 1984)

9.7 Tidal flat sculptures.

11.0 North edge of Eureka. Both Eureka and Arcata contain numerous examples of Victorian house and business architecture. The rectilinear street patterns of Eureka were laid out by speculators on planning maps in San Francisco in the early 1850s. In the nineteenth century, Eureka was a center of commerce and trade for the Trinity River mines. Today, the main industries are timber and wood products, government, fishing, and tourism. The population of Eureka is approximately 40,000. Total population of Humboldt County is about 100,000.

11.4 Look to the right (west) into Old Town Eureka for glimpses of Victorian buildings. Two Street in Eureka is one of the most interesting parts of urban Humboldt County.

12.8 Sulfurous smoke from pulp mills to west.

13.8 More terrace deposits on left, across from Olympic Motel.

14.4 Fort Humboldt historical site to left. U. S. Grant was stationed here before the Civil War and reportedly began drinking heavily, perhaps because of the depressing effects of the weather.

15.5 Elk River interchange. Well-preserved marine terrace level east of the highway.

16.1 Humboldt Bay Power Plant. This plant was originally designed as a dual-purpose nuclear and fossil fuel plant, but has been running only on fossil fuel since 1975, when the nuclear facility was closed due to concerns about seismic hazard. The plant was challenged initially by a citizens group concerned about earthquake stability. Geologic investigations conducted for Pacific Gas and Electric Company by Woodward-Clyde Consultants (1980) confirmed Late Pleistocene displacements on the Little Salmon Fault 2.5 km south of the plant and also discovered that Late Pleistocene units were displaced by the Bay Entrance Fault, which runs beneath the plant site, a few hundred meters from the reactor (see Fig. 2). Plans for decommissioning the nuclear power plant are now underway, a process being watched closely by observers nationwide, since it is one of the first nuclear power plants to be decommissioned in the country.

Tidal deposits and the mouth of Elk River are ahead on the right (west).

17.7 Fields Landing, one of the main points of export of logs to Japan. The logs are milled in Japan, where advanced milling facilities have been constructed, and then the planks are shipped back to the United States.

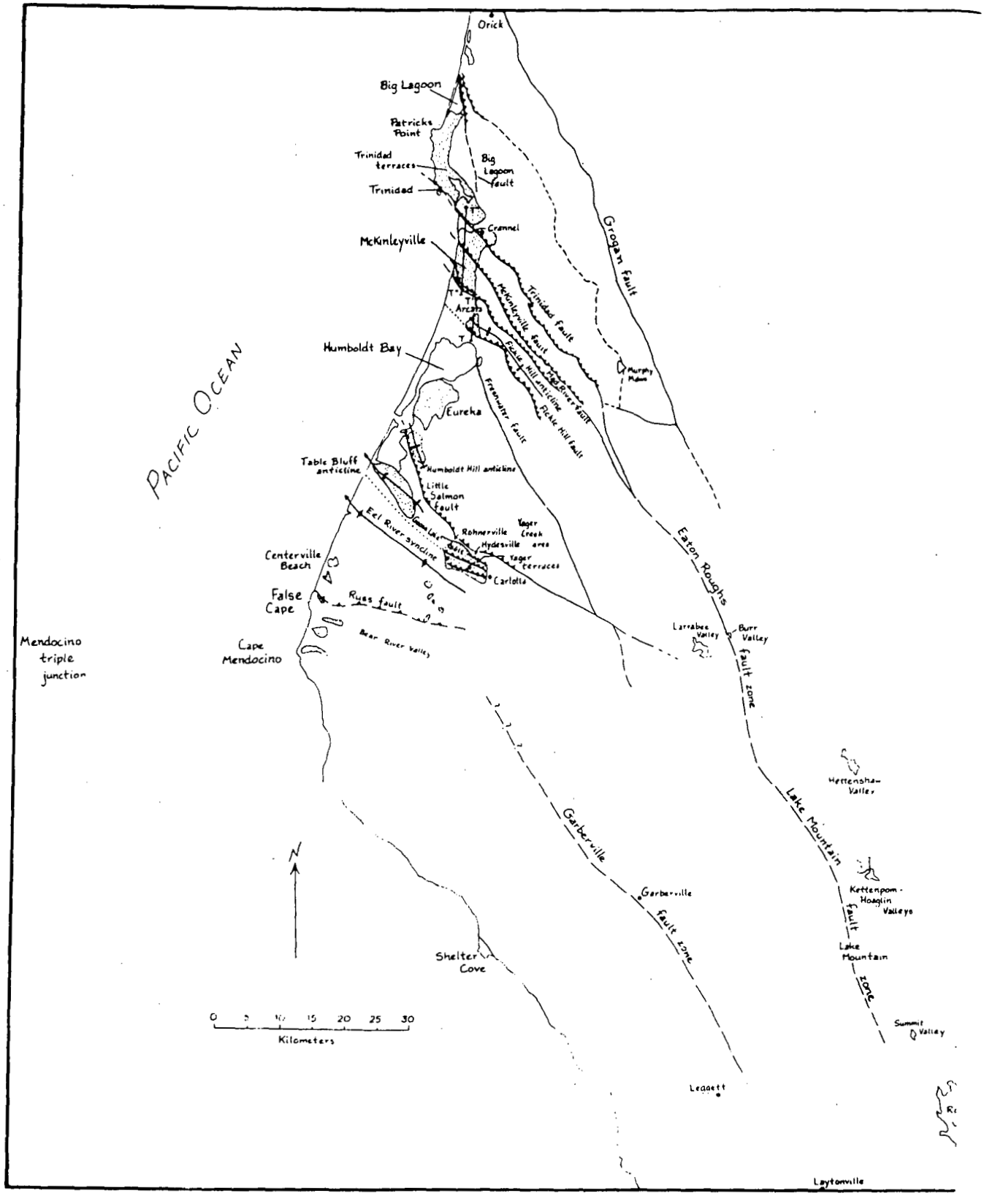

Figure 2. Location map showing major faults, folds, and marine and fluvial terrace surfaces (stippled) in the field conference area.

Boat building and storage, and commercial and charter fishing are the other main industries in Fields Landing.

19.2 Across the Bay, Table Bluff is a prominent marine terrace surface, warped into an anticline. It is the most prominent of a series of east-west trending anticlines in Humboldt County, related to north-south compression associated with the Mendocino triple junction (see Fig. 2). Gas wells have been drilled along the axis of the anticline at Thompkins Hill, to the east of Highway 101.

20.8 Eroded terrace deposits to left.

22.4 Highway climbs over Table Bluff anticline.

23.9 At crest of hill, overlook of Eel River mouth to west (right). The lower Eel River runs in a major east-west trending syncline, which contains approximately 2700 m of sediment deposited in this major depocenter since the mid-Miocene (Fig. 2). Evidently, the basin subsided nearly continuously, as only a few unconformities have been found in the sediments. Almost all of the interest in offshore oil in northernmost California has been centered on the Eel River basin, and there is a great potential for conflict between oil interests and fisheries resources.

8859

25.6 Ferndale exit. The village of Ferndale has preserved nearly all of its Victorian architecture. It is on the south side of the Eel River, connected to the main highway by a small road going over Fernbridge, which you can see to the west a little past the exit. The Eel River Valley near Fernbridge has been famous for its dairy industry for more than 100 years. The valley is so wide at this point that the 1964 flood that devastated much of the upper Eel Valley did not take out Fernbridge because the water slowed down and spread out in the lower Eel Valley.

A tremendous amount of sediment was transported out of the Eel River basin during the December 1964 flood. For instance, based on U.S.G.S. gage records at Scotia, only 20 km upstream of Fernbridge, the Eel River transported, during the 30-day period December 23, 1964 to January 23, 1965, 51% of the entire suspended sediment discharge for the 10 year period 1958 to 1967 (Brown and Ritter, 1971). The extent of aggradation in the Eel River Valley can be seen from overlooks in the next few miles. In the nineteenth century, it was possible to navigate ships as far upstream as Fernbridge, where a port was located. Of the major river basins in the United States where sediment discharges have been monitored by the U.S.G.S., the Eel, along with Redwood Creek, has the highest average annual suspended-sediment yield per square mile of drainage area (Brown and Ritter, 1971).

26.7 Terrace deposits on left (east).

28.7 Fortuna bridge. Fortuna, east of the highway, is the third largest city in Humboldt County. The highway turns south and crosses terraces at the mouth of the Van Duzen River. The lower Van Duzen River flows along the axis of an east-west trending anticline. Terraces along the north side of the Van Duzen tilt toward the north; those to the south of the river tilt

to the south. The south-tilting terraces will be most visible this afternoon as we emerge from the Van Duzen basin.

30.0 Good view to east on the skyline of northward tilting terrace level.

31.1 Strath terrace on left. Alluvial sediments are deposited on top of eroded Neogene conglomerates and sandstones. In some exposures, the difference between the tilt of the beds beneath the strath surface and the tilt of the strath is particularly clear.

31.8 Across the Eel River to the south are the edges of the south-dipping terraces.

32.4 Alton

32.7 Turn left onto Highway 36 (follow signs to Bridgeville). The route followed by Highway 36 in the lower Van Duzen River basin is the original stage coach route for traffic between Eureka and San Francisco. Northbound stages from San Francisco originally followed dirt roads northward along north-trending Coast Range ridges, rather than following the densely vegetated river valleys.

33.0 Steeply dipping Neogene Wildcat Group beds crop out on left; they dip more steeply than the terrace surface they underly. Kelsey interprets this to be a Van Duzen River terrace, not an Eel River terrace. The road will gradually climb onto this surface.

34.2 To south (right) is the Van Duzen River, eroding the south valley wall into Pleistocene sediments. The Van Duzen is named after a Mr. Van Duzen, who was a member of the Dr. Josiah Gregg party. After nearly drowning Dr. Gregg at the mouth of the Mad River in late 1849 (see discussion mile 0.00), the party "re-discovered" Humboldt Bay just before crossing the Van Duzen River. The vegetation differences observable from the road reflect microclimate control of north- and south-facing slopes. Timber on the slopes to the south is all second growth. Isolated patch cuts are second harvest, beginning third growth.

35.2 The alluvial veneer on the terraces is probably five to eight meters thick.

35.4 The town of Hydesville is located on the lower of two prominent tilted surfaces. The scarp of the higher surface, tilted to the north, is visible ahead. Hydesville's original name was Goose Lake, after an undrained depression on the back-tilted edge of the lower terrace.

35.5 Right turn

36.2 View to left, up Yager Creek valley. The road crosses a number of terraces of Yager Creek. To the north of the road, Yager Creek terraces are offset by the WSW-trending Goose Lake fault scarp. The fault shows two distinct zones of reverse faulting, the most recent displacement being younger than 16,000 yrs. (Woodward Clyde Consultants, 1980). The Goose Lake fault is part of the Little Salmon fault system, the western margin of which passes close to the Humboldt Bay nuclear power plant.

36.8 Road crosses last of the terraces. Some of the last remaining old growth in the Van Duzen basin is present upstream in Yager Creek Valley to the left.

37.0 Hogback of resistant Scotia Bluffs Sandstone on skyline ahead.

37.4 At 11 o'clock, one of the two notches in the skyline is the Little Salmon Fault. The other is another fault branch.

37.6 Crossing Yager Creek; town of Carlotta.

37.9 Good view of Van Duzen floodplain. Much of this area was inundated in the 1964 flood.

38.3 The terraces at the foot of the hillside on the left (at 10 o'clock) do not consist of Van Duzen River deposits. These are eroded remnants of debris fans from landslides in small tributaries of the Van Duzen. Earthquakes may have triggered these debris releases.

42.3 View of Van Duzen to right (south).

43.6 Old growth trees of Pamplin Grove.

44.2 The Van Duzen River in this reach has large meander bends where it cuts through erodible Tertiary deposits of the Wildcat Group that were deposited on top of the Yager Formation (Late Cretaceous to Eocene sedimentary rocks of the Coastal Belt Franciscan). Upstream, where the river cuts through to the level of the Yager, the course is much straighter, the valley is narrower and the stream gradient is steeper (Figs. 3 and 4).

44.4 Lower terrace (right) and upper terrace (left).

45.0 Van Duzen County Park

45.4 First of two bridges constructed as road crosses two meander bends. To left is a good view of marine sediments of the Wildcat Group. This grove is maintained by the Nature Conservancy as a research grove for the University of California.

46.1 Second old bridge. Debris slide at 3 o'clock.

47.0 River emerges from narrow valley upstream where it flows through the Yager formation. Most of the riparian vegetation is post-1964.

48.1 Entering narrow part of river valley. The debris slides on valley sides involve Yager Fm. bedrock; they are not soil slips.

49.0 Grizzly Creek Redwoods State Park. This stretch of road, called Dead Horse Grade, runs along a narrow canyon reach that is lined with debris slides.

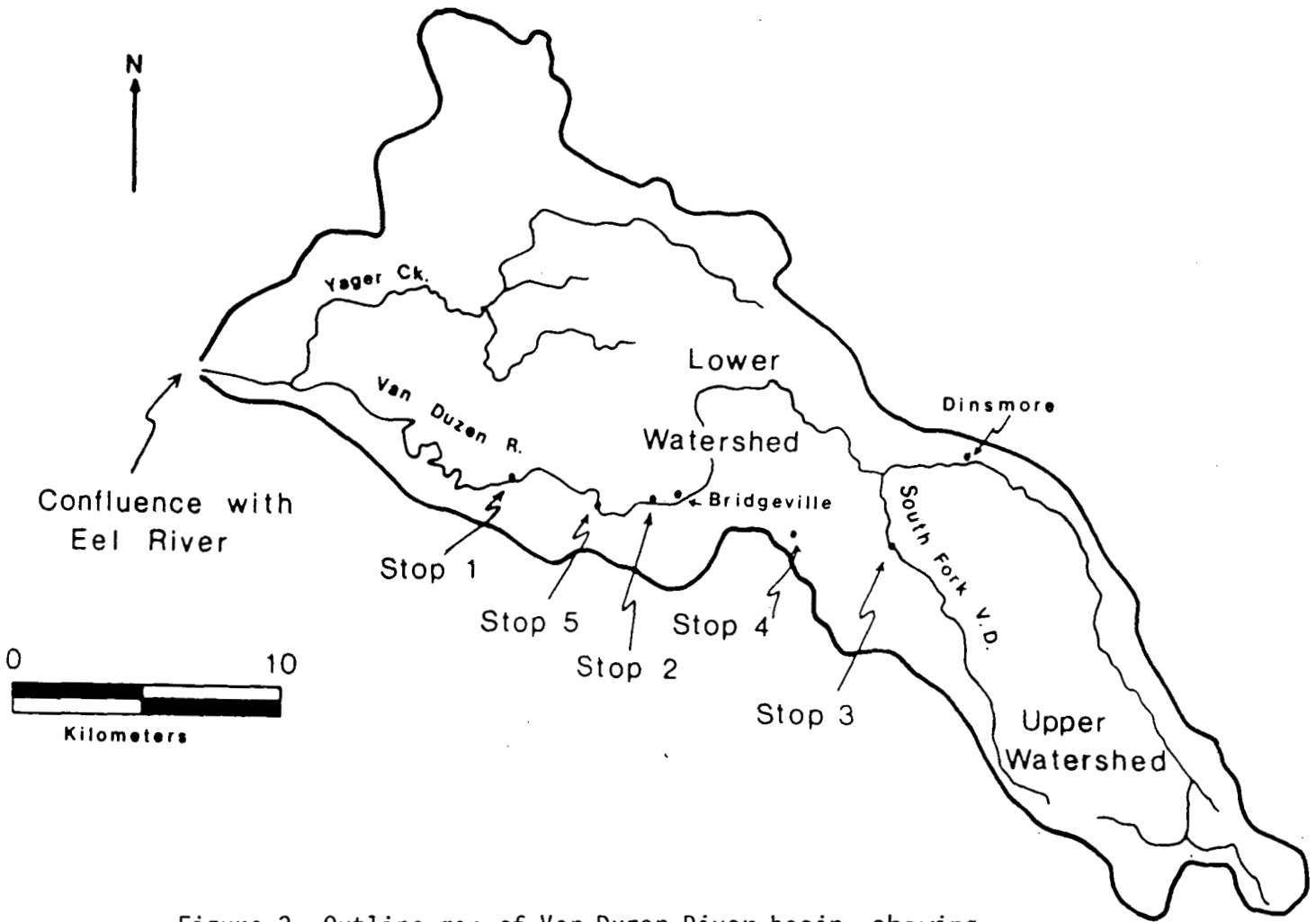

Figure 3. Outline map of Van Duzen River basin, showing locations of field stops, Day 1. Note change in sinuosity downstream of Stop 1.

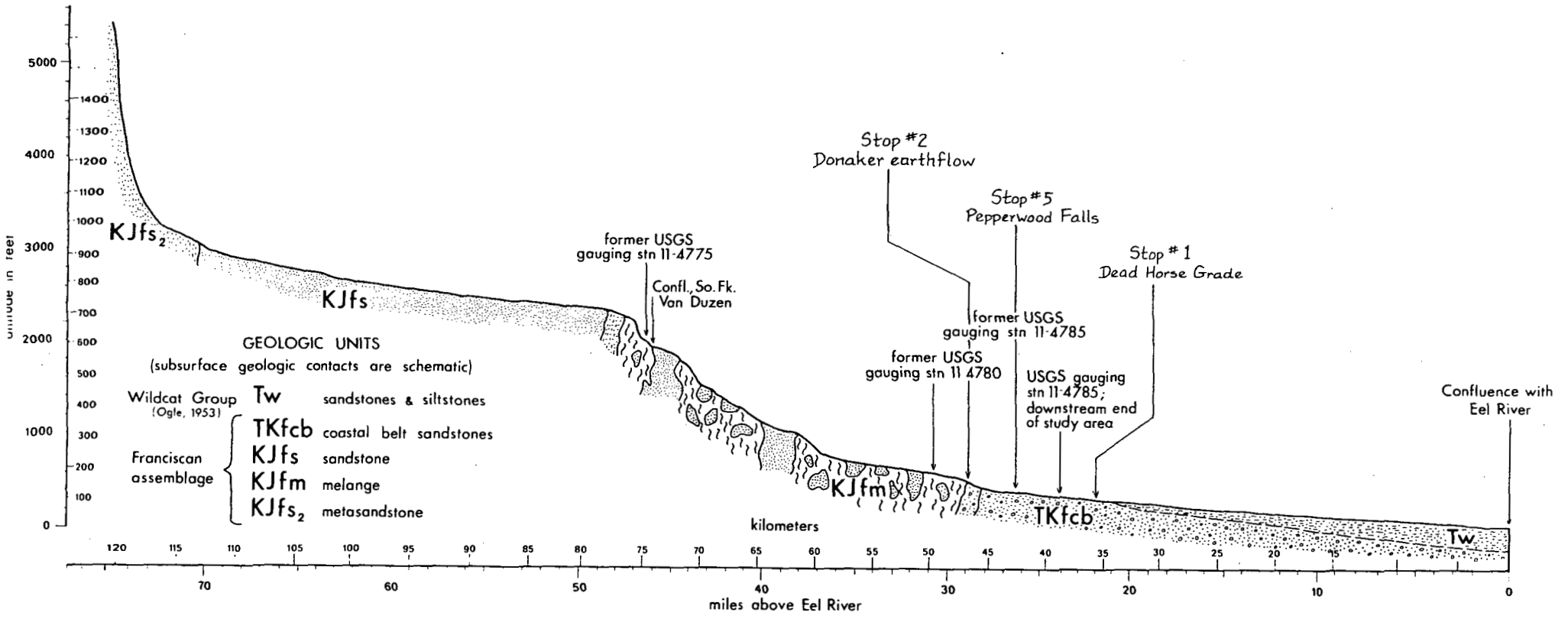

Figure 4. Longitudinal profile of Van Duzen River, showing relation of gradient to lithology. Figure from Kelsey.

49.1 STOP 1 - DEBRIS SLIDES AT DEAD HORSE GRADE.
Pull off to right at parking lot above bend in river called Devil's Elbow. We will look at the debris slides on the south valley wall from the parking lot and then walk back along the road to a caterpillar trail along the northern embankment.

USE EXTREME CARE WHEN WALKING ALONG THE HIGHWAY, CROSSING THE ROAD, AND CLIMBING ON THE EMBANKMENT.

Features to note at this stop include the size, geometry, and thickness of the debris slides. A variety of processes, including both sliding and sediment flow, are apparent from scars. Many of these slides have the capability of damming the river and affecting fluvial processes. The debris slides and flows almost all occur below a convex break in slope, in what many authors have called the "inner gorge" (see Road Log, day 2, mile 22.6). At least one older, revegetated landslide scar can be seen across the channel.

The types of landslide present at this stop are associated most commonly with lithologies within the Franciscan assemblage that produce soil and colluvium with relatively low clay contents and high sand contents. Debris slides and flows are thus found most often in areas underlain by sandstone, greenstone, and schist. The exposures in the roadcuts and along the tractor trail at this location show considerable variability within the Yager sandstone, especially in shearing and shale content.

Above the bedrock are scattered patches of colluvium. The size, geometry, and degree of weathering of these patches vary. We will see more patches of colluvium this afternoon on the Larabee Buttes access road where they fill bedrock hollows.

Figure 5 shows the distribution of debris slide landslides along a reach of the Van Duzen River further upstream before and after the 1964 flood. Major storms, such as that associated with the 1964 flood, greatly increase debris slides and flows into the major rivers. During the 35-year period 1941-1975, debris slides and associated shallow, rapidly moving slope failures, such as we see here at Dead Horse Grade, contributed 17% of total sediment to the Van Duzen River from less than 1% of the total basin area. The relation of debris slides to channel aggradation and subsequent channel recovery will be discussed at Stop 5 this afternoon.

We plan to leave Stop 1 at 10:30 a.m.

49.6 Grizzly Creek crossing

50.2 Terrace remnant on left

50.5 Cable for gaging station. Figure 17 shows changes in the channel at this cross-section since 1965. Significance of these changes will be discussed at stop 5 today.

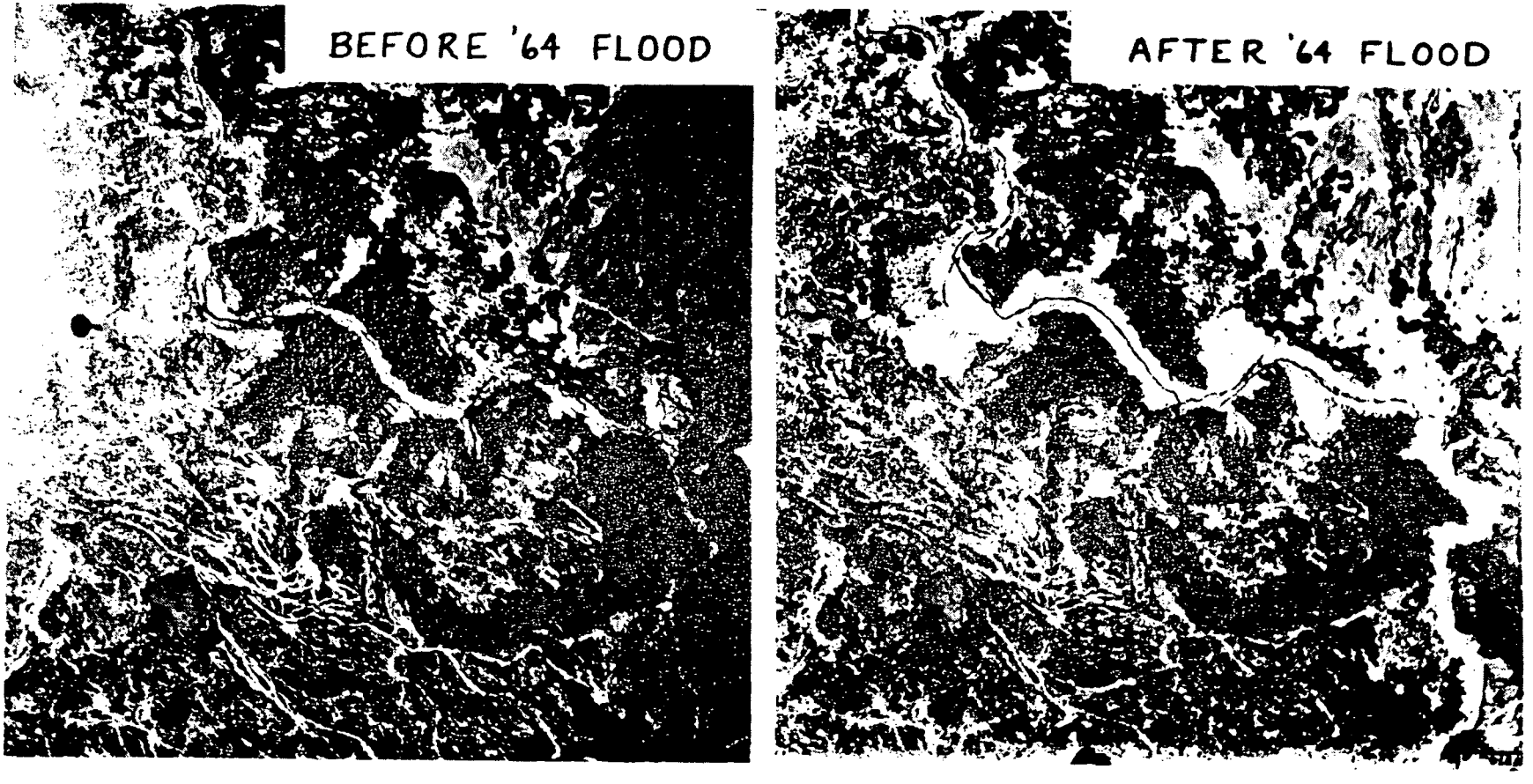

Figure 5. Comparative aerial photos, taken in 1963 and 1966, showing debris slides and avalanches that occurred in 1964 upstream of a landslide dam (shown by white arrow on left photo). Van Duzen River flows from right to left. Confluence of the South Fork Van Duzen is in the center of the right side of the photos. Photos from Kelsey, 1977.

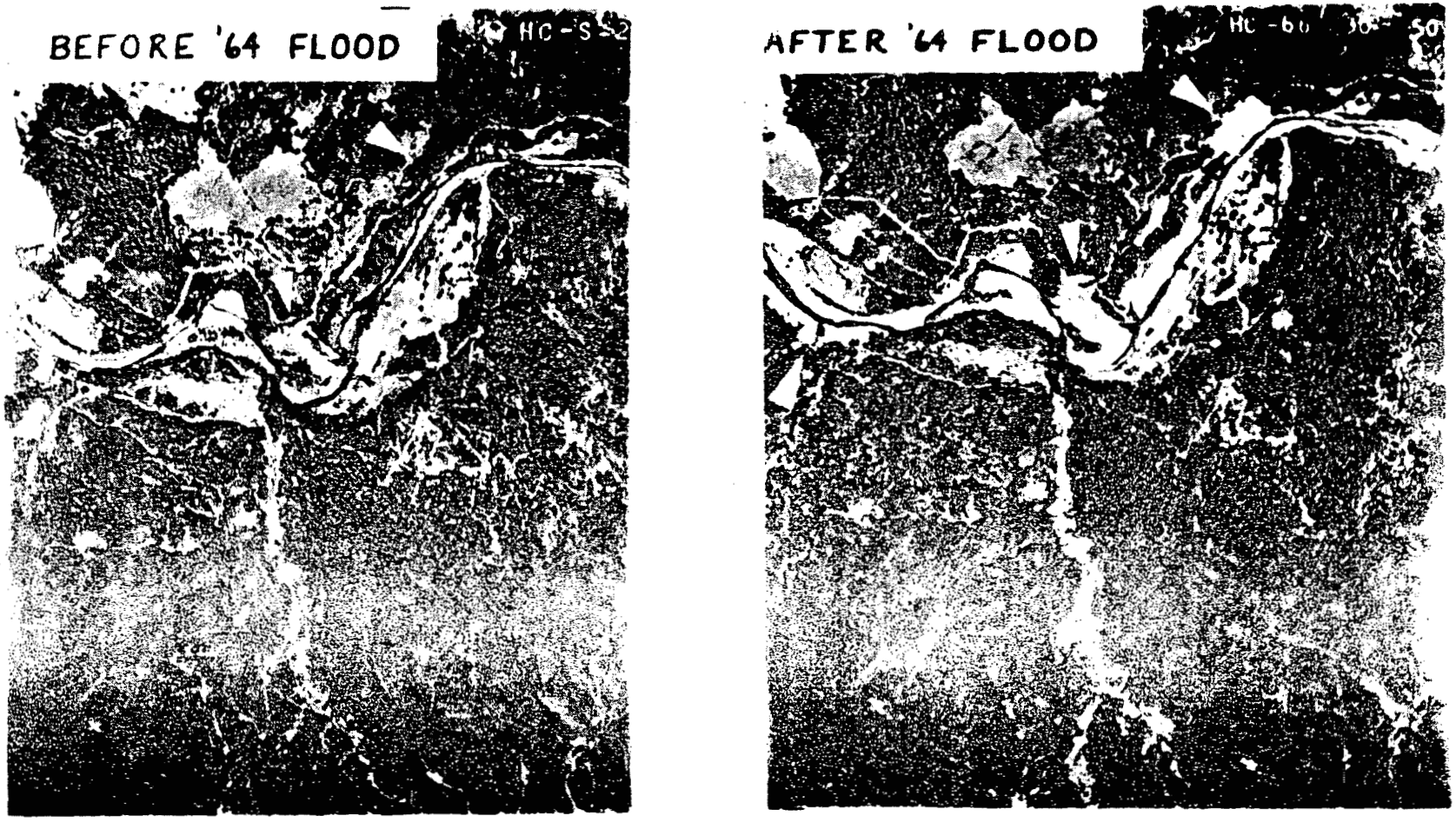

Figure 6. Comparative aerial photos, taken in 1963 and 1966, showing debris slides that occurred along a 3.5 km reach of the Van Duzen River during the 1964 flood (arrows). Fish Creek, site of a 1964 debris torrent, enters the Van Duzen from the south. Pepperwood Falls, location of the surveyed cross-sections in Figure 15, is at the downstream (left) end of this reach. Photos from Kelsey, 1977.

50.7 New bridge over the Van Duzen where the road has been straightened. The old bridge, however, will be saved because it is a historical landmark, one of the first reinforced concrete arch bridges in this area.

51.3 Dunn Creek on right. This small drainage was monitored by Kelsey during the 1975 and 1976 seasons.

51.9 Swains Flat, a prominent strath terrace.

52.1 Debris avalanche at 9 o'clock dammed the Van Duzen river in 1941 for a brief time. The valley at this point was wide enough so that the river was quickly diverted around the end of the landslide toe. Had the avalanche occurred only 100 m further downstream in the narrow canyon reach, a sizeable landslide dam would have totally blocked the river.

52.2 Good view of the contact between Yager Formation (underlying the steep slopes) and Franciscan Assemblage (underlying the gentle slopes to left). These units are in contact along the Freshwater Fault.

52.6 This trailer court was under water in 1964.

52.9 Van Duzen Bridge

53.0 VFW hall, Pepperwood Falls. This will be the final stop (Stop 5) of the day.

53.4 Exposure on left in a strath terrace shows the contact of bedrock with sediments. There are two terraces between Pepperwood Falls and Little Golden Gate Bridge. The lower terrace matches up with Swains Flat.

53.8 Valley at 3 o'clock is Fish Creek, site of a debris torrent in 1964 (see Fig. 6 for before and after pictures of the debris torrent).

54.1 Topography on Franciscan melange, straight ahead.

54.5 Bedded Yager formation in roadcuts to left. At 1 o'clock, prominent rock is Goat Rock, also in the Yager, at the base of Donaker earthflow in Franciscan melange.

55.1 STOP 2 - DONAKER EARTHFLOW Turn off at parking area on right. We will walk partway up the earthflow and then follow a path from the parking area to an overlook of the toe. This earthflow was monitored by Kelsey, who measured both the rate of earthflow movement and the water and sediment discharge from the axial gully. Although the earthflow has challenged road engineers for decades (see Fig. 7 and note modern condition of road), it is not the fastest moving earthflow in the Van Duzen basin. From 1974 to 1976, the earthflow moved at an average rate of 0.7 m per year, whereas the Halloween earthflow, further upstream, moved an average of 24 m per year for the three winter seasons from fall 1973 to spring 1976 (Kelsey, 1978, reprinted in Part II of this guidebook). The

Figure 7.

Plank road for the San Francisco-to-Eureka stage-coach across the toe of the Donaker earthflow in 1909. The barren, disheveled ground and the temporary nature of the road testify to the mobility of the earthflow toe (photo courtesy of Donald C. Tuttle).

erosion rate calculated for the Donaker earthflow, based on both mass movement surveys and measurement of suspended sediment and bedload discharge in the axial gully, is 51,200 metric tons/km ^{2} /year. Kelsey (1978) estimates that half the volume of sediment contributed to the Van Duzen River from earthflows comes from fluvial processes associated with the axial gully and its tributaries. The other half of the sediment influx comes from the mass movement of the earthflow itself.

Dwight May, whose family owns much of Donaker earthflow, told Kelsey in 1974 that old-timers said the earthflow moved much faster before they blasted away part of the protruding point of Goat Rock. Apparently the removal of the obstruction allowed the Van Duzen River to occupy the left side of the channel, lessening its lateral cutting against the toe of the earthflow.

The rockfall from the prominent greenstone block at the top of the earthflow occurred a few years before Kelsey began his field work in 1973.

The Van Duzen River is not competent to move the large rocks introduced into its channel by the earthflow. As a result, the channel in reaches affected by earthflows is narrow, boulder-choked, and considerably steeper than in other reaches (Fig. 4).

Tomorrow, the first stop of the day will be at an earthflow in the Redwood Creek basin that is presently being monitored by Dick Iverson. Like the Donaker earthflow, that earthflow is grass-covered. However, in other parts of the Coast Ranges, including parts of Redwood National Park, large blockglides with some similarities to these earthflows occur in forested terrain. These forested landslides, despite their large size, are difficult to observe on air photos (Sonnevil, personal communication).

Features to observe:

a) Prominent axial gully.

b) Variety of lithologies: The stones in the axial gully include the range of Franciscan lithologies: greenstone, chert, sandstone, serpentinite, blueschist. Gully banks show the shaly melange matrix.

c) Distinction of melange matrix in place from moving colluvium: in many exposures of Franciscan melange, it is difficult to tell what material has been affected by movement and what material has not moved. Many earthflows are, in fact, slides with movement concentrated in one or two zones and only small amounts of creep deformation within the material above the zones of shearing (see Iverson's description of Minor Creek Landslide on Day 2). In these cases, moving material may appear relatively undeformed. Kelsey estimates the depth of the Donaker earthflow at 20 meters at Rte. 36.

d) Morphology of the earthflow: You can walk across the northern margin of the earthflow and look back, noting the contrast between the stable and unstable areas. Figure 8 from Kelsey, 1978, is a schematic diagram of a typical earthflow. Figure 9 is a topographic map of Donaker earthflow.

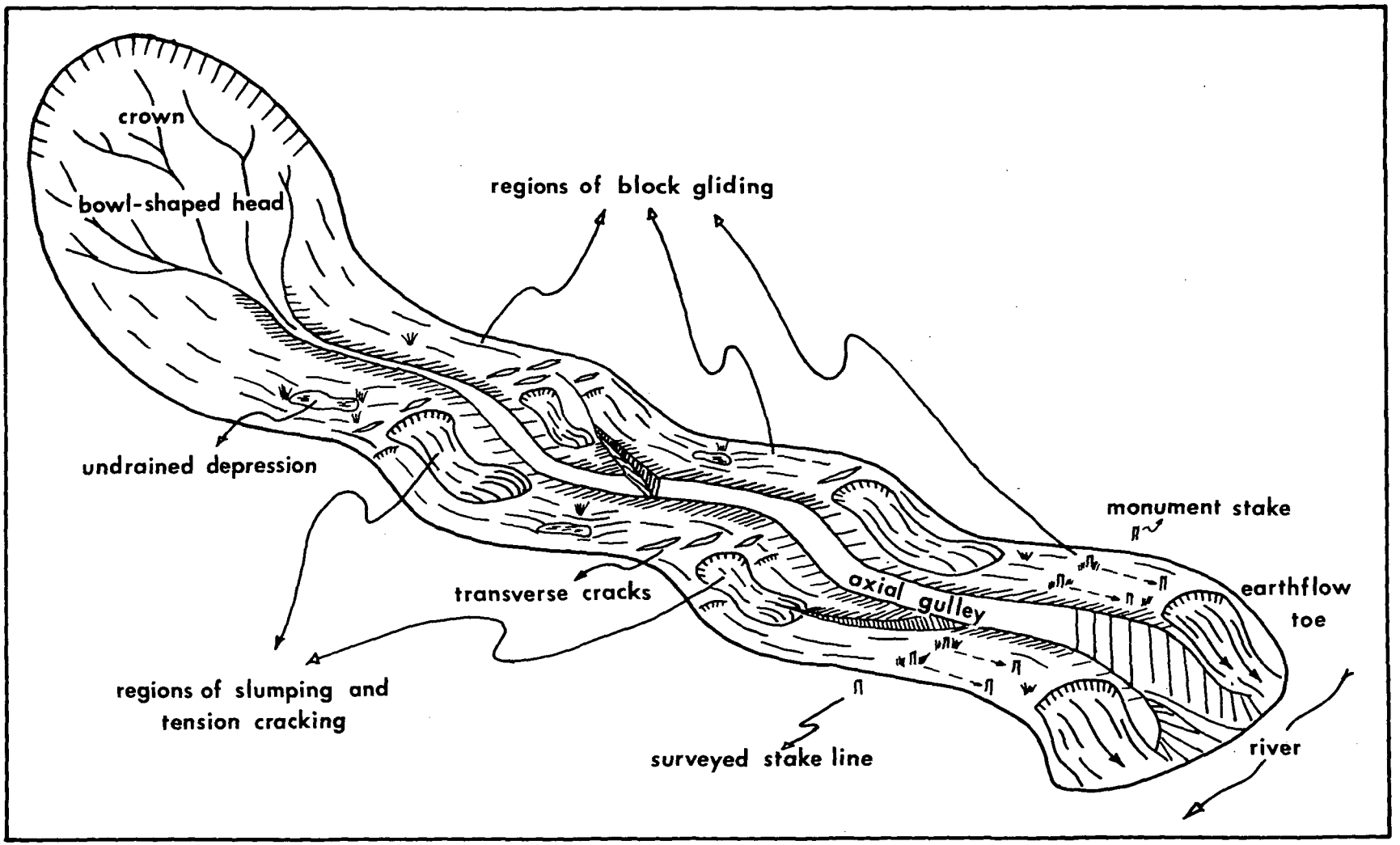

Figure 8. Schematic diagram of typical earthflow (from Kelsey, 1978).

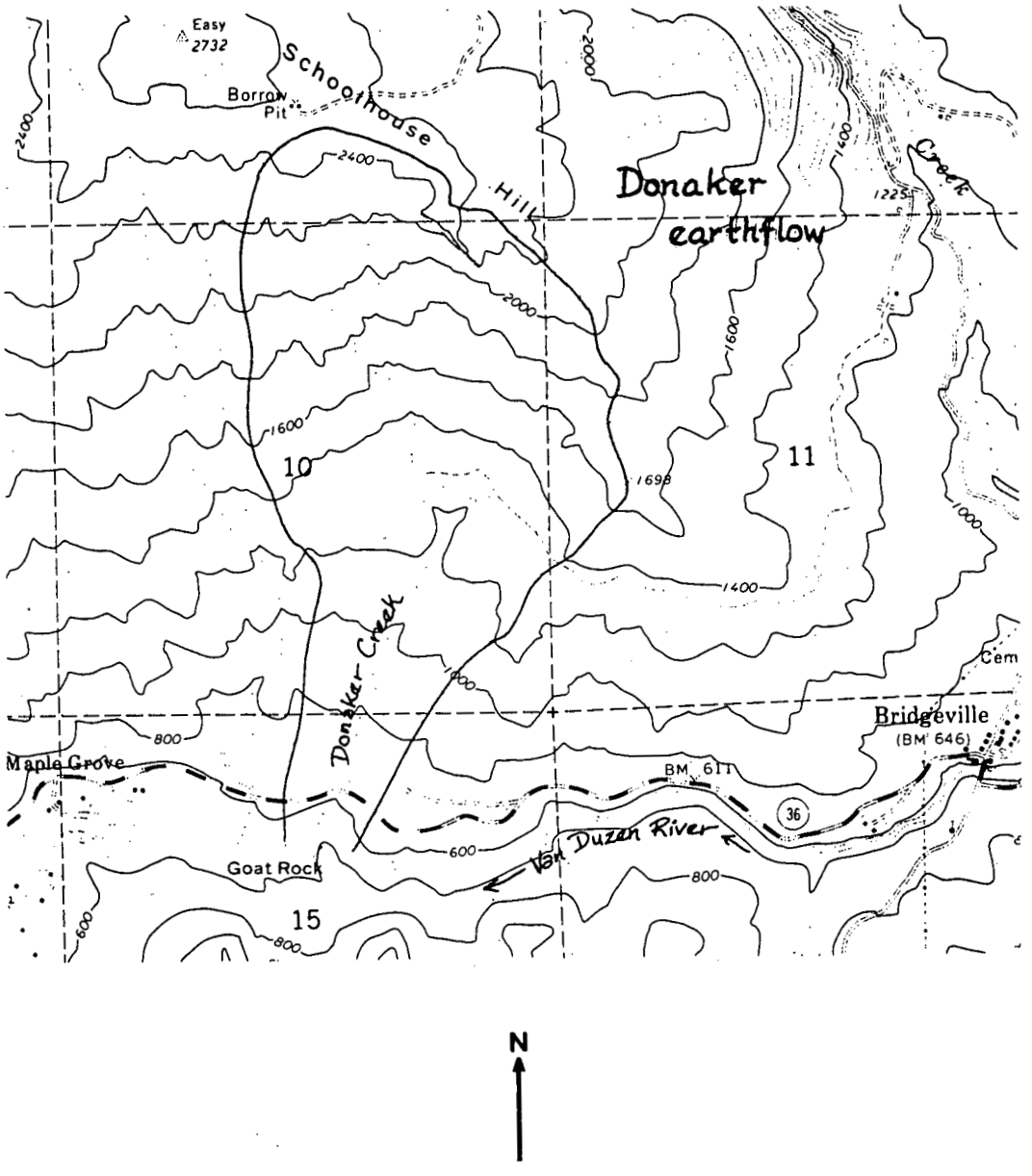

Figure 9. Topographic map of the Donaker earthflow, showing bowl-shaped topographic depression. Scale - 1:24,000; contour interval 40 ft. From Kelsey, 1977.

e) Toe of the earthflow: Note the boulder-clogged channel, fresh debris slide scars at toe of earthflow, and change in channel width compared to upstream and downstream.

We will leave stop 2 at 11:45 a.m.

56.6 Bridgeville

56.7 Take right over bridge, left turn on 36. 600 meters upstream from the Bridgeville bridge is a former U.S.G.S. gaging site. Channel changes at this section are illustrated in Figures 13 and 14.

56.9 Strath terrace on left, typical hillslopes on melange visible above channel.

57.8 The Van Duzen has incised into alluvium left by the 1964 flood since 1978. Most of the alders and other riparian vegetation have grown up since that time. These and other changes in the channel will be discussed at stop 5.

58.0 Crossing Little Larabee Creek, a tributary of the Van Duzen. The road leaves the Van Duzen at this point and follows the Little Larabee Creek drainage to the east, cutting off a loop of the Van Duzen.

58.5 Larabee Buttes, to south (right) form the divide between the Van Duzen basin and the Eel basin. The road visible in the distance, about one-third of the way from the crest of the Buttes to the stream channel, is the Larabee Buttes access road, where we will stop this afternoon (see Stop 4). Note the steep slopes below Larabee Buttes and the divides to the west of the road. Patch cuts of timber are visible for the next several miles.

61.6 Colluvium exposed on the left.

62.0 Deerfield Ranch. One of the many large ranch holdings now being subdivided into smaller parcels.

62.5 Sheared rock on left

63.0 McClellan Mtn. Road on left. McClellan Rock, near the headwaters of Little Larabee Creek, is a big greenstone block with well-developed pillows that should be visible from the vehicles.

64.7 Divide separating Little Larabee Creek basin from Larabee Valley and the basins of Butte Creek and the South Fork of the Van Duzen. Note the gentle slopes of Larabee Valley to the east compared to the steep slopes entering Little Larabee Creek. Larabee Valley has thick fill terraces in its lower part and may once have been a closed depression. It now drains into the South Fork Van Duzen. On the skyline, at 10 o'clock the unvegetated peak is Black Lassic, a klippe of black mudstone.

64.8 A recent landslide on the right has exposed weathered fluvial gravels at a high landscape position on the divide, about 50 m above Larabee Valley below. The weathered zone is enriched in clay, and has a 5 YR 7/6 dry color. These deposits were discovered during the field investigation for this road log. Ahead at 11:30 o'clock is the South Fork Van Duzen Valley; at 1:00 o'clock is Butte Creek Valley.

65.0 Larabee Buttes Access Road on right. Stay on Rte. 36.

65.1 Bedrock and surficial materials in exposure on left.

66.2 Larabee Valley Road. Most of Larabee Valley originally belonged to Deerfield Ranch and has now been subdivided into 40 acre parcels.

67.1 Gravels in roadcut at left.

67.2 Butte Creek crossing.

67.9 Church camp on left.

68.0 Bridge over South Fork Van Duzen.

68.1 STOP 3 - SOUTH FORK VAN DUZEN RIVER - LUNCH
Pull off the road to the left, pick up a lunch, and walk down the spur road to the river. This site is another of the temporary U.S.G.S. gaging sites installed in September 1958 to measure flow rates on tributaries and headwaters of several North Coast rivers. These flow determinations were designed to test the feasibility of a plan to divert water from north coastal rivers into the Middle Fork of the Eel and thence into the Central Valley aqueduct system and on to southern California. Nothing came of the project, although similar schemes are still being proposed. Nevertheless, the establishment of the cross-sections has proved useful in monitoring the changes of the stream channels with time.

This particular cross-section is one of the upstream-most locations of channel monitoring done by Kelsey (1977). At this site, recovery from the aggradation induced by the 1964 flood was already underway by the time Kelsey remeasured the cross-section in 1974. Since then, there has been gradual, continued degradation (see Fig. 12). In addition to the picturesque scenery, note that the channel cross-section here is partly on bedrock and that both valley walls expose bedrock near stream level.

This is the most upstream point of our trip. Highway 36 continues east and crosses the divide between the Van Duzen River basin and the Mad River basin east of Dinsmore.

We plan to leave Stop 3 at 1 p.m. Return west on Rte. 36

71.2 Turn left on Larabee Buttes Access Road. This road winds upward through private and BLM land for about 6 miles.

74.9 STOP 4 - BEDROCK HOLLOWS WITH COLLUVIAL FILLS

Vehicles will drop people off just beyond road ditch with debris catcher. Vehicles will proceed 1.25 miles (2 km) to turnaround and wait. Field trip stop is a walk down the road for 1.25 miles. Stragglers will be picked up along road on return.

The exposures in the 1.25 miles beyond the dropoff point contain a variety of hollows excavated into the bedrock and now filled with colluvium. Bedrock underlying Larabee Buttes is resistant sandstone with included sections of red chert. This sandstone unit is most likely a fault-displaced fragment of the Yolla Bolly terrane of the Franciscan assemblage, exposed in the Yolla Bolly Mountains 110 km southeast of here. The hollows we will see are more common in terranes of resistant rocks like these than in melange terranes.

Bedrock hollows with colluvial fills have been described by Lehre (1982) and Dietrich and Dunne (1978) and studied in detail in Redwood Creek basin by Marron (1982, 1985). Dietrich and Dorn (1984) most recently described the detailed geometry of a hollow in north-central California and dated the colluvial fills. All researchers agree that the hollows are probably excavated initially by debris slides or flows and subsequently filled by different types of processes. Figure 10 is a map from Marron (1985) showing the distribution of colluvium-filled hollows in Miller Creek basin, a tributary basin of Redwood Creek. Figure 11 (also from Marron, 1985) shows common sedimentologic features of colluvium-filled bedrock hollows in the Redwood Creek basin.

Along the Larabee Buttes road section, it is obvious that hollows occur in a variety of positions relative to the present topography, including adjacent to modern channels, within prominent swales, and near the crests of ridges. The dimensions of the hollows differ. In a few places, the entire hollow is visible: both of the lateral contacts and the basal contact with bedrock are preserved. Near the end of the traverse, one hollow is exposed along upper and lower road cuts. The width of this hollow is identical in both cross-sections, showing the linear nature of the hollow (length much greater than width, a typical feature of debris flow scars).

Sedimentology of the colluvial fills also differs from hollow to hollow. Near the beginning of the traverse, one hollow is filled with a homogeneous mass of matrix supported colluvium containing about 40% large angular sandstone clasts. We interpret this as a landslide deposit. Most of the other hollows are filled with finer grained material, some of which shows a crude stratification. Marron (1982) interpreted the hollow-filling processes as slopewash, creep, windthrow of trees, raveling of scar edges, and small landslides. The filling processes are periodically interrupted by debris slides that excavate part or all of the fill (Dietrich and Dunne, 1978; Marron, 1982) (see Fig. 11). A few of the colluvial deposits visible on the Larabee Buttes road have an indistinct stone line at the base of the colluvial fill. Dietrich and Dunne (1978) and Marron (1982) postulate that the stones are a lag produced when slope wash removed finer material after the debris flow that excavated the hollows. Some colluvium-filled bedrock hollows have

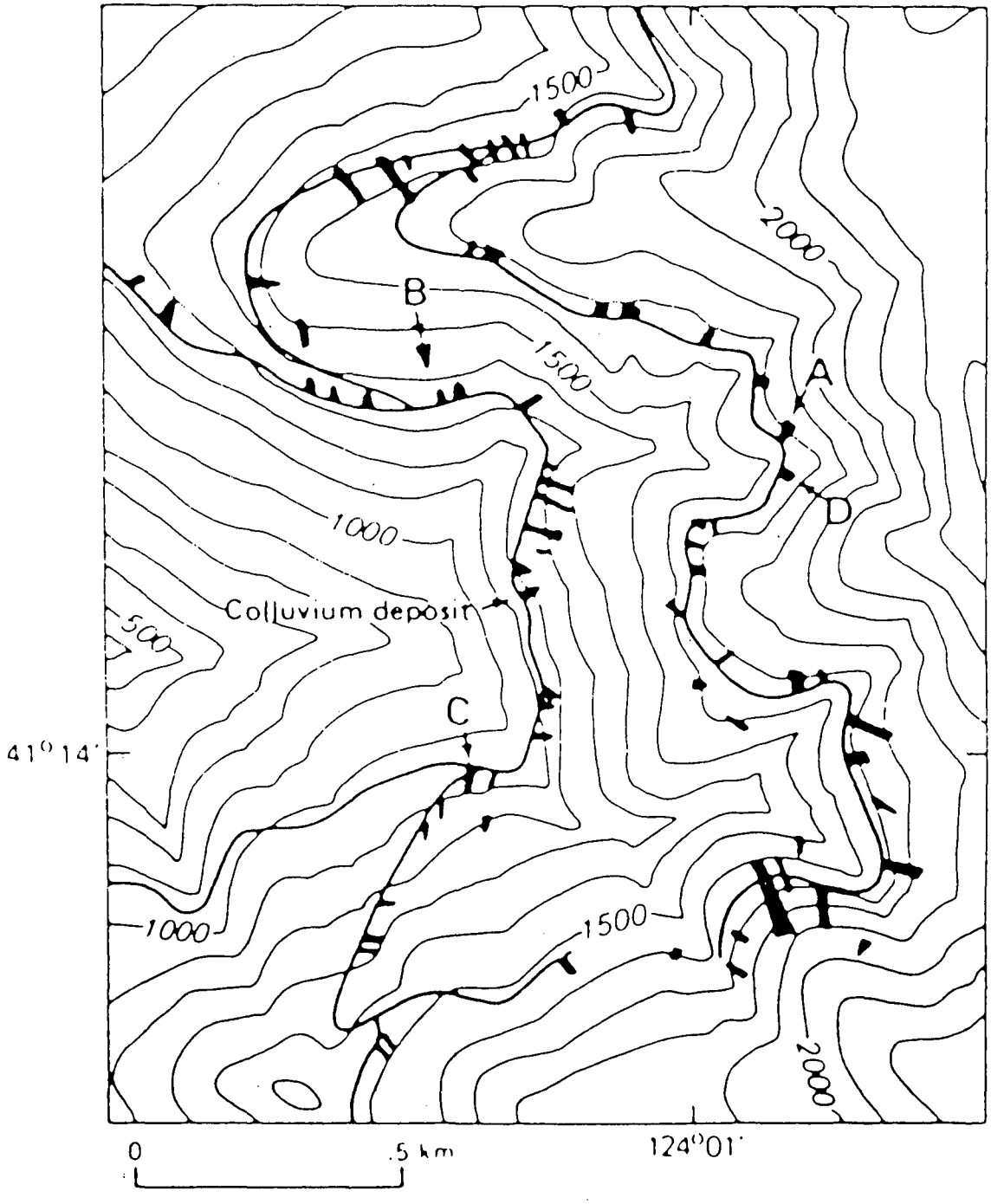

Figure 10. Distribution of colluvial deposits along major haul roads in Miller Creek watershed, Redwood Creek basin. Letter A marks colluvial deposit shown in Figure 11. From Marron, 1985.

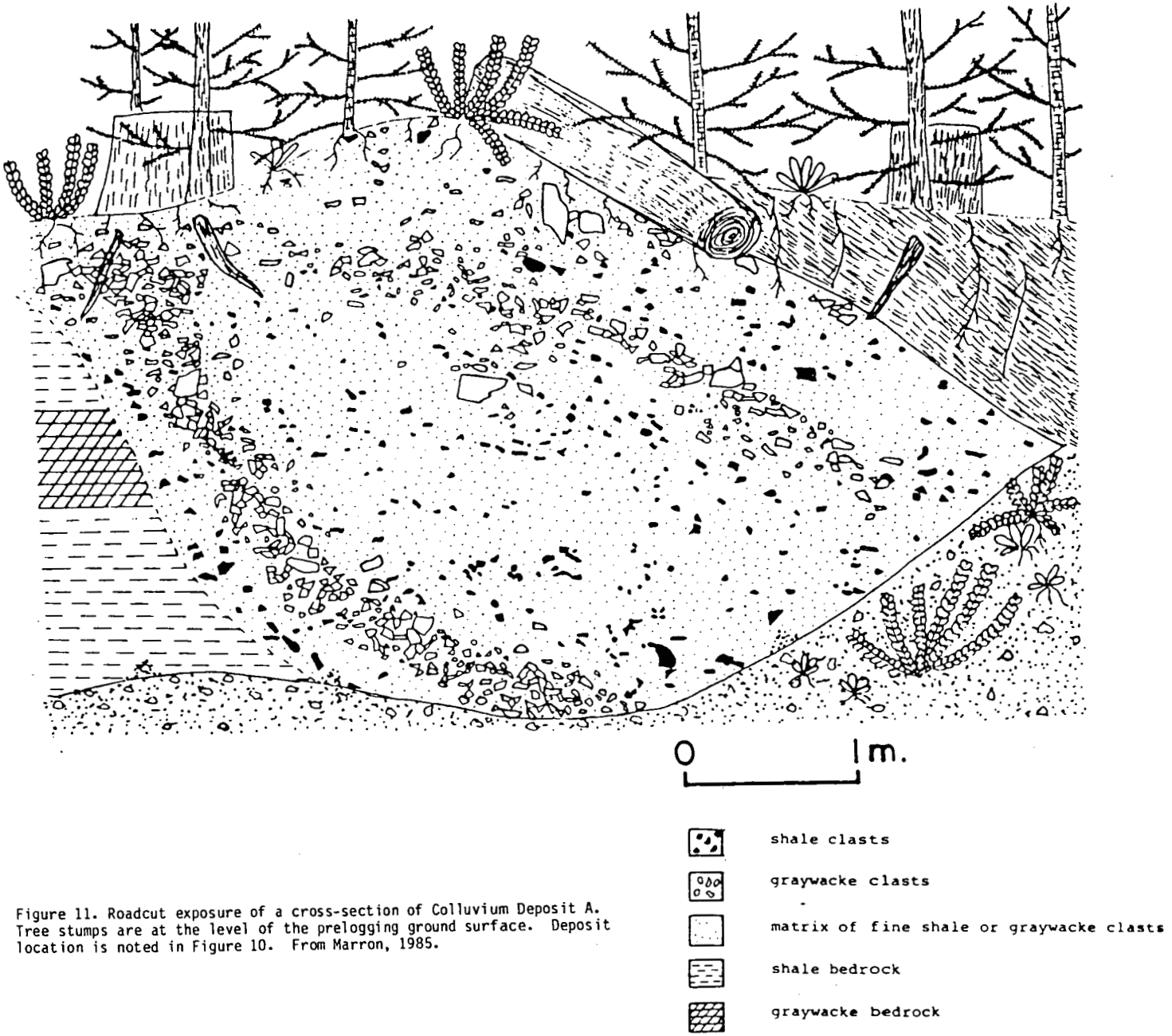

Figure 11. Roadcut exposure of a cross-section of Colluvium Deposit A. Tree stumps are at the level of the prelogging ground surface. Deposit location is noted in Figure 10. From Marron, 1985.

topographic positions and/or weathering features that suggest long-term stability (Marron, 1985).

Another interesting feature of the Larabee Buttes hollows is the fact that they have developed both on the sandstone and on the chert. The character of the colluvial fill in the chert hollows differs from the fill of the sandstone hollows.

We have found charcoal near the base of one of the colluvial fills here at Larabee Buttes. It has given an age of 35,530 [± 2300] years B. P. Marron (1985) found that the lower fill in a hollow in Redwood Creek basin gave dates of 9625 [± 310] to 9900 [± 260] years B.P. Dietrich and Dorn (1984), who studied a hollow north of San Francisco Bay, near Clear Lake, CA, found that the hollow began to fill with sediment between 11,000 and 13,500 years ago. Reneau and others (abstract, this volume) note a clustering of charcoal dates from 11,000 to 14,500 years B. P. and suggest that long duration-high intensity storms capable of eroding the hollows were particularly common during the latest Pleistocene.

In the course of planning this field trip, we have realized that both of us are latecomers to a true appreciation of the importance of these colluvium-filled bedrock hollows. Now, we think it no exaggeration to claim that these hollows are the single most important element in the landscape for the understanding of geomorphic processes in this area. The hollows contain the record of the landscape-forming processes of at least the last 10,000 years and are particularly critical in determining the role played by low magnitude, high frequency processes like creep and windthrow that are difficult to measure in the length of time covered by most geomorphic studies. Also, the hollows provide a graphic illustration of the ephemeral nature of most landscape elements like ridges and stream channels. Presumably, most of the hollows are depressions in the landscape produced by rapid landslides. Now, however, the present landscape has been sculpted around these old landslide scars, leaving many of them perched in improbable positions adjacent to ridges. Although we do not have enough dates to estimate the speed of hollow filling and landscape alteration, it is clear that the landscape has changed rapidly in this environment.

We plan to leave Stop 4 at 3:30 p.m. We will return to Highway 36.

'8.6 Intersection of Larabee Buttes Access Road with Highway 36. Turn left (west) onto Highway 36. Retrace road log from Larabee Buttes Access Road to Pepperwood Falls.

'0.6 STOP 5 - VAN DUZEN RIVER AT VFW HALL, PEPPERWOOD FALLS. This is the site of a monitored cross-section (Kelsey, 1977, 1980), recently remeasured by Kelsey and Savina in summer 1984. There are three channel cross-section survey sites in the lower Van Duzen. Survey data on all three are included in the guidebook: 1) above Bridgeville (Fig. 13), 2) Pepperwood Falls (Stop 5; Fig. 15), and 3) near Grizzly Creek State Park (Fig. 17). At this site, we will discuss the results of these cross-section surveys, the results of Kelsey's sediment budget for the Van Duzen basin and the

response of the Van Duzen channel to high magnitude events. One such event occurred in December 1964 and caused basin-wide landsliding and stream aggradation. Most of the riparian vegetation along the Van Duzen and other north coast rivers was removed by the flood (see Figs. 7 and 18). The varied lithologies and sub-basin geometries within the Van Duzen system resulted in a complex pattern of aggradation in response to the 1964 flood and subsequent channel recovery by degradation of the thalweg, stabilization of bars with vegetation, and partial stabilization of valley sides. In general, however, the most upstream sites such as stop 3, received the 1964 sediment slug first and were also the first to recover. Degradation at the three monitored sites lower in the basin, including this site at Pepperwood Falls, has been much slower. Such sites aggraded over a longer period of time after the 1964 flood and recovery (degradation) at some sites also appears slower than further upstream. Sequential photos showing channel recovery at Pepperwood Falls are shown in Figure 16.

A summary of sediment budget studies for the Van Duzen basin is included in Part II of this guidebook as a reprint of Kelsey (1980). Furthermore, Figure 19 summarizes the sediment budget for the area upstream of the U.S.G.S. gage near Grizzly Creek State Park, 4.0 km downstream of Stop 5. The relative importance of different source areas to total sediment yield (Fig. 20) shows that a major portion of the sediment discharge (45%) comes from a small fraction of the basin study area (5.5%) that consists of 1) densely gullied grasslands, 2) earthflow landslides, and 3) debris slides and avalanches. Most of the remaining sediment comes from moderately gullied grassland slopes with no landsliding evident.

Downstream to the north of the bridge is a large debris flow that dammed the Van Duzen (see comments under mile 52.1 of this log).

We plan to leave stop 5 at 6 p.m. Return to west on Highway 36 and north on Highway 101.

132.6 Take Highway 255 exit at the north end of Eureka and proceed west on 255 to Samoa spit. Dinner tonight at Samoa Cookhouse, a moderately authentic lumber camp restaurant. Steam trains used to haul loggers to the nearby woods from this cookhouse.

After dinner, return to campground at Mad River.

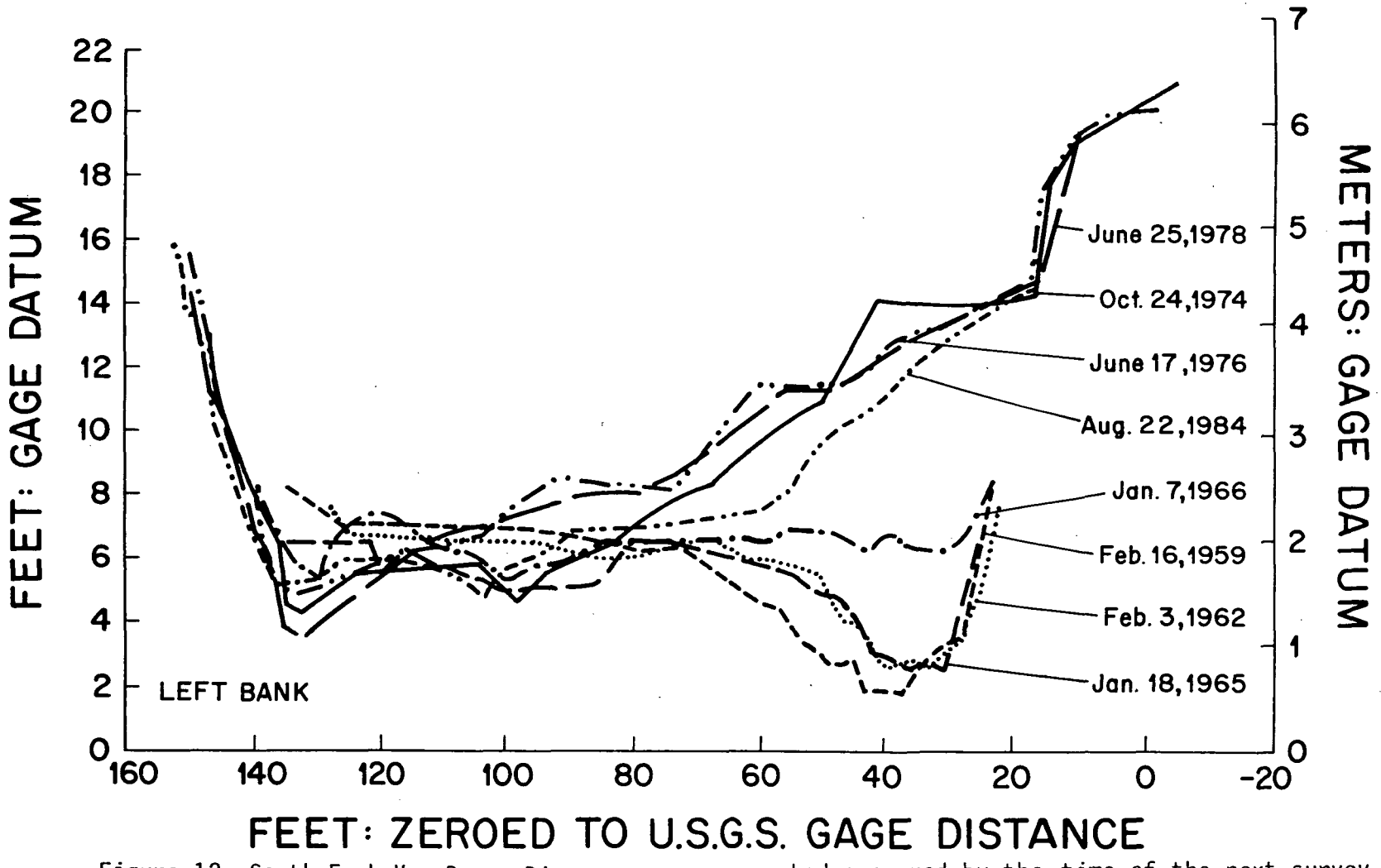

Figure 12. South Fork Van Duzen River: cross-section surveys at site of former U.S.G.S. gaging station #11-477700. This series of cross-sections show the delayed channel response at this site to a major erosion event (debris avalanches in headwater basins) that occurred 21 km upstream during the storm of December 1964. Immediate post-storm channel response was minor (1966 survey). The largest amount of aggradation had occurred by the time of the next survey in 1976. Between 1976 and 1978, minor aggradation continued, and the survey in August shows degradation. Note that the thalweg on the left bank has been on or near bedrock since 1976, indicating the depth of fill here is not substantial compared to the other three Van Duzen channel sites (above Bridgeville, at Pepperwood Falls and near Grizzly Creek).

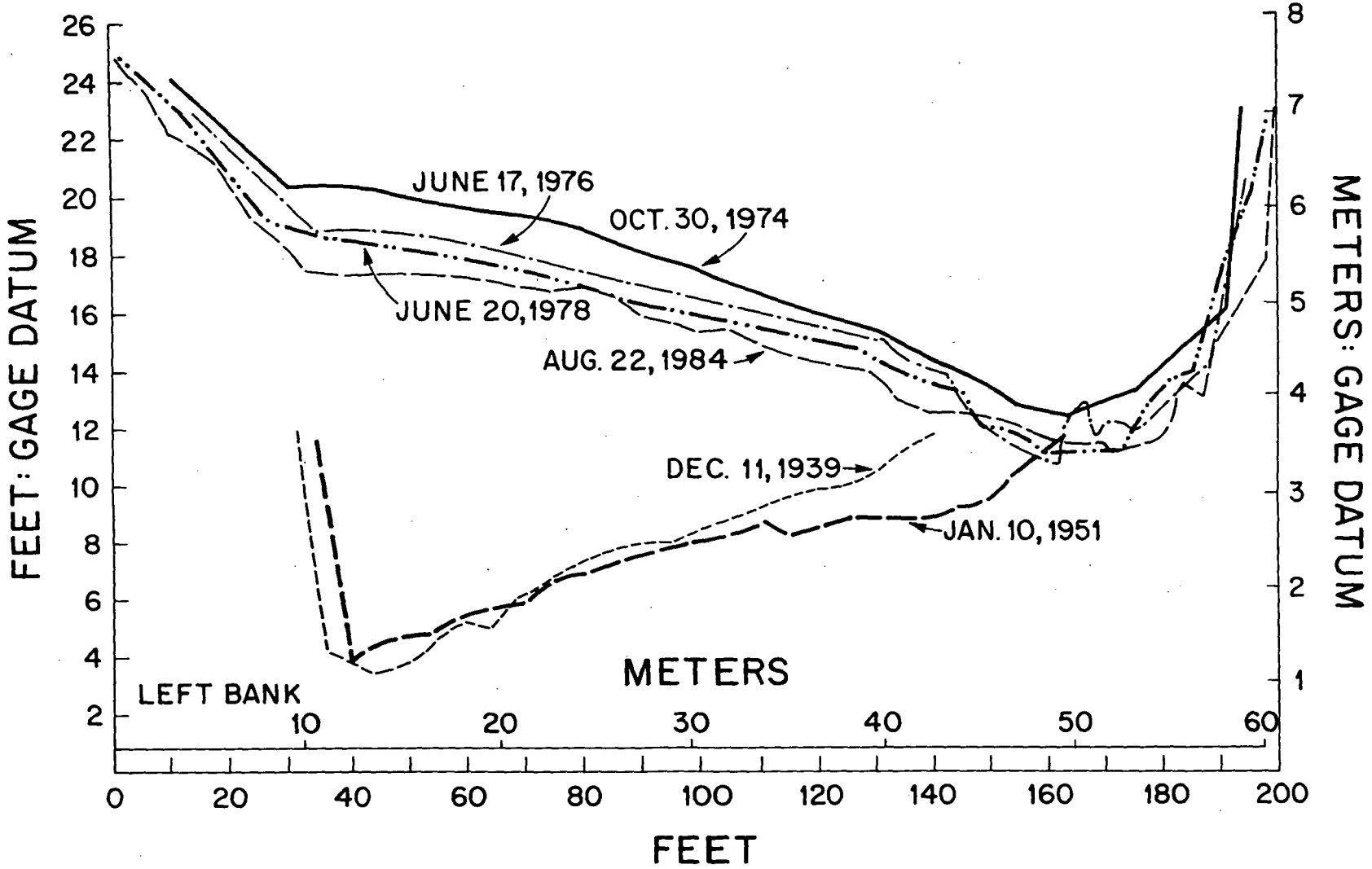

Figure 13. Van Duzen River 600 m above Bridgeville: cross-section surveys at site of former U.S.G.S. gaging station #4780. The six channel cross-sections at this site depict the stable pre-1964-flood channel as it appeared in 1939 and 1951, and post-1964-flood channel changes that span the years 1974 to 1984. The major aggradation that occurred between the 1951 and 1974 survey resulted from the late December 1964 flood event and the 1974 to 1984 set of surveys records progressive degradation. Since 1976, bedrock has been exposed at the thalweg near the right bank. The rate of degradation has slowed over the 1974 to 1984 period, perhaps due to increasing erosional resistance of the left bank bar due to a developing armor layer.

Figure 14. Looking downstream at the flood bar on the left bank of the Van Duzen River cross-section site 600 m above Bridgeville. a) taken in 1976? This flood bar appears armored with small boulders and larger cobbles that were deposited during the 1964 flood. b) taken in 8/1984.

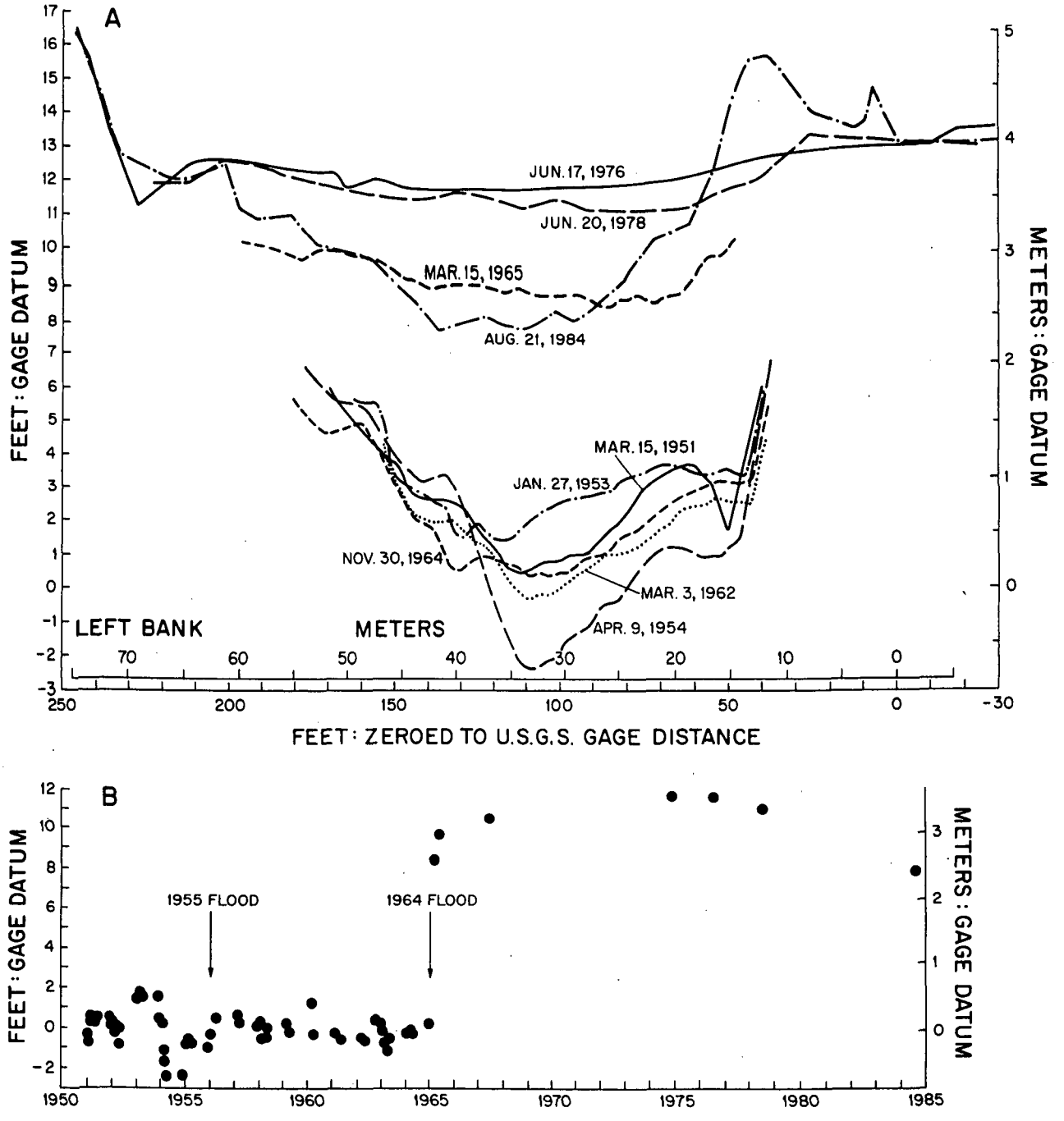

Figure 15. Van Duzen River at Pepperwood Falls: cross-section surveys at the old site of U.S.G.S. gaging station #11-4785. Upper graph (A): changes in channel bed elevation, 1951-1984. Lower graph (B): changes in thalweg elevation, 1951-1984. Both graphs show that bed elevations dramatically rose as an immediate consequence of the December 1964 flood. Note change from an inner trapezoidal channel (1953-1964 surveys) to a flat channel bed with no inner channel (1965-1978 surveys). Peak channel bed elevation occurred in 1976 and minor downcutting is evident by the 1978 survey. Water years 1976 through 1981 were low-flow years on the Van Duzen. Substantial downcutting (one third of the way back to pre-1964 flood elevations) had occurred by August 1984. Most of the downcutting must have occurred in the wet 1983 and 1984 water years. Between 1978 and 1984, a dense riparian fringe of willow grew on the right bank at horizontal gage distance = 50 feet. This vegetation promoted build-up of an inner channel bank, which became the right bank of the new trapezoidal inner channel. This observation emphasizes the importance of riparian vegetation in establishing the new channel during recovery from an aggradation event. Note that the new trapezoidal channel is becoming established in the same channel position as the pre-1964 flood channel.

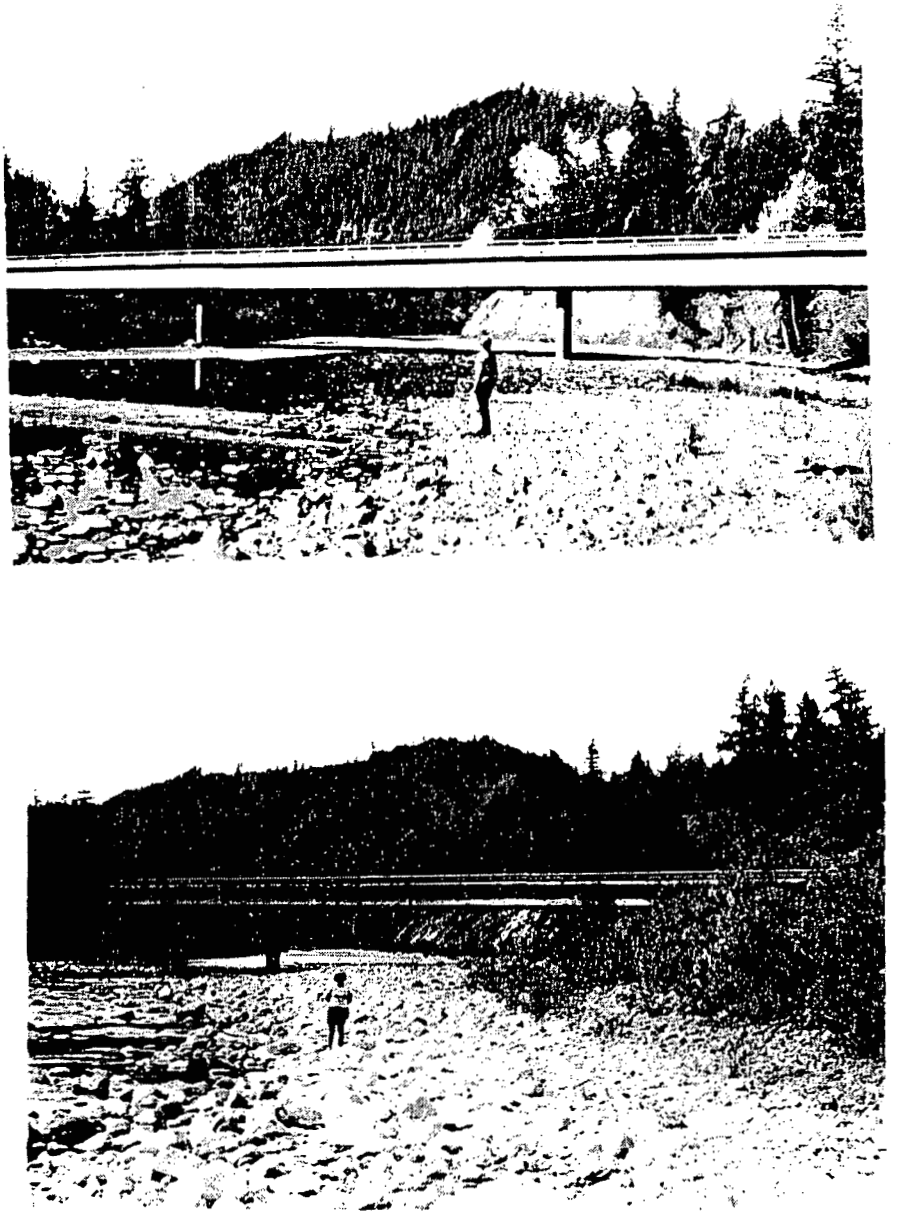

Figure 16. View looking downstream at the Van Duzen River at the site of the former U.S.G.S. gaging station at Pepperwood Falls. a) taken November 1976. b) taken August 1984. The new highway bridge is a replacement for an old concrete arch bridge that was washed away by the 1964 flood. Note growth of riparian vegetation on right bank since 1976. Figure 15 shows changes in the channel cross-section at this site.

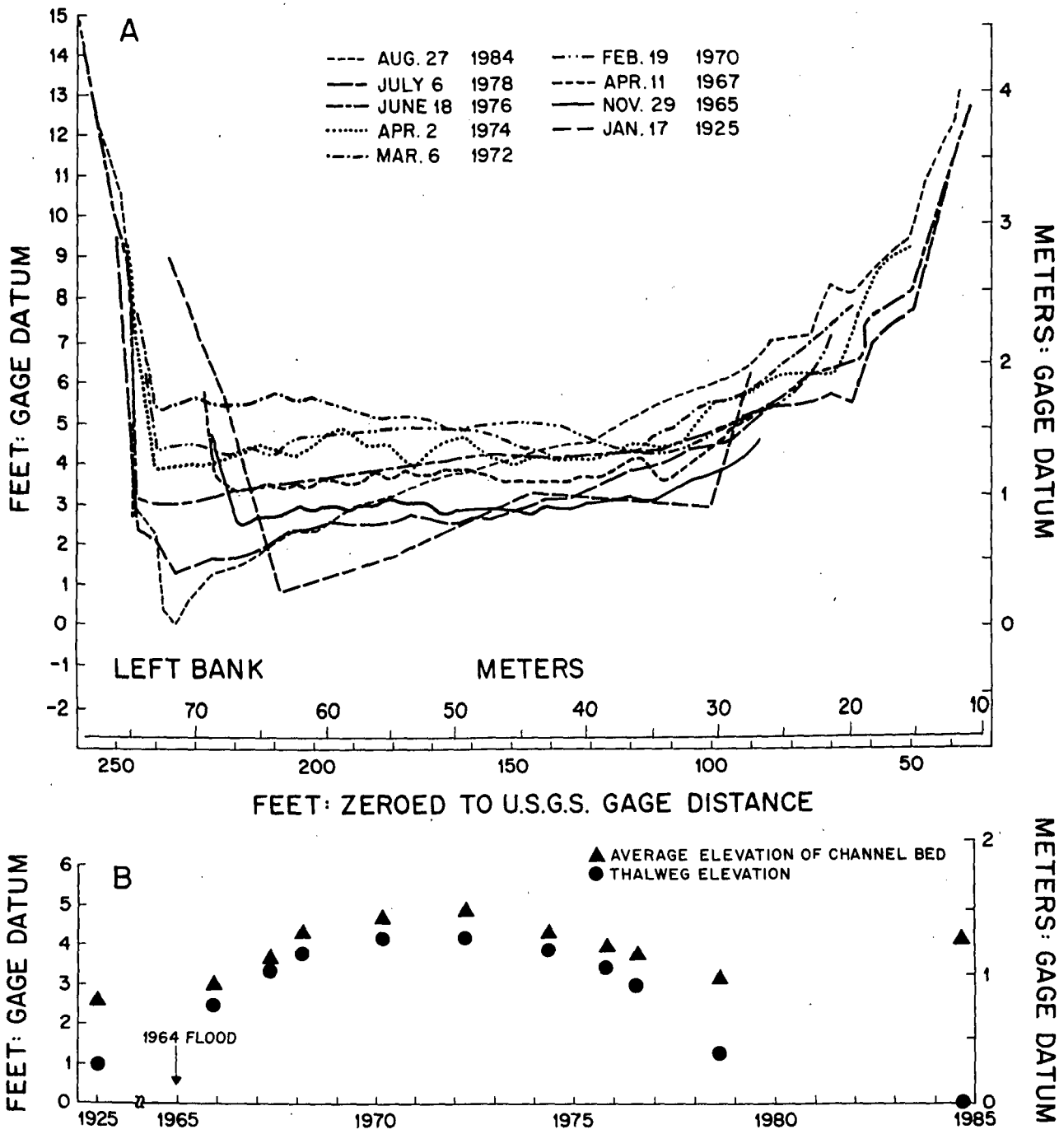

Figure 17. Van Duzen River near Grizzly Creek State Park: cross-section surveys at the U.S.G.S. gaging station #11-4785 (new site). Upper graph (A): changes in channel bed elevation, 1965-1984. The single survey in 1925 is at the concrete arch bridge approximately 100 m upstream of the rest of the surveys. Lower graph (B): changes in thalweg elevation ( ) and average elevation of channel ( ), 1966-1984. Average elevation is approximated for the bankfull width and is a more useful index of net elevation change than thalweg elevation. Thalweg elevations for 1976, 1978, and 1984 reflect pronounced scour due to a root wad embedded in the channel. This cross-section is 5.0 km downstream from the last major sediment sources due to debris slides and debris torrents triggered during the 1964 storm and flood. Because of this distance downstream of sediment sources, bed elevations gradually increased at this section by approximately 0.6 m from 1965 (date of first survey) to a peak height in 1972. The channel showed gradual degradation between 1972 and 1978. The 1984 survey showed net aggradation, despite deep thalweg scour because of a local obstruction. This aggradation may reflect deposition of sediment from reaches of accelerated downcutting 4.0 km upstream at Pepperwood Falls in the winters of 1982-83 and 1983-84 (see Figure 15).

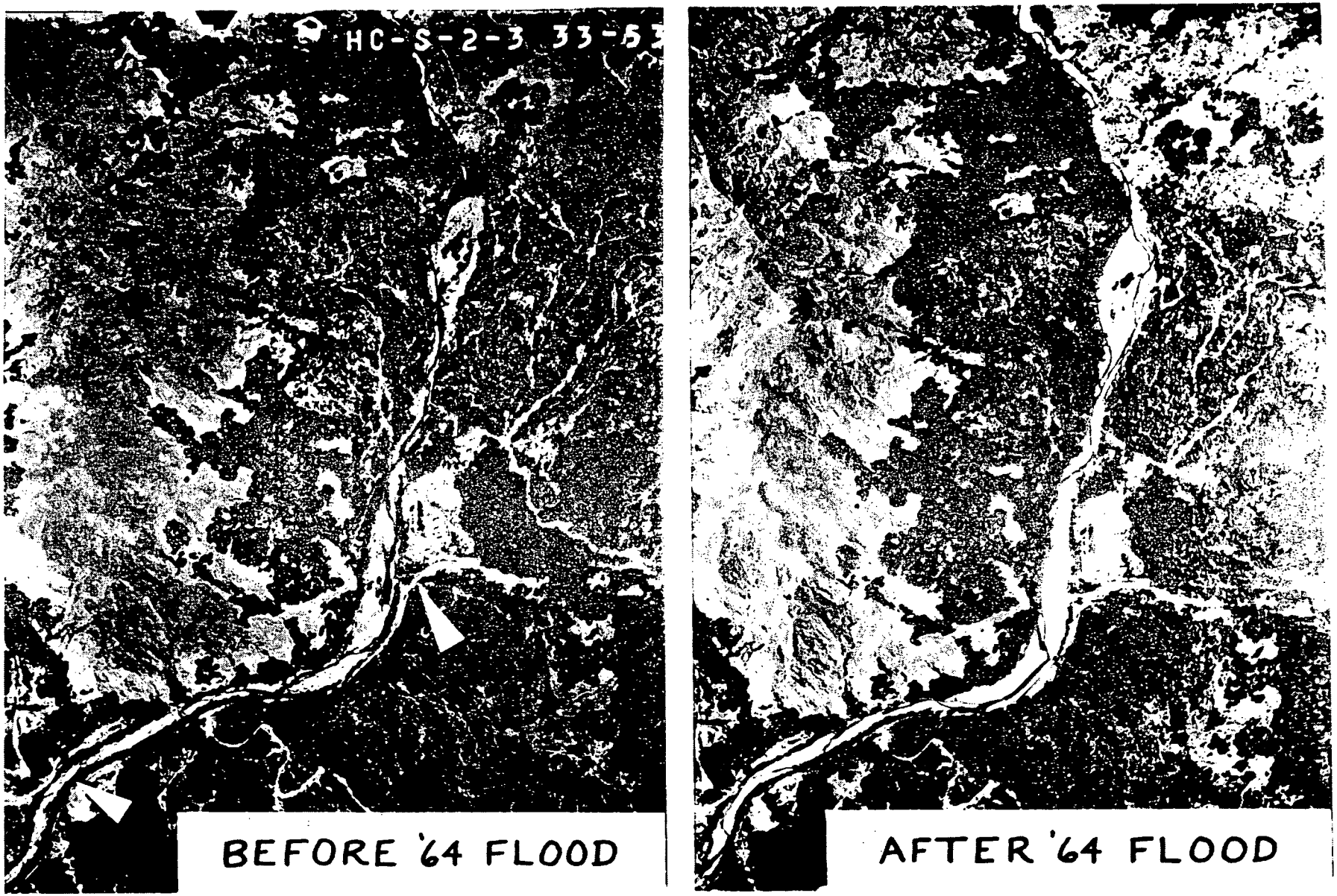

Figure 18. Comparative aerial photographs taken in 1963 and 1966 showing the effects of the 1964 flood on riparian vegetation and slopes in a 4.2 km reach of the Van Duzen river upstream of the gaging station 600 m above Bridgeville (left arrow). See Figure 13 for the record of channel changes at this location. Right area is the confluence of Little Larabee Creek with the Van Duzen. Photos from Kelsey, 1977.

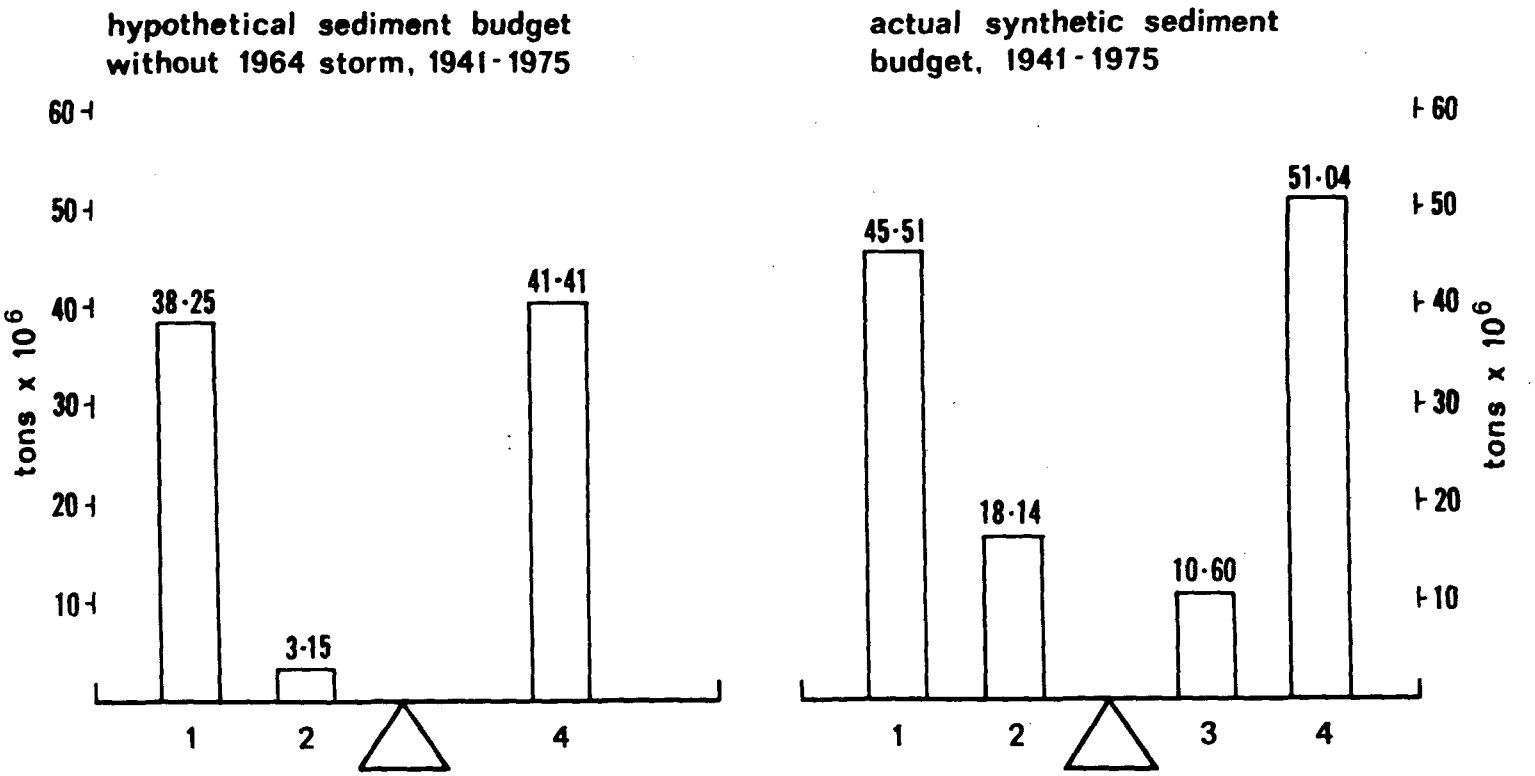

1. sediment yield by fluvial transport from hillslopes
2. sediment yield by streambank erosion and landsliding along major channels and in headwater basins
3. aggradation in major river channels
4. total sediment discharge past gauging station near Bridgeville

Figure 19. Comparative histograms showing two synthetic sediment budgets for the Van Duzen basin, 1941-1975. The left histogram shows a hypothetical sediment budget that excludes the effects of the December 1964 storm. The right histogram shows the actual synthetic sediment budget for the Van Duzen. Figure from Kelsey, 1980.

SEDIMENT SOURCE AREAS

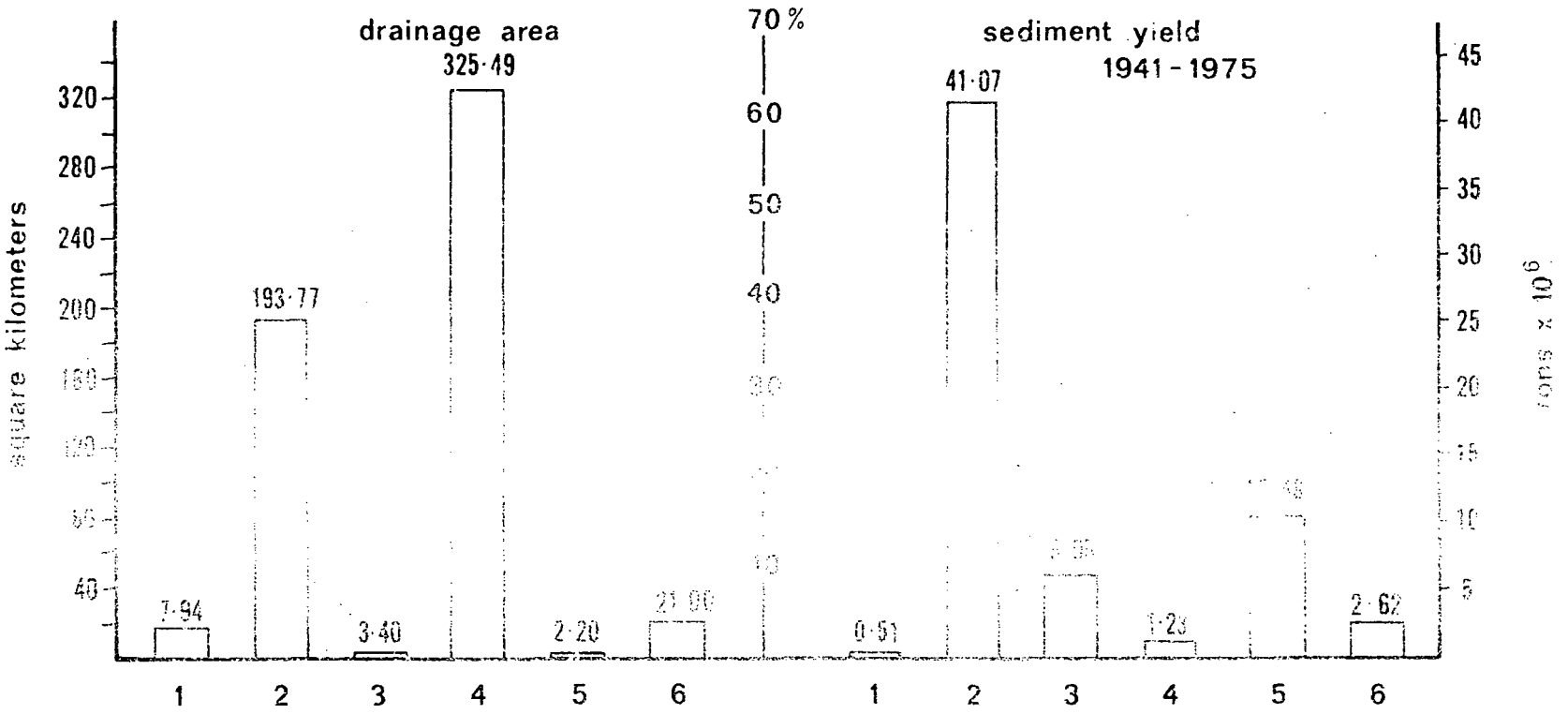

1. stable and ungullied melange slopes (type Ia & Ie)
2. eroding melange slopes (type Ib & Ic)
3. earthflow slopes (type Id)
4. sandstone slopes (type II, III a & III b)
5. debris slides, debris avalanches (type II & III a)
6. alluvial floodplains, fill terraces (type IV b)

Figure 20. Sediment source areas in the Van Duzen River basin. The left histogram shows the percentage and total amount of drainage area of each source area. The right histogram shows the sediment yield from each source area. Sediment source areas are split into six categories, based on physiographic slope types outlined in Kelsey, 1980. Figure from Kelsey, 1980.

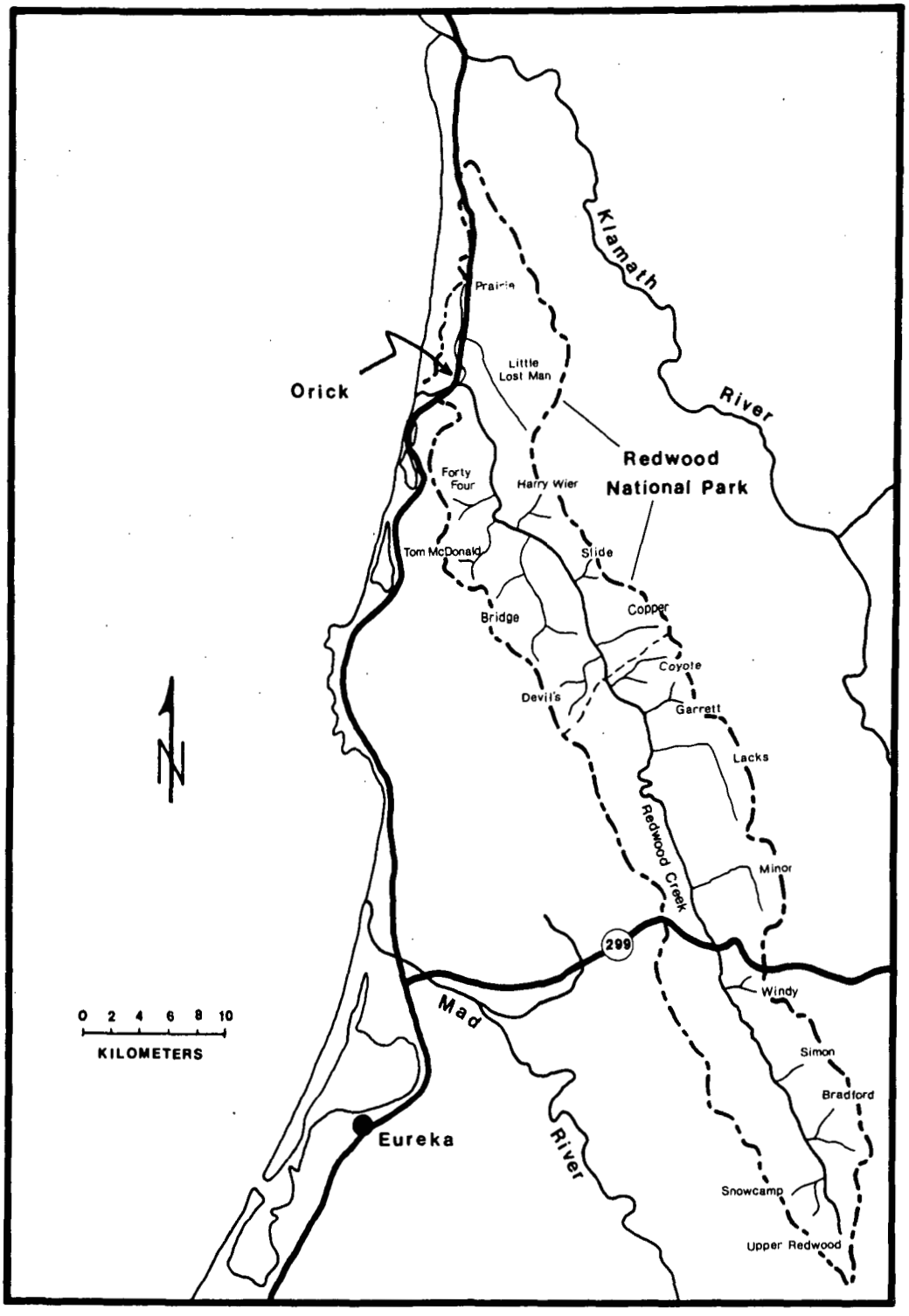

Figure 21. Index map of Redwood Creek Basin, showing boundaries of Redwood National Park and general route for Day 2 of Field Conference. Stop 1 is in the Minor Creek Basin, north of highway 299.

Field Guide Day 2 - Redwood Creek Basin

By Harvey Kelsey, Department of Geology, Western Washington University, Bellingham, WA; Mary Savina, Department of Geology, Carleton College, Northfield, MN; Iverson, R. M., U.S.G.S. David A. Johnston Cascades Volcano Observatory, Vancouver, Washington; Sonnevil, Ron, Redwood National Park, Orick, CA; LaHusen, Richard, Redwood National Park, Orick, CA, Popenoe, James, Redwood National Park, Orick, CA; Ricks, Cynthia, Siskiyou National Forest, Gold Beach, OR; and Madej, Mary Ann, Redwood National Park, Arcata, CA.

The Redwood Creek basin is underlain by somewhat different rock types from those we saw yesterday in the Van Duzen basin. The geomorphic processes, however, are comparable. In addition, the Redwood Creek basin has been studied in depth since the establishment and subsequent expansion of Redwood National Park in 1968 and 1978. The park now occupies the lower third of the basin. The extensive work of Janda and others (1975) provided the background for many of the more recent studies that will be discussed today. Among the many geomorphic studies in Redwood Creek, recent studies by Iverson (1984), Sonnevil and others (this volume), LaHusen (this volume) and others have concentrated on the detailed mechanics of landslide movement, including the relation between movement rates and styles and ground water. Both the technical aspects of these studies (including the instrumentation designs and placement of piezometers and movement monitors) and the geologic implications of the results are of great interest, and can be applied to similar types of landslides in other parts of the north coastal area.

Redwood Creek basin has also been the site of detailed sediment budget and sediment storage measurements (Madej, 1984). We will see Redwood Creek at two places: one at mid-basin in Redwood Valley near the confluence of Minor Creek (a major tributary) and one at the estuary of Redwood Creek near the town of Orick (see Fig. 21 for locations). Madej will discuss the results of her sediment budget studies at the lunch stop at Redwood Creek estuary.

One of the main reasons for concern and interest in the geomorphic processes of Redwood Creek basin is the potential for disruption of the natural environment within the national park, which originally included only the old-growth forests near the downstream end of Redwood Creek. The park was expanded in 1978 to include parts of the basin upslope of the initial park boundaries. The upper two-thirds of the Redwood Creek basin, including the area we will see from Stop 1, are still in private hands. Treatment of the newly-acquired park lands, most of which were logged and had roads built on them in the 1950s, 1960s, and early to mid-1970s, is a continuing source of concern to the Park Service. In recent storms, for instance, many road fills failed in debris flows. Debris torrents moving downstream from these flows entered the old-growth areas of the park. Redwood National Park has embarked on a process of rehabilitation of the formerly logged areas, in order to protect the natural environment of the old-growth forests. Most of the rehabilitation

is concentrated on the removal of the logging road system in that portion of the park acquired in 1978. For those interested, Redwood National Park geologists will lead an informal field trip through some of the rehabilitation sites on June 22. Today, we will be shown some of the research aimed at determining what rehabilitation measures will be the most effective in preventing slope failures from previously-logged areas. This research is also leading to a better understanding of landslide processes, soil genesis, and groundwater movement in the Redwood Creek basin.

Road Log:

We plan to leave the campground at 7:30 a.m. An early, prompt start is necessary because of the amount of driving between stop 1 and Orick.

Mileage:

0.0 Highway 299 East on-ramp near West End Road. For the first 16 miles of the trip, Highway 299 runs in the north part of the Mad River Basin.

10.2 Bridge over North Fork of Mad River.

16.4 Lord Ellis Summit, 2262 ft., the divide between Mad River basin and Redwood Creek basin. Mr. Lord and Mr. Ellis were two gentlemen around the turn of the century who were instrumental in having this road built. At about the summit, the road crosses the Bald Mountain Fault, separating Franciscan melange on the southwest from Redwood Creek schist on the northeast. The southwest side of the Redwood Creek basin is formed on the Redwood Creek schist. Through much of its length, Redwood Creek parallels the Grogan Fault, which separates schists on the southwest from Franciscan Assemblage rocks on the northeast which in this area are sandstones and mudstones (see Fig. 22).

17.4 Junction Redwood Valley Road. Take a left onto Redwood Valley Road. (Highway 299 continues east into the Trinity River basin and on to the Central Valley.) We are now travelling northeast into the axis of the Redwood Creek valley.

17.65 View ahead across the Redwood Creek basin to the Minor Creek drainage and Minor Creek earthflow.

18.4 Roadcuts on the left expose the Redwood Creek schist. The schist is similar in lithology and metamorphic grade to the South Fork Mountain Schist which is the easternmost unit of the Franciscan Assemblage in much of the northern Coast Ranges. The Redwood Creek schist may be a sliver from South Fork Mountain, moved northwest along the Grogan fault (Kelsey and Hagans, 1982).

When we worked on the road log for this part of the trip in August, 1984, Redwood Valley Road, a major county road, was in terrible shape. Slope failures had removed the entire northbound lane in some places, and tension cracks and bumps were ubiquitous. While we hope that the road

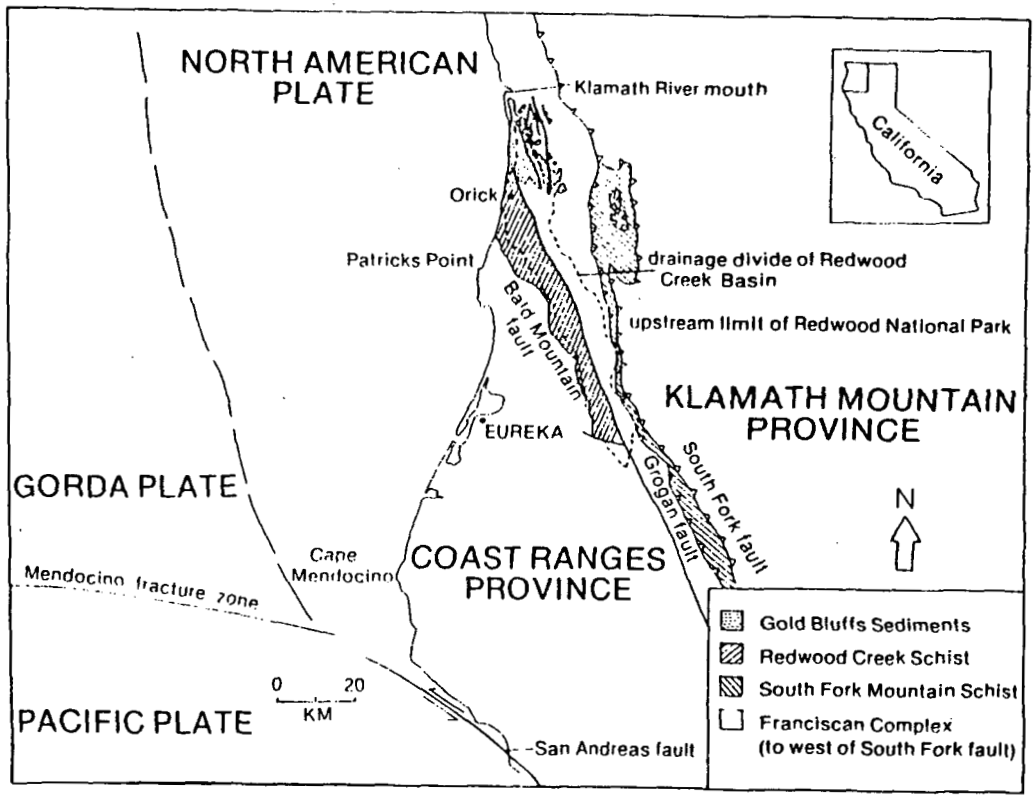

Figure 22. Generalized geologic and tectonic map of north coastal California showing major faults and rock units in the Redwood Creek drainage basin. Note that the Grogan fault separates Redwood Creek schist from Franciscan Assemblage sandstones and mudstones. From Kelsey, in press.

will be open for us on this trip, we also hope that some of the evidence of the stability problems in the Redwood Creek schist remains for you to see. This afternoon, we will have a detailed look at the soils formed on the Redwood Creek schist and the stability problems posed by those soils, which are the subject of Rick LaHusen's thesis.

20.0 View ahead to Minor Creek earthflow, our first stop.

20.8 Bridge over Redwood Creek. The bridge is near the upstream end of Redwood Valley, a mile-long alluvial valley in the middle of the Redwood Creek basin. This low-gradient, wide-channel reach separates steep-gradient, narrow reaches upstream and downstream which have a well-developed inner gorge morphology. Kelsey (in press) has proposed that the head of Redwood Valley marks the downstream end of a reach of Redwood Creek where the creek is capable of moving sediment down channel. In Redwood Valley, the channel gradient has decreased to the point where the stream can no longer transport sediment, so it has been deposited, forming the wider valley. With a reduced sediment load, Redwood Creek begins to re-incise at the downstream end of Redwood Valley, creating a second reach with inner gorge slopes (see Fig. 23).

21.25 Junction with Hoopa Road, take right. Road in this section crosses the Grogan Fault Zone within a few hundred meters of the road junction. Note the change from schist to sandstone in the road cuts.

21.7 Outcrops of sandstone indicate that road is now east of the Grogan Fault.

22.05 Chert block on right.

22.3 Road begins to traverse Minor Creek earthflow.

STOP 1 - MINOR CREEK LANDSLIDE
Park here along the north (left) side of the road and walk about 150 m upslope along the west edge of the earthflow. We will immediately convene near the upper west edge of the earthflow for a brief lecture. We will then have about 1 1/2 hours to examine the earthflow and its instrumentation.

MINOR CREEK LANDSLIDE, By R. M. Iverson

Minor Creek landslide has been monitored by the U.S. Geological Survey for the past 13 years. As part of a broad-based study of the effects of upstream sediment sources on the behavior of Redwood Creek, transverse stake lines and rain gages were installed on Minor Creek landslide and several nearby landslides in the early 1970s (e.g. Harden, et. al., 1978). During the late 1970s and early 1980s, more instrumentation was added to the monitoring network at Minor Creek landslide. This instrumentation included two flumes in which water and sediment discharges of axial gullies were measured; 15 inclinometer tubes in which subsurface deformation was measured, two continuously recording surface extensometers or "strain

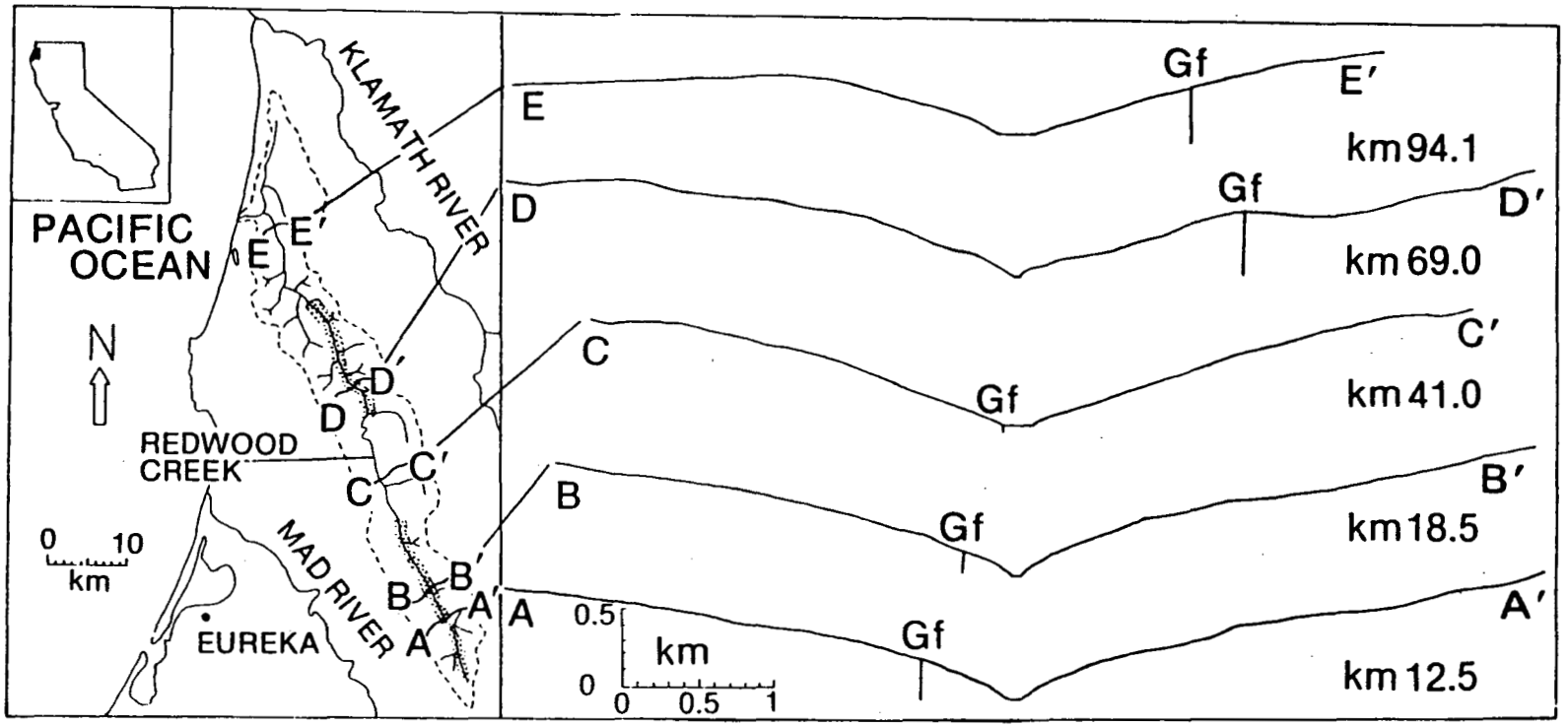

Figure 23. Topographic profiles, perpendicular to the course of Redwood Creek, drawn along interfluves between tributary basins. For each profile, the two halves represent the nearest opposing interfluves, which are offset along the creek by no more than 500 m. Map of Redwood Creek basin shows locations of the topographic profiles and the two mainstem channel reaches (stippled areas) where an inner gorge is moderately to well developed. Gf: location of Grogan fault on profile, sandstone and mudstone to east of fault and schist to west of fault. From Kelsey, in press.

gages"; 64 open standpipe piezometers; three electrical piezometers, one of which was fitted with a continuous recorder; and a longitudinal stake line that incorporated several strain rhombs. Most of this instrumentation is still in service. The density and longevity of the data collection network at Minor Creek landslide make it nearly unique among landslides that have not been modified by extensive geotechnical engineering.

The current data collection network and morphology of Minor Creek landslide are depicted on maps shown here as Figures 24, 25, and 26. These maps provide a good basis for a self-guided tour of the landslide. So that you may easily locate the mapped features, several key areas will be marked in the field. These include the west ends of the five transverse stake lines, the recording extensometer, several inclinometer tubes, and the recording electrical piezometer. Morphological features you should be certain to examine include the highly disrupted landslide toe and the discontinuous "mole tracks" of dilated soil along the landslide's lateral shear zones.

Conspicuous on the landslide surface are many stakes and standpipes. Orange stakes are members of transverse stake lines and red stakes are longitudinal-line or strain-rhomb stakes. Stakes of other colors are also present but are no longer monitored. Small-diameter, white plastic pipes are open piezometers with casing perforated at specific depths. The pipes are numbered on the outside and the perforation depths are generally written inside the pipe caps. Large-diameter, white plastic pipes contain electrical piezometer leads and air ports and green pipes and aluminum pipes are inclinometer access tubes. Most of these pipes contain water all year long. Many of the pipes have been sheared off or constricted where they pass through the base of the landslide.

The status of Minor Creek landslide data collection and analysis through June 1984 has been summarized by Iverson (1984). Several reports in press or in review as of January 1985 describe interpretation of the data and theoretical work that has been motivated by the data (Iverson, 1985 a, b, c, d, e; Nolan and Janda, 1985). Salient aspects of the data are summarized in Figures 27 through 33 shown here.

Figure 27 depicts rainfall, piezometric response, and landslide displacement data recorded at the extensometer site during two annual landslide movement cycles. These data are representative of most movement cycles and they provide many insights to the behavior of Minor Creek landslide. Particularly interesting are the remarkably steady landslide movements that follow brief annual periods of acceleration. Acceleration is motivated by gradual changes in ground-water seepage, pore pressure, and effective stress that occur during the onset of the rainy season, whereas steady motion occurs in response to a temporally steady stress state and reflects a dynamic balance between driving and resisting forces. This dynamic force balance is suggestive of a viscous component of deformation resistance, which holds major implications for understanding long-term landslide behavior.

Subsurface deformation of Minor Creek landslide has been monitored by repetitive inclinometer surveys of bore-hole casing displacement.

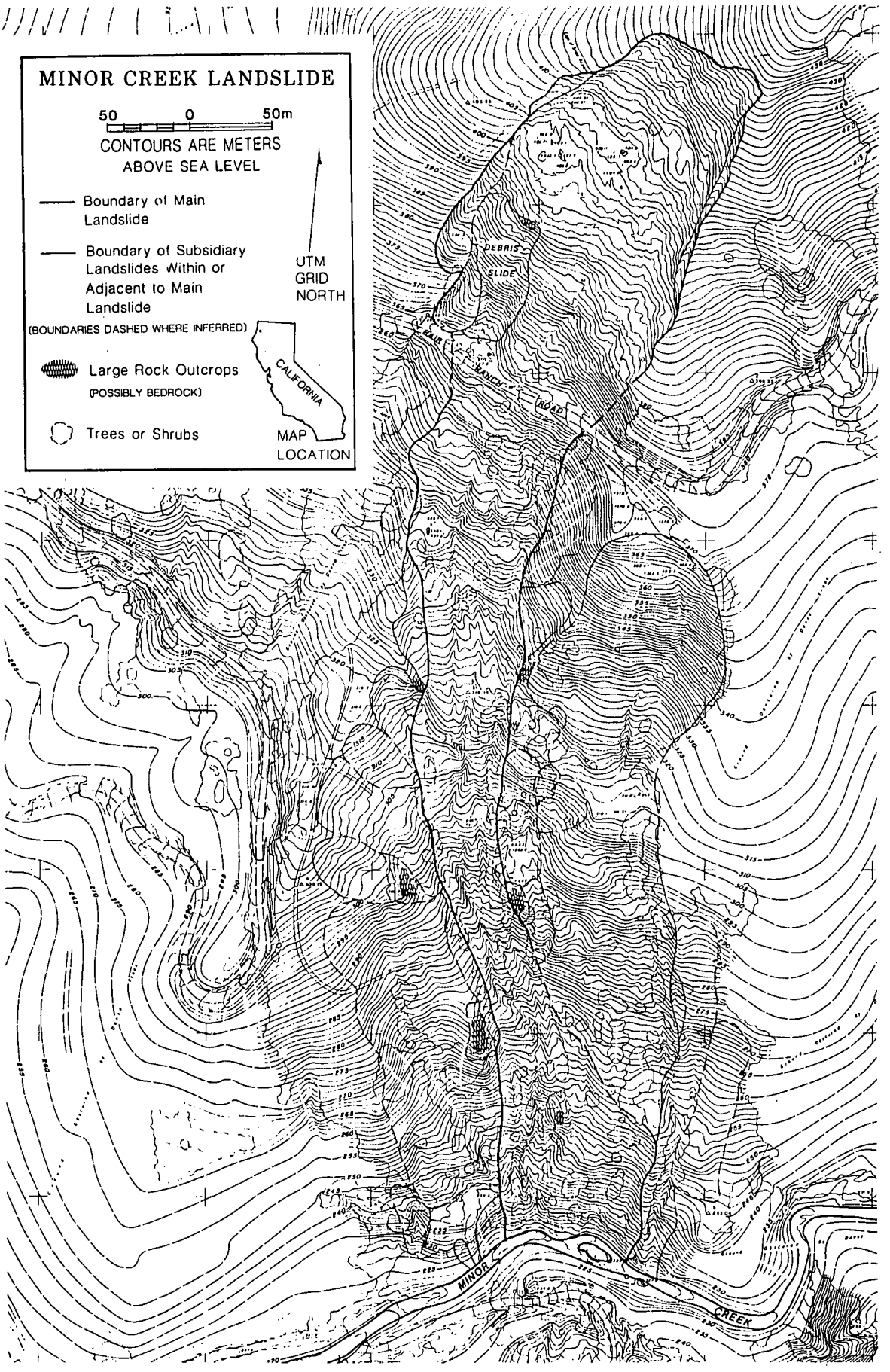

Figure 24. Topographic map of Minor Creek landslide. Photogrammetric topographic mapping was done to U.S.G.S. national mapping standards from aerial photographs taken on July 13, 1982. Morphological mapping was done in field during 1982 and 1983.

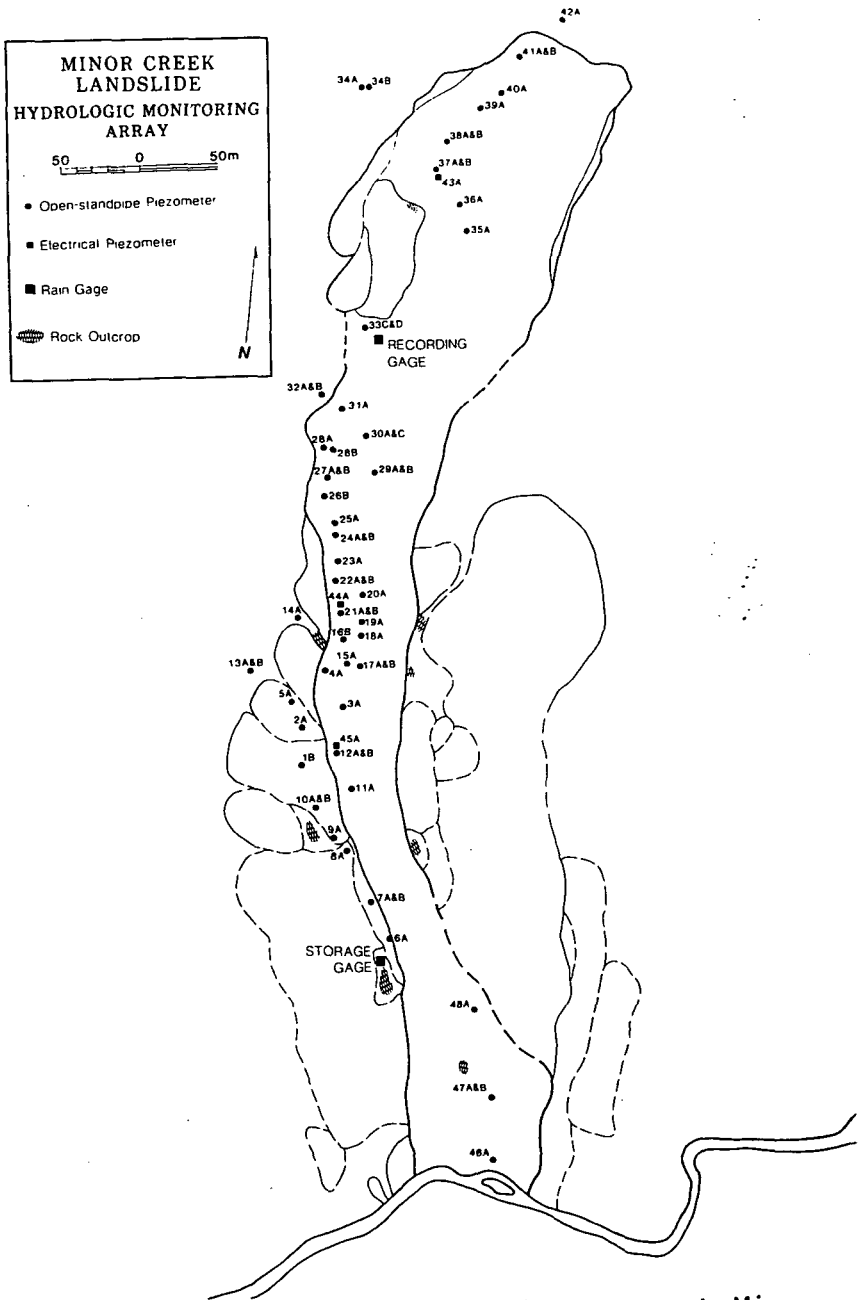

Figure 25. Hydrologic monitoring array at Minor Creek landslide, 1984.

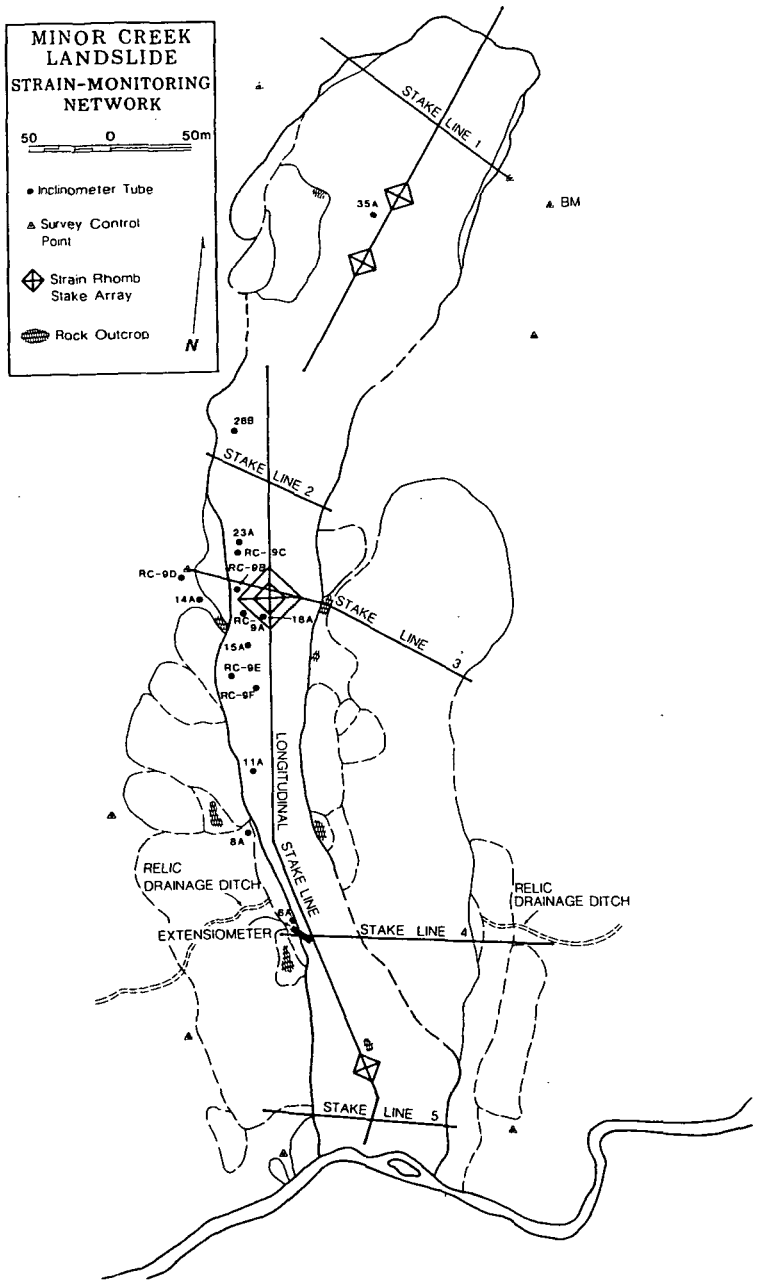

Figure 26. Strain monitoring network at Minor Creek landslide, 1984.

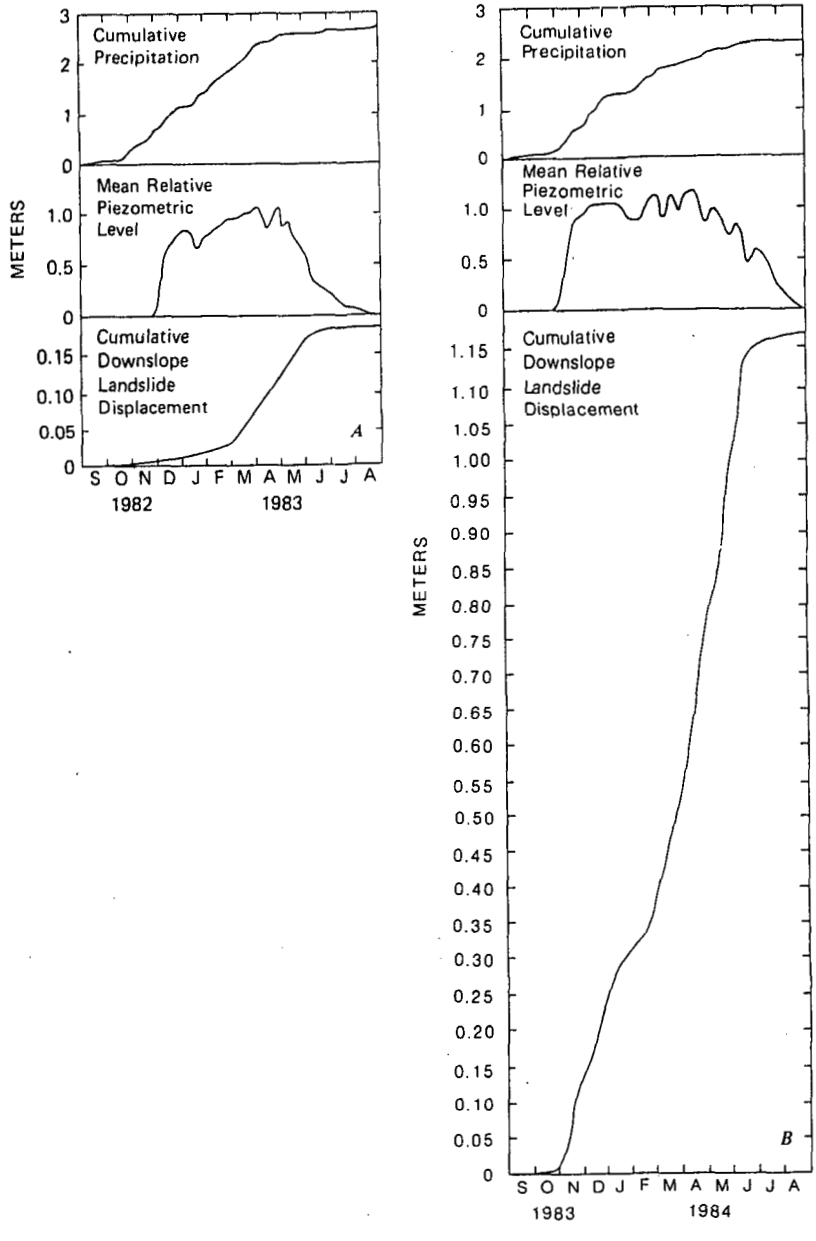

Figure 27. Temporal patterns of precipitation, piezometric response, and surface displacement at the extensiometer site, Minor Creek landslide, during two movement seasons. Piezometric levels are referenced to a datum 2.1 m below the ground surface.

Some typical vertical velocity profiles inferred from the inclinometer surveys are shown in Figure 28. These profiles show that subsurface deformation in the main body of the landslide occurs principally in a basal shear zone that averages roughly one meter in thickness and five meters in depth. Some creep deformation occurs above the basal shear zone, both in the main landslide and outside its margins. Sampling, inspection, and testing of the shear zone material shows that it differs little from the surrounding material. The lack of distinctive shear zone material and the shape of the landslide velocity profiles are both consistent with viscoplastic or pseudoplastic continuum material behavior.

Figures 29, 30, and 31 depict the surficial components of landslide displacement measured at transverse stake lines 1, 3, and 5 from the time of their installation (1973 or 1974) through April, 1984. An intriguing aspect of the displacement patterns shown in Figures 29, 30, and 31 is that the timing and amount of displacement varies along the length of the landslide. The upper portion of the landslide moved rather slowly and steadily for ten years (Fig. 29), while midslope portions of the landslide underwent movement pulses during the 1973-1974 and 1983-1984 seasons (Fig. 30). The toe of the landslide, in contrast, accelerated dramatically throughout the early 1980's, with very large displacements that culminated in 1982-1983 (Figure 31). These large displacements were catalyzed by transient undercutting of the landslide toe by Minor Creek. It appears clear, therefore, that the landslide does not translate downslope as a rigid body. Instead, different parts of the landslide respond to a variety of impetuses at different rates and different times.

Further evidence of the nonuniform motion of Minor Creek landslide is depicted in Figure 32 which shows the distribution of strain measured along the longitudinal stake line during 1982-1983 and 1983-1984. In response to the culmination of landslide toe undercutting by Minor Creek, very large extensional strains occurred near the toe in 1982-1983.

The overall movement pattern of Minor Creek landslide is summarized in Figure 33. This figure illustrates the spatial distribution of downslope sediment flux through Minor Creek landslide during the movement cycles of 1981-1982, 1982-1983, and 1983-1984. Sediment fluxes were calculated from stake-line data, inclinometer data, and field mapping data, and they may be in error by as much as 50%. Despite this considerable potential for error, Figure 33 clearly shows that major disparities exist between sediment fluxes in different portions of the landslide. These disparities appear to result from transient, nonuniform loading phenomena like fluvial undercutting of the landslide toe and spatially varied ground-water flow. Responses of the landslide to such phenomena are strongly time- and space-dependent. This reinforces the idea that Minor Creek landslide, and probably many other landslides, cannot be viewed as classic Coulomb sliding bodies. Instead, a complex suite of viscous and plastic rheological components must be considered in assessing landslide behavior.

From this vantage point, the inner gorge slopes in the upstream part of Redwood Creek basin can be seen. Project the long, visible slopes

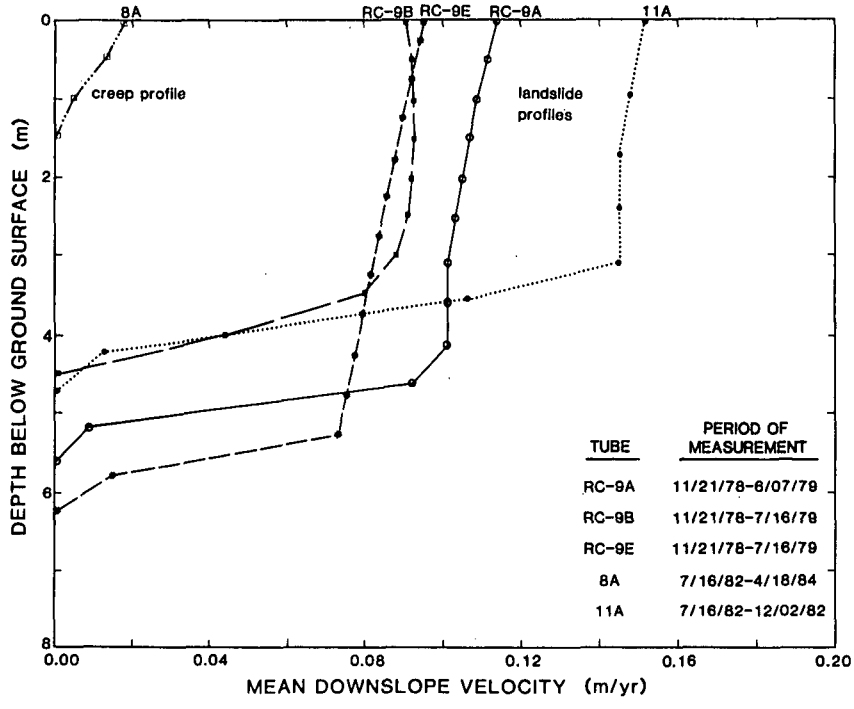

Figure 28. Representative vertical velocity profiles inferred from repetitive inclinometer surveys of bore-hole casing displacement, Minor Creek landslide.

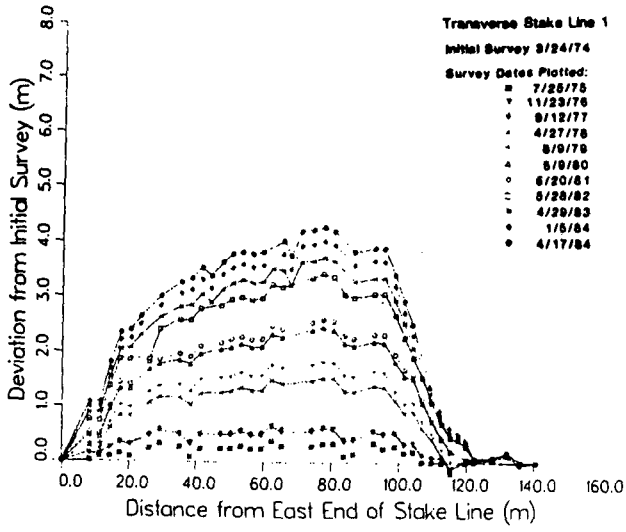

Figure 29. Surveyed displacements of transverse stake line 1, Minor Creek landslide.

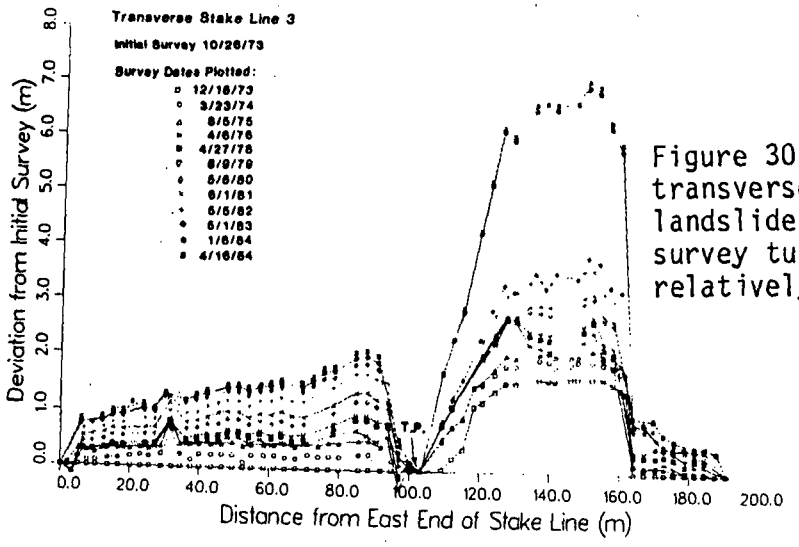

Figure 30. Surveyed displacements of transverse stake line 3, Minor Creek landslide. The point marked "T.P." is a survey turning point situated on a relatively stable rock outcrop.

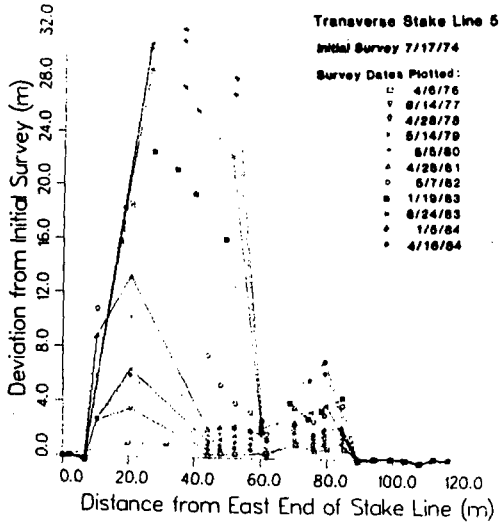

Figure 31. Surveyed displacements of transverse stake line 5, Minor Creek landslide.

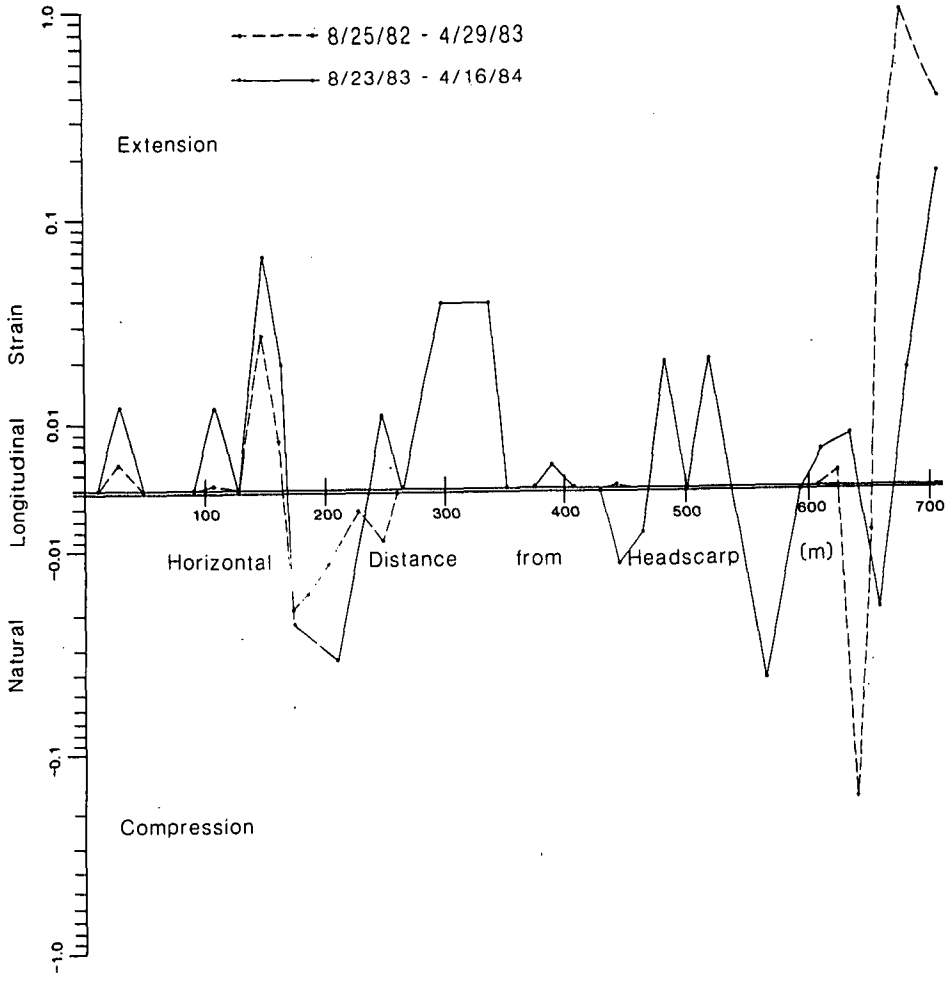

Figure 32. Distribution of measure longitudinal strains along the longitudinal stake line, Minor Creek landslide. Strains smaller than 0.005 are not plotted because strain measurement errors could be as large as 0.005.

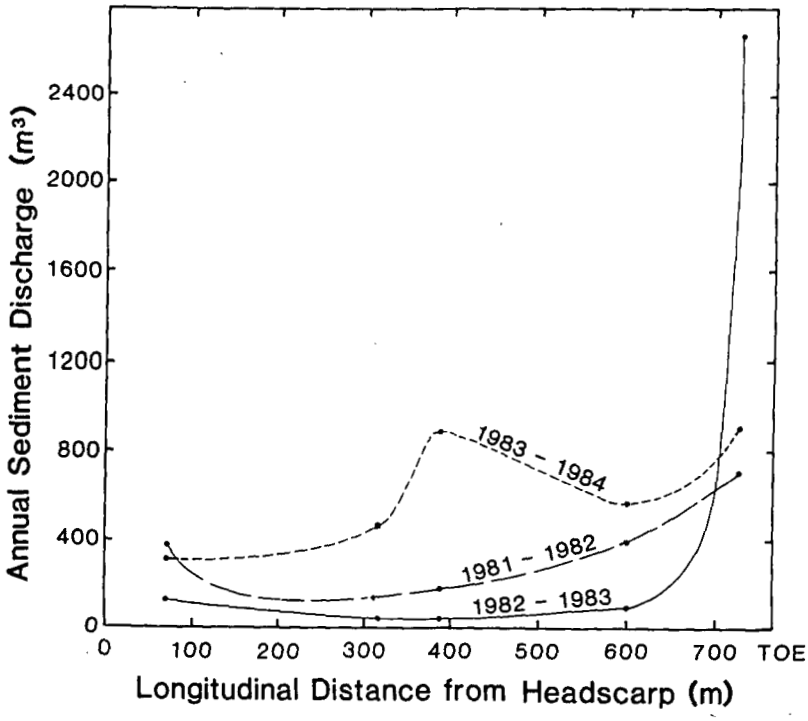

Figure 33. Spatial distribution of downslope sediment flux through Minor Creek landslide during three movement seasons.

toward each other and note that they intersect in the air, above the stream channel. Inner gorge slopes are formed below this point of intersection and can be just barely seen from this view (Fig. 34). Some of the inner gorge slopes visible from here are sites of debris slides: this is presumably the major process that forms such slopes.

The term "inner gorge" was first used by Clarence E. Dutton (1882) in his descriptions of the Grand Canyon. Francois Matthes (1930) applied the term to slopes above Yosemite Valley and the term has been subsequently applied to slopes in north coastal drainage basins in California by Farrington and Savina (1977), and Furbish and Rice (1983). In an inner gorge, slopes directly adjacent to the channel are steeper than those further up the hillslope. A clearly defined break-in-slope separates the steeper inner gorge slopes from the more moderate, higher hillslopes. Inner gorge slopes do not appear to have one common angle, and slope steepness probably depends in large part on the underlying rock type. A full account of the morphology and genesis of inner gorge slopes in the Redwood Creek basin is given by Kelsey (in press).

We plan to leave Stop 1 at 10:30 a.m. Retrace route to west end of Highway 299.

46.2 Junction 299 and Highway 101. Take 101 North. For the next 1.4 miles the highway crosses alluvial flats at the mouth of the Mad River.

47.6 Mad River crossing. See yesterday's road log for the story of this river's elegant name. The lowermost Mad River flows in a structural trough. On the north side of the valley is graywacke brought up along a reverse fault. The Mad River trough formed on the downthrown side of one of a series of tilted blocks produced by reverse faulting in the Mad River Fault Zone (see road log for third day).

49.3 School Rd. Exit. The flat surface along which we have been travelling is a marine terrace surface called Dows Prairie. Both the Arcata Airport and McKinleyville lie on this surface. They are separated by a northwest trending scarp that proved, on trenching, to be produced by a high-angle reverse fault. This fault is the northernmost of seven reverse faults between here and central Arcata, which together comprise the Mad River Fault Zone (Carver, et. al., 1983). We will see an exposure of one of these faults on the third day of the conference.

The town of McKinleyville was first called Dows Prairie, then Minorville, after one Isaac Minor, who founded the town. Minor changed the town's name to McKinleyville after the 1901 assassination of the president. Minor's name is still applied to the Minor Creek, the tributary of Redwood Creek that we visited earlier today.

51.7 At Arcata Airport exit, look east (right) to see a Holocene fault scarp (not to be confused with the airport runway, just to the northwest). Until recent work (Woodward-Clyde consultants, 1980) established that this and similar scarps were indeed tectonic, most people believed that they were marine terrace scarps.

A

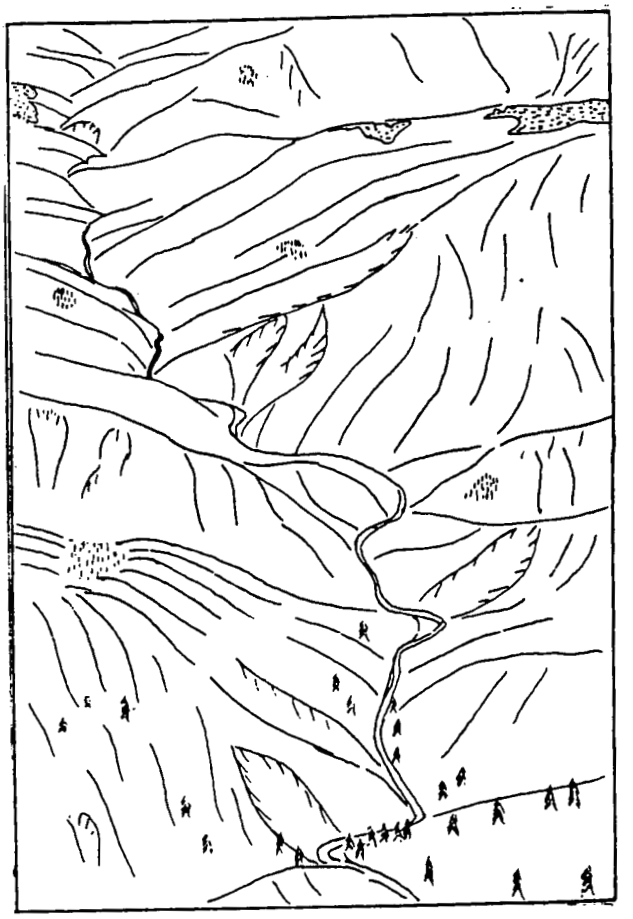

B

Figure 34. Oblique aerial photo (A) and accompanying sketch based on the photo (B) looking upstream at a 12 km reach of the Redwood Creek basin in the upper third of the watershed. The inner gorge is well developed along this reach of Redwood Creek.

From here, the road descends from the marine terrace to Clam Beach. Trinidad Head, visible ahead to the west, is underlain by an intrusive complex of diorite, keratophyre, tonalite, etc. It is a block in the Franciscan melange. Trinidad Head is attached to the mainland by a marine terrace. Sea stacks on the modern marine platform are visible south of Trinidad Head. Between Trinidad Head and Patricks Point, the coast is formed on Franciscan melange with at least seven distinct terrace levels rising to the east inland. These terraces have been warped into an east-west trending anticline (see Figs. 35 and 36, from Stephens, 1982). Both the heavy vegetation and the fact that the highway was constructed without attention to geologic points of interest make it impossible to discern the terrace steps from the road.

53.9 Highway is constructed across Holocene dunes in Clam Beach, visible on the west side of the road.

55.1 Vegetated dunes are visible to the west near the Crannell Road exit. Most dunes trend northwest and formed in response to winter winds from the southwest.

55.2 Little River crossing

56.1 Melange and Crannell dune sands are exposed in roadcuts along highway. Relief visible from road is produced by the marine terrace scarps, but pattern of scarps is obscured.

58.8 Trinidad exit. Trinidad is the oldest town in the Humboldt Bay area. It was used as a harbor until Humboldt Bay was rediscovered, and was even incorporated as the county seat of "Klamath County." However, soon after the rediscovery of Humboldt Bay, the bulk of shipping and commerce moved south and Trinidad was all but abandoned.

59.3 Sea stacks have been preserved on some of the old terraces, now uplifted above sea level. One such stack is Strawberry Rock, composed of greenstone, which can be seen to the east.

64.1 Patricks Point turnoff. Patricks Point State Park is on the lowest marine terrace and contains a number of preserved sea stacks.

64.6 Sands in roadcuts. The magnitude of Quaternary deformation in this area is well illustrated by the fact that the marine terrace the road is built on here is about 100 to 150 m high and tilts down to sea level in the next few miles. Unconformities within the terrace deposits show the progress of the tilting.

65.9 Big Lagoon exit. Big Lagoon is almost totally unaltered except for the causeway built for Highway 101. During most winters, the lagoon fills and the spit breaches one to four times, depending on the runoff from Maple Creek. Most of the breaches occur at the north end of the spit. When the spit breaches, the lagoon empties in less than one day and the breach remains open anywhere from a day to a week before winter waves rebuild a berm across the breach. Stone Lagoon to the north behaves in the same way, but its spit does not breach as often because of the smaller drainage

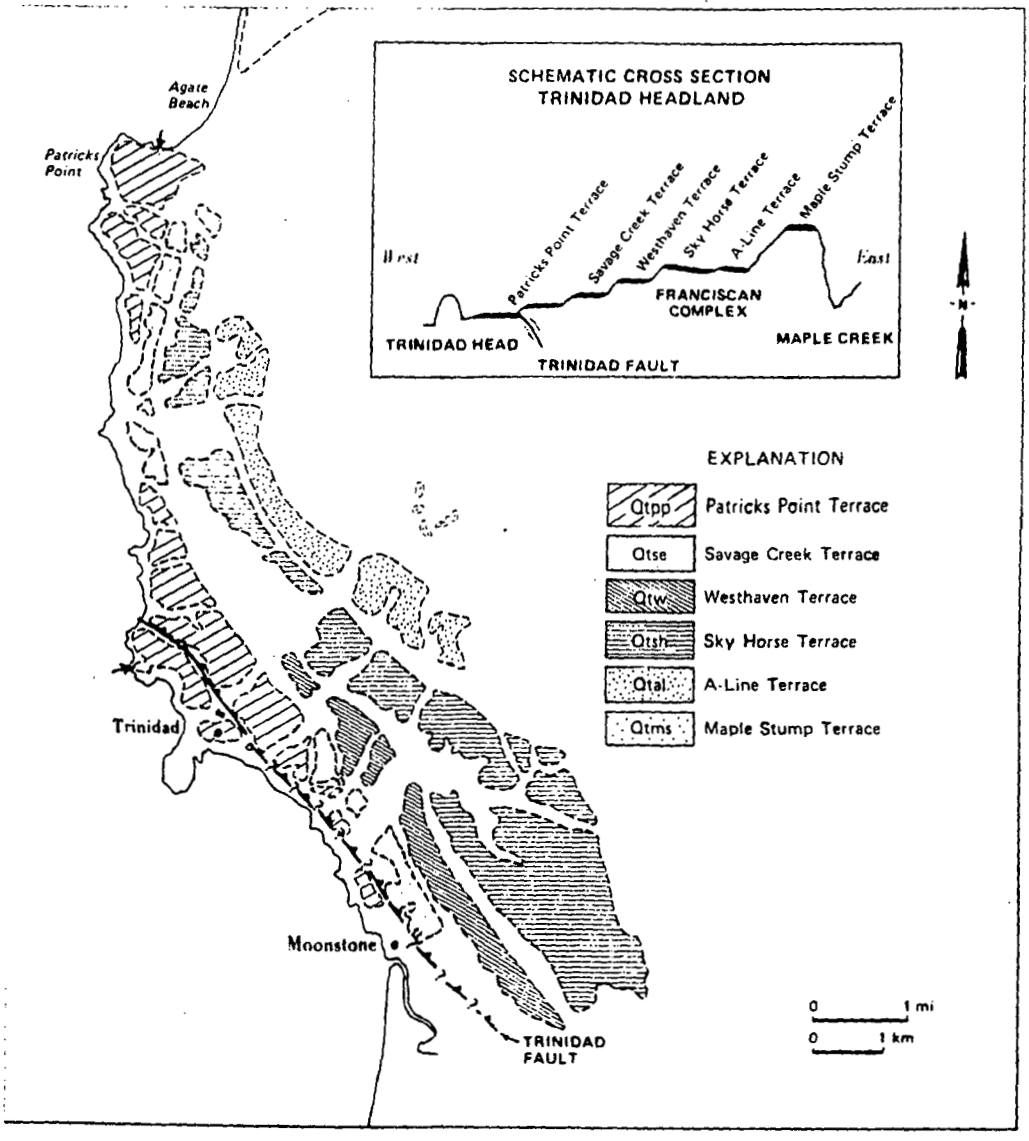

Figure 35. Map of Late Quaternary marine terraces on the Trinidad Headlands. From Stephens, 1982.

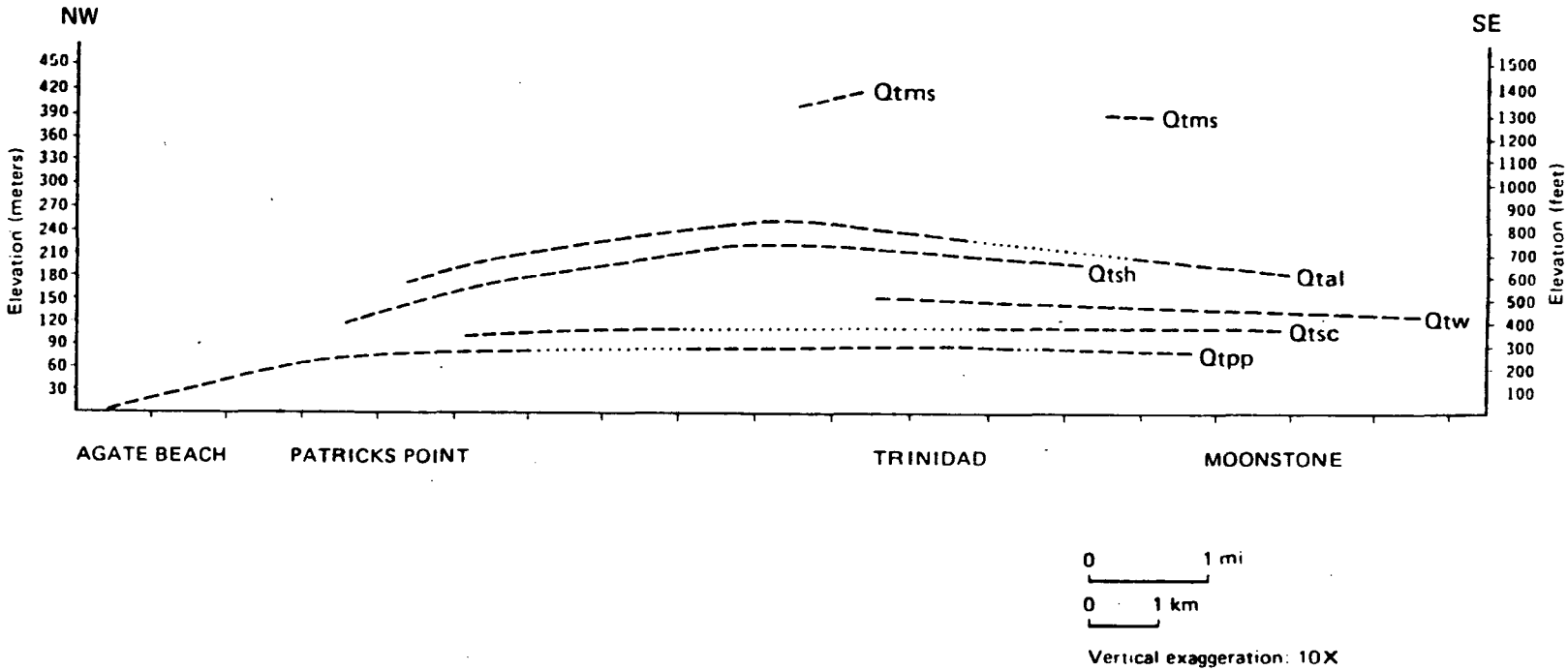

Figure 36. Longitudinal profiles of marine terraces on the Trinidad Headlands. From Stephens, 1982.

basin supplying the lagoon with water. Big Lagoon apparently formed within a structural depression similar to the one at the lower end of the Mad River. The controlling structure is the Big Lagoon Fault, a high angle reverse fault that offsets Neogene sediments that blanket the Franciscan melange to the east of Big Lagoon. The Big Lagoon Fault parallels the northwest side of the lagoon.

66.2 Freeway ends. The road in this area follows the trace of the Big Lagoon Fault. The 1981 earthquake, centered offshore, caused sand volcanoes and other liquefaction features along the lagoon side of the Big Lagoon spit.

70.3 Divided highway begins.

71.4 You may be able to catch a glimpse of Dry Lagoon to the west (left).

71.7 End of divided highway.

73.4 At about this place, the highway crosses the Bald Mountain Fault, separating Franciscan melange on the south from Redwood Creek schist on the north.

73.9 Stone Lagoon to west.

76.2 Highway traverses spit of Freshwater Lagoon. The lagoon has a very small drainage area. Even before the highway was built across the Freshwater Lagoon spit, the spit almost never breached, which probably accounts for the name of the lagoon.

76.6 New visitors center, Redwood National Park, at south end of Redwood Creek beach.

78.5 Road crosses lower Redwood Creek. Note levees along both sides of the Creek. The levees extend from the mouth of the creek to the head of the bottom lands approximately four km upstream.

We are entering the town of Orick, which used to be supported exclusively by logging until the creation of the National Park. Now, tourism is one of the major sources of income. All of the forested hillslope land visible from the road is within Redwood National Park, but the bottomlands occupied by the town of Orick and the prairies to the northwest are entirely privately owned.

78.6 Left turn onto road marked "Coastal Access". Follow fishing signs to parking at estuary. Note that the last downstream meander of Redwood Creek was bypassed during channelization.

80.5 STOP 2 - MOUTH OF REDWOOD CREEK - LUNCH STOP
Figure 37 shows the location of the afternoon stops.
Before lunch, Cindy Ricks will discuss the dynamics of the Redwood Creek estuary, including the effects of the levees on sediment transport and deposition in lower Redwood Creek and the estuary.

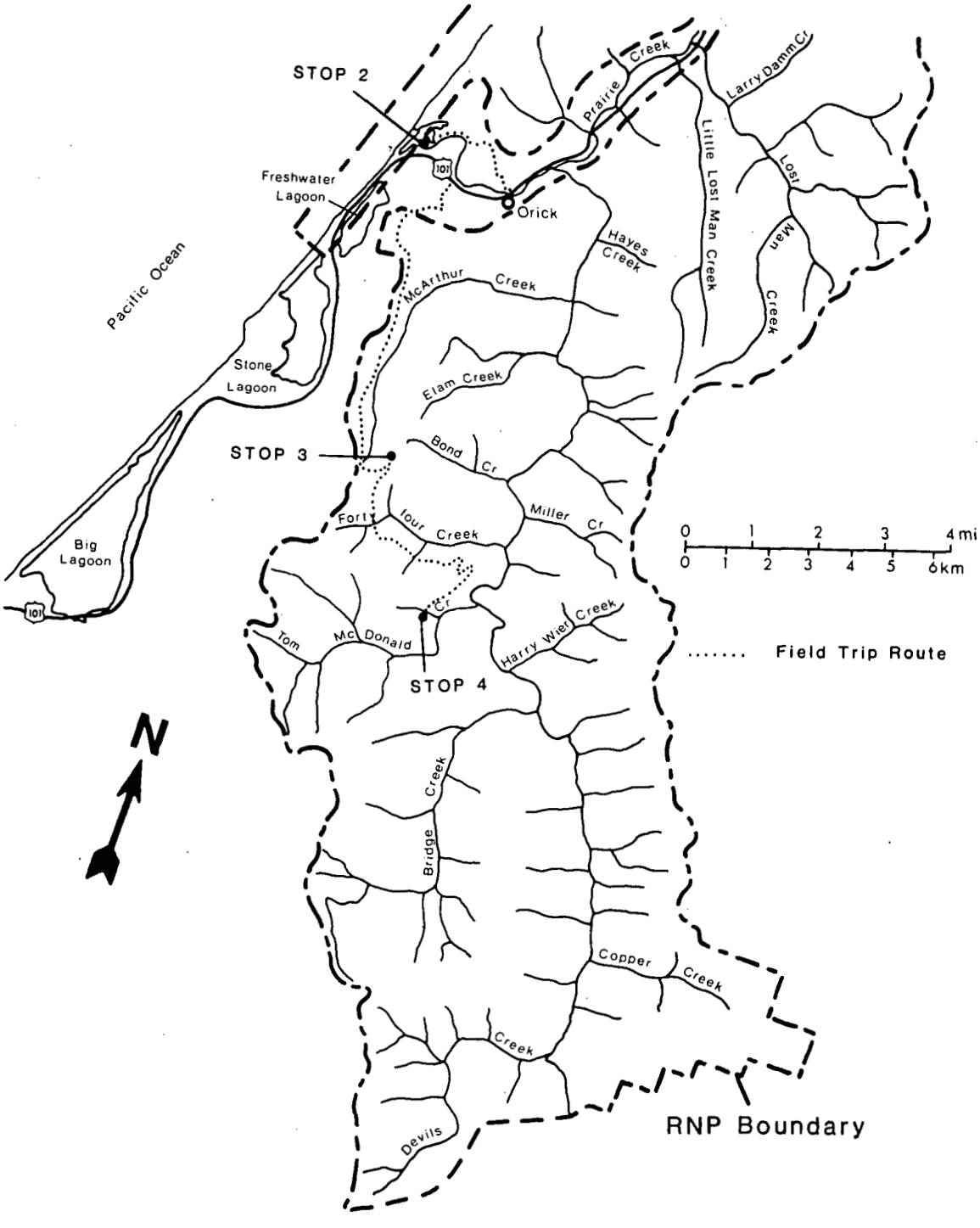

Figure 37. Map of the lower Redwood Creek basin showing location of field trip route and stops within Redwood National Park.

I. REDWOOD CREEK ESTUARY, By Cynthia Ricks

Since the early 1950s, the distribution of sediment at the mouth of Redwood Creek has been altered by the effects of channel aggradation and channelization along the lower reach. Severe flooding in 1953, 1955, and 1964 caused bank erosion, landsliding, and channel geometry changes along Redwood Creek. The increased sediment load resulted in channel aggradation and widening along the lower floodplain (see Fig. 38). Prior to 1966, floods scoured the north slough, middle slough, and main channel, thus maintaining a hole adjacent to the north cliffs at least 20 feet deep. The December 1964 flood scoured the entire beach from the north cliffs south to the former Cal-Pacific Mill site. Floods generally deposited material across the floodplain from the confluence with Prairie Creek to the middle island. Flood damage in the town of Orick prompted channelization of Redwood Creek in 1966-1968. The distribution of erosional and depositional sites at the mouth has been more drastically altered by the effects of channelization than of aggradation.

As we drive along the south levee toward the mouth of Redwood Creek, note the last downstream meander which was bypassed and isolated from the main channel of Redwood Creek during channelization. Channelization was accompanied by removal of bed roughness elements, shaping a trapezoidal channel with an increased hydraulic radius, and steepening the channel gradient. This caused an increase in the mean velocity and frequency of mobilization of the substrate between the levees. With streamflow confined between the levees, sediments deposited in the last downstream meander (south slough) and north slough are no longer flushed from the mouth of Redwood Creek. Since 1966, 47 to 54 percent of the lower estuary (between zero and four feet above mean sea level) has filled with sediment or become isolated from the embayment (see Figures 39 and 40).

Sediment yield of Redwood Creek is among the highest for a basin of its size in North America, but under present conditions fluvial sediment is not accumulating at the mouth. Heavy mineral and textural data indicate that during high to moderate streamflow, sand- and gravel-sized sediment is flushed through the embayment. Overwash across the storm berm and tidal current transport are the dominant processes of deposition in the sloughs, delivering marine sediment to the estuary.

Sediment accumulation has also altered the seasonal sequence of migration and closure of the outflow channel which determines the embayment water volume, substrate distribution, and water quality during the low flow period from spring to early fall. Since the volume of water subject to tidal fluctuations (tidal prism) has decreased, the ebb tide current velocity has also decreased, resulting in earlier migration and closure of the outflow channel. When the rates of outflow, seepage, and evaporation do not exceed the stream discharge, the embayment expands, becoming connected with the productive north and south sloughs (Figure 41). More frequent closure and flooding of backwater areas and adjacent pastures has historically led to artificial breaching of the berm. In the past, such premature breaching released 75 percent of the embayed water volume being used by 20,000 juvenile salmonids for summer rearing habitat.

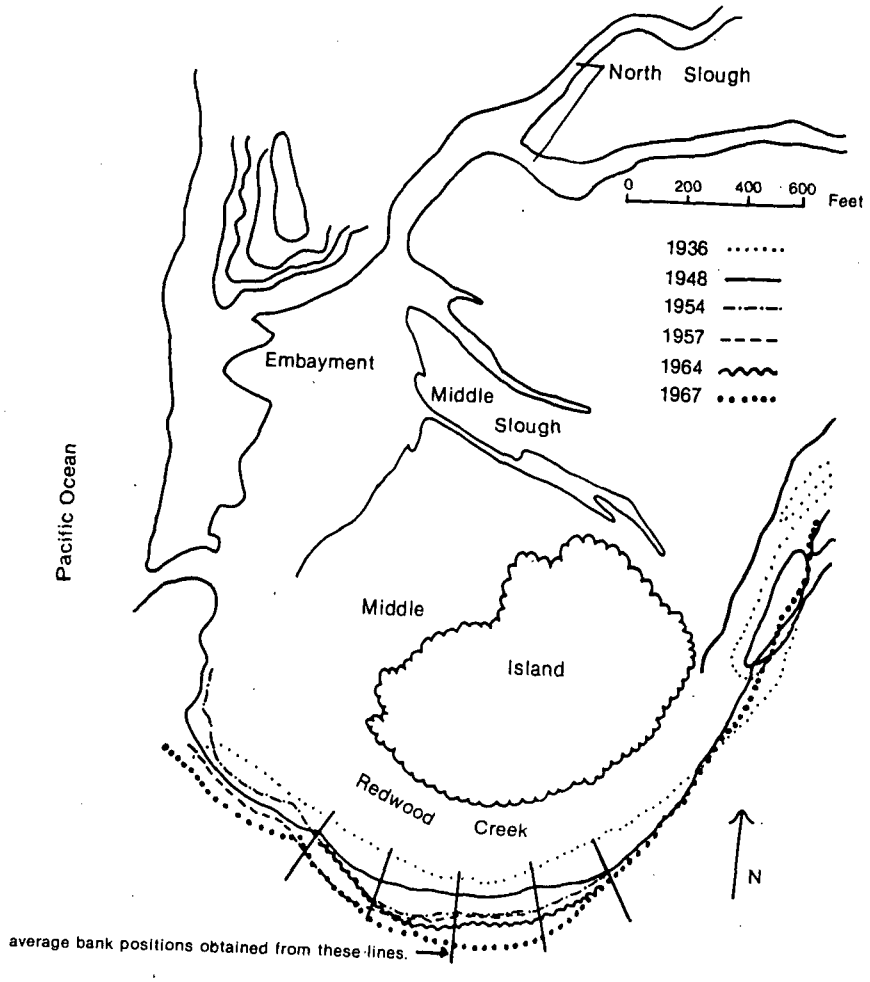

Figure 38. Bank positions along the last downstream meander of Redwood Creek, 1936-1967. Figure from Ricks, in press.

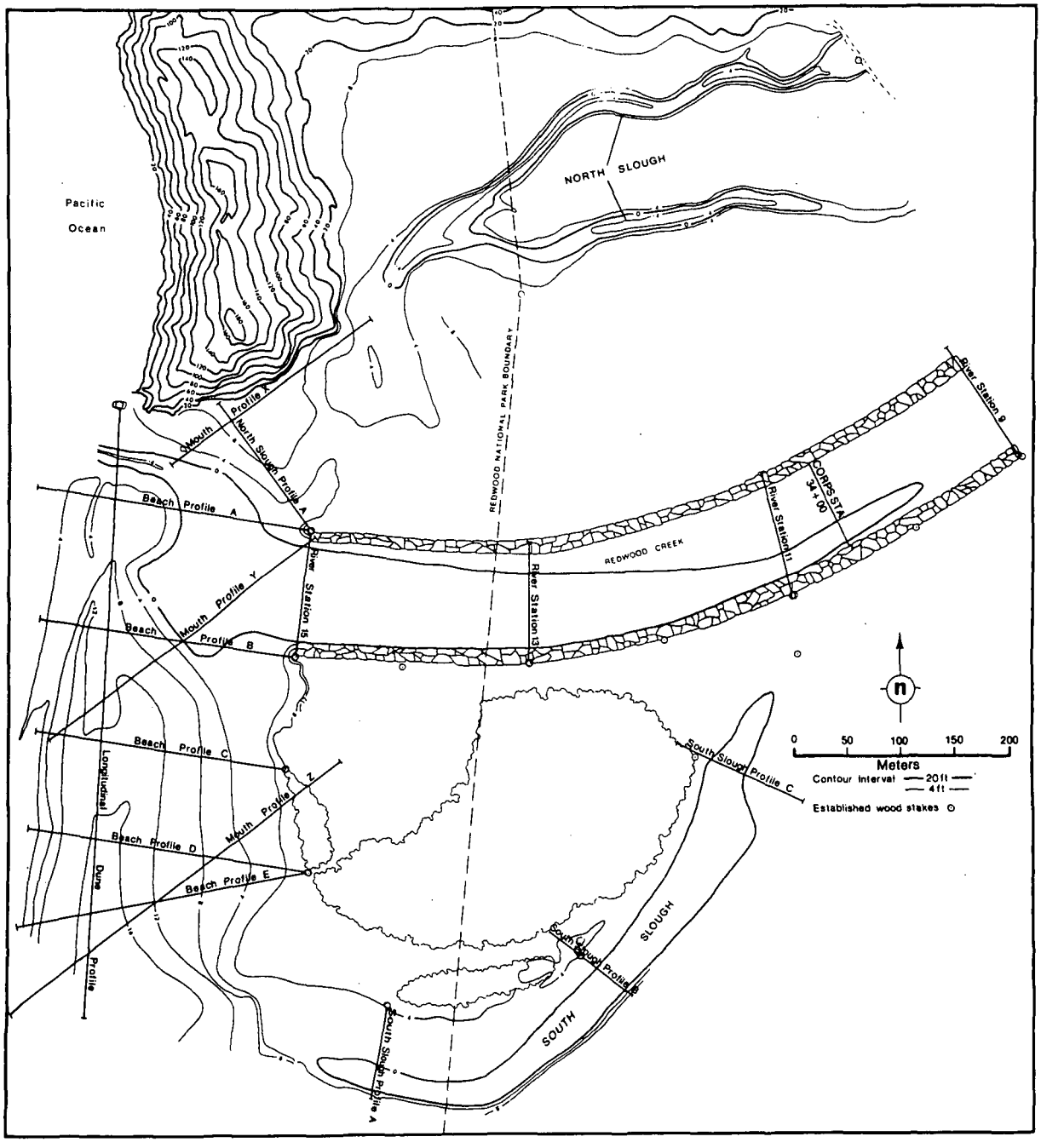

Figure 39. Profile locations for cross-sections at the mouth of Redwood Creek. Figure from Ricks, in press.

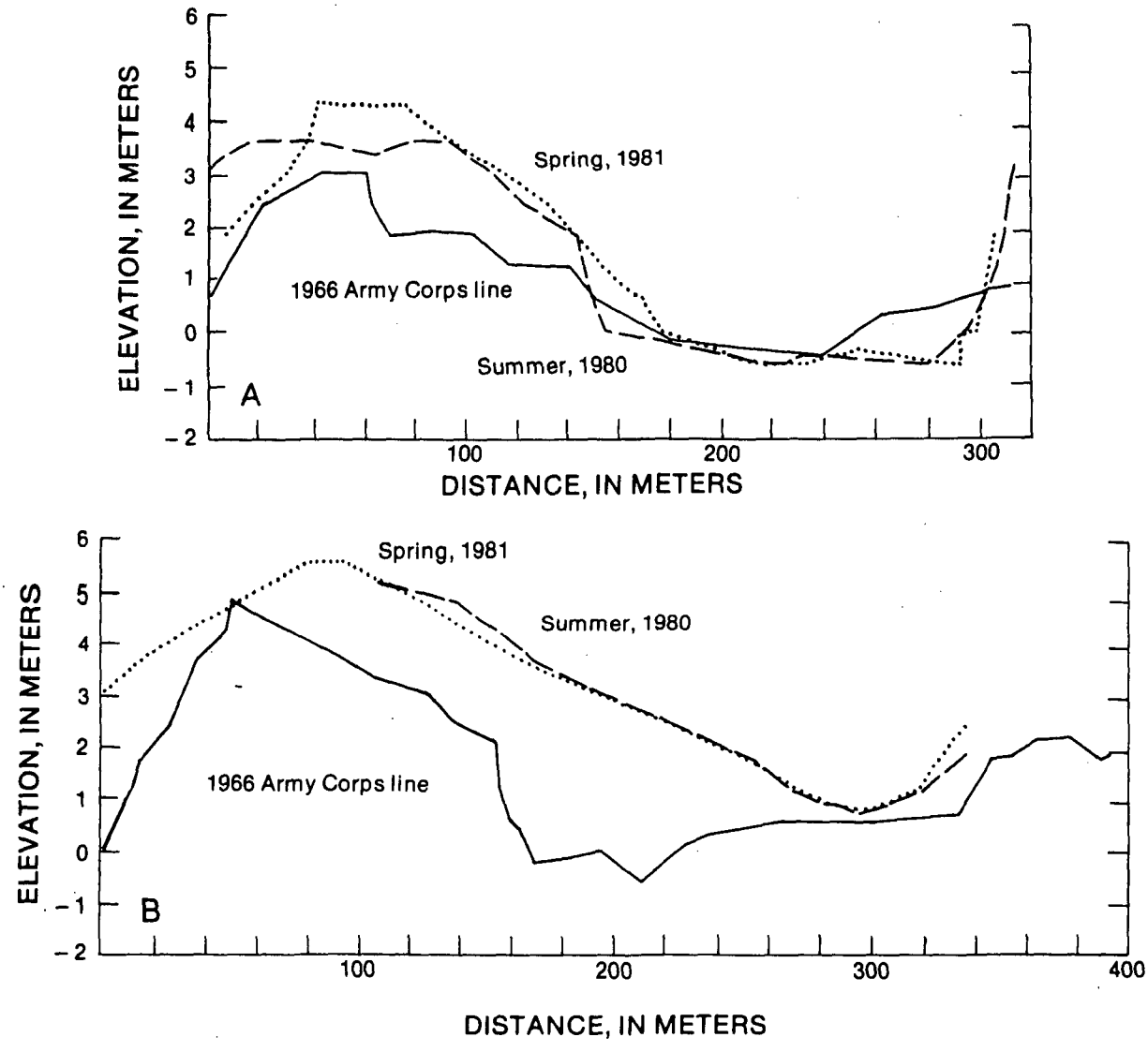

Figure 40. Topographic profiles across the mouth of Redwood Creek. Both profiles run from SW to NE across the longitudinal dune into the embayment. Top (A), mouth profile Y. Bottom (B), mouth profile Z. Profile locations on Figure 39. Figure from Ricks, in press.

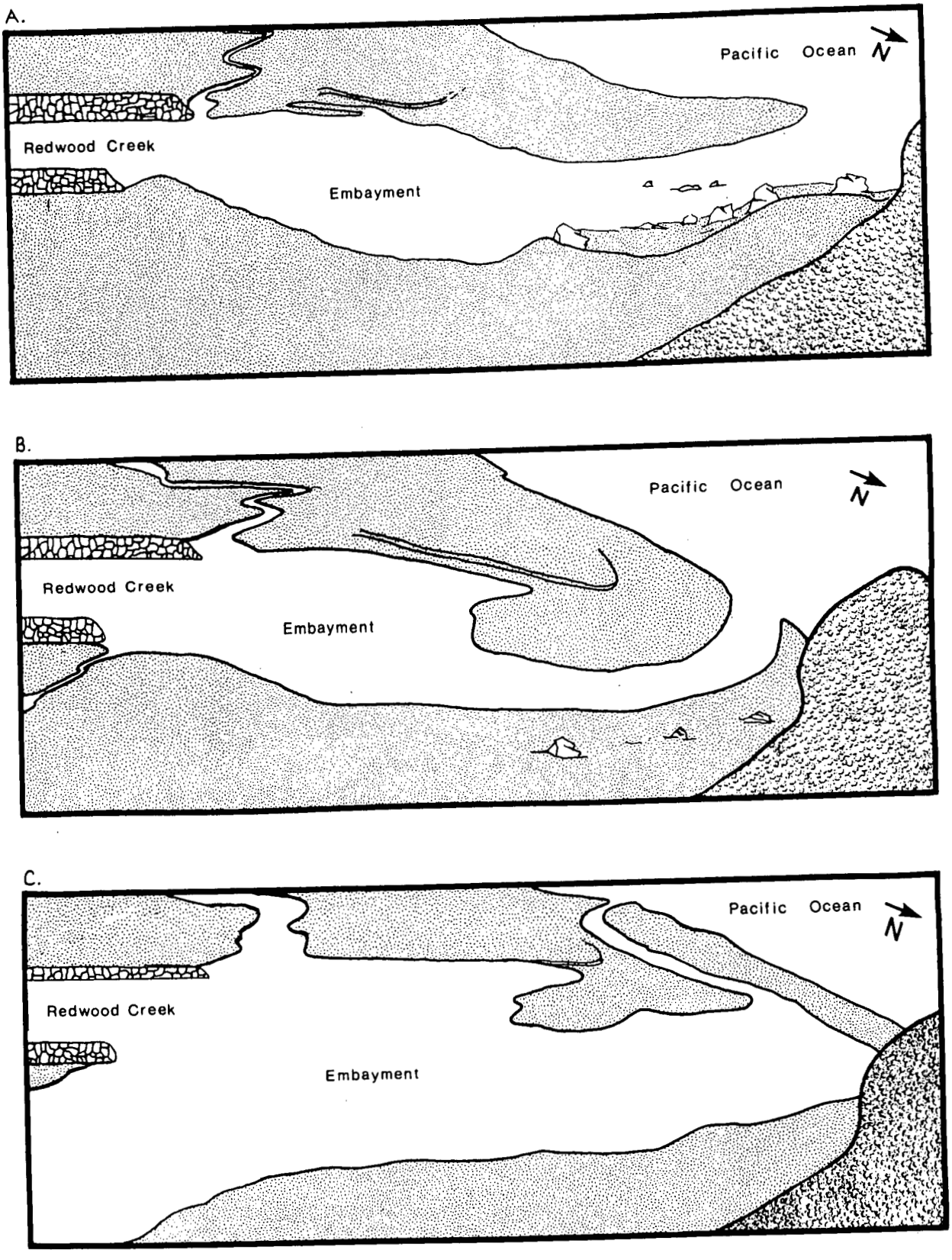

Figure 41. Mouth of Redwood Creek: oblique views from the top of the north cliffs looking to the south. A, January 12, 1980. B, April 19, 1980. C, June 14, 1980. Figure from Ricks, in press.

II. MAGNITUDE AND DYNAMICS OF SEDIMENT STORAGE IN REDWOOD CREEK (From Madej, 1984)

We have now seen Redwood Creek at a mid-basin location (the upper end of Redwood Valley) and we have seen the Redwood Creek channel in its lowermost reaches at the channelized estuary. Mary Ann Madej, geologist for Redwood National Park, has conducted extensive studies of the magnitude and dynamics of sediment storage along the 105 km long main channel of Redwood Creek and will discuss results of this investigation during the lunch stop. The following paragraphs are edited from Madej, 1984.

Storage of alluvium in the mainstem of Redwood Creek was quantified for three time periods spanning 35 years, 1947, 1964 (post-flood), and 1980. An unusual amount of aggradation occurred during the December 1964 flood (a 50-year flood), increasing the total volume of sediment stored on the valley floor by almost 1.5 times to 16×10^6 m^3. High landslide activity during the 1964 flood contributed to 5.25×10^6 m^3 to the mainstream of Redwood Creek, and channel storage increased by 4.74×10^6 m^3. Fig. 42 shows cumulative landslide input to the mainstem and deposition in the channel resulting from the December 1964 flood. Moderate to high flood flows (2 to 20 year recurrence intervals) following 1964 eroded sediment in the upper basin and redeposited it in downstream reaches. In addition, floods in 1972 and 1975 deposited sediment in downstream reaches. As a result, there was little change in the total sediment on the valley floor. This migration of a slug of sediment down Redwood Creek was easy to follow on successive resurveys of channel cross-sections along the main channel. Figure 43 shows three cross-sections from representative reaches of Redwood Creek. Cross-section 40 is located in the upper basin and shows the increase in channel bed elevation in the 1960s and a subsequent decrease to almost the 1953 level. Downcutting through sediments deposited in 1970 occurred at cross-section 25, but aggradation is still occurring near the mouth, at cross-section 6. Because of the relatively simple, elongate basin geometry of Redwood Creek compared to the Van Duzen basin, downstream movement of the locus of aggradation was straightforward in Redwood Creek, but complex in the Van Duzen River.

Presently, sediment is stored in several geomorphic compartments, and some compartments (such as recent gravel flood terraces, debris jams, stable alluvial terraces and strath terraces) are only found in particular reaches of Redwood Creek. Boundaries of the upper, middle, and lower reaches are shown in Figure 44. Figure 45 is a longitudinal profile of Redwood Creek showing the distribution of localized sediment compartments. Potential mobility of sediment stored in Redwood Creek was characterized as active, semi-active, inactive and stable, depending on its distance from and height above the thalweg, and the age and type of vegetation on the deposit. Fig. 46 a, b is a schematic cross section and plan view of these four types of sediment reservoirs in Redwood Creek.

To identify active sediment in the channel bed, the amount of scour and fill occurring during various flows was determined through scour chains and discharge measurement notes. In this gravel-bedded stream, depth of

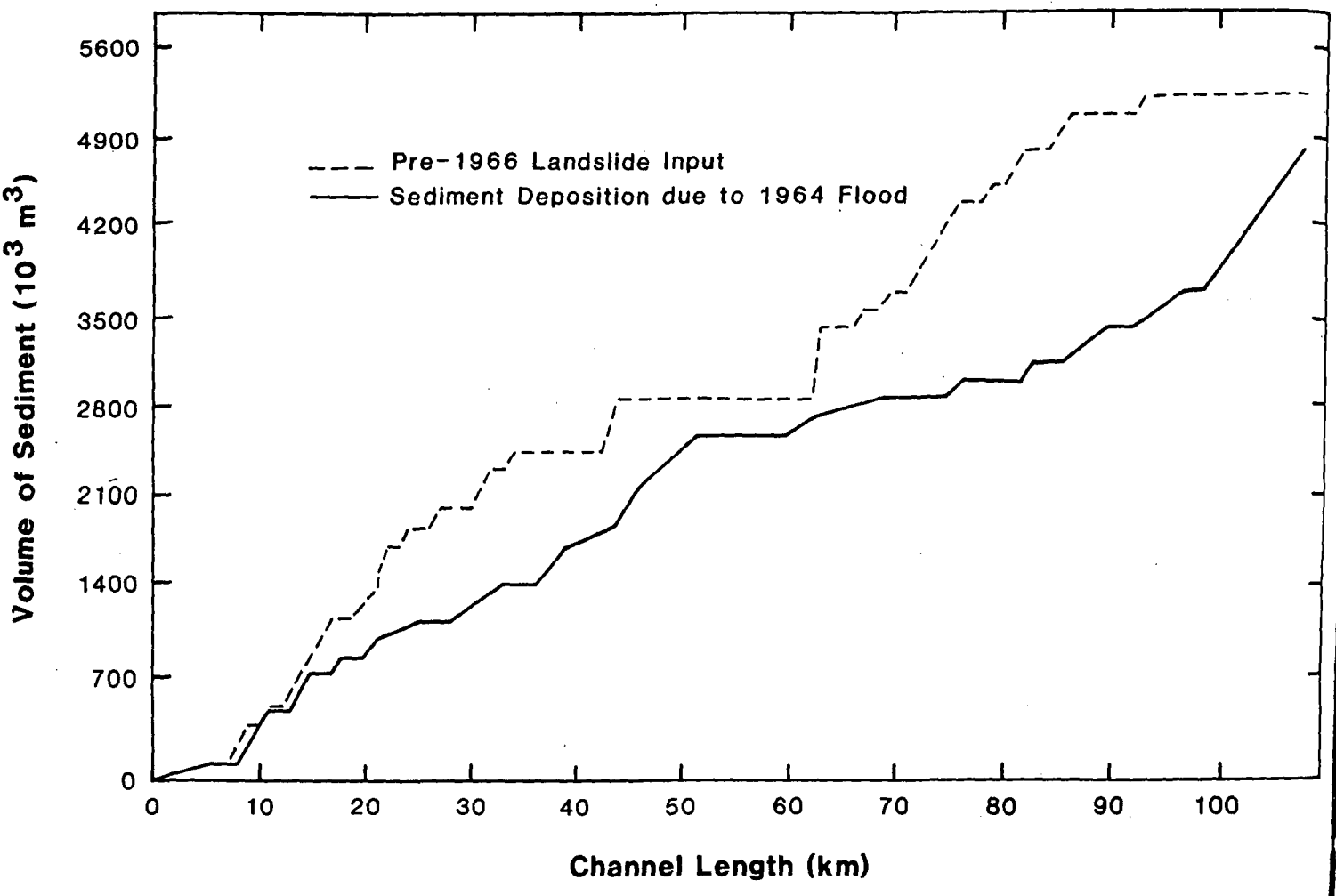

Figure 42. Cumulative volumes of total landslide input to the mainstem of Redwood Creek and the deposition in Redwood Creek resulting from the December 1964 flood. Landslide data are from Kelsey and others (in press). Figure from Madej, 1984.

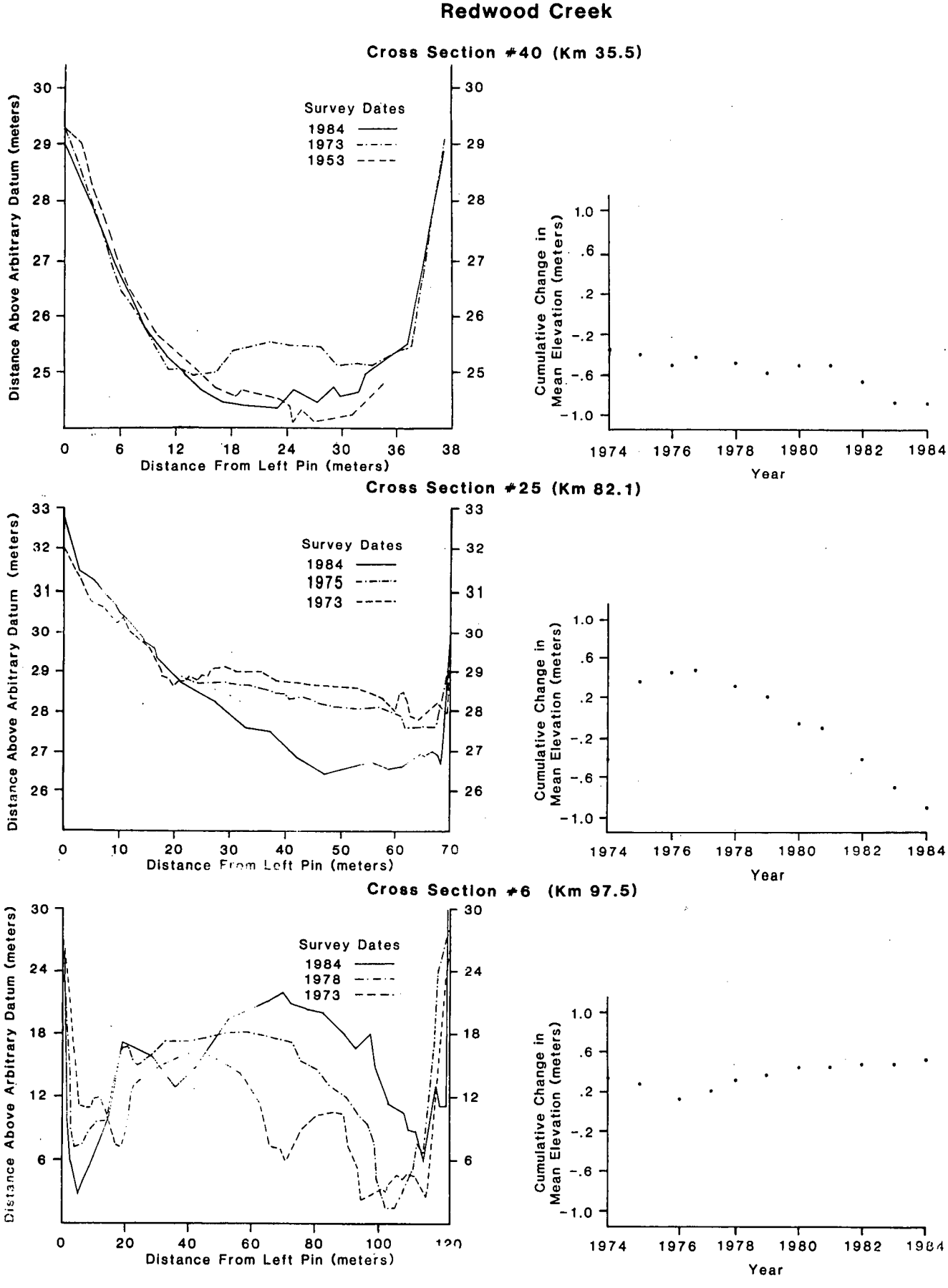

Figure 43. Cross-section surveys and cumulative changes in mean bed elevation for three stations in Redwood Creek. Cross-section 40 is in the upper third of the basin and documents progressive downcutting after aggradation. Cross-section 25 also shows consistent downcutting, whereas Cross-section 6 near the mouth of Redwood Creek shows progressive aggradation. Figure from Madej, 1984.

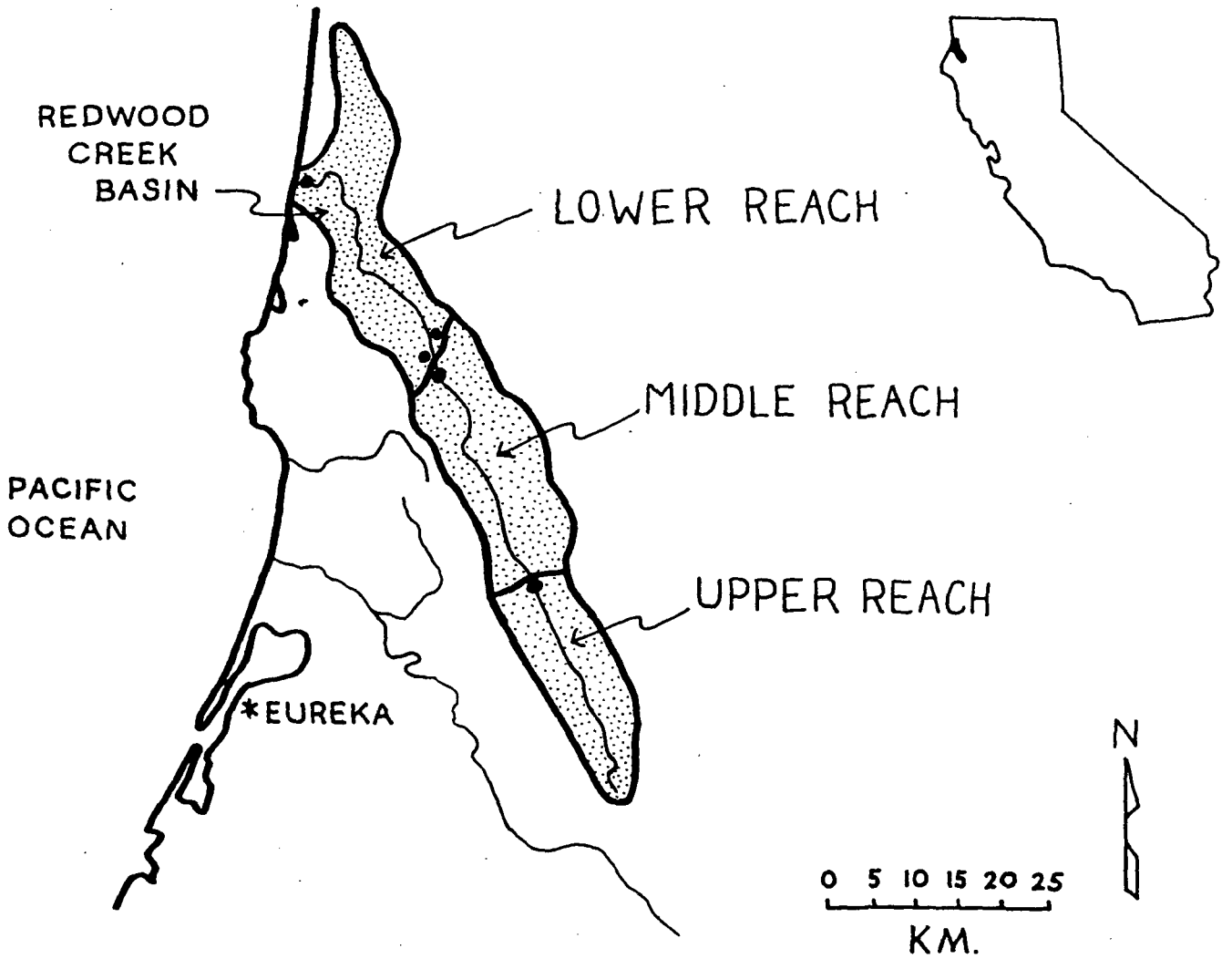

Figure 44. Sketch map of Redwood Creek showing lower, middle and upper reaches.

● = U.S.G.S. gaging stations

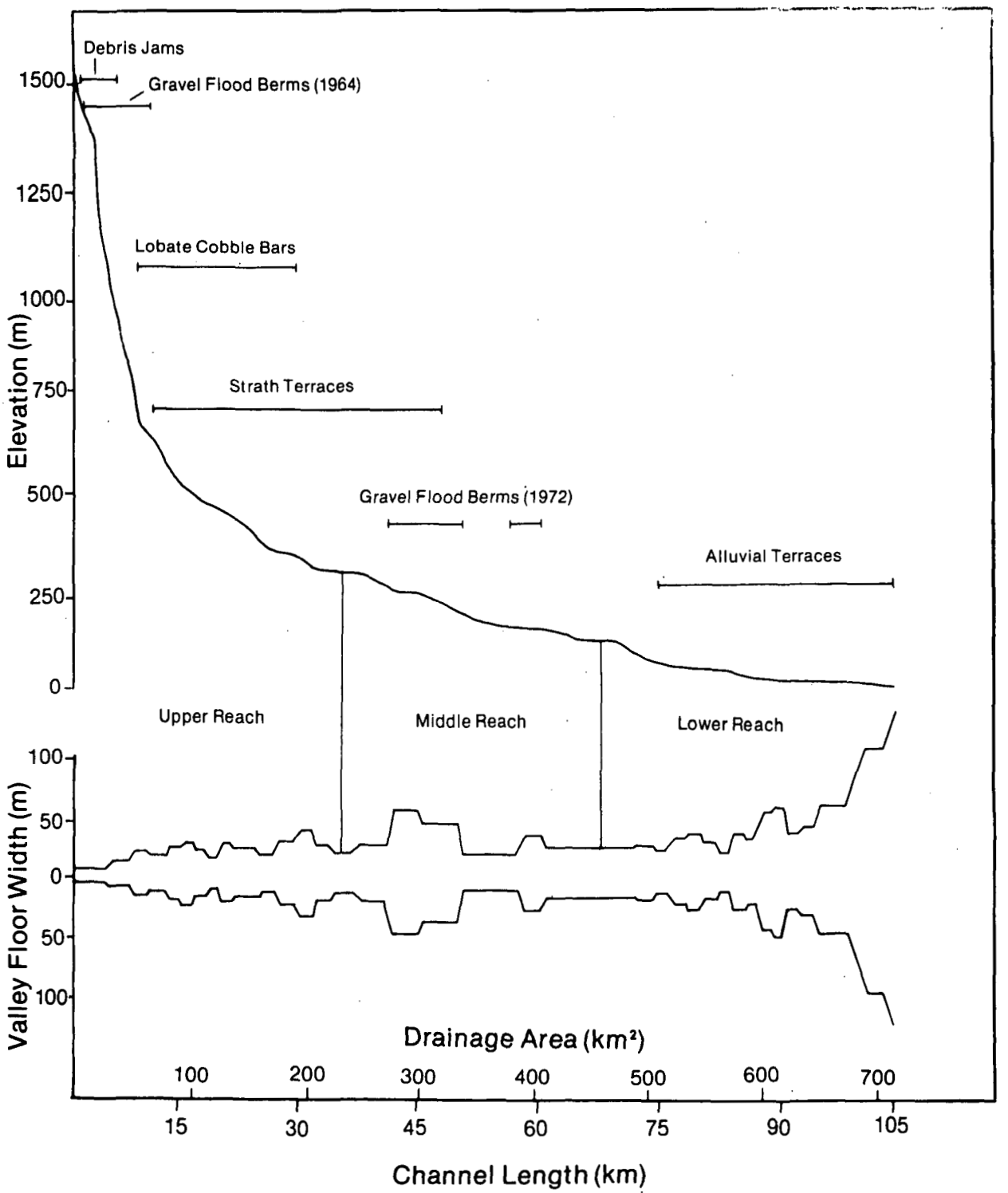

Figure 45. Longitudinal profile of Redwood Creek showing distribution of localized sediment compartments along certain reaches of the creek. Valley widths for Redwood Creek are drawn on the same horizontal scale as the profile. Figure from Madej 1984.

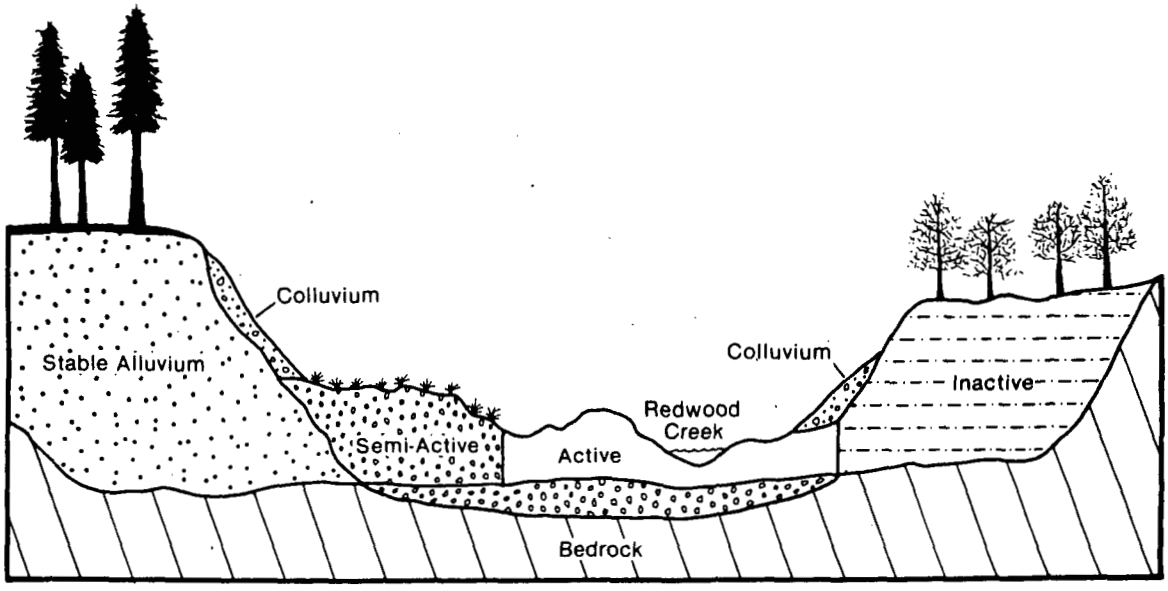

Figure 46.a. Schematic cross section of four sediment reservoirs in Redwood Creek: active (Ac), semi-active (Sa), inactive (Ia) and stable (St) sediment. Figure from Madej, 1984.

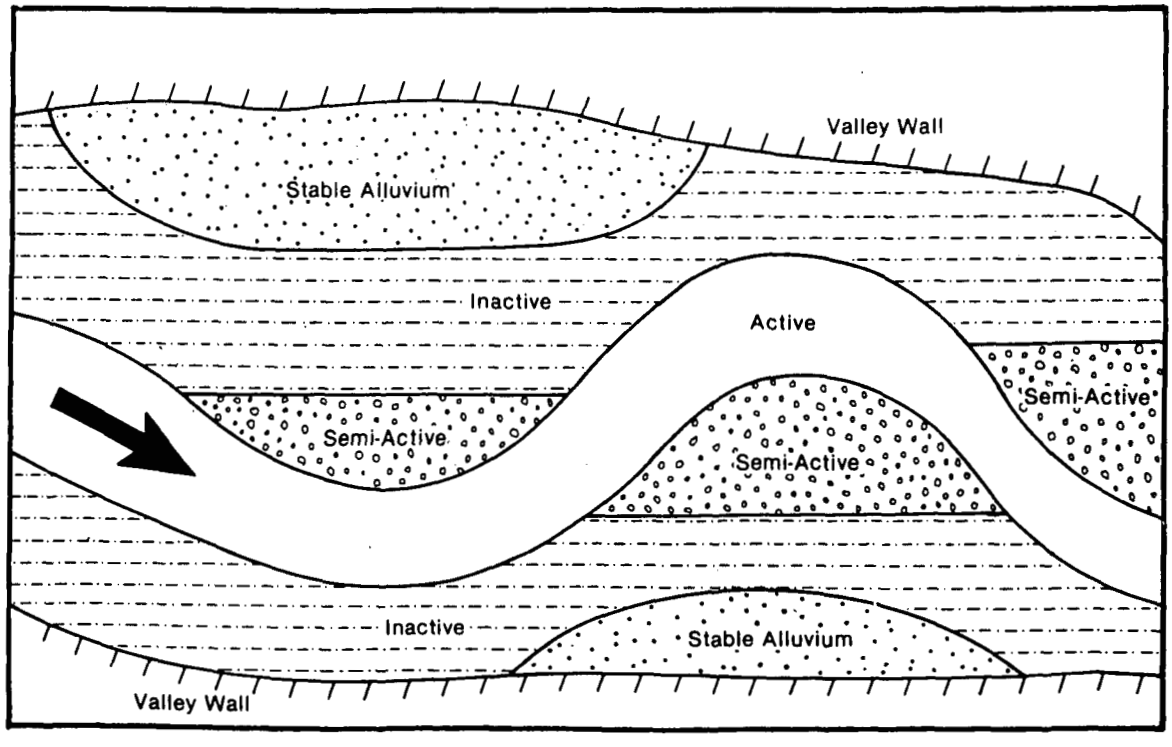

Figure 46.b. Schematic plan view of four sediment reservoirs in Redwood Creek. Figure from Madej, 1984.

scour increases downstream for equivalent discharges and depth of scour increases with increasing discharge at a given station. Sediment was not distributed uniformly downstream and maximum recent deposition occurred in areas of previous deposition. Sediment distribution is controlled more by valley width than by channel gradient, sites of sediment input, or drainage area. Fig. 47 shows the cumulative volume and spatial distribution of stored sediment in Redwood Creek for 1947, 1964, and 1980.

Erosion of bed sediment that had been deposited in the 1964 flood contributed greatly to annual bedload transport in the upper reaches of Redwood Creek for several years after the 1964 flood. Current sediment yields for Redwood Creek are 2,700 metric tons per square kilometer per year (t/km^2 /yr) in the upper basin and 2,200 t/km^2 /yr at the mouth, and bedload constitutes 20% and 11% of the total load at these stations, respectively.

Residence times of active and semi-active sediment generally decrease downstream, but increase for stable sediment. Residence times range from decades for sediment in the active channel bed to thousands of years for sediment in stable floodplain deposits. Table 1 shows residence times for sediment in the four different sediment storage reservoirs for the upper, middle, and lower study reaches (located on Figures 44 and 46a). Average velocities of stored sediment are highest for active sediment, and decrease with decreasing activity levels. Recovery time for the channel in response to the 1964 flood has been slow, and total recovery will take more than a century.

We will leave stop 2 at 1:30 p.m. Return to Highway 101.

82.4 Highway 101; turn right.

83.5 Junction with Hilton Rd.; turn left on Hilton Rd. We are entering part of the previously-logged portion of Redwood National Park. All around us is relatively new vegetation, mainly hardwoods; which impair our ability to see any vistas. Our route through this part of the park is southeast along the divide between Redwood Creek drainage and Stone Lagoon drainage, and then northwest into the tributary basin of McArthur Creek and southeast into the Tom McDonald Creek basin (Fig. 37).

Slope processes active in the part of Redwood Creek underlain by schist include debris flows, block glide-earthflow complexes and soil creep. Our two stops within the park will be at debris flows, but it is important to note that much larger translational landslides do occur in the forested area of the park underlain by schist (see Sonnevil and others, this volume).

Recent rainy winters have caused extensive landsliding in the park. Sonnevil and LaHusen (personal communication) have located 40 debris flows which occurred in the winter of 1981-82 and 28 resulting from storms in the winter of 1982-83, virtually all on schist terrain. These debris flows are associated with a) steep slopes, b) topographic position below convex breaks-in-slope in headwater swales and inner gorges (see below),

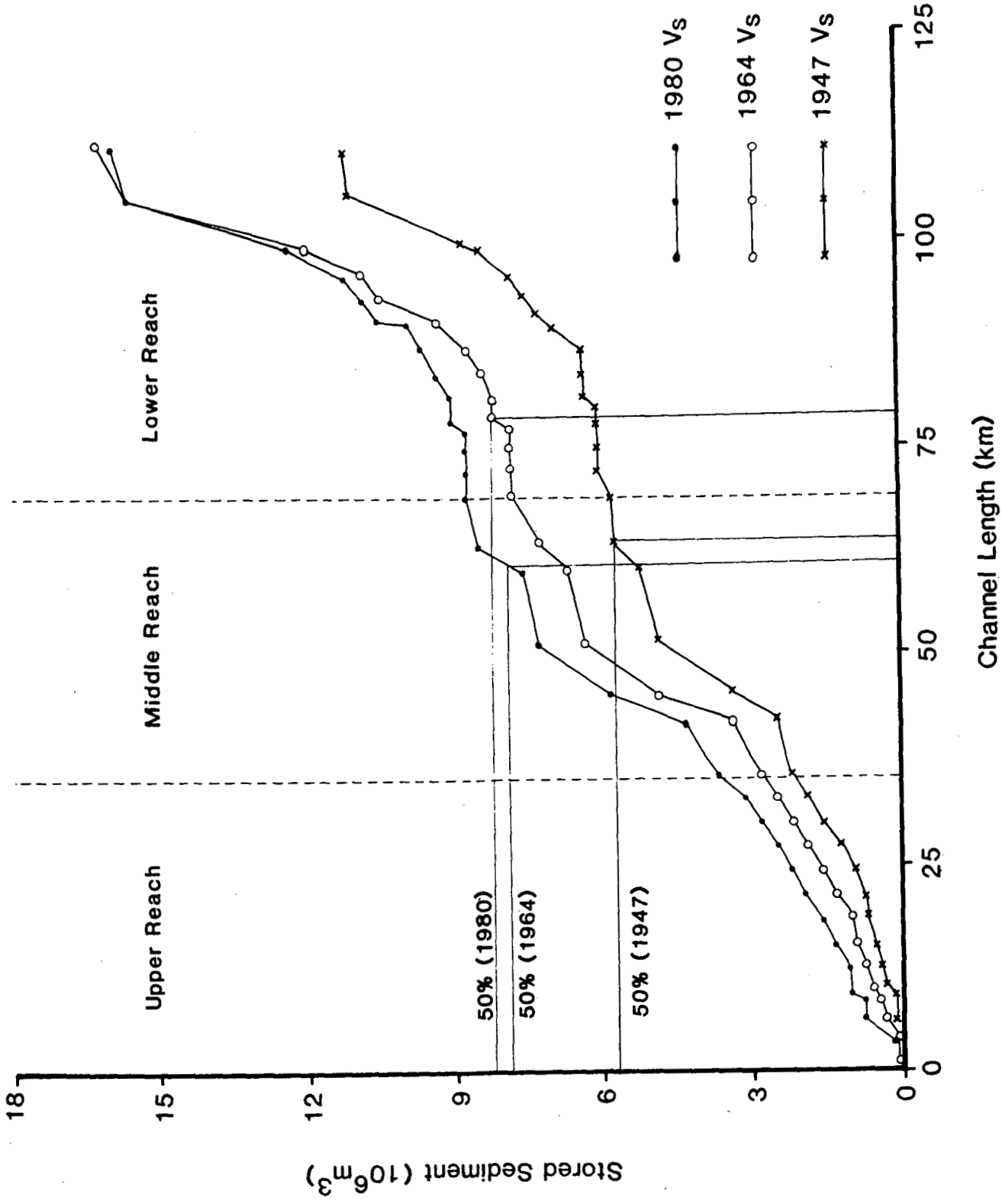

Figure 47. Cumulative volume and spatial distribution of stored sediment in Redwood Creek as of 1947, 1964 and 1980. Center of mass for each time period is indicated by the "50%" line. Note that the center of mass moved upstream after the 1964 flood, subsequently shifting 17 km downstream (as of 1980) as Redwood Creek redistributes sediment. Figure from Madej, 1984.

TABLE 1

Residence times of sediment in storage reservoirs.

Sediment Reservoirs	Residence Time Functions	Years	Velocity, V m/yr
Active	$0.09\ [X_2^{0.54} - X_1^{0.54}]$		
-upper reach (35.5 km)		26	1365
-middle reach (33.3 km)		11	3030
-lower reach (35.6 km)		9	3950
Semi-active	$0.33\ [X_2^{0.48} - X_1^{0.48}]$		
-upper reach		50	710
-middle reach		19	1750
-lower reach		15	2370
Inactive	$2.63 \times 10^{-3}\ [X_2^{1.01} - X_1^{1.01}]$		
-upper reach		104	340
-middle reach		99	335
-lower reach		106	335
Stable	$1.76 \times 10^{-9}\ [X_2^{2.55} - X_1^{2.55}]$		
-upper reach		700	50
-middle reach		3100	10
-lower reach		7200	5

c) specific soils (especially the Devilscreek soils) with a mottled subsurface horizon indicative of periodically saturated conditions, and d) the position of logging roads and skid trails (LaHusen, 1984). LaHusen (1984) postulates that compaction of soil horizons due to the placement of the road and skid trail fills may have lowered the permeability of the Devilscreek soils. Consequently, increased pore water pressures and partial saturation of the road fills caused by elevated groundwater levels may be important debris flow initiation mechanisms.

In the Van Duzen basin, we saw the prevalence of debris slides at slope positions just below the break-in-slope of the inner gorge. In lower Redwood Creek basin, shallow debris flow-type failures are also prevalent just downslope of the broad, convex divides of many Redwood Creek tributaries. Figure 48, a sketch taken from LaHusen (1984), shows both of the common hillslope positions of debris slides and debris flows in the Redwood Creek basin: inner gorge and below broad, convex divides. Our first stop this afternoon will be at a slope break just below a broad divide.

Figure 49 depicts a hillslope profile illustrating a typical debris flow initiation site. Although soil thickness and, in some instances, soil types may vary, locally all debris flow initiation sites exhibit common hydrologic and physical controls. These include a marked decrease in permeability and increase in cohesion of materials below failure surfaces. All failures examined occurred at the boundary between regolith (predominantly colluvium) and bedrock. In some locations, particularly those occurring in the upper hillslope positions, bedrock consists of hard schist. However, at many initiation sites, particularly most of those occurring within Devilscreek soils, bedrock consists of a highly sheared, dark black, quartz-mica-feldspar schist with abundant carbonaceous material.

The focus of the on-going research we will see at the next two stops is the development of models for the debris flows, with particular emphasis on determining the hydrologic characteristics of the soil and the groundwater response during storms.

86.5 Road is on a flat beveled alluvial surface between McArthur Creek and Stone Lagoon.

87.6 Road drops into McArthur Creek. Road cuts expose Redwood Creek schists.

90.1 The high bankcut on the right exposes soils of the Trailhead series (Ultisols: clayey, oxidic, isomesic Orthoxic Tropohumults). These soils have reddish (5YR to 2.5YR) clay argillic Bt horizons ranging from about 1.5 to 3 meters thick. There is 40 to 60 percent clay in the argillic horizon. Trailhead soils are found on most of the broad, rolling ridges and upper sideslopes underlain by schist in Redwood National Park. Some Trailhead profiles contain remnants of terrace sediments, including rounded clasts of Franciscan sedimentary or Klamath River (plutonic) lithology. The underlying schist bedrock is strongly weathered and reddened to a depth of several meters below the paralithic contact. Advanced soil development and deeply weathered bedrock illustrate the

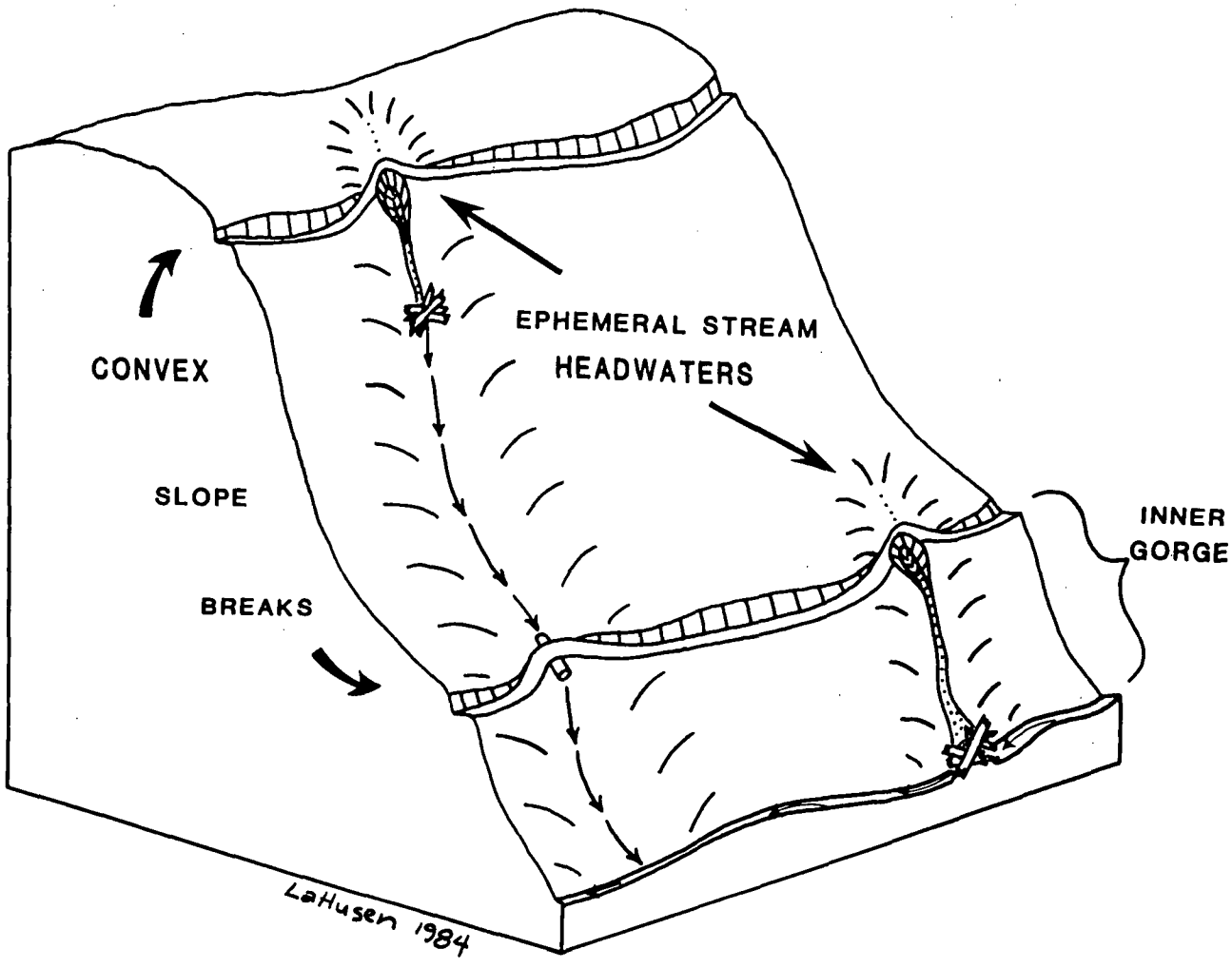

Figure 48. Diagrammatic view illustrating debris-flow-prone locations in ephemeral stream headwaters and inner gorge areas below convex slope breaks.

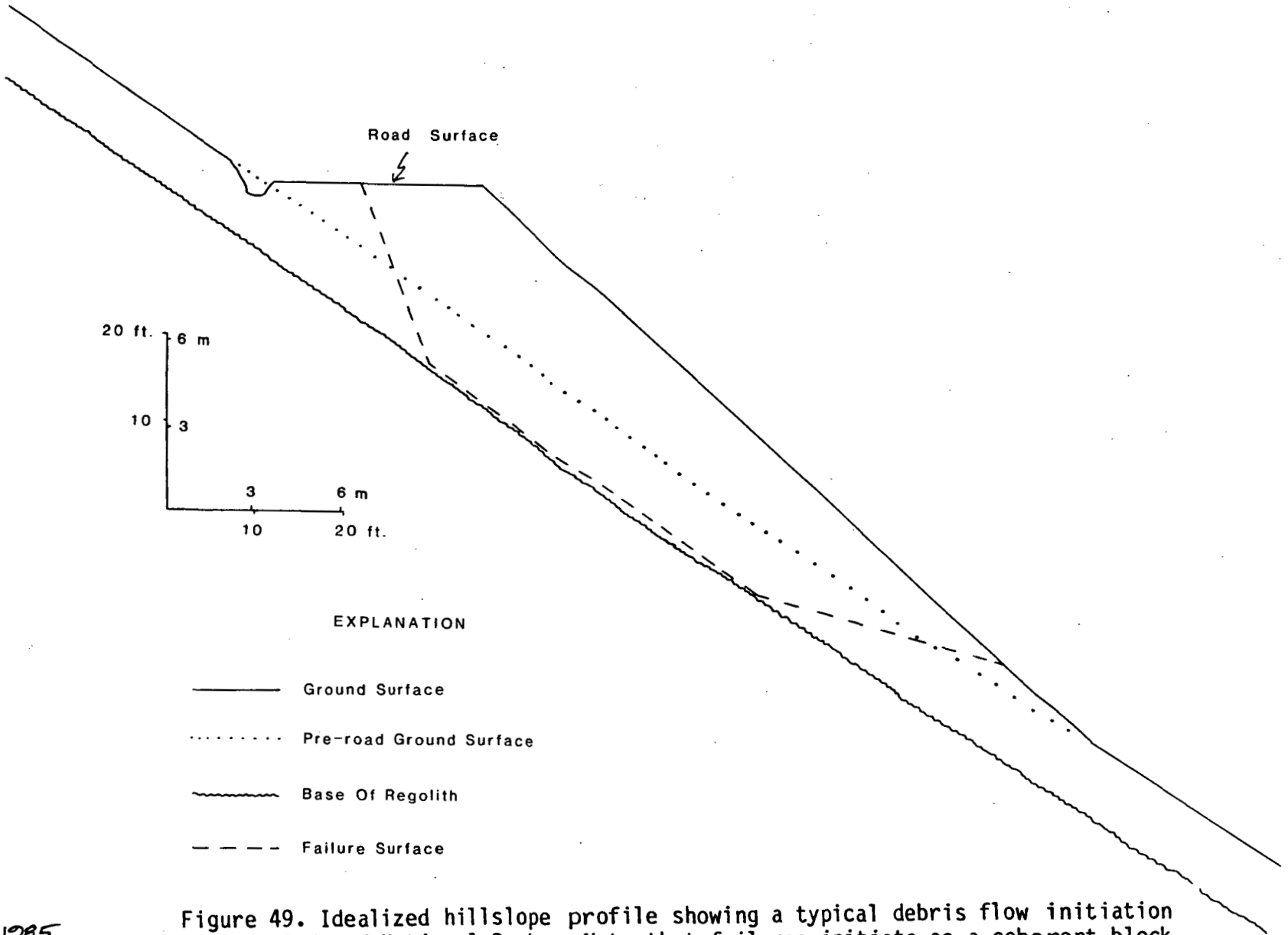

Sonnevil 1985

Figure 49. Idealized hillslope profile showing a typical debris flow initiation site in Redwood National Park. Note that failures initiate as a coherent block or "sliding wedge" and that much of the failure surface coincides with the base of the regolith.

importance of chemical dissolution in this climate on relief with comparatively low erosional activity.

90.4 Junction with L-line Road; take L-line Road to the south.

90.7 Vehicles will park in this area and we will walk 0.2 miles to Stop 3.

STOP 3 - DEBRIS FLOW ON L-LINE AND ADJACENT MONITORING SITE

This landslide failed in the winter of 1981-82, producing a debris torrent that extended into McArthur Creek and dammed the low gradient upper reach of McArthur Creek. A debris dam lake still exists in the channel (see Fig. 50.) The failure incorporated 3300 cubic yards of road fill, soil, and colluvium at the initiation site and approximately 8,000 cubic yards of regolith and organic debris were deposited in McArthur Creek. The failure occurred near the head of a swale, just below a broad, convex ridge.

Soil profiles at this stop are transitional in color and development between the strongly developed Ultisols on gentle, upper slopes and the moderately developed, brownish Inceptisols that dominate steep sideslopes. The contrast, here, between the very deep regolith in hollows and thin regolith on adjacent, convex slopes seems to be typical of upper mountain slopes in northwestern California. The well-defined soil-topographic boundary at the break-in-slope creates for us a colorful illustration of hillslope processes at work. Note the transition from reddish soils and deeply weathered bedrock at the top of the ridge to brownish soils and much fresher bedrock downslope. Note the inhomogeneity of colluvium in the hollows. It contains soil and rock in a variety of weathering states, some stratified and some mixed, all roughly traceable to a particular soil or rock source on the landscape. Use of soils as tracers could be a valuable technique for documenting geomorphic patterns and processes.

Sonnevil and LaHusen have established a monitoring network on an adjacent swale (Fig. 51) to define the groundwater movement and relate groundwater to precipitation and to slope movement processes. There were tension cracks present in this swale when the piezometers were installed. Figure 51 is a topographic map of this monitoring site showing piezometer locations and relevant morphologic features. Drilling during piezometer installations indicated that over six meters of colluvium exists within the swale upslope of the road while less than three meters are present in the swale at the base of the roadfill. This contrast indicates that this site is a colluvium-filled bedrock hollow with a bedrock lip between the road surface and the base of the roadfill.

Groundwater data at this site are being collected from an array of 24 piezometers. Piezometric stages are recorded from all piezometers on a weekly basis or after each significant rainfall event. Piezometric crests are recorded on crest staff gages (Fig. 52) and several piezometers have pressure transducers with data recorders sampling at 15 minute intervals. The data recorders and pressure transducers were designed and constructed by LaHusen. Figure 53 is a cross-section of the hillslope profile along the centerline of the swale. Piezometric data recorded in February, 1984 were used to construct this flow net for

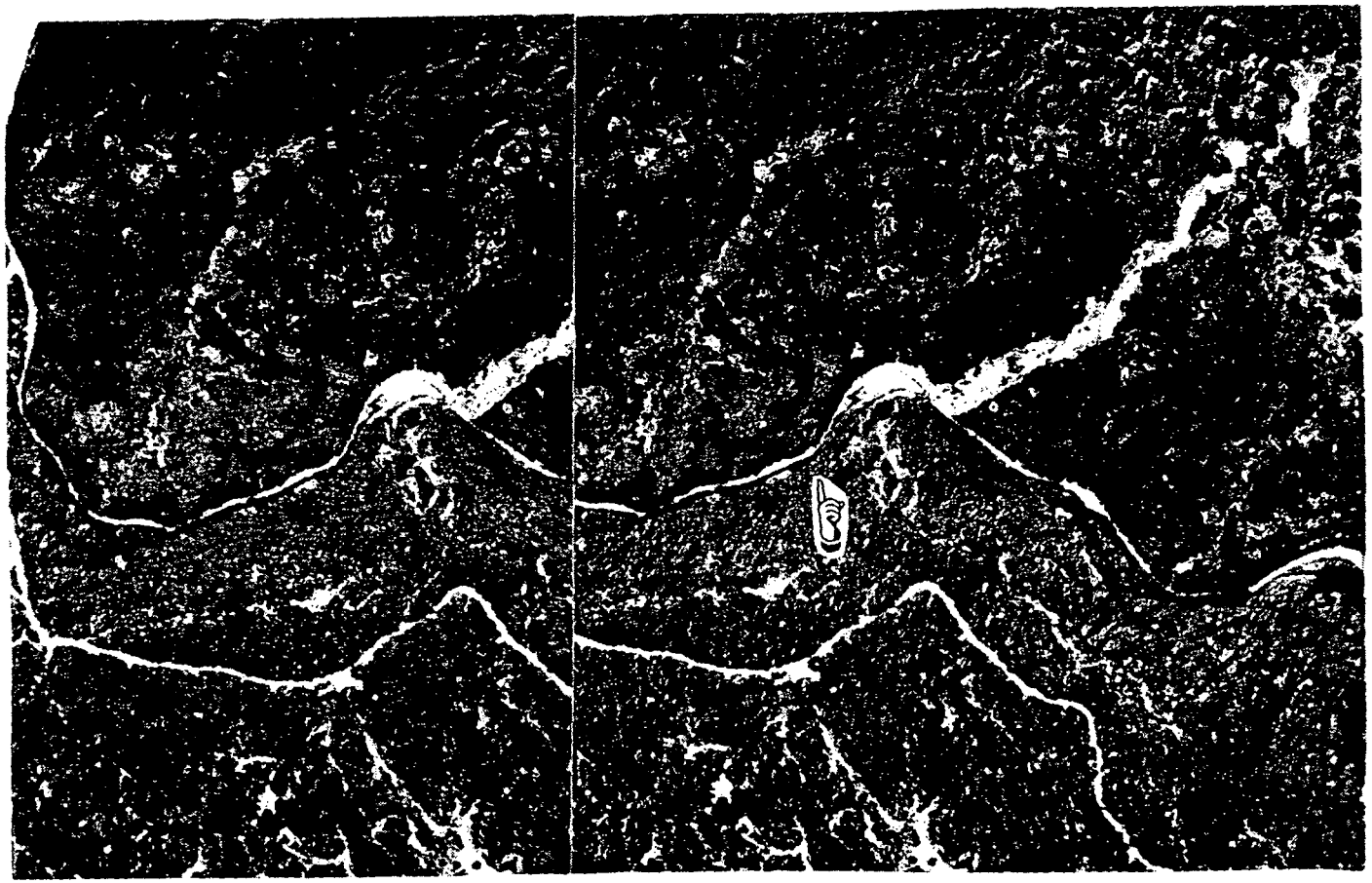

Figure 50. Stereo photo pair showing vicinity of Stop 3. Note debris torrent originating at the L-line road and resultant debris dam in McArthur Creek. Adjacent swale (marked on photo) is the groundwater monitoring site depicted in Figure 51. Debris torrent failure occurred in December 1981 and photo was taken in June 1984.

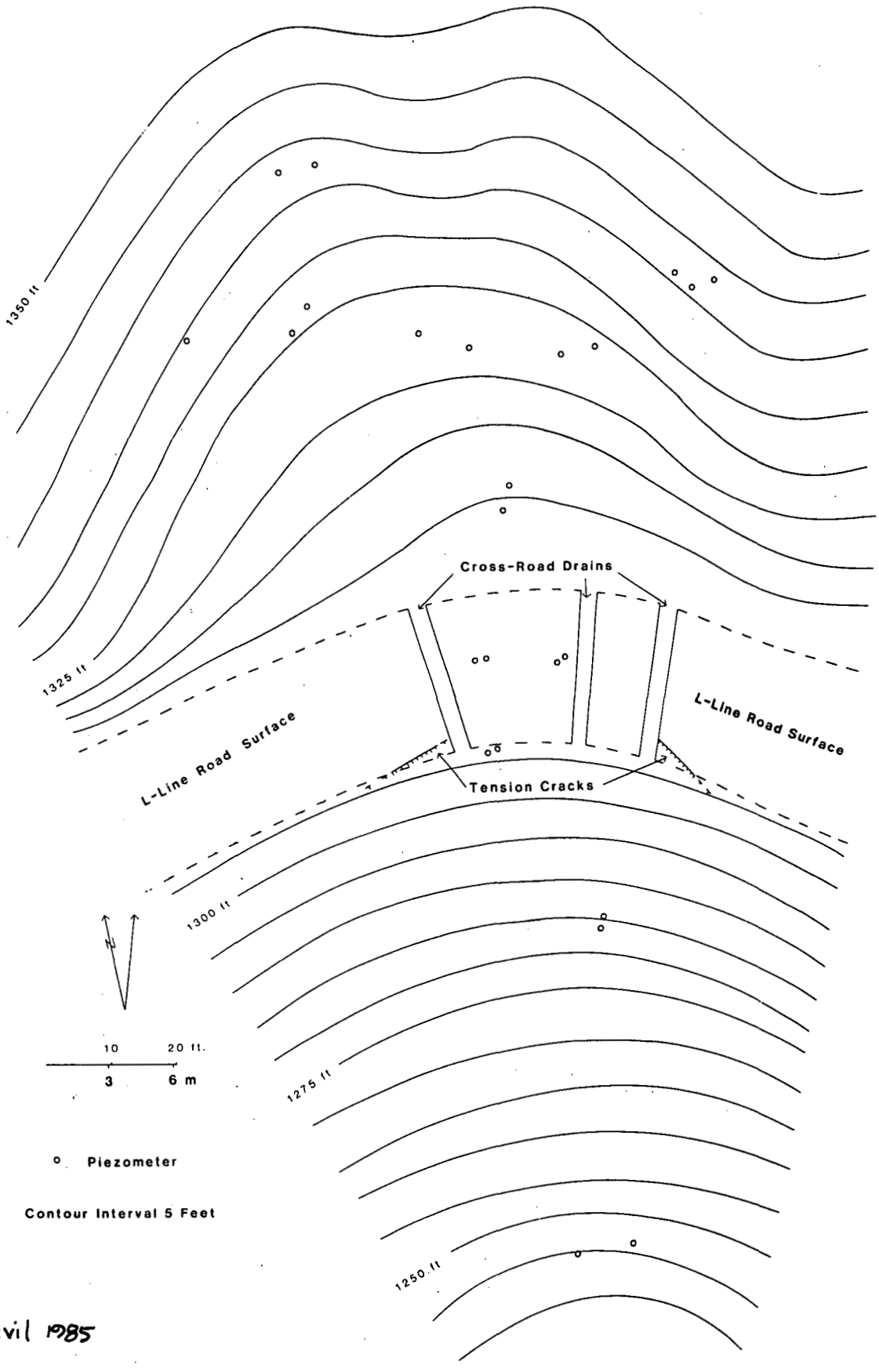

Figure 51. Topographic map showing piezometer network on and upslope of an incipient debris flow initiation site. The lower limit of roadfill coincides with the lowest piezometers. Tension cracks appeared in December 1981 and were continuous before construction of crossroad drains. Piezometers were installed in January, 1984.

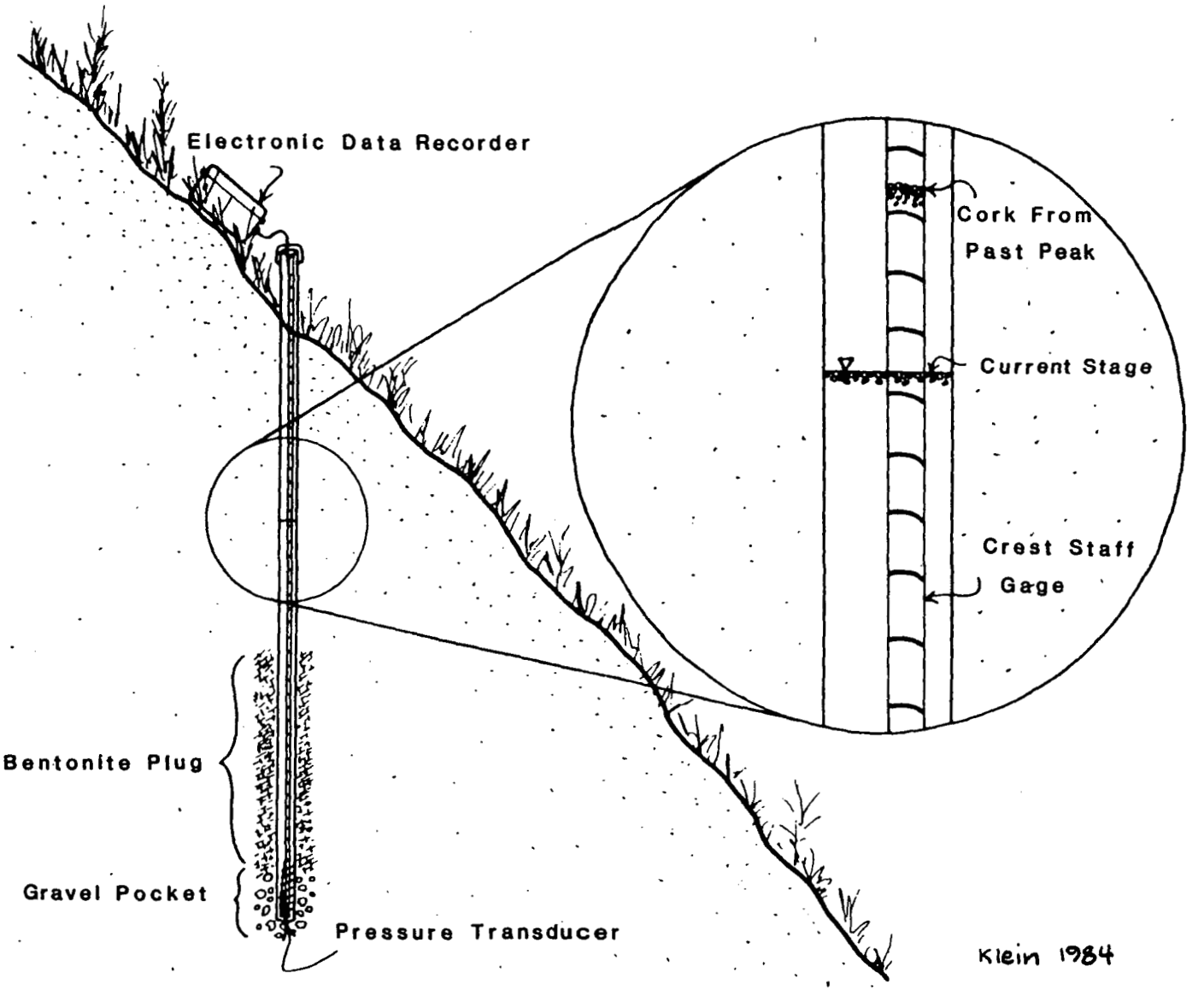

Figure 52. Diagrammatic view of piezometer installation. Piezometer casing consists of 24 mm diameter PVC pipe with the lower 45 cm slotted. Piezometers vary from 2 to 8 m in depth. Crest staff gage is a strip of PVC 12 mm wide. Past crest and current stage may be read by removing gage and noting locations of granulated cork lines. Home-made electronic instruments record piezometric stage every 15 min. on memory modules suitable for direct transfer to microcomputer system.

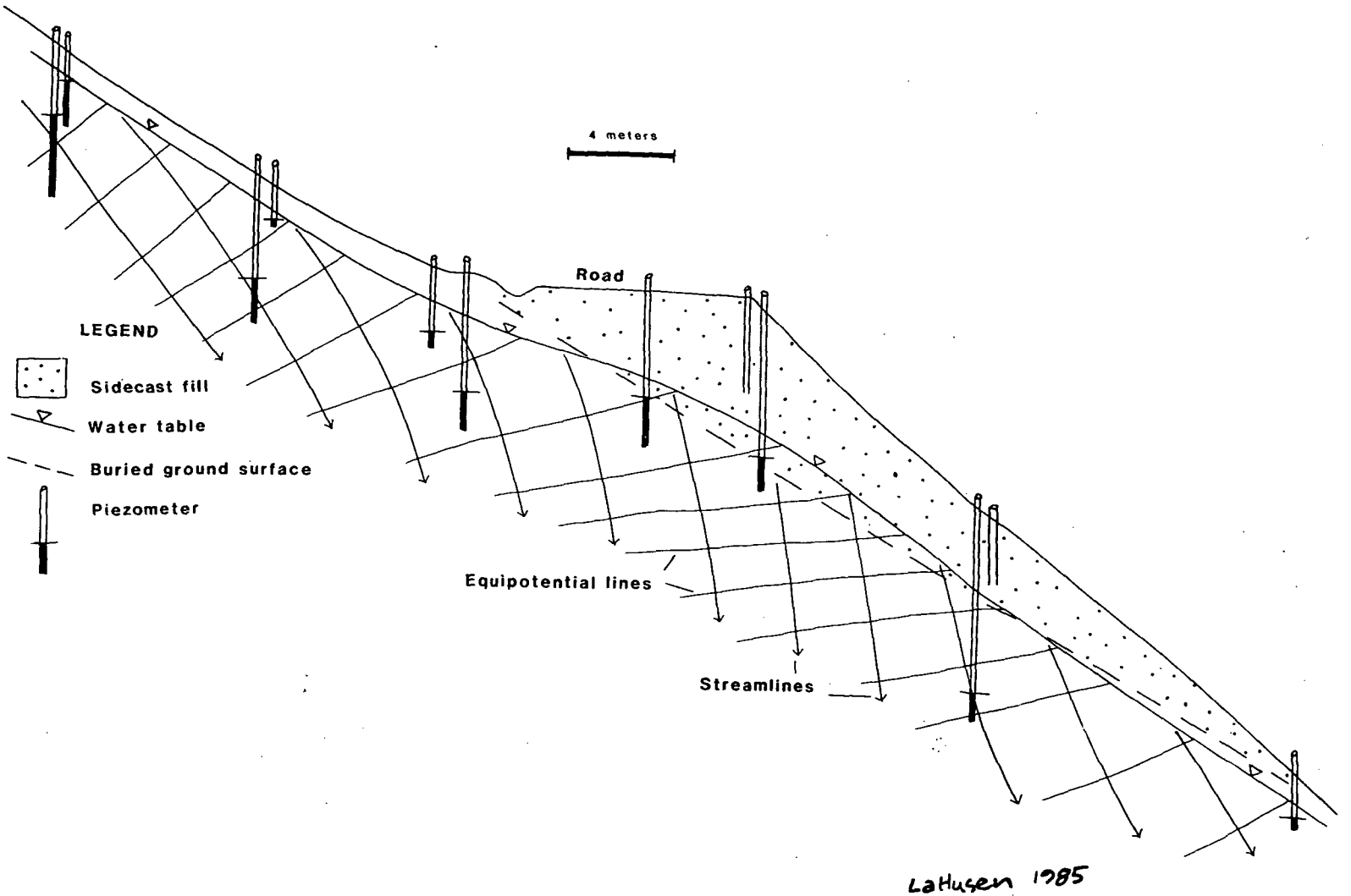

Figure 53. Hillslope cross-section along centerline of swale at Stop 3. Flow net developed from piezometric data shows elevated ground water level beneath road. Refracting streamlines are consistent with a decrease in hydraulic conductivity due to compaction of underlying soil horizons.

the saturated zone. Although only relatively minor antecedent storms (< two year return interval) occurred, evidence of groundwater perturbations is present. Note that positive pore water pressures were found within the roadfill material above the original ground surface. In addition, the downward refraction of the streamlines as they pass under the road indicate that a two- to five-fold decrease in hydraulic conductivity has occurred. More intense rainfall events would create a more pronounced "groundwater mound" eventually culminating in debris flow initiation.

Besides the hyrologic data collected at this site, four additional locations along the L-line road alignment are being monitored at a much less intensive level. Two of these locations are observable on the walk back to the vehicles. These additional monitoring sites expand the data base for a stability analysis of the L-line road fills.

Ultimately, Sonnevil and LaHusen hope to create a model of debris flow formation at this hillslope position. They will discuss some preliminary results of their modeling. One practical result of their research will be to tell rehabilitation crews how much material needs to be removed from old road fills to prevent the kind of debris flow failures obvious at this site. Removal of the entire road and landing fill prism, for instance, would have cost about $13,000 (Sonnevil, personal communication). This cost does not justify complete removal of fills, except in cases of documented imminent hazard. Twelve road fills of varying sizes are still present in swales along a mile-long reach of the the L-line road. If a way can be found to identify the fills most prone to failure and then define the minimum amount of material that needs to be removed to stabilize the slopes or greatly reduce downslope impacts, then significant savings in rehabilitation costs may result.

We plan to leave stop 3 at 3:30 p.m.

91.0 Intersection of L-line road at A-9 deck. Take A-9-9 road south.

91.9 The high, red-clay bankcut on the right exposes a Trailhead soil. This site was described and sampled by James A. DeLapp in 1960. The description and laboratory data (Sample No. 60-12-18) are published in Begg, et. al. (1984).

94.1 Turn left onto C-12 road.

94.5 Turn sharply right onto G-6-1 road. Note that the regolith generally deepens as we descend from the crest of a spur ridge onto a smooth, steep slope along the G-6 road. Smooth, steep middle and lower slope positions tend to have a continuous mantle of deep soils. Deep soils are not confined to bedrock hollows as they were at the last stop.

95.1 Exposed in the roadcut to the right are Coppercreek soils (Inceptisols: fine-loamy, mixed, isomesic Typic Humitropepts). This series and other associated Inceptisols dominate steep sideslopes in Redwood National Park. Coppercreek soils have brownish (10YR to 7.5 YR) cambic B horizons ranging from about 40 to 100 cm thick. There is 25 to 35 percent clay in the B horizon and a gradual decrease in the C horizon. Depth to bedrock

is one to three meters. The Coppercreek series is the most extensive in the park.

95.2 There are thin soils in the roadcut as we round a narrow spur and cross a well-incised stream. Thin soils are generally associated with high relief and competent bedrock. The soil profiles here were disrupted by road building. Typically, the regolith on bedrock spurs is about 50 to 100 cm deep. The Lackscreek series (loamy-skeletal, mixed, isomesic typic Humitropepts) and Ahpah series (fine-loamy, mixed, isomesic Typic Humitropepts) are the principal series. These soils have colors, horizons, and clay percentages similar to the Coppercreek series.

The valley of the next stream crossing is underlain by incompetent rock that is disintegrating and deforming downslope. The valley is broader and more irregular than the first stream valley and there are Devilscreek and Elfcreek soils on both sides of the stream. The Devilscreek series (fine-loamy, mixed, isomesic Typic Humitropepts) consists of soils similar to the Coppercreek series, except that they have a 2Cg horizon with gray matrix and brownish mottles. Water is perched during the winter rainy season and its level fluctuates within the mottled zone. The A and B horizons of Devilscreek soils probably originated by soil creep from surrounding, higher Coppercreek soils. The 2Cg horizon, which has only 8 to 20 percent clay, seems to have originated from disintegrating, but pedogenically unaltered material from within the hollow itself. The Elfcreek series (loamy-skeletal, mixed, isomesic Typic Eutropepts) have gray C horizons and grayish brown A and B horizons with 15 to 25 percent clay. They occur in locations where debris slides have removed the A and B horizon of a Devilscreek soil and also on some lobate debris flow deposits. Here, as at the last stop, contrasting soil characteristics help us keep track of slope processes.

95.3 Vehicles will park at pull-off on left. We will walk about 0.2 miles to G-6-1 debris flow.

STOP 4 - G-6-1 DEBRIS FLOW AND MONITORING SITE

This landslide failed in 1981-82 into the channel of a tributary of Tom McDonald Creek, removing some old-growth redwoods. We will look at the landslide and at the slope to the east that is being monitored by LaHusen and Sonnevil. Figure 54 is a sketch map showing the failure, groundwater monitoring sites and relevant morphologic features. The majority of soil movement and resultant debris flow at this site involved roadfill and regolith located within an intermittent stream channel. Streamflow was diverted to the north by road construction. It is evident, due to numerous tension cracks, that instability extends along the road east of the stream channel. This unstable segment of road and the adjoining hillslope is the driest of three locations being studied in detail by LaHusen who is completing a thesis at Humboldt State University on the movement of groundwater through logging road prisms constructed on Devilscreek soils.

The piezometer network at this locality consists of two parallel transects extending from upslope of the road surface to the base of the

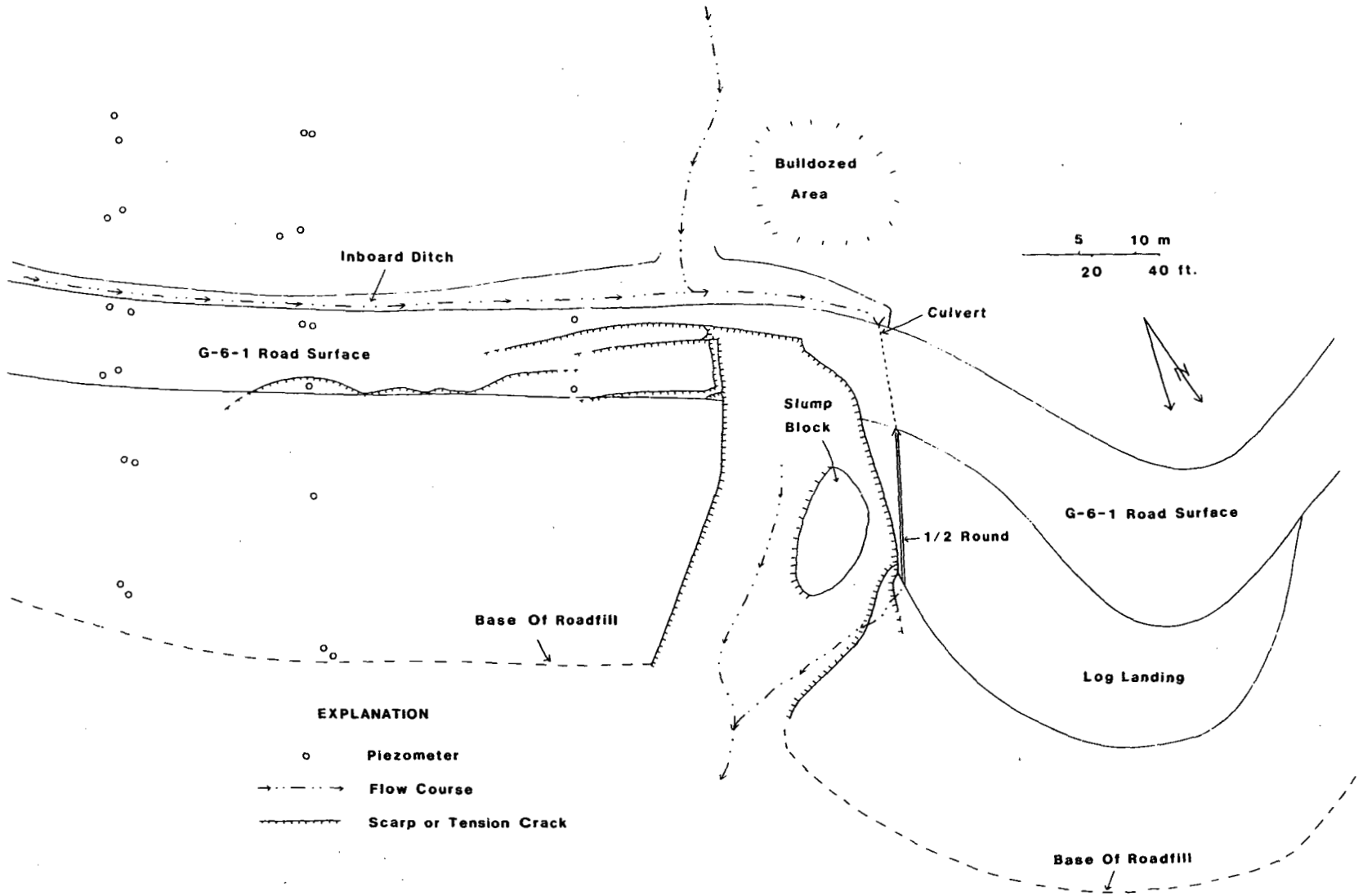

Figure 54. Map showing vicinity of Stop 4. Failure occurred in winter 1981-1982. Piezometer transects were installed in September 1983.

roadfill. Figure 55 shows a flow net generated from data collected at one of these transects in February 1984. At this site, a less obvious effect is seen compared to our last stop. Only a minor "groundwater mound" is observable beneath the road. The lesser effect is probably due to the planar hillslope where streamlines don't converge, contrasting with monitoring sites located in swales. Furthermore, for the soils along this piezometer transect, the depth from the ground surface to the top of the saturated zone is greater than in the more typical Devilscreek soils located in the next swale west of the debris flow.

Exposed along the road are examples of the wetter soils typically associated with road-related debris flows underlain by schist. Figure 56 is a sketch and description of the soil profile exposed at the piezometer transect.

We plan to leave stop 4 at 5 p.m. Those interested in a closer look at the soils in the Redwood Creek basin are encouraged to stay a little longer with Jim Popenoe, soil scientist at Redwood National Park. As many vans or buses will stay for the additional soils trip as are required. Retrace route on G-6-1, C-12, C-line and A-9-9 roads.

99.6 Mileage at deck; return to Highway 101 on Hilton Rd.

106.5 Junction Highway 101, turn south (left). We will retrace the morning's route on Highway 101 back to camp. At the south edge of Freshwater Lagoon is a prominent cliff face cut into deeply weathered Redwood Creek schists.

140.8 Junction 101 and 299. Take 299 and West End Road east, back to campground. Tonight's dinner will be a barbeque at the campground.

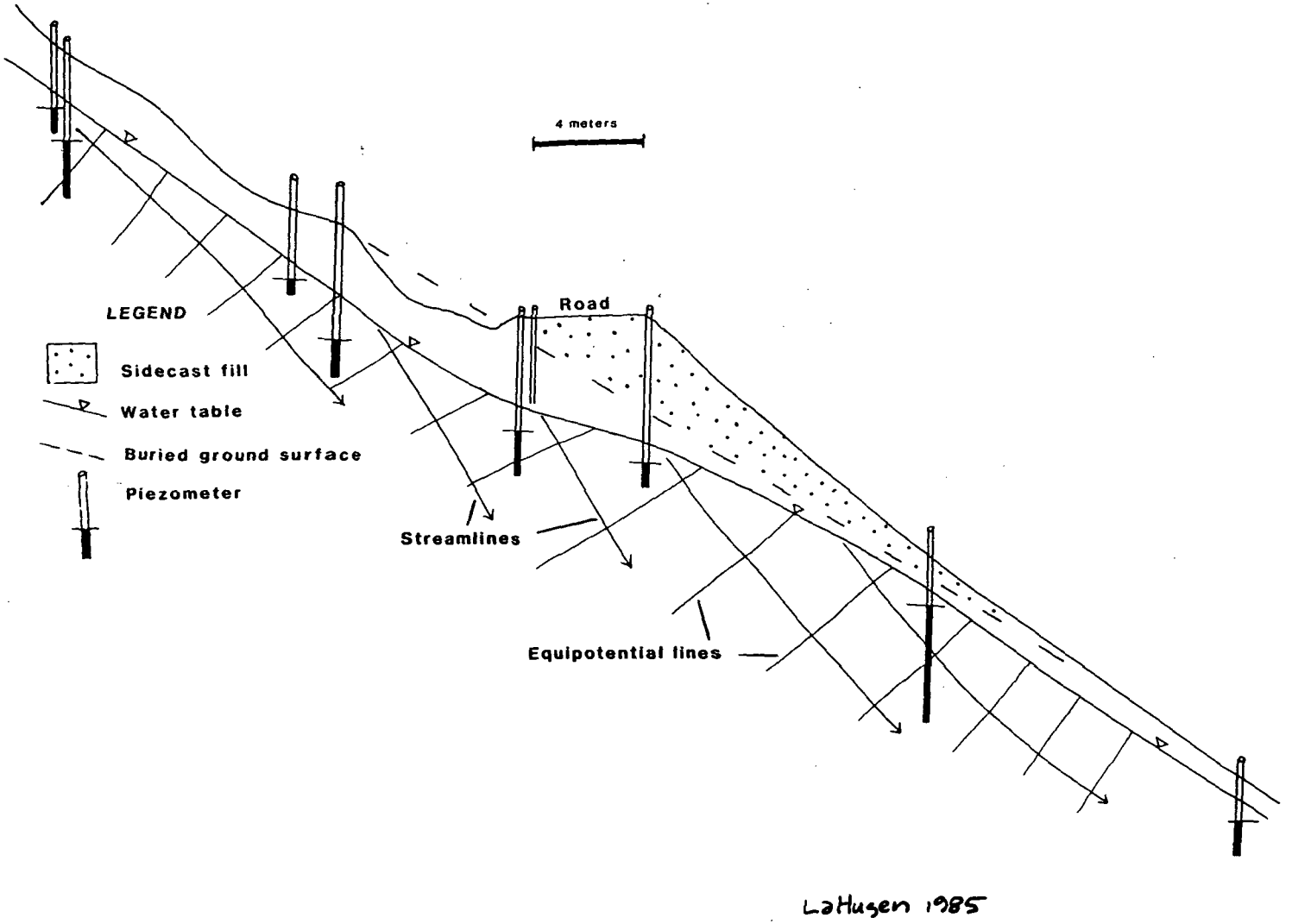

Figure 55. Hillslope cross-section of planar slope adjacent to debris flow at Stop 4. Minor "ground water mound" is evident under the road prism. A much greater elevation in ground water has been demonstrated in swales and in wetter phases of the Devilscreek soil.

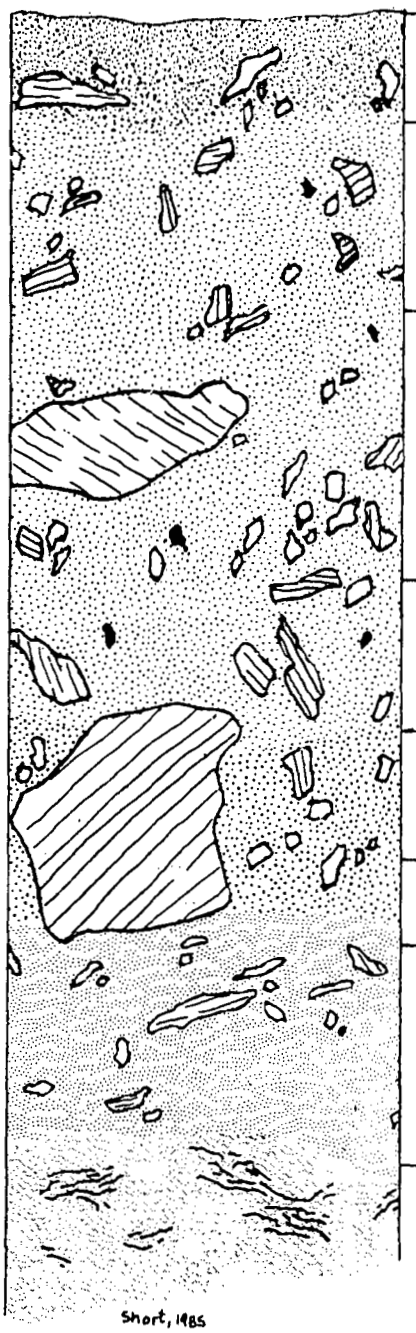

Depth (cm)		
0	A	Dark brown (10YR 3/3) very gravelly silt loam, weak fine and medium subangular blocky structure.
15	Bw1	Yellowish brown (10YR 5/6) gravelly silt loam, weak coarse & medium subangular blocky structure.
45	Bw2	Variegated strong brown, yellowish brown (7.5YR 5/6, 10YR 5/6) very cobbly silty clay loam, weak coarse subangular blocky structure.
89	Bw3	Yellowish brown (10YR 5/8) silty clay loam, weak medium subangular blocky structure.
110	BC1	Yellowish brown (10YR 5/8) very stony silty clay loam, no soil structure.
132	BC2	Yellowish brown (10YR 5/6) very stony loam, no soil structure.
145	2Cg	Variegated pale olive, gray (5Y 6/4, 5Y 5/1) gravelly loam, few brownish yellow (10YR 6/6) mottles, common brownish yellow (10YR 6/6) weathering rinds.
180	2Cr	Schist saprolite, variegated dark gray (N4/) and olive gray (5Y 5/2) few brownish yellow (10YR 6/6) weathering rinds, no mottles.

Figure 56. Sketch and description of soil profile exposed along the G-6-1 Road near piezometer transect. All colors are for moist soil.

ROAD LOG - TECTONIC GEOMORPHOLOGY OF THE MAD RIVER - FICKLE HILL AREA

G. A. Carver and A. K. Lehre
Department of Geology
Humboldt State University

0.0 Leave the campground and turn right onto Warren Creek Road. You are traveling west along the Mad River. The prominent hills on either side of the Mad River represent the westernmost extension of Fickle Hill, a large extensively faulted pleistocene anticline. This Quaternary structure will be the principal focus of the morning portion of today's trip. The narrow canyon we will be driving through for the next several miles is a water gap cut by the Mad River in response to tectonic uplift of Fickle Hill during the late Pleistocene.

0.2 Railroad Trestle Underpass - Warren Creek Valley near the confluence of Warren Creek with the Mad River. Warren Creek is a greatly disrupted drainage system which follows the Mad River Fault. The stream has recently reversed its drainage direction and is now flowing northwest. All of Warren Creek's tributaries flow northeast, as did the trunk stream prior to the late Pleistocene drainage reversal. The railroad trestle is a part of the Annie and Mary Short line R.R., operated until this year by the Simpson Timber Co. The railroad is presently for sale.

0.3 Junction with West End Road. Turn right and follow West End Road. Here the antecedent Mad River cut through upfaulted imbricate blocks within the Mad River fault. The fault zone is about a half mile wide at this point.

1.8 Railroad Crossing - Exit the narrow canyon of the Mad River where it crosses the Mad River Fault and proceed onto the Holocene floodplain of the Mad River. At least five levels of Holocene terraces are present within this broad floodplain, which grades to the modern Humboldt Bay margin and coastline about 1 km to the West. The Mad River fault and its associated complex scarp form the prominent hillslope (Bella Vista Hill) to the North of the Mad River and Highway 299.

2.3 Junction with Giuntoli Lane. Turn right and follow Giuntoli Lane across the Holocene Mad River floodplain to intersection with U.S. 101. Giuntoli Lane represents the approximate high water limit reached during the 1964 Christmas flood.

3.0 Junction with US 101 - Turn right onto US 101 and continue north across the Mad River to the Central Avenue (McKinleyville) exit.

4.1 Central Avenue exit to McKinleyville. Central Avenue leaves US 101 and climbs the Mad River Fault scarp. Narrow strips of Franciscan rocks are in fault contact with early and mid Pleistocene Falor Formation sediments in the scarp face. At least three major faults cut this scarp.

4.9 Top of Bella Vista Hill. The top of Bella Vista Hill consists of strongly warped late Pleistocene marine terrace deposits.

5.4 Stop light, intersection with School Road. Turn left. School Road traverses the warped and tilted marine terrace surface correlated with the Patricks Point Terrace at Trinidad.

6.1 Intersection of School Road and Winsor Road, Turn right on Winsor Road and park at the McKinleyville Baptist Church Parking Lot.

STOP 1 Mad River Fault - Deformed Patricks Point Terraces

The Mad River Fault, one of the principal faults of the MRFZ, intersects and displaces the Patricks Point terrace at School Road (Figure 1). Three prominent southwest-facing scarps are evident. The terrace is warped and vertically displaced more than 30 meters down to the south. A trench excavated across the northern scarp near its intersection with School Road revealed Franciscan rocks thrust over terrace sands along a shallow northeast dipping (10^{0}-20^{0}NE) fault surface. The curved trace of the faults and highly variable scarp form also suggest a shallowly dipping fault. These faults continue to the southwest and form the large south facing scarp seen along the Mad River near Bella Vista Hill.

Returning to School Road, turn right and cross over U.S. 101, turn left on south bound freeway ramp and proceed south on U.S. 101 to Arcata.

8.2 Cross the Mad River onto its Holocene floodplain.

9.6 Junction with U.S. 299 - continue south to the next exit.

10.6 Exit freeway at Sunset Avenue offramp and proceed straight ahead (south) into Arcata on H Street. The gently sloping surface on which the northern part of Arcata is situated is a northward tilted marine terrace. Soils on this terrace are much better developed than those on the Patricks Point terrace at School Road and the terrace is interpreted to be much older.

11.4 12th and H Streets - Larry's Market. The terrace on which Arcata is sited is cut by the Fickle Hill fault at this point. The gentle south facing slope between here and the downtown plaza is a fault scarp. The south side of the fault is downdropped. A second smaller scarp is present on the south side of the plaza, passing under the Jacoby Storehouse, a historic building on the corner of 8th and H Streets. The flat surface at the central plaza is a fault-bounded terrace remnant with a structural position in the fault zone similar to the remnant at the church at STOP 1 on the Mad River fault. Both the Mad River fault at School Road and the Fickle Hill fault in Arcata have been zoned by the State of California as Alquist-Priolo special study zones. Certain types of development within these zones must include

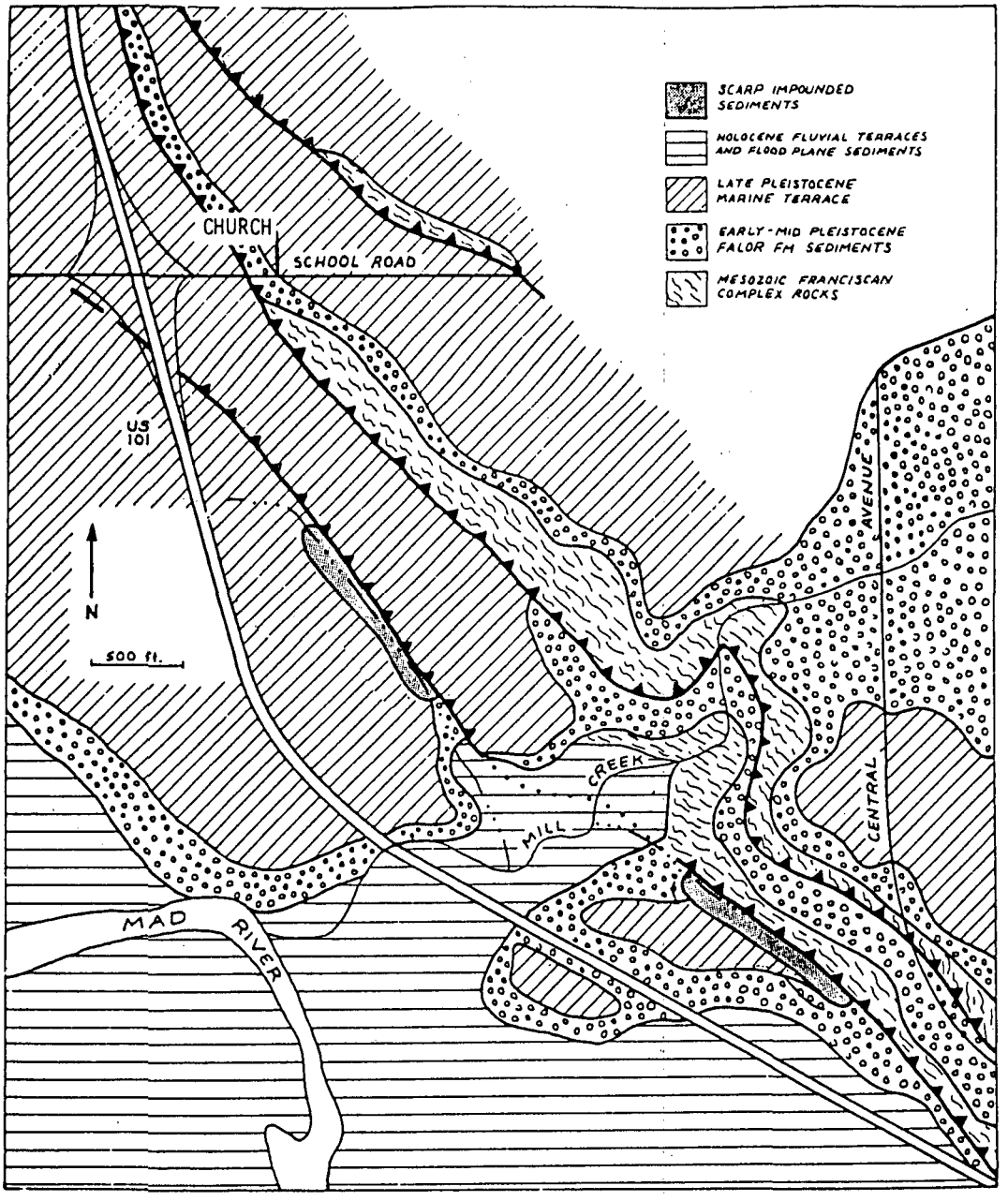

Figure 1. STOP 1 - The church on School Road. Geologic map of the Mad River Fault in the vicinity of School Road. Three prominent scarps mark down to the south fault displacement of the late Pleistocene (.85 ma) Patricks Point terrace. A shallow trench excavated across the northern scarp revealed Franciscan sandstone thrust over terrace sand on a fault surface dipping 10^{o}-20^{o} to the northeast. The church (STOP 1) is situated on a tilted fault bounded terrace remnant. Total dip slip displacement across the three prominent traces of the fault at this location is estimated to be about 110 meters.

geotechnical analysis of seismic hazards.

11.7 7th and H Streets, Arcata. Turn left on 7th and proceed east across the freeway. To the left just before the freeway overpass is the scarp of the Fickle Hill fault. Note the location of the City Hall and Arcata City Police Department on the scarp.

12.2 7th and A to 7th and B Streets, Arcata. 7th Street traverses the Fickle Hill fault at this locality. The fault forms a large complex scarp. Holocene sediments marginal to Humboldt Bay form the low plain below the fault scarp.

12.3 Turn left onto Fickle Hill Road just past the intersection of 7th and A Streets and proceed uphill. Sparse outcrops along the road consist of Falor Formation sediments and deeply weathered Franciscan sandstone which underlies the Falor sediments. Fickle Hill Road climbs the plunging nose of the eroded Fickle Hill anticline for the next several miles.

15.2 Lazy "L" Ranch - In this vicinity the road climbs onto the crest of Fickle Hill. Most of the outcrops consist of weathered Franciscan sandstone and melange, but scattered patches of Falor Fm marine sands mantle the crest inland for the next 20 miles. To the south Fickle Hill slopes steeply down to Jacoby Creek. Steeply SW dipping beds of Falor Fm marine sands and fluvial gravels compose the lower half of this slope. These sediments have been thrust under the Franciscan rocks of the upper part of Fickle Hill along the Fickle Hill fault. The more gentle north-facing slope of Fickle Hill is mantled with NE dipping Falor Formation sediments cut by the Mad River fault. Fickle Hill represents a large asymmetrical anticline with an oversteepened and locally overturned southern limb. Both limbs have been displaced by northeast dipping thrust faults.

For the next several miles the road follows the crest of Fickle Hill. Along this part of the route of graben-like depressions can be seen cutting obliquely across the ridge top, and the headscarps of several of large slump-earthflows are evident.

17.2

STOP 2 Top of Fickle Hill (1260') This is the starting point for an approximate 1.5 mile walk down the south side of Fickle Hill to Jacoby Creek. This walk is along an improved logging road on private land. Please respect the land owner's property, don't litter. Please don't stray from the road, it is relatively easy to get lost. Points along the way corresponding to entries in this guide are marked with numbered signs. (Figure 2)

1 The first part of the walk down the S. flank of Fickle Hill traverses Franciscan Melange terrain. Dark, highly sheared shaley melange matrix containing blocks of graywacke sandstone, chert, greenstone, greenschist and blueschist is exposed along the route. These rocks make up the thrust sheet comprising the top of Fickle Hill. Basin like

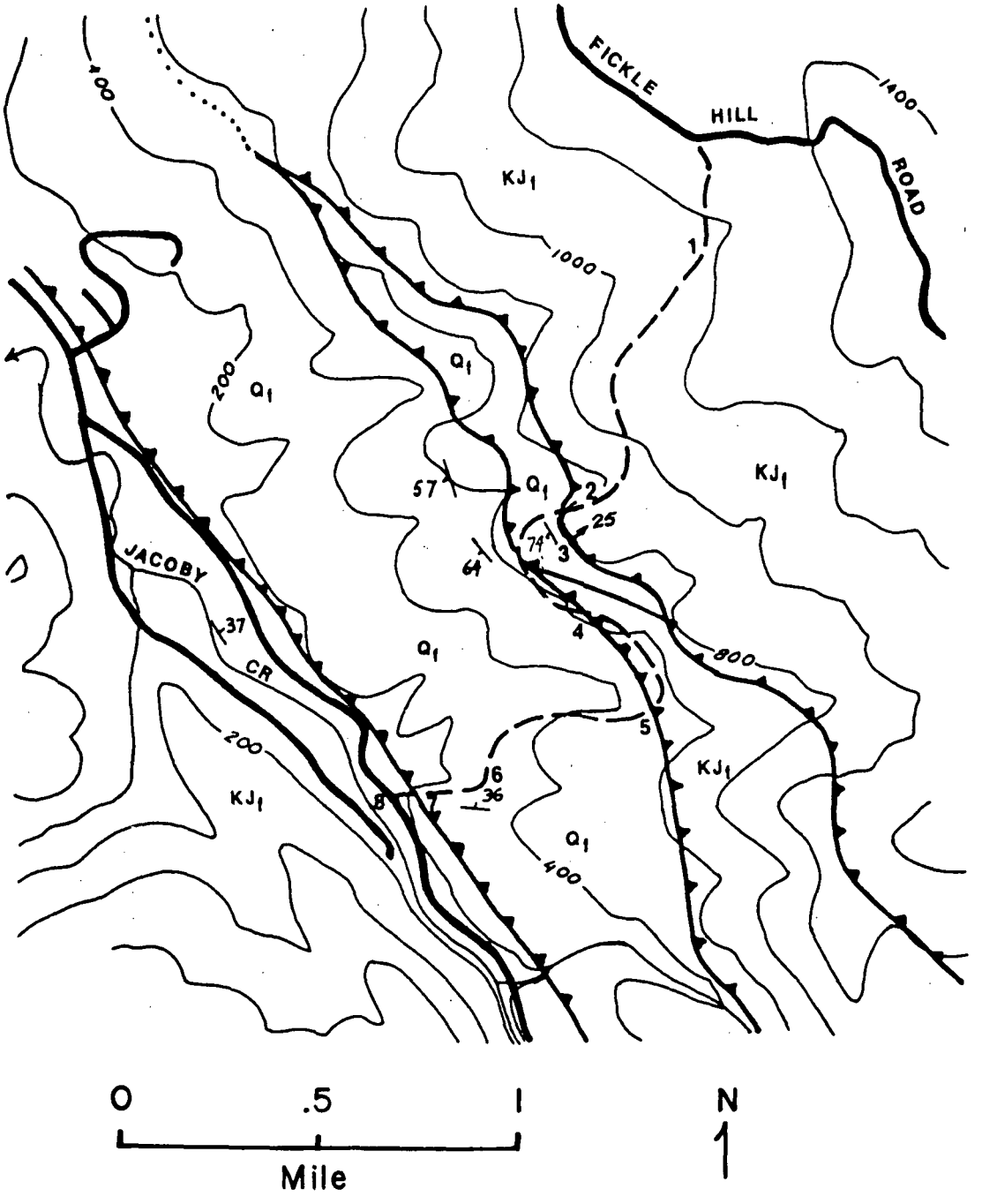

Figure 2. Generalized geologic map of the south slope of Fickle Hill along the field trip route. The dashed line shows the approximate location of the logging road followed on the walking part of the trip. Locations discussed in the field guide are numbered along the route. Q_f - Falor Formation. K_{Jf} - Franciscan Complex. The three thrust faults represent the main traces of the Fickle Hill fault.

heads of large slump-earthflows scallop the hillcrest. One of these forms the broad depression at the beginning of the walk.

Panoramic views of Humboldt Bay and the coast south to Cape Mendocino are afforded along this part of the route. The Samoa Peninsula, a late Holocene spit, separates the north part of Humboldt Bay (Arcata Bay) from the ocean. Humboldt Bay is surrounded by Holocene floodplains and delta complexes of the Mad River, Jacoby Creek, and several other streams. Holocene and latest Pleistocene fluvial terraces are present in Jacoby Creek Valley at the base of Fickle Hill. Eureka sits on a slightly elevated late Pleistocene marine terrace. Further south, Humboldt Hill, Table Bluff, and Cape Mendocino form headlands. Each is uplifted by large Quaternary faults and folds. The area occupied by the bay is tectonically depressed.

2 Fickle Hill fault. The Fickle Hill fault is exposed in the roadcut at this location. Sheared and faulted Franciscan melange is thrust over Falor Formation sand and pebbly sand on a fault surface oriented N65W25NE. Slickensides show that predominately dip-slip movement has occurred. The fault is marked by a brownish clay gouge containing broken and crushed sand grains of the Falor Formation and sheared fragments of Franciscan rocks. Closely spaced sub-paralled gouge filled faults cut the overthrust Franciscan. A conjugate pattern of fractures and faults also cuts the Falor sediments in the underthrust block. These are much better seen at STOP 3. Mapping along the southside of Fickle Hill suggests the Franciscan has been thrust over the Falor Formation a total of about 1 km on this and several parallel traces of the Fickle Hill fault.

3 Exposure in a logging landing on the Fickle Hill fault. The cut bank bordering this landing exposes a cross section through faulted Falor Formation sand and gravel. The fault contact between Franciscan rocks and Falor sediments is about 25 meters upslope. Intersecting sets of northeast and southwest dipping thrust faults and fractures from a conjugate fault pattern. Displacements on these secondary faults of the Fickle Hill fault range from a few millimeters to 0.5 meters. Bedding dips steeply to the south west. Conjugate faults and fracture like these are typical of exposures of northcoast thrust faults where they cut poorly consolidated Quaternary sands.

4 Limestone Creek. Near this location the walk crosses the second of the two main traces of the Fickle Hill fault. The massive Franciscan sandstone seen along the road for the next several hundred meters overlies a thick sequence of Falor sediments which extend from the fault contact to Jacoby Creek at the bottom of the canyon. Blocks of limestone derived from the Franciscan melange are present in the creek.

5 Junction with the J220 Road. The route crosses the concealed Fickle Hill fault near this road junction. Downslope from here to Jacoby Creek Falor Formation sediments are present but poorly exposed. A blanket of slump-earthflow deposits mantles the lower slopes of Fickle Hill and covers the Falor sediments with 10 to 20 meters of mixed landslide debris principally derived from Franciscan terraine upslope.

6 Junction with unnumbered logging spur. Roadcut exposures in the vicinity of this road junction show slump-earthflow deposits of Franciscan composition overlying Falor sands. The slump-earthflow deposits are relic to an early period of valley cutting and are now perched on interfluves of incised Jacoby Creek tributaries. Active slump-earthflows are present to the north and south of this locality where they follow the younger tributary drainages to Jacoby Creek. Derived from the overthrust Franciscan block which makes up the top of Fickle Hill, these slump-earthflows provide the sediment transport link between the tectonically supplied material in the upper slopes of the Fickle Hill and the fluvial system of Jacoby Creek.

7 The Jacoby Creek trace of the Fickle Hill fault. Conjugate northeast and southwest faults and fractures cut Falor Formation sand at the Jacoby Creek strand of the Fickle Hill fault. The fault pattern and outcrop expression is very similar to that seen at STOP 3. A late Pleistocene Jacoby Creek terrace is inset into the fault zone in the southern end of the roadcut exposure and its northern margin appears to be faulted, suggesting late Pleistocene movement of the fault.

8 Junction of the logging road with Jacoby Creek Road, end of the walk - rejoin the vans and eat lunch.

Earthflows in Franciscan melange, Van Duzen River basin, California

Harvey M. Kelsey
National Park Service
Redwood National Park
Orick, California 95555

BSTRACT

Large earthflows are a significant source of sediment in the highly ıeared and easily eroded Franciscan melange of the northern California oast Ranges. They are active during the winter wet season, and their ıovement averages 2.4 to 4.0 m/yr. Fluvial sediment yield from the gullied ıd broken earthflow surface is about equal to sediment yield by mass ıovement. Indirect evidence suggests that changes in vegetation cover due) grazing beginning in the nineteenth century may have increased the rate f earthflow movement.

ITRODUCTION

Giant earthflows are among the spec- cular geomorphic features of the Cali- rnia Coast Ranges. These are complex ndslides whose movement includes block iding, slumping, and viscous flowing. hey occur on many kinds of rock ranging age from pre-Jurassic to Cretaceous it reach their greatest development on anciscan melange, a rock unit consisting highly sheared sandstones and siltstones which are dispersed blocks and boulders greenstone, chert, schist, and serpen- ıe. Franciscan melange attains its great- t outcrop extent in the California Coast anges north of San Francisco. Earth- ɔws comprise roughly 10% of this elange area.

The earthflows in the Van Duzen River ısin, a 1,110-km² coastal watershed (lat 1°30'N, long 123°45'W) approximately 5 km north-northwest of San Francisco, e the subject of this report. The basin ıs dry summers, mild, wet winters, and ı annual precipitation from 100 to 250 ɑ, 90% of which falls between October ıd April. It is one of a number of ɔrthern California coastal basins with spended sediment discharges 5 to 50 nes that of any basin of comparable ze in the United States (Brown, 1973; own and Ritter, 1971; Judson and itter, 1964; Janda and others, 1975; ıott, 1971); the average long-term sus- nded sediment load of the Van Duzen is proximately 2,600 metric tons/km²•yr. he causes of these high sediment dis- ıarges are a subject of controversy, and rthflows are recognized as one of the significant sediment sources (Wahrhaftig and Curry, 1967; Kelsey, 1977).

EARTHFLOW SURFACE MORPHOLOGY

The Van Duzen earthflows head in large bowl-shaped hollows and have narrow, elongate midportions that terminate in bulbous toes at the river bed (Fig. 1). Smaller, less active earthflows are confined to midslope. Individual flows are 0.15 to 2.5 km long and 0.1 to 2.0 km² in area. The majority of earthflows occur on dry, south-facing slopes. Annual grasses are the predominant vegetative cover.

Active earthflow surfaces are bouldery and hummocky, have undulatory profiles, and commonly contain undrained depressions (Fig. 2). Because the surfaces are severely disrupted by mass movement, they have a dense network of parallel or dendritic bare-walled rill and gully systems; some of the parallel gully systems originate along longitudinal tension cracks. The drainage pattern constantly changes because of continued earthflow movement. The smaller rills and gullies that drain the bowl-shaped earthflow heads merge downslope into one axial gully, as much as 3 to 4.5 m deep (Fig. 2). The lateral margins of active earthflows are defined by vertical planes of shear along which slickenslides frequently develop. Commonly, 3- to 6-m-high, steep-walled colluvial ridges occur on the stable ground bordering the lateral margins.

Numerous dormant earthflows also occur in slope hollows on melange terrain and have a rolling, hummocky, "melted ice cream–type" topography. The margins of dormant flows are subdued, and creep has smoothed out the formerly sharp scarps and deep gullies.

Recurrent earthflow movement occurs each winter after fall and early winter rains thoroughly wet the colluvium. During seasonal movement, the earthflow toe protrudes out into the river and is gradually eroded back by high winter streamflows. Large blocks 2 to 15 m or more on a side, carried as part of the earthflow colluvium, are left in the channel when the finer debris is winnowed .

Figure 1. View of Halloween earthflow: this hummocky, gullied earthflow annually moves material into the Van Duzen River (river in foreground flowing toward earthflow toe).

away. The channel reaches adjacent to most earthflow toes are therefore clogged with these blocks; because these blocks armor the channel against downcutting, channel reaches adjacent to earthflow toes are unusually steep. As a result, the river gradient markedly steepens across melange terrain, even though hillslopes in the melange are generally not as steep as the neighboring, competent Franciscan sandstone slopes. Therefore, hillslope gradients are not clearly tied to channel gradients where earthflows move melange blocks into the river channel.

The mode of movement, surface morphology, and appearance of most earthflows is similar to that of alpine glaciers. In both earthflows and glaciers, movement is slow and the flow is laminar or confined to discrete shear planes. Both have stepped longitudinal profiles with alternating convex and concave segments; the profiles in both cases probably result from alternation between compressing flow in the concave segments and extending flow in the convex segments (Nye, 1952; Colman, 1976). The lateral ridges on the margins of earthflows are similar morphologically to moraines; but, unlike moraines, these ridges are due to the lateral pressure of the moving earthflow forcing up a welt in the stable ground along its sides.

SURVEYS OF EARTHFLOW MOVEMENT

Currently, 19 earthflows seasonally move into the Van Duzen River; I established stake lines across the lower portion of six of them to measure surficial movement. The stakes were placed 3 to 5 m apart in a line perpendicular to the direction of movement approximately 10 to 30 m above the earthflow toe scarp (Fig. 2), with end stakes positioned on stable ground. The stake lines were resurveyed each summer. The calculated downslope movement is the average displacement along the stake line. Most of the earthflows moved as one coherent unit, but some moved more rapidly in the center or near one margin.

Table 1 summarized movement histories and annual precipitation for the monitored earthflows. One flow was surveyed for three seasons, one for two seasons, and four for one season only, because the landowners denied access after the first year. The season during which all six were monitored had average precipitation, and earthflow movement ranged from 26 m on the Halloween earthflow to 0.6 m on the Donaker earthflow. The average annual movement rate for the earthflows other than the Halloween flow was 2.4 m, with a standard deviation of 1.8 m. Studies by the California Department of Water Resources (1973) of eight earthflows in Franciscan melange along the Eel River (35 to 100 km south of the Van Duzen) gave similar movement rates: practically all movement ranged from 0.3 to 9.0 m/yr and averaged 4.0 m/yr; however, three of the flows surged tens of metres during winters of exceptionally heavy rainfall.

On Halloween earthflow, the most thoroughly studied, three stake lines were monitored for three winter seasons (Table 1). The repetitive surveying of these stake lines showed that the flow accelerated as it moved downslope (Fig. 3). The lowest stake line (58 m wide and 26 m above the river) moved 5.5 times as fast as the upp stake line (124 m wide and 235 m upslo of the river). The downslope acceleratio in earthflow motion is shown especially well for seasonal movement on stake line In the first two seasons, stakes were lost solely due to bank sloughing into the axi gully; by the end of the third season, the stake line had moved to the vicinity of th earthflow toe, and more than half the stake line was lost by slumping of the t into the river. The lowest stake line continuously slumped into the river and wa abandoned at the end of the second seas

The acceleration in flow going downslope is accompanied by a decrease in earthflow thickness. Assuming that the thickness of the Halloween earthflow at line 2 is 12 m (a bit more than the 10.5

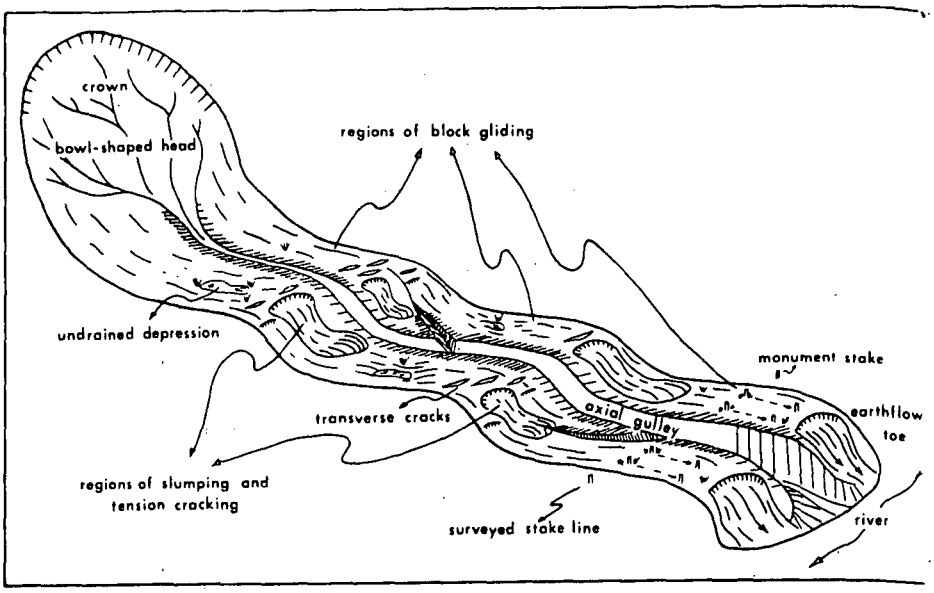

Figure 2. Schematic drawing of an earthflow landslide showing prominent geomorphic featu and position of earthflow stake line.

TABLE 1: EARTHFLOW MOVEMENT HISTORIES FOR SIX MONITORED EARTHFLOWS: VAN DUZEN RIVER BASIN

Name of Earthflow	1973-74 Winter Season A*	B†	C§	D#	1974-75 Winter Season A	B	C	D	1975-76 Winter Seas A	B	C
Donaker earthflow					166	0.8	0.6	1.02	114	1.1	0.8
Cashlapooda Cr. earthflow					197						
west tongue						3.5	1.7	0.62			
east tongue						3.1	1.7	0.65			
Broken Road earthflow					197						
west tongue						1.8	1.7	0.48			
east tongue						1.6	1.2	0.51			
Chimney Rock earthflow					197	8.1	5.3	4.19			
Falling Tree earthflow					197	4.5	2.7	2.78			
Halloween earthflow	244	21.3	20.1	8.84	197	29.0	25.6	11.24	117	28.7	25.9

* Annual precipitation (cm).
† Maximum movement at earthflow toe (m).
§ Average movement across earthflow toe (m).
# Volume of sediment discharged to channel ($m^3 \times 10^3$).

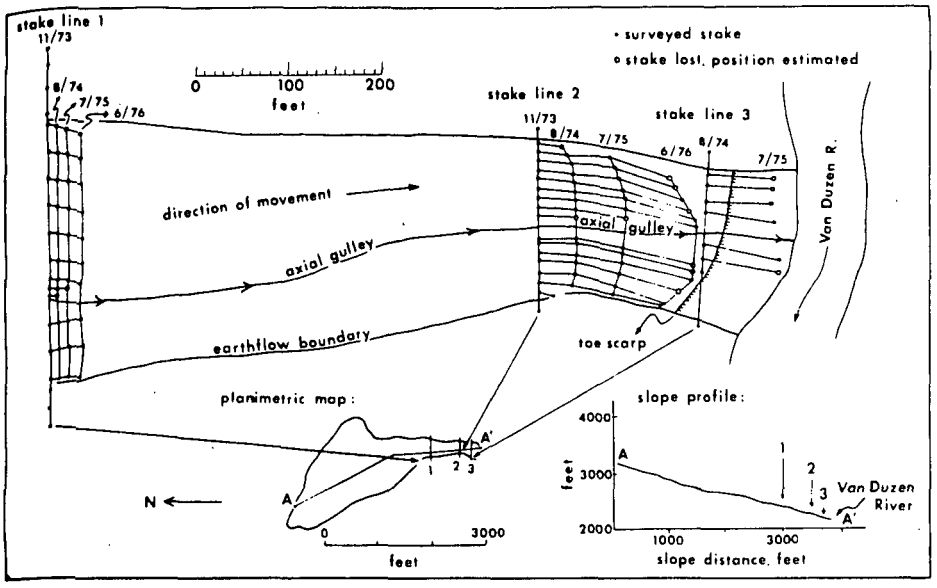

Figure 3. Planimetric map of lower portion of Halloween earthflow showing movement on three surveyed stake lines for three winter seasons.

thickness of the nearby toe), and that an approximately equal amount of earthflow material moves past lines 1 and 2, then the thickness at line 1 is approximately 30 m. The thickness of the slower-moving upper half of the earthflow must, therefore, exceed 30 m. For comparison, the California Department of Water Resources (1970) drilled into two Eel River earthflows at midslope localities to determine their depths. Deformation of the casings in these drill holes over the following winter showed that the depth of these earthflows ranged between 30 and 35 m.

The Halloween earthflow surveys also document the substantial sediment yield each winter by bank erosion along the axial gully. On each of the upper two stake lines, approximately 20 ft of gully bank retreat occurred in three years due to bank corrasion by high flows as well as to the inward mass movement of the flow toward the low created by the axial gully. Though the gully banks continually moved inward as the entire gully moved downslope, a net widening of the gully occurs due to bank sloughing.

EARTHFLOW SEDIMENT PRODUCTION: 1941–1975

The total movement and the total amount of sediment production from active earthflows for the period 1941–1975 was determined from the surveying data as well as from five sets of aerial photographs going back to 1941. Measuring the displacement of vegetation on sequential aerial photography enabled a determination of movement rates for the 13 unmonitored earthflows. The average movement rate for the 19 Van Duzen earthflows during this period was 3.1 m/yr, with a standard deviation of 2.0 m. Total sediment discharge to the Van Duzen River by earthflow mass movement during this period was 1,409,500 m^3 or 2,960,000 metric tons ($\rho_{colluvium}$ = 2.1 g/cm^3). This erosion by mass movement is equivalent to an annual sediment yield of 24,900 metric tons/km^2 from the 3.4 km^2 of earthflow surface, or an average of 1.0 m of surface lowering per century (ρ_{rock} = 2.5 g/cm^3).

Sediment sampling, between October 1974 and May 1976, of the creek that drains the Donaker earthflow (Kelsey, 1977) showed that gullying on the earthflow surface produces approximately 26,300 metric tons/km^2•yr. If it is assumed that the yield for this earthflow watershed is representative of gully and rill erosion from active earthflows with highly disrupted surfaces, then most earthflows contribute approximately equal amounts of sediment to the channel by gullying and mass movement. The total annual sediment yield from earthflow slopes (51,200 metric tons/km^2) undoubtedly is one of the highest in the U.S., and is more than an order of magnitude greater than the average sediment yield for the upper 570 km^2 of the Van Duzen basin for the same period (2,570 metric tons/km^2).

INFERENCES ON THE NATURE OF EARTHFLOW MOTION

The seasonal ground wetting of earthflow slopes, which increases pore water pressure and reduces intergranular friction, is the major factor contributing to earthflow movement. Monitoring studies indicate that after initial wetting during the first two or three rains, major episodes of movement coincide with periods of heavy rainfall.

Though ground wetting initiates seasonal earthflow movement, a major factor contributing to both the seasonal duration and the rate or motion appears to be the removal of lateral support by erosion of the toe. The toes of some of the most active flows, including the Halloween slide, are located on the outside of sharp river bends that receive the maximum erosive force of winter streamflows. In the case of the Donaker flow, the blasting away—more than a century ago—of a protruding ledge that diverted the river into the toe resulted in a notable decrease in earthflow movement rate. As another example of the influence of toe erosion, a major flood in December 1964, which caused a tremendous amount of streambank erosion, reactivated eight dormant earthflows and significantly increased the rate of movement of at least six other already active flows. Because lateral support exerts a significant control on movement, sliding appears to be a more important movement mechanism than true flow.

The surface of most earthflows alternates in appearance between a smooth, relatively unbroken grassy surface showing only a small amount of internal rotation, shear, or distortion, and a broken, hummocky, relatively steeper surface with small scarps and surficial slumps indicating shearing within the moving layer (Fig. 2). The flatter, less disrupted earthflow segments move downslope in a manner best described as block glides. In contrast, the steeper, more disturbed earthflow segments are the regions where extensional deformation over the slope convexities is being transferred to compressional deformation over the concave slope segments. Surficial expression of compressing flow is not common, though pressure ridges or furrows develop parallel to the slope contour on the higher portion of some earthflows. Extending flow in the convex slope portions results in transverse tension cracks, which are probably the precursors of the shallow slumps that are common on the steeper earthflow slopes. The movement mechanism of most larger earthflows, therefore, alternates between

gliding without significant internal deformation and slumping-flowing with substantial internal shear (Fig. 2). The lobate form of the toe plus the piling up of earthflow colluvium behind large blocks in the earthflow are evidence of flow within the earthflow mass above the sliding plane. Small earthflows are not as complex but rather are one large slump block with secondary surficial slumping and flowing.

Earthflow surges (abnormally large displacements in one or a few seasons) have been observed in some earthflows and may be a phenomenon of many. Surges can probably be triggered during a major streamflow when the toe is substantially eroded back, changing the distribution of mass above the sliding plane and altering the balance of forces. An example of such a surge is the recent activity of the Halloween earthflow, whose current movement (Table 1) is much greater than the average movement rate of 7.0 m/yr for 1941–1973. Surges can also be caused by earthquakes: during the 1906 San Francisco quake, an earthflow surge caused a temporary blockage of the Eel River (California Department of Water Resources, 1973). Intermittent pulses of accelerated earthflow movement have also been suggested for slower-moving, forested earthflows in the western Cascades of Oregon (Swanston and Swanson, 1977).

INCREASED EARTHFLOW ACTIVITY SINCE EUROPEAN SETTLEMENT

Earthflows erode faster than the melange terrain on either side of them, and they create bowl-shaped depressions in their upper portions. Given the current measured erosion rate of an active earthflow and the volume of the depression formed by the flow, it is possible to calculate the time necessary for the depression to form. For the two Van Duzen earthflows with the deepest headward depressions (Donaker and Halloween flows), the time required to create the depressions by both mass movement and fluvial processes is 2,400 and 650 yr, respectively. Considering that climatic and tectonic conditions were probably conducive to earthflow movement during a large portion of the Quaternary (even though it is unlikely any single earthflow moved continuously throughout this time), these time intervals are quite short and suggest that current earthflow erosion rates are anomalously high.

The melange grasslands have been extensively grazed since 1870, and the onset of grazing caused an almost immediate change in vegetative cover from the native, deep-rooted, perennial grasses to introduced, shallow-rooted annual grasses (Gene Conrad and Dennis Anderson, 1977, oral communs.). The grass-species change resulted in a weaker vegetation mat with less root-induced shear strength (Waldron, 1977). The weaker grass cover may well have led to the increased surface breakage, gullying, and slumping that promote ground wetting and increase the potential for earthflow movement.

EARTHFLOWS AND EROSION OF THE VAN DUZEN BASIN

Active earthflows in the Van Duzen basin erode an order of magnitude faster than the surrounding Franciscan terrain, and this terrain is the most rapidly eroding region of its size in the conterminous United States. The 19 active Van Duzen earthflows comprise less than 1% of the upper 570 km^2 of the basin, yet they account for approximately 10% of the total sediment yield from this rapidly eroding watershed.

REFERENCES CITED

Brown, W. M., III, 1973, Streamflow, sediment, and turbidity in the Mad River basin, Humboldt and Trinity Counties, California: U.S. Geological Survey Water Resources Investigations 36-73, 57 p.

Brown, W. M., III, and Ritter, J. R., 1971, Sediment transport and turbidity in the Eel River basin, California: U.S. Geological Survey Water Supply Paper 1986, 70 p.

California Department of Water Resources, 1970, Middle Fork Eel River landslide investigation: California Department of Water Resources Memorandum Report, 120 p.

—1973, Geology and sediment production for ten Eel River landslides: California Department of Water Resources Memorandum Report, 29 p.

Colman, S. M., 1976, Inherent factors in the flow of valley glaciers as a possible influence in the formation of stepped glacial valleys: Zeitschrift Geomorphologie, v. 20, p. 297-307.

Janda, R. J., Nolan, K. M., Harden, D. R., and Colman, S. M., 1975, Watershed conditions in the drainage basin of Redwood Creek, Humboldt County, California, as of 1973: U.S. Geological Survey Open-File Report 75-568, 267 p.

Judson, S., and Ritter, D. F., 1964, Rates of regional denudation in the United States: Journal of Geophysical Research, v. 69, p. 3395-3401.

Kelsey, H. M., 1977, Landsliding, channel changes, sediment yield, and land use in the Van Duzen River basin, north coastal California, 1941-1975 [Ph.D. thesis]: Santa Cruz, University of California, Santa Cruz, 370 p.

Knott, J. M., 1971, Sedimentation in the Middle Fork Eel River basin, California: U.S. Geological Survey Water Resources Division Open-File Report, 60 p.

Nye, J. F., 1952, The mechanics of glacier flow: Journal of Glaciology, v. 2, p. 82-93.

Swanston, D. N., and Swanson, F. J., 1977, Timber harvesting, mass erosion, and steepland forest geomorphology in the Pacific northwest, *in* Coates, D. R., ed., Geomorphology and engineering: Stroudsburg, Pa., Dowden, Hutchison and Ross, p. 199-221.

Wahrhaftig, C., and Curry, R. R., 1967, Geologic implications of sediment discharge records from Northern Coast Ranges, California, *in* Man's effect on California watersheds: Report of the California Assembly Committee on Natural Resources, Planning, and Public Works, Subcommittee on Forestry and Watershed Management, Part III, p. 35-58.

Waldron, L. G., 1977, The shear resistance of root-permeated homogeneous and stratified soil: Soil Science Society of America Journal, v. 41, p. 843-849.

ACKNOWLEDGMENTS

Reviewed by R. J. Janda, F. Swanson, and C. Wahrhaftig. Financial support from Sigma Xi Grants-in-Aid of Research. Logistical support from University of California at Santa Cruz; Department of Public Works, Humboldt County, California; California Department of Water Resources, Red Bluff, California; and U.S. Geological Survey, Menlo Park, California. Surveying assistance from J. Duls, A. Allwardt, T. Stephens, and T. Pratte.

MANUSCRIPT RECEIVED DEC. 23, 1977
MANUSCRIPT ACCEPTED MARCH 24, 1978

A sediment budget and an analysis of geomorphic process in the Van Duzen River basin, north coastal California, 1941–1975: Summary

HARVEY M. KELSEY *National Park Service, Redwood National Park, P.O. Box SS, Arcata, California 95521*

The Coast Ranges of northern California are the most rapidly eroding region of comparable size in the United States (Judson and Ritter, 1964; Brown and Ritter, 1971). This area has undergone recent (post-Miocene) uplift and is underlain by highly deformed and faulted sandstone and melange units of the Franciscan assemblage. This study investigates the sources of the large amount of sediment, the processes by which the sediment moves, and the times of sediment transport in the upper half of the Van Duzen River basin in the California Coast Ranges (Kelsey, 1977). The Van Duzen is the northernmost tributary of the Eel River and flows into the Eel at a point ~ 480 km north of San Francisco (Fig. 1). I documented sediment transport and changes in hillslope and channel morphology during the period 1941–1975 by using six sets of aerial photographs, early land surveys, U.S. Geological Survey water and sediment discharge records, and data from surveying and sediment sampling for 1973 to 1978.

The climate consists of high annual rainfall (125 to 250 cm) that occurs mostly from October through April; the majority of the sediment transport occurs each winter during the two to six most intense storms. Infrequent high-intensity storms of long duration, which are major sediment-transporting events, recur every 100 to 500 yr. One such storm occurred in December of 1964, and it serves as a major focus of this study.

The two main physiographic types in the Van Duzen basin are (1) grasslands and grass-oak woodlands underlain by melange; and (2) the more competent, forested sandstone slopes. Whereas the competent sandstones and siltstones form straight, forested slopes with relatively sharp ridge crests and V-shaped canyons, the Franciscan melange hillslopes range in morphology from smooth, undulating grassland or grass-oak woodland slopes to hummocky, boulder-strewn, poorly drained grasslands sculpted by active mantle creep or earthflow landslides. Since European settlement in the 1870's, grazing has been the major grassland land use. Timber harvesting on the sandstone slopes started in about 1950 and still continues. The lower portion of the study area was extensively logged prior to the 1964 storm, but the upper watershed was not logged until after 1965.

This study presents a sediment budget that summarizes the major erosional and depositional processes in the Van Duzen basin during the 35-yr study period (Table 1). Although the budget spans 35 yr (1941–1975), major changes in slope sta-

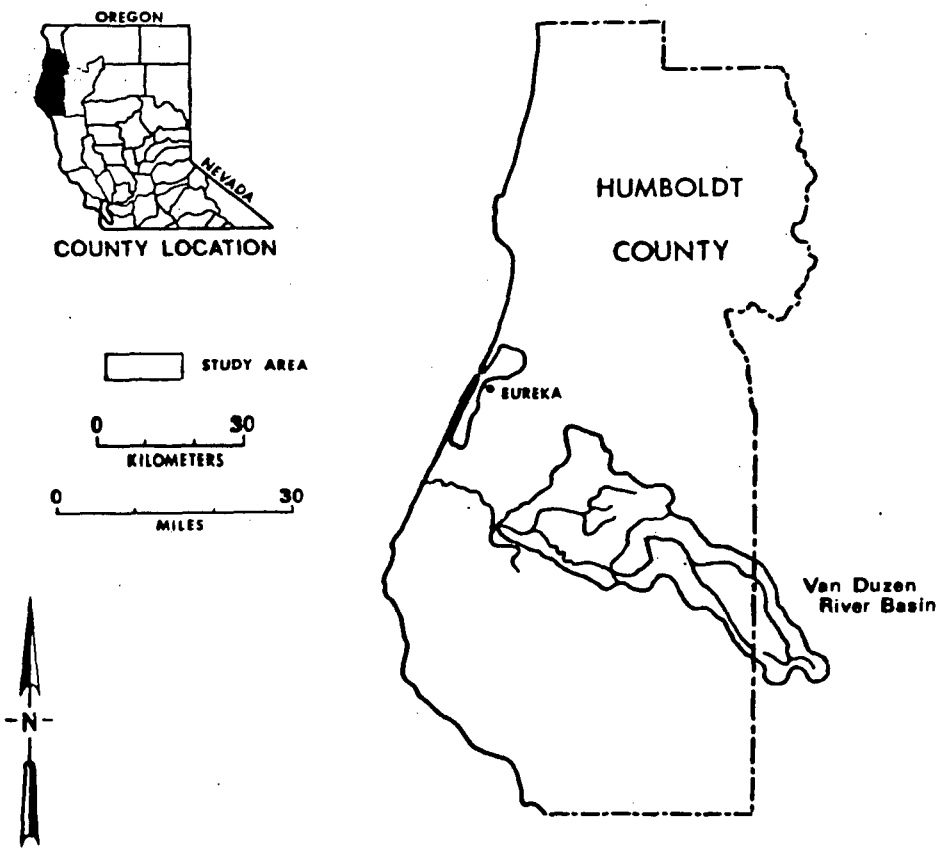

Figure 1. Location map of the 1,111-km² Van Duzen basin, showing the 575-km² study area in the upper half of the basin. This illustration appears as the upper part of Figure 1 in the accompanying article in *Part II*.

The complete article, of which this is a summary, appears in *Part II* of the *Bulletin*, v. 91, no. 4, p. 1119–1216.

Geological Society of America Bulletin, Part I, v. 91, p. 190–195, 4 figs., 2 tables, April 1980, Doc. no. S00402.

TABLE 1. COMPARISON OF ACTUAL COMPUTED SEDIMENT BUDGET TO HYPOTHETICAL SEDIMENT BUDGET EXCLUDING THE EFFECTS OF THE DECEMBER 1964 STORM FOR THE VAN DUZEN BASIN, 1941–1975

	Actual sediment budget (metric tons)	Hypothetical budget without 1964 storm (metric tons)
Fluvial sediment yield from hillslopes	45,509,000	38,254,000
Landsliding		
Debris slides, debris avalanches	10,630,000	1,120,200
Earthflows	2,931,000	1,834,500
Streambank erosion		
Melange bank erosion	426,000	66,100
Flood plain and fill terrace erosion	2,619,000	131,000
Aggradation	10,601,000	none
Total sediment discharge out of basin	51,036,000	41,405,000

bility, channel morphology, and sediment transport are largely due to the effects of the December 1964 storm and flood, and the budget is therefore weighted by the effects of the storm. Because the 1964 storm is an infrequent event, I also present a hypothetical budget that estimates sediment transport if the 1964 storm had not occurred (Table 1). The differences between the two budgets point out those geomorphic processes most influenced by the 1964 storm.

The vast majority of landslides occur on basin slopes immediately adjacent to the main channels or on headwater slopes where landslide debris moves directly into headwater tributaries. Earthflow landslides (Kelsey, 1978) are confined to grassland slopes underlain by highly sheared Franciscan melange. They seasonally move colluvial debris into the major channel at rates that average from 2.4 to 4.0 m/yr. Earthflow colluvium is composed primarily of fine-grained, sheared siltstone and is carried away in suspension upon entering the river. In contrast, debris slides occur in competent massive Franciscan sandstone units on basal slopes bordering the Van Duzen and South Fork Van Duzen Rivers. Debris avalanches are most common on competent sandstones and siltstones in the headwater region where they occur in the mid-slope or upper-slope areas. Both debris slides and debris avalanches deliver coarse material to the channels, ~ 70% of which cannot be carried away in suspension and remains in the channel to be slowly transported as bedload during major streamflow events. A large amount of debris sliding and avalanching occurred during the December 1964 storm, which resulted in widespread channel aggradation.

Bank erosion along main channels and in headwater reaches is confined mainly to unconsolidated alluvium in flood plains and along stream reaches where bare melange colluvium makes up the channel margins. Bank erosion is a slow, persistent process each winter, but relatively short periods of accelerated bank retreat triggered by unusually high streamflows and associated channel aggradation probably account for most of the bank erosion.

Fluvial erosion from hillslopes is a highly significant sediment transporting process on melange grassland and grass-oak woodland slopes but is of negligible importance on forested sandstone slopes. High fluvial erosion rates in melange terrain are mainly due to extensive gullies developed on slopes subject to active mantle creep or faster, earthflow movement. The more mobile hillslopes have increasingly greater surface breakage and disruption and subsequently a higher density of gullies than more stable terrain. Mobile earthflow melange slopes with high gully density have the greatest fluvial erosion rate.

The text of the extended report in *Part II* describes in detail the geomorphic processes operating in the basin and the quantitative data which form the basis for the sediment budget and the estimates of recurrence intervals of episodic events such as debris sliding and major channel aggradation. Following are the most significant findings of the study.

A major portion of the sediment discharge (45%) comes from a small fraction of the basin study area (5.5%) that consists of (1) the most densely gullied grassland slopes, (2) earthflow landslides in the melange, and (3) debris slides and avalanches in the Franciscan sandstone units. Most of the remaining sediment comes from moderately gullied grassland slopes with no large landslides. Forested slopes not directly adjacent to major streams contribute a minimal amount of sediment, even though they constitute 57% of basin area.

The December 1964 flood, which lasted for about three days, mobilized a large quantity of sediment; it alone accounted for 7% of the suspended sediment discharge during the 35-yr study period and mobilized, for the short flood period, almost as much bedload as moves out of the basin in a century.

The storm and flood caused massive amounts of debris sliding and avalanching. On streamside sandstone slopes in the lower portion of the study area, timber harvesting initiated debris sliding even before the 1964 storm, but many of the areas of the most extreme debris sliding were those where the 1964 storm and flood greatly enlarged slope failures initiated by timber harvest and road construction. In addition, bank corrasion by flood flows initiated many new debris slide failures on both logged and unlogged slopes. Table 2 shows the influence of large storms and timber harvesting on the time of initiation of debris slides in the lower part of the basin. Although logging significantly influenced the number and location of debris slides on basal slopes, the 1964 flood was responsible for actually mobilizing most of the material that entered the river from these debris slide failures. Logging is an effective trigger for debris slide events, but significant amounts of mass slope movement and sediment transport require the geomorphic work provided by large storms and floods.

Extensive storm-caused debris avalanching occurred on the unlogged headwater slopes, indicating that the 1964 storm would have been a major erosional event without any human modification of the basin (Fig. 2). The increase in bare slope and channel areas caused by this avalanching and channel widening in the headwater region significantly increased upper basin water yields compared to hydrologic conditions before the 1964 storm.

A storm and flood of similar magnitude to that of 1964 occurred in December of 1955, but the 1955 storm had minimal impact on streamside slope stability and channel geometry. The reason for the difference in geomorphic response is not obvious because the storms were more notable for their similarities than their differences (Harden and others, 1978). Perhaps the

TABLE 2. DEBRIS SLIDES IN LOWER WATERSHED — INITIAL OCCURRENCE OF SLOPE FAILURES AND AMOUNT OF SEDIMENT DELIVERED TO CHANNEL

	Total number of failures*	Occurrence of initial failures relative to time of 1964 flood†			Amount of sediment delivered to channel, metric tons × 10^3 (ρ = 1.92 g/cm^3)		
		Pre-flood	At time flood	Post-flood	Pre-flood	At time of flood	Post-flood
Slope failures in logged areas	56	52%**	37%††	11%	477	4769	123
Slope failures in unlogged areas‡	26	19%	77%	4%	77	1139	4

* Logged and unlogged land approximately equal in area.
† Pre-flood: 1941 through Dec. 1964; time of flood: Dec. 1964; post-flood: 1965–1975.
‡ Unlogged areas do not have any logging roads.
** 79% of these failures occurred on slopes traversed by logging roads.
†† 59% of these failures occurred on slopes traversed by logging roads.

1955 storm did initiate cracks on the steeper hillslopes, priming the slopes for massive failure during a succeeding large storm. It is certain that the timing of logging operations in the lower Van Duzen basin rendered hillslopes more prone to failure in 1964 than in 1955 because sufficient time had elapsed after logging to allow for the loss of slope shear strength due to the decay of tree roots.

Debris sliding and avalanching during the 1964 flood contributed a large amount of coarse alluvial debris (10,601,000 t) to main river channels, causing from 1 to greater than 3 m of aggradation (Figs. 3 and 4); this aggradation buried former incised channels and triggered a period of prolonged and widespread bank erosion. In the 15 yr following the flood, some aggraded channel reaches have started to degrade after reaching peak stream-bed elevations 5 to 8 yr after the flood (Fig. 4), while other reaches are not degrading (or degrading very slowly) due to channel armoring by large flood-deposited clasts, as well as to the continued supply of coarse alluvium from aggraded upstream reaches (Fig. 3). Bank erosion is still continuing on many reaches, regardless of whether the reach is degrading or not (Fig. 4). Almost one-fifth of the total

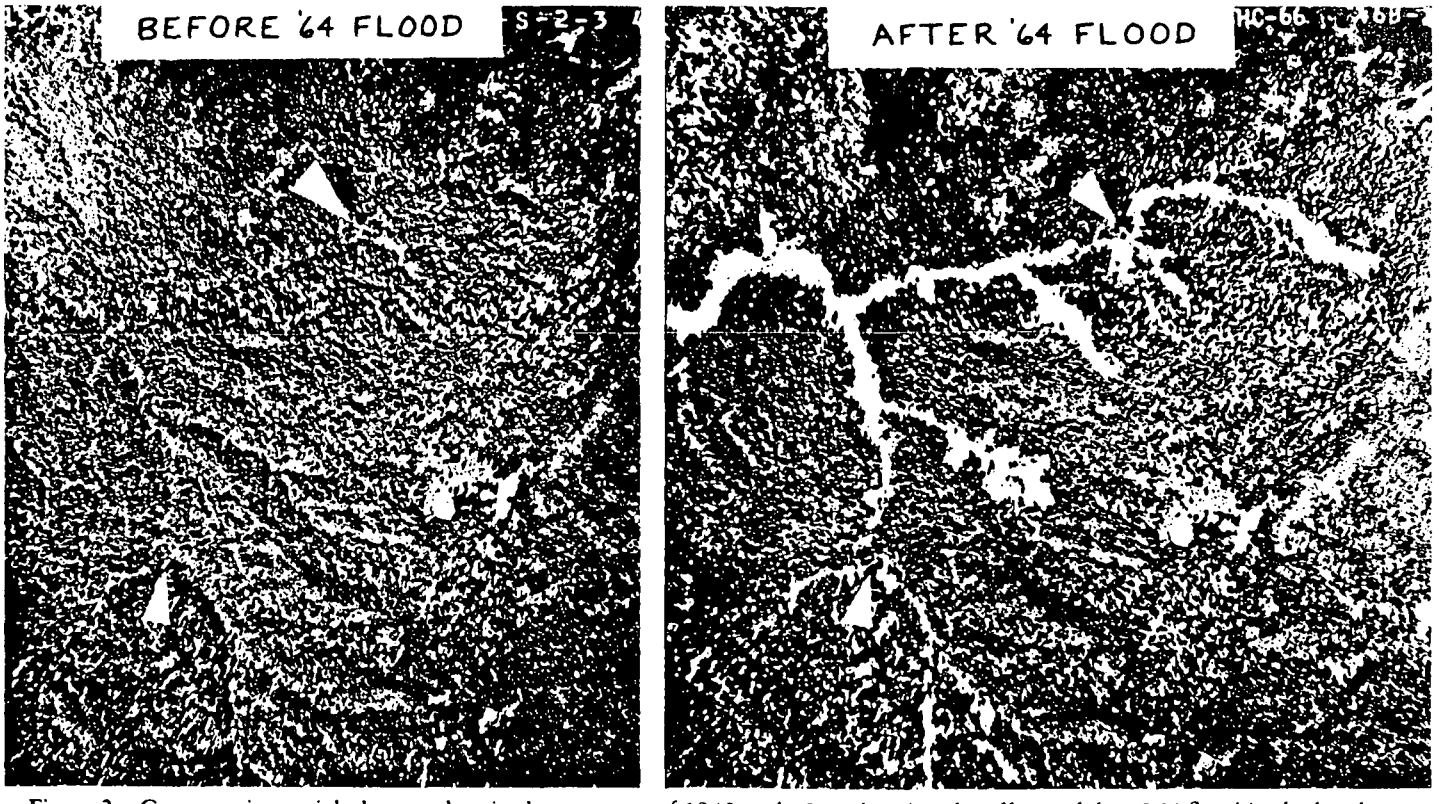

Figure 2. Comparative aerial photos taken in the summers of 1963 and 1966 showing the effects of the 1964 flood in the headwaters of the South Fork Van Duzen. White arrows identify the same channel locations on both photos. The post-flood photo shows four elongate debris avalanches that converge downslope into debris torrents along existing channels. Bank erosion in the channel reaches downstream of the avalanches initiated smaller streamside slides that can be seen in the post-flood photo. This illustration appears as Figure 11 in the accompanying article in *Part II*.

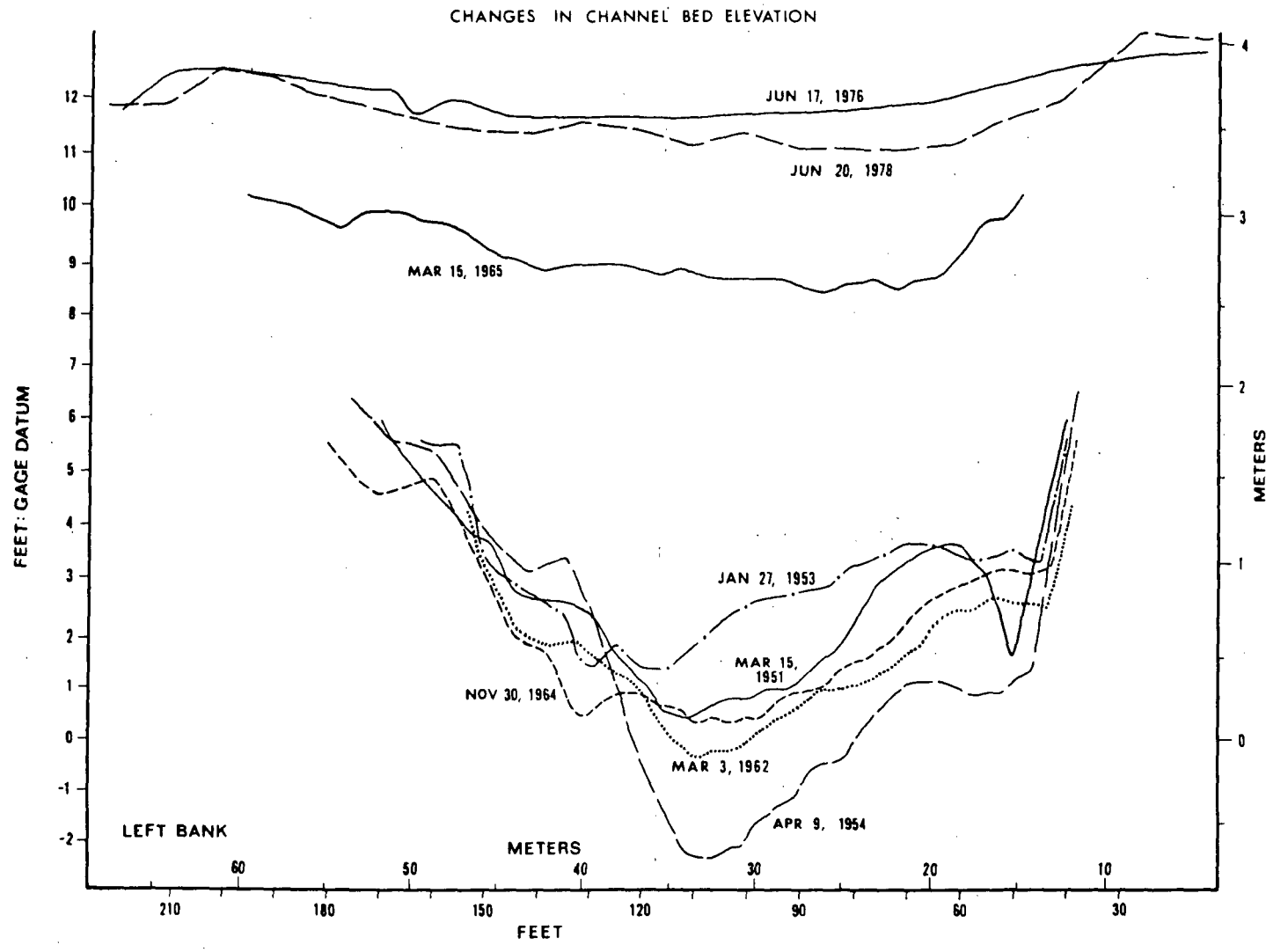

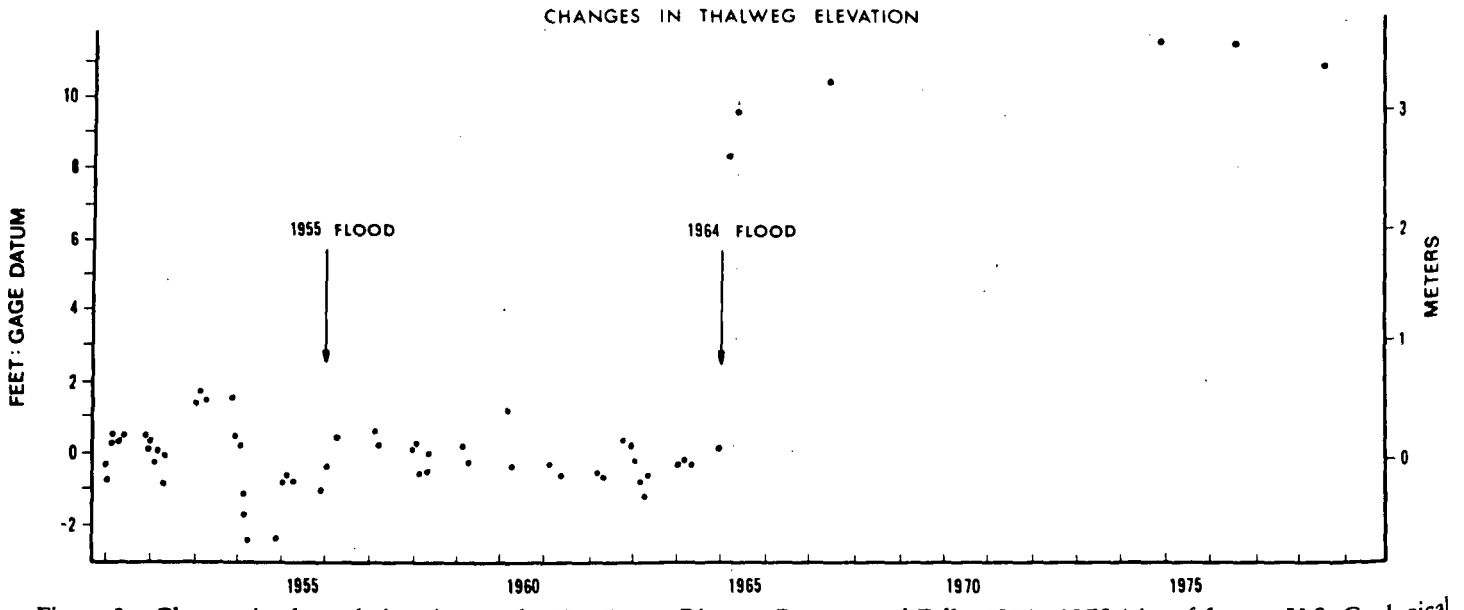

Figure 3. Changes in channel elevation on the Van Duzen River at Pepperwood Falls, 1951–1978 (site of former U.S. Geological Survey gage 11-4785). This illustration appears as Figure 18 in the accompanying article in *Part II*.

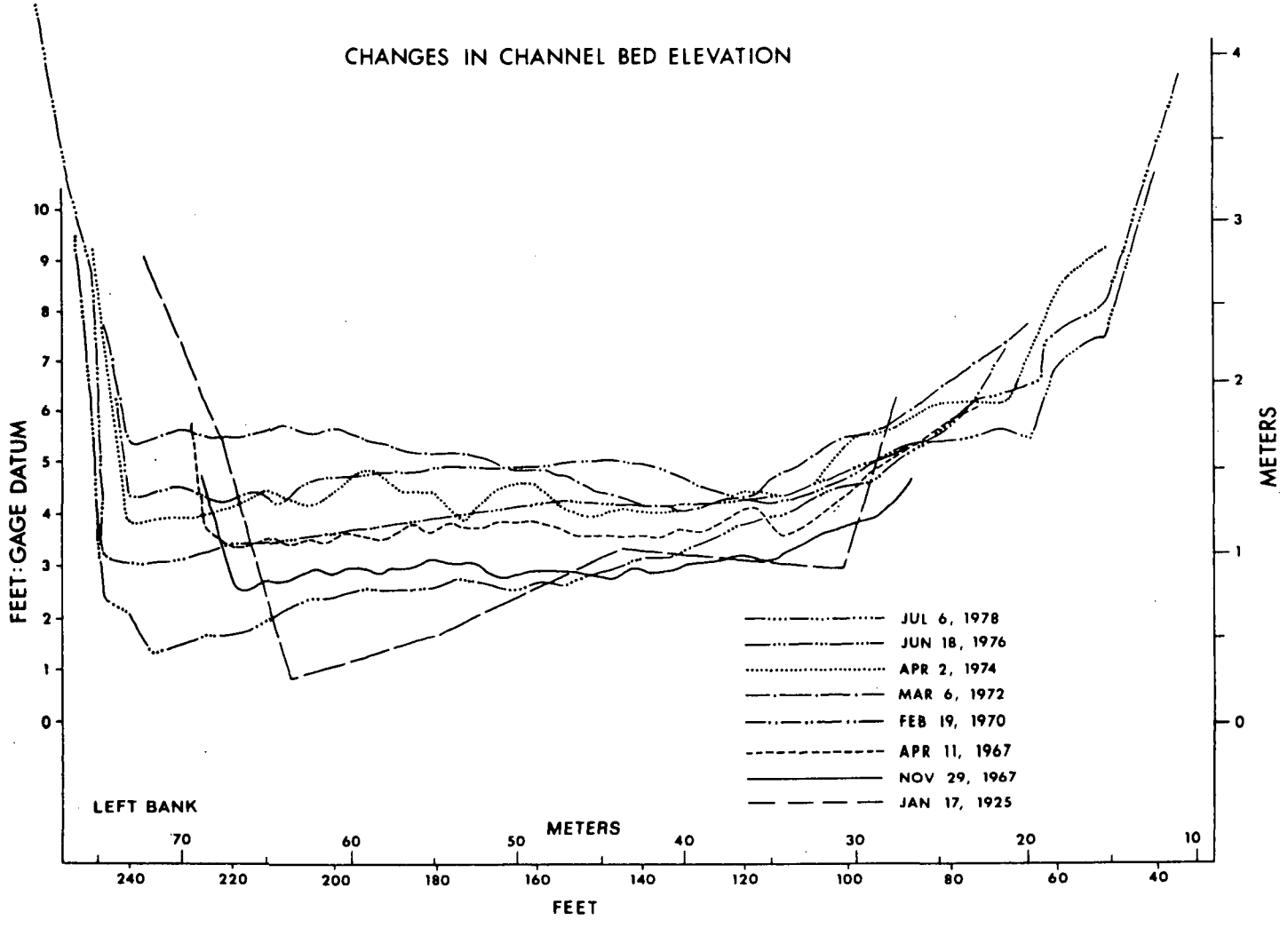

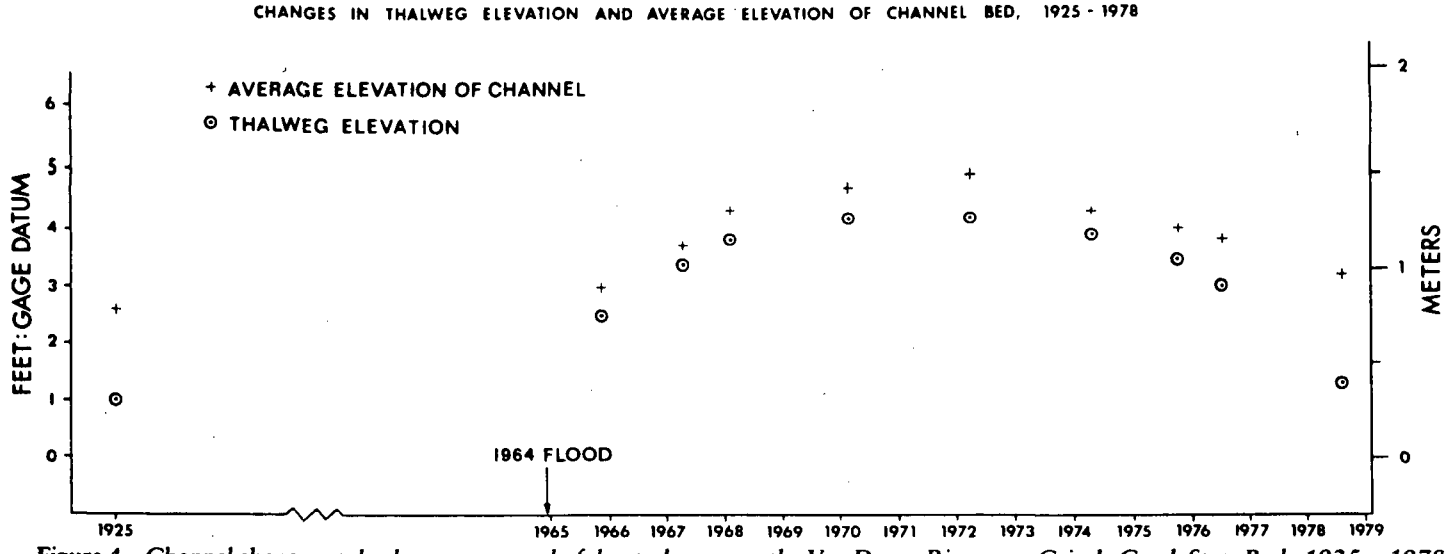

Figure 4. Channel changes at the downstream end of the study area on the Van Duzen River near Grizzly Creek State Park, 1925—1978 (U.S. Geological Survey gage 11-4785). This illustration appears as Figure 20 in the accompanying article in ***Part II***.

sediment supplied to the channel during the study period is stored (as of 1975) as aggraded sediment in major stream channels.

On the basis of dating of debris avalanche-originated channel fills which form multiple levels of terraces along headwater channels, it appears that episodes of debris avalanching on steep headwater slopes in the upper basin have recurrence intervals of from ~ 300 to greater than 500 yr. The episodic introduction of large quantities of avalanche debris to headwater channels results in a pulse of aggradation which migrates down upper watershed channels at ~ 1 km/yr. Similar migrating pulses of aggradation cannot be documented in the higher-order channel of the Van Duzen River in the lower part of the study area, despite substantial aggradation in this channel reach, because of the fluctuations in channel gradient and the more complex routing of alluvium from diverse source areas through the main channel.

In summary, the major sediment source areas are the erosive grassland slopes (including earthflows) underlain by melange and debris slides and avalanches in the sandstone units, which together account for more than 90% of the sediment introduced to the Van Duzen River from only one-third of the basin area. Landslide areas alone (earthflows, debris slides, and debris avalanches) account for a quarter of the total sediment input to trunk streams from only 1% of basin area.

The 1964 storm caused 49% more sediment to enter the Van Duzen basin in the period 1941–1975 than would have been the case without the storm (Table 1). This increase was due to landsliding and bank erosion on trunk streams (64%) and increased fluvial transport off hillslopes (36%). No channel aggradation would have occurred without the 1964 storm. It appears that major landscape-altering storms such as that of 1964 recur on the average every 200 to 600 yr, on the basis of studies of alluvial fills generated by avalanching in the Van Duzen basin and elsewhere (Helley and LaMarche, 1973). The sediment budget for 1941–1975 therefore represents relatively high sediment transport that occurs approximately once every third or fourth century. However, recent land use has affected the land surface to a significant but undetermined extent, and the 35-yr budget that I present may now be more representative of future long-term rates of sediment transport than it would have been prior to intensive land use.

The current large sediment yield from melange grassland slopes results from extensive gullying and slumping that appear, in large part, to be recent features of the landscape; these features most likely reflect the impacts of grazing, and especially the weakening of the vegetation mat by the replacement of the native prairie bunch grasses by weaker, short-rooted annual grasses. This grassland species conversion occurred quite rapidly after the advent of grazing in about the 1870's, and many of the most obvious sources of sediment from the grasslands, such as shallow, extensive gully networks and small slump failures, do not appear more than a century old and could have commenced after prairie vegetative change.

Of the many factors which influence the sediment budget of the basin and the manner of sediment routing through the basin, it is evident that the role of major storms is crucial in initiating or accelerating large landslides, generating tremendous quantities of runoff, causing widespread gully widening and headward cutting, and mobilizing large amounts of bedload for short time spans. More frequent but less severe climatic events are important sediment transporters, but a significant amount of the sediment they move (especially bedload) is delivered to the stream network by the infrequent larger events. Much of the streamside landsliding and bank erosion during the smaller, more frequent storms are indirectly caused by channel and slope changes initiated by the high magnitude, infrequent storm event. In addition, catastrophic, rapid debris avalanching and sliding during major storms are the most important means of landform evolution on otherwise competent sandstone slopes. Therefore, large-magnitude and infrequent storms, such as that of 1964, have a significantly greater effect on total sediment discharge and on landscape formation and a much longer lasting effect on channel morphology in this region of high sediment yield than similar types of floods have on less mountainous terrain underlain by more stable geologic units.

The current sediment yield from the basin, 2,570 t/km^2/yr, is from three to six times the maximum possible long-term rate since the late Miocene, based on a landform reconstruction of the basin. The current rate, which is probably one of the highest ever, may in part reflect recent uplift, but land use of the past century has been a major contributing factor.

REFERENCES CITED

Brown, W. M., and Ritter, J. R., 1971, Sediment transport and turbidity in the Eel River basin, California: U.S. Geological Survey Water-Supply Paper 1986, 70 p.

Harden, D. J., Janda, R. J., and Nolan, K. M., 1978, Mass movement and storms in the drainage basin of Redwood Creek, Humboldt County, California — A progress report: U.S. Geological Survey Open-File Report 78-486, 161 p.

Helley, E. J., and LaMarche, V. C., 1973, Historic flood information for northern California streams from geological and botanical evidence: U.S. Geological Survey Professional Paper 485-E, 16 p.

Judson, S., and Ritter, D. F., 1964, Rates of regional denudation in the United States: Journal of Geophysical Research, v. 69, no. 16, p. 3395–3401.

Kelsey, H. M., 1977, Landsliding, channel changes, sediment yield and land use in the Van Duzen River basin, north coastal California, 1941–1975 [Ph.D. thesis]: Santa Cruz, California, University of California, 370 p.

——1978, Earthflows in Franciscan melange, Van Duzen River basin, California: Geology, v. 6, p. 361–364.

MANUSCRIPT RECEIVED BY THE SOCIETY JULY 2, 1979
REVISED MANUSCRIPT RECEIVED DECEMBER 17, 1979
MANUSCRIPT ACCEPTED JANUARY 11, 1980

reprinted from Peter D. Jungerius (Ed.):
SOILS AND GEOMORPHOLOGY
Catena Supplement 6, Braunschweig 1985

COLLUVIUM IN BEDROCK HOLLOWS ON STEEP SLOPES, REDWOOD CREEK DRAINAGE BASIN, NORTHWESTERN CALIFORNIA

Donna C. Marron
U.S. Geological Survey
Denver Federal Center, M.S. 413
Denver, Colorado 80225

SUMMARY

Colluvial deposits in small U- to V-shaped bedrock hollows are common on coherent graywacke slopes in the Redwood Creek watershed in northwestern California. The deposits average 10 to 15 meters in width and 3 to 4 meters in thickness. Both the deposits and the bedrock hollows they fill extend linearly downslope toward stream channels. The geometry and distribution of the hollows indicate that they result from landsliding. The textural and weathering characteristics of the colluvial deposits indicate that hollows can be filled episodically and that partial removal of deposited colluvium and subsequent refilling are common. However, dates of charcoal above and below a textural discontinuity in one deposit indicate that the colluvial deposits can remain stable for thousands of years. The long-term stability of colluvium may result from repeated removal of colluvium from hollows by erosional events that do not lower the hollows themselves.

1. INTRODUCTION

Although considerable research has been done on erosional processes in steep forested watersheds in northwestern California (JANDA et al. 1975; NOLAN et al. 1976; HARDEN et al. 1978; KELSEY 1980; KELSEY et al. 1981), little is known about the characteristics of the surficial materials affected by those processes. Colluvium and soils developed on colluvium provide valuable information on erosion and slope evolution because their characteristics reflect the activity of different weathering and erosional processes. Because these surficial materials are commonly formed over long time periods, studies of their characteristics can provide long-term information not obtainable through direct measurements of current or recent erosion and deposition.

Colluvial deposits filling small U- to V-shaped bedrock hollows are commonly exposed in roadcuts across slopes underlain by coherent bedrock in the Pacific Northwest (DIETRICH AND DUNNE 1978; DIETRICH et al. 1982; LEHRE 1982; DIETRICH AND DORN 1984). In places, these deposits are exposed in the headscarps of recent landslides (DIETRICH et al. 1982). The widespread occurrence of

the colluvium-filled bedrock hollows and their occasional association with landslides suggest that they may be useful in understanding erosion history in steepland watersheds. Extensive roadcut exposures created during timber harvesting in the Redwood Creek drainage basin north of Eureka, California (fig. 1), have provided an opportunity to document the topographic positions, textural features, and weathering characteristics of these deposits on slopes underlain by coherent graywacke in that basin. Landslide terminology in this paper follows that of VARNES (1978).

2. PREVIOUS WORK

Early studies of slope deposits in small bedrock hollows interpreted the deposits as filled gullies. BRYAN (1940) described pockets of regolith in small bedrock hollows that he observed on slopes in New Mexico, Texas, and the southern Appalachians. He attributed the formation of these deposits to the filling of gullies, which form on slopes when regolith becomes sufficiently weathered and clay-rich to prohibit infiltration and to promote runoff. PARIZEK & WOODRUFF (1957) described small U- to V-shaped deposits in the southern Appalachians. They also interpreted the deposits as gully fills.

More recent studies in the Pacific Northwest have linked the formation of pockets of colluvium on slopes to landsliding. DIETRICH & DUNNE (1978) and DIETRICH et al. (1982) referred to colluvium-filled U- to V-shaped bedrock hollows on steep forested slopes in the Oregon Coast Range as "wedges" and suggested that the deposits are filled landslide scars and sites of repeated landslide activity. LEHRE (1982) described colluvial deposits in bedrock hollows on slopes approximately 14 km northwest of San Francisco and also interpreted them as filled landslide scars. DIETRICH & DORN (1984) quantified the age of colluvium that was mostly removed by landsliding from a bedrock hollow in northwestern California.

3. THE STUDY AREA

Colluvial deposits described in this paper occur on slopes underlain by coherent graywacke in the Redwood Creek basin in the Coast Ranges of northwestern California (fig. 1). Gradients of these slopes commonly range from 20 percent to over 50 percent, and average approximately 35 percent. Below gently sloping interfluves, slope profiles are usually straight to slightly concave. Maximum relief in the Redwood Creek watershed is 1615 m.

The climate of the Redwood Creek drainage basin is characterized by wet winters with mild temperatures and dry summers. Yearly precipitation, which occurs almost exclusively from October to June, ranges from 1800 to 2300 mm. Before logging, forests that were chiefly composed of redwood (Sequoia sempervirens) and Douglas-fir (Pseudotsuga menziesii) covered

most hillslopes in the Redwood Creek watershed. Prairies covered by grasses and shrubs occur on gently sloping interfluves in the study area. These prairies were present before the start of timber harvest.

Bedrock in the study area consists primarily of unmetamorphosed bedded graywacke, which is interbedded with lesser amounts of mudstone and still lesser amounts of conglomerate. Beds are usually 0.1 to 3.0 m thick but can be as thick as 10.0 m (HARDEN et al. 1981). The graywacke includes tectonically emplaced blocks of conglomerate and particularly resitant graywacke, which are surrounded by sheared and broken graywacke and shale.

4. DESCRIPTION OF COLLUVIAL DEPOSITS AND BEDROCK HOLLOWS

4.1. GEOMETRY AND TOPOGRAPHIC DISTRIBUTION

Sharp contacts with bedrock make colluvial deposits in the study area easily distinguishable from bedrock and shallow soils that have developed on bedrock. Both the deposits and the bedrock hollows they fill are U- to V-shaped in cross section and are commonly 10 to 15 m in width and 3 to 4 m in depth. Three-dimensional exposures show that the colluvial deposits and their associated bedrock hollows extend linearly downslope toward streams or ravine bottoms. Some of the bedrock hollows have a concave upward longitudinal profile.

Mapping of the U- to V-shaped colluvial deposits along major haul roads in a particularly well-exposed tributary basin within the study area (fig. 2) indicates that the deposits are abundant and widely distributed. Approximately 15 percent of major haul roads traversing the area shown in figure 2 intersect colluvium-filled bedrock hollows. Deposits are found in topographic positions ranging from the borders of deeply incised stream channels to the sides of prominent interfluves. Many deposits do not completely fill the bedrock hollows in which they occur, and are consequently associated with a slight topographic depression or swale. Not all topographic swales in the study area contain colluvium-filled bedrock hollows, however, and some colluvium-filled bedrock hollows lack topographic expression.

The bedrock hollows are probably formed by debris avalanches, as indicated by their geometry and distribution. The U-shaped cross sections of many hollows and the lack of fluvially cut notches or alluvial deposits associated with any of the hollows strongly suggest that they were not caused by gullying. Locations of some colluvial deposits on or near ridgetops resemble topographic positions of debris avalanche scars rather than fluvially cut channels in forested watersheds. A landslide origin for the widespread and abundant hollows is compatible with observations of erosional processes that are presently active in the Redwood Creek basin. Dense vegetation and highly permeable surface materials inhibit gully development on forested slopes in

CHARACTERISTICS OF MANAGEMENT-RELATED DEBRIS FLOWS, NORTHWESTERN CALIFORNIA[1]

Richard G. LaHusen[2]

Abstract: An inventory of landslides in the lower Redwood Creek basin, California showed that erosion due to shallow landslides has been accelerated by logging-road and skid trail construction. The analysis of landslides occurring during the 1981-82 rainfall season showed that all debris flows (40) originated from roads or skid trails on slopes with gradients of at least 30 degrees. Furthermore, 90 percent of the inventoried features originated less than 30 meters below a major convex break-in-slope and 87.5 percent of the failures occurred in a poorly drained soil having a mottled horizon less than one meter from the surface. These site characteristics commonly occur at the headwaters of ephemeral drainages or in streamside gorge slope positions. Results of this study are being applied in an erosion control program to selectively identify road reaches with high failure potential.

Since the expansion of Redwood National Park in 1978 to include nearly 13,000 hectares of cutover forest lands in the lower Redwood Creek basin, no severe storms ($T_r \geq 5$ yrs) have impacted the area. However, the winter of 1981-82 produced several moderate precipitation events which resulted in numerous shallow hillslope failures on steep forest land in the area. An inventory and analysis of the resultant debris slides, avalanches, flows and torrents was accomplished in 1982. These failures are hereafter collectively referred to as debris flows, reflecting the dominant type of failure (Varnes, 1958).

The purpose of the study was to develop a better understanding of the hillslope processes and to develop criteria useful for selecting mass erosion prone sites for treatment in an ongoing erosion control program. Previous studies in the northwestern United States have described and quantified characteristics of shallow landslides on forest steeplands (Dyrness, 1967; Swanson and others, 1981; Gresswell and others, 1979). Computer assisted multivariate analysis of a wide spectrum of site characteristics has been used to predict the loci of landslide occurrence (Rice, 1967; Furbish and Rice, 1983; Neely, 1983). This study examined some common field associations recognized by other researchers as well as additional factors which were associated with debris flow location and hillslope failure in the study area.

STUDY AREA

The study area comprises 200 km^2 of Redwood National Park located in the lower Redwood Creek basin, northwestern California (fig. 1). Approximately 34 percent of the study area is virgin redwood forest, 51 percent has been clearcut and tractor yarded and 7 percent has been clearcut and cable yarded. The Redwood Creek basin lies within the rugged Coast Range province and is underlain by folded and sheared sandstones, mudstones and schists of the Franciscan assemblage (Harden and others, 1982). The region is subject to high erosion rates due to geologically rapid tectonic uplift, the pervasively sheared and faulted condition of the underlying lithologies and the imprint of complex, highly disruptive landuse activities (Janda and others, 1975). The Mediterranean climate results in an annual average precipitation of 205 cm occurring mostly as rain during a single eight-month period.

METHODOLOGY

A total of 40 recently activated debris flows, visible in June 1982 during low altitude aerial reconnaissance flights, was included for this analysis. The entire study area was aerially searched to avoid biases created by reliance on ground observations which tend to miss failures in non-roaded terrain. Locations of debris flows were plotted on a master inventory map (1:48000). True color (1:6000), color infrared (1:25000) and black and white (1:12000) aerial photographs were examined to gain topographic, hydrologic and historical information. A field inventory addressing 39 variables was completed for each failure. Lengths, widths, and runout distances were measured with an optical range finder. Failure depths were estimated. Aspect and hillslope gradients were measured with compass and clinometer, respectively. Distance to streams and

---

[1]Presented at the Symposium on The Effects of Forest Land Use on Erosion and Slope Stability, 7-11 May, 1984, Honolulu, Hawaii.

[2]Hydrologist, Redwood National Park, National Park Service, U.S. Department of Interior, Orick, California, U.S.A.

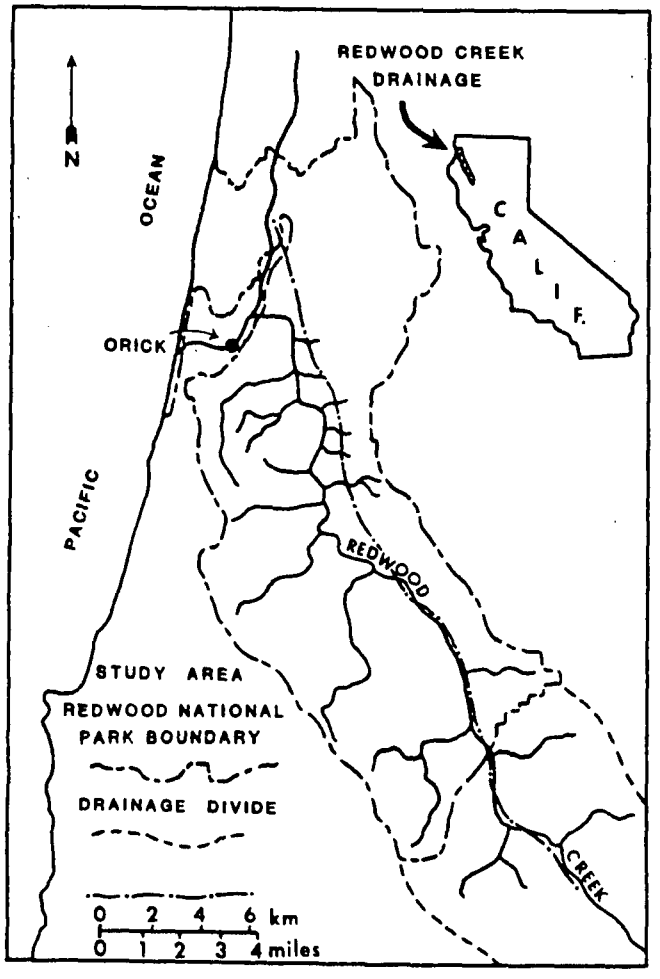

Figure 1--Location map of the lower Redwood Creek basin, Northwestern California, U.S.A. Study area is encompassed by Redwood National Park boundary.

major convex breaks in slope were estimated and hillslope morphology was categorized as planar, concave or convex along horizontal and downslope axes. Spatial relationships of the landslides to roads, skid trails and harvest units were also noted.

Soil characteristics were identified from exposures of the soil profiles at landslide scarps or adjacent road cutbanks. Soil texture was judged by feel and diagnostic surface and subsurface soil horizons were determined. Where exposures permitted observation of the underlying lithology, total depth of the regolith, bedrock competency and dip of bedding or foliations was documented.

Continuous rainfall records were obtained from two tipping bucket precipitation recorders located within the study area. Additional hydrologic data collected during field inspections included the location of surface water flow routes, ponded water, springs, and the presence of vigorous hydrophilic vegetation.

RESULTS

The inventoried debris flows deposited about 14,000 cubic meters of sediment into intermittent and perennial streams. Two thirds of that volume was deposited by a single debris torrent (fig. 2F and 3).

The first and most intense storm known to have induced many of the slope failures occurred on 19 December 1981. The maximum recurrence interval for the storm was only 3 years for the 24-hour total of 160 mm. However, that storm was preceded by 80 cm of rain over the preceding 38 days (fig. 4). The recurrence intervals for shorter durations for the same storm were less than 2 years (Miller and others, 1973).

Although the failure dimensions varied widely (fig. 2), the debris flow source areas exhibited several important similarities (table 1). The most prominent similarity was that all of the debris flows originated in landing, road or skid trail sidecast material where the local hillslope gradients exceeded 30 degrees. More than half of the failures had multiple skid trails crossing the source area.

A bimodal distribution of failures on the hillslope profile was found to coincide with the typical occurrence of two convex slope breaks in the area. Ninety percent of the failures occurred less than 30 meters below these major convex slope breaks. The two steep, convex sections of the hillslope, illustrated in figure 5, are inherently geomorphically active zones. The upper convexity is formed as a result of headward downcutting of an uplifted surface by first and second order streams. The lower "inner gorge" areas are formed by rapid incision of higher order streams into stream valleys. Consequently, the oversteepened slopes at both locations are prone to landsliding.

Another important topographic relationship noted was the tendency for failures to originate in minor swales at the heads of ephemeral drainages (figs. 5 & 6). At these locations, culverts or other drainage provisions through the road prism were noticeably absent.

Eighty-eight percent of the features were located in a single soil type characterized as a moderately deep (>1.5 meters) inceptisol having a fine-loamy texture overlying saprolitic schist. This soil exhibits mottling in a subsurface g-horizon within one meter of the surface. The mottled g-horizon is significant because it develops in poorly drained soils as a result of periodically saturated conditions (Brady, 1974).

The inherently wet conditions of most of the failure sites were often revealed by the presence of springs and unusually dense and vigorous hydrophilic vegetation including Red alder (Alnus rubra) and rushes (Juncus sp.). Color infrared aerial photographs highlighted vigorous vegetative growth on wet sites indicative of persistently shallow groundwater.

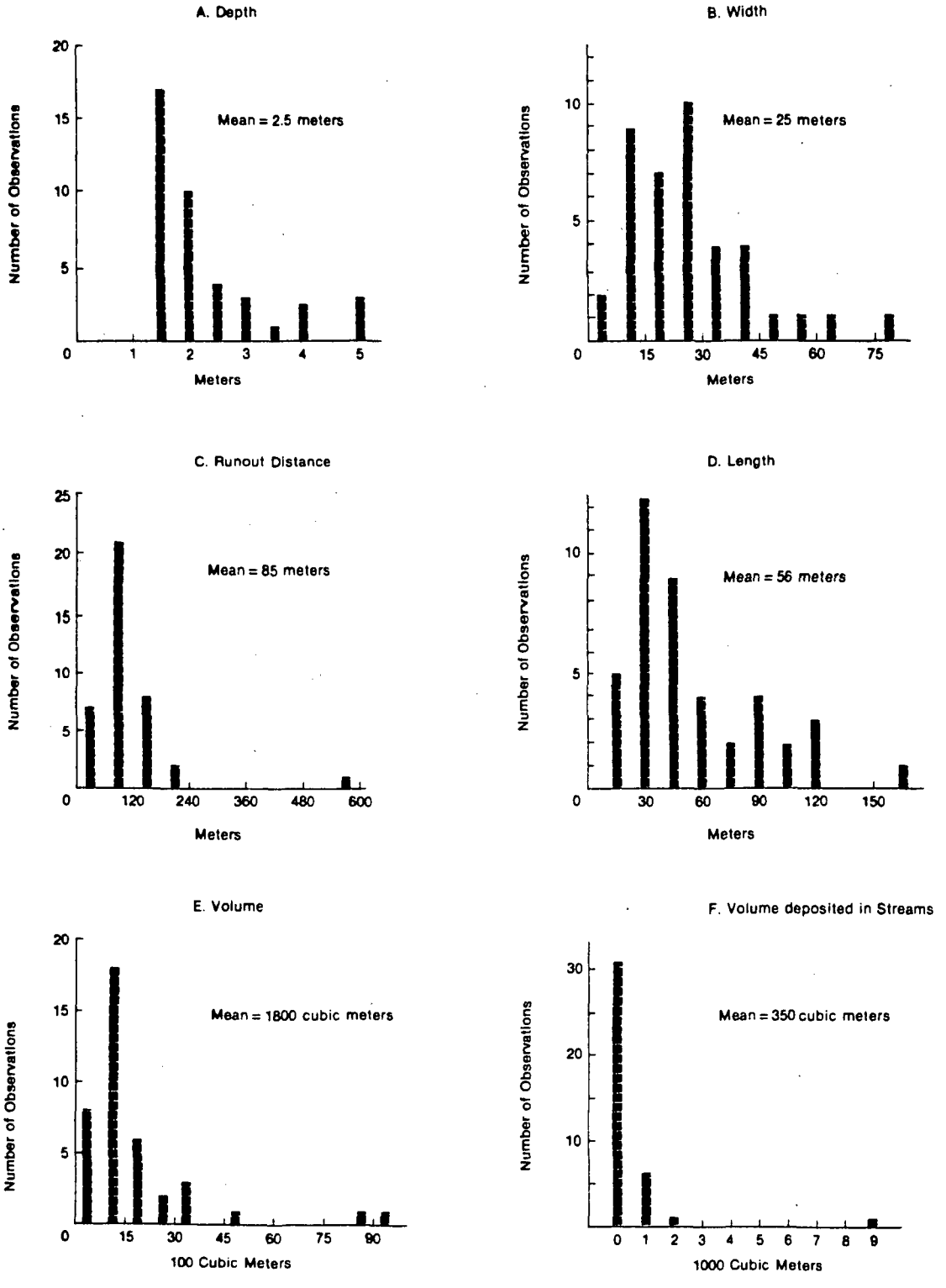

Figure 2--Histograms of A) depths, B) widths, C) runout distances, D) lengths, E) volumes and F) sediment delivery to intermittent and perennial streams. Data collected from 40 debris flows active during Winter, 1981-1982, lower Redwood Creek basin, California.

Table 1--Common associations of debris flows and other site variables in the lower Redwood Creek basin, Winter 1981-1982.

Site Variables	Number of Debris Flows	Percent of Total
1) Origin at:		
a. Road or Landing	22	55
b. Skid Trail	18	45
Total	40	100
2) Hillslope Gradient>30°	40	100
3) <30 Meters Below Slope Convexity	36	90
4) Soil exhibits Mottling<1m Deep	35	88

DISCUSSION

The ability to define specific areas with high failure potential is essential to effectively manage forest steeplands. Through the analysis of various extrinsic and intrinsic factors potentially related to landsliding, high risk areas may be delineated. The methodology employed in this inventory and analysis can be utilized elsewhere to pinpoint sensitive areas and compile an appropriate set of diagnostic criteria for risk classification.

This study has shown that the greatest potential for slope instabilities in the study area occur where roads and skid trials cross steep slopes and wet soils located in headwater swales or along inner gorge slope positions. These findings agree in part with other studies done in the region.

Neely (1983) tested a proposed erosion hazard rating system for logging-related debris slides in Northern California (California Board of Forestry, 1981) and found that only four criteria were significant in predicting debris slide locations in his study area. Those factors were: 1) slope gradient, 2) distance to springs, 3) distance to a major convex break-in-slope, and 4) density of incipient drainages (swales). Neely's results, indicating that the greatest instabilities occur on steep, wet hillslopes beneath major convex slope breaks, corroborate the results of this investigation.

Gresswell and others (1979) pooled data from forest lands which show that 70 percent of landslides in the northwestern United States are related to roads and the greatest number of these are sidecast fill failures. Swanston (1974) contends that roads cause failures due to slope loading, inadequate provision for slope and road drainage and oversteepened cutbanks. Direct severence or burial and subsequent decay of forest root systems also decrease hillslope stability (Ziemer, 1981).

As suggested by this study, an additional factor to be considered is the potential influence of road fills on natural subsurface flow characteristics. As forest roads cross a hillslope, the fill/cut ratio is greatest within swales. The weight of these deep, wide fill wedges may compact underlying soil horizons thus reducing their permeability. Consequently, subsurface flows which naturally concentrate in topographic depressions are restricted causing elevated pore water pressures beneath the road prism (fig. 7). Furthermore, a cap of structureless and permeable sidecast fill prevents exfiltration and relief of building pressures. As a result, continued buildup of pore water pressure beneath and within the road prism may lead to eventual failure.

Although the landslides observed during this study were clearly associated with road

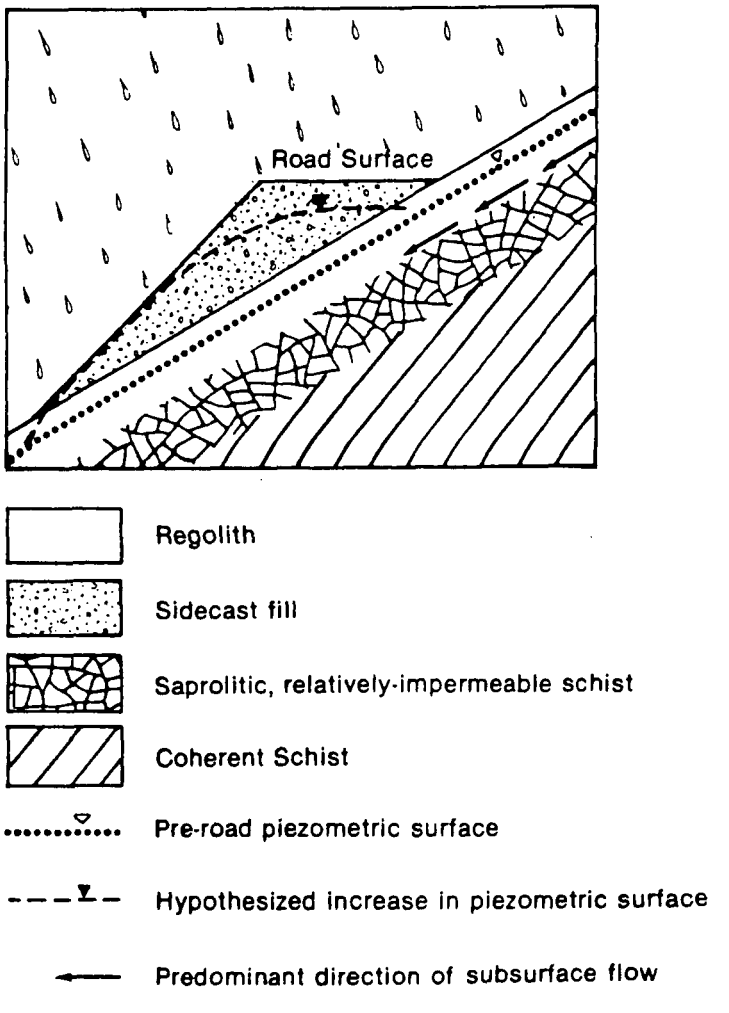

Figure 7--Diagrammatic cross section of forest road having no cut into hillslope. Dual piezometric surfaces show hypothesized conditions before and after road construction.

construction, it should not be inferred that only roaded sites in the study area are unstable. However, this study does confirm that roads decrease the stability of geomorphically active sites. The fact that no debris flows were found in non-roaded areas only indicates that the failure thresholds for these locations were not exceeded.

If a geomorphic threshold for landsliding is defined as a ratio of driving and resisting forces, hillslope failure occurs when the ratio become unity (Bull, 1980). This mechanistic definition, also known as the factor of safety, has been used extensively in slope stability analyses. Ward and others (1981) used a factor of safety model to predict general landslide hazards on forest hillslopes in southeast Alaska. More detailed stability analyses covering large forest management units are impractical. Since the intrinsic variables influencing slope stability such as cohesion and frictional strength vary spatially, attempts to identify absolute threshold values should be approached on a site specific basis. Therefore, it is crucial to identify additional criteria, such as soil characteristics or microtopographic position, which will limit the areas requiring further analysis.

CONCLUSIONS

The short period of record for timber harvesting on steep and unstable hillslopes prevents a direct magnitude-frequency analysis for debris sliding. However, utilizing a mechanistic analysis of hillslope stability, it may be possible to define a set of recurrence intervals for the conditions for which a landslide threshold is attained. The intrinsic variables within the factor of safety equation can be measured or derived for a particular site and act as constants for stability calculations. Because porewater pressure ultimately induces slope failure, it is the recurrence interval of the piezometric surface, not rainfall, for which estimates need to be determined.

Obviously rainfall creates fluctuations in piezometric levels. Where rainfall records are available, precipitation could be a surrogate variable potentially suitable for analysis. However, studies using stochastic methods to directly correlate precipitation with debris flow occurrence (Caine, 1980; Wieczorek and Sarmiento, 1983) have yielded inconclusive results.

A more suitable approach for magnitude-frequency analyses was taken by Swanston (1967), who utilized piezometric data to define a precipitation-piezometric head relationship for some thin soils in southeast Alaska. To develop such a predictive model for deeper colluvium-derived soils, current research at Redwood National Park involves continuously monitoring precipitation and piezometric levels at roads in debris flow prone locations. Through these efforts, we hope to more closely define both the precipitation-pore pressure relationship and the influence of road location on subsurface flow regimes.

There are several methods available to reduce debris flows related to construction of new roads, maintaining existing roads and rehabilitation of abandoned roads. Most obviously, sensitive slopes can be delineated and avoided when new roads are built. Total mileage requirements for new roads can be reduced by increasing road spacing in conjunction with complementary yarding systems (e.g. multiple span skylines, balloon or helicopter yarding). Road alignments which closely follow contours of the slope reduce the volume of sidecast fill placed in swales. Permeable blankets or horizontal drains can be used to improve drainage of the road prism and underlying soils. Finally, structural reinforcement of fillslopes can be an effective means of preventing fillslope failures on new and existing roads.

The erosion control program at Redwood National Park concentrates on erosion control and prevention by the excavation of unstable fill material from abandoned roads and skid trails. Results of this study are being used to selectively identify those road sections with high failure potential. Such specific road or skid trail reaches receive more extensive treatments including total fill removal. The ability to selectively prioritize treatment sites has helped to optimize the cost-effectiveness of logging road rehabilitation.

Acknowledgements: I wish to thank all the geologic field personnel of Redwood National Park whose diligent work in adverse terrain and climate has led to a greater understanding of forest hillslope erosion processes. Special thanks go to Ron Sonnevil for his insightful input at all stages of this endeavor and to Dr. Bill Weaver for his unsurpassed gift of constructive review. He and Jill Albert also did a skillful job of editing and transforming the draft manuscript into the final required format. Lastly, thanks to Randy Klein for his professional and moral support.

REFERENCES

Brady, N.C. The Nature and Properties of Soils, New York, MacMillan Co.; 1974. 639 p.

Bull, W.B. Geomorphic thresholds as defined by ratios. In Coates, D.R. and Vitek, J.D. eds. Thresholds in Geomorphology, Boston, George Allen and Unwin; 1980. 259-263.

Caine, N.A. The rainfall intensity-duration control of shallow landslides and debris flows. Geografiska Annaler; 1980. 62A; 23-27.

California Board of Forestry. Technical Rule Addendum Number 1: Procedure for estimating surface soil erosion hazard rating and completing mass movement checklist; Sacramento, California; December 15, 1981. 16 p.

Dyrness, C.T. Mass soil movements in the H.J. Andrews Experimental Forest. U.S. Department of

Agriculture, Forest Service, Research Paper PNW-42; 1967. 12 p.

Furbish, D.J.; Rice, R.M. Predicting landslides related to clearcut logging, Northwestern California. Mountain Research and Development; 1983. Vol.3, No. 3, 253-259.

Greswell, S.; Heller, D.; Swanston, D.N. Mass movement response to forest management in the central Oregon Ranges. U.S. Department of Agriculture, Forest Service, Resource Bulletin PNW-84; 1979. 26 p.

Harden, D.R.; Kelsey, H.M.; Morrison, S.D.; Stephens, T.A. Geologic map of the Redwood Creek drainage basin, Humboldt County, California. U.S. Department of Interior, Geol. Survey Water Resour. Invest. Open File Report 81-496, Menlo Park, Calif.; 1982. 1 p.

Janda, R.J.; Nolan, K.M.; Harden, D.R.; Colman, S.M. Watershed conditions in the drainage basin of Redwood Creek, Humboldt County, California, as of 1973. U.S. Department of Interior, Geological Survey Open-File Report 75-568; 1975. 266 p.

Miller, J.F.; Fredrick, R.H.; Tracey, R.J. Precipitation-frequency atlas of the western United States, California. U.S. Department of Commerce, National Oceanic and Atmospheric Administration, National Weather Service, Washington, D.C., Volume XI; 1973. 71 p.

Neely, M.K. Testing a method of predicting debris slides on logged hillslopes. Unpublished M.S. Thesis, Humboldt State University, Arcata, California; 1983. 54 p.

Rice, R.M. Multivariate methods useful in hydrology. Proceedings International Hydrol. Symposium. Fort Collins, Colorado; September 6-8, Volume 1; 1967. 471-478.

Swanson, F.J.; Swanson, M.M.; Woods, C. Analysis of debris-avalanche erosion in steep forest lands: an example from Mapleton, Oregon, USA. In Proceedings of a Symposium on Erosion and Sediment Transport in Pacific Rim Steeplands, International Association of Hydrological Sciences, Publication No. 132, Washington, D.C.; 1981. 67-75.

Swanston, D.N. Soil-water piezometry in a southeast Alaska landslide area. U.S. Department of Agriculture, Forest Service, Research Note PNW-68; 1967. 17 p.

Swanston, D.N. Slope stability problems associated with timber harvesting in mountainous regions of the Western United States. U.S. Department of Agriculture, Forest Service, Gen. Tech. Report. PNW-21; 1974. 14 p.

Varnes, D.J. Slope movement types and processes. In Schuster, R.L.; Krizek, R.S., eds. Landslides - analysis and control. National Academy of Sciences, Transportation Research Board Special Report 176; 1958. 12-33.

Ward, T.J.; Li, R.; Simons, D.B. Use of a mathematical model for estimating potential landslide sites in steep forested drainage basins. In Proceedings of a Symposium on Erosion and Sediment Transport in Pacific Rim Steeplands, International Association of Hydrological Sciences, Publication No. 132, Washington, D.C.; 1981. 21-41.

Wieczorek, G.F.; Sarmiento, D.B. Significance of storm intensity duration for triggering debris flows near La Honda, Calif. In Abstracts with Programs, Joint meetings of Rocky Mountain and Cordillean Sections of Geological Society of America. Boulder, Colo.; 1983. p. 289.

Ziemer, R.R. Roots and the stability of forest slopes. In Proceedings of a Symposium on Erosion and Sediment Transport in Pacific Rim Steeplands, International Association of Hydrological Sciences, Publication No. 132, Washington, D.C.; 1981. 343-357.

Blocksliding on Schist in the Lower Redwood Creek Drainage, Northwest California

Ronald Sonnevil, Randy Klein, Richard LaHusen,
Darcia Short and William Weaver

ABSTRACT

Mass-movement is an important process for shaping landforms and producing sediment in the Redwood Creek basin, northwest California. Previous investigations, based on analysis of aerial photographs, depict an abundance of ancient and recent landslides on sedimentary terrane, but relatively few landslides in the heavily timbered schist terrane. This study, based on field mapping in the lower Redwood Creek basin, has identifed at least 33 active block slides on forested land underlain by the Schist of Redwood Creek. Most of the block slides occur immediately west of the Bridge Creek lineament.

Most block slides in the study area are discrete, translational landslides ranging in size from 0.4 to 2.0 hectares. Some of the larger features, which are not bounded by well-defined lateral scarps, range up to 40 hectares in areal extent. Episodic movement of the monitored block slides is closely related to rainfall events. Total annual measured displacement ranges from 0 to 7 meters. Observed depths to failure surfaces range between 3.4 and 6.9 meters. Nearly all block slides are associated with a highly sheared, black schist which is a metamorphosed argillaceous rock. Block-slide movement has been detected near the boundary between sheared black schist and overlying brownish-gray regolith. This preferential failure surface development is probably a result of permeability and cohesion differences between these materials.

Block slides differ from typical grassland-covered earthflows on Franciscan sedimentary terrane in northwest California. Major differences include size, morphology, lithologic controls on failure depths, and temporal characteristics of movement.

Blocksliding may be an important process responsible for sculpting schist terrane, producing many of the smaller, "trough-shaped" first-order drainages common to this lithologic unit within the lower Redwood Creek basin. Block slides also probably exist on schist terrane in the upper two thirds of the basin. Aside from along the Bridge Creek lineament, block slides are most likely to be found in other areas where the bedrock consists predominately of sheared black schist. They may also be found on terrain underlain by lithologies similar to the Schist of Redwood Creek, such as the South Fork Mountain Schist in northwest California and the Colebrooke Schist in southwest Oregon.

INTRODUCTION

Redwood Creek, a 730km² drainage basin in northwest California (Fig. 1), contains some of the most rapidly eroding terrain in North America (Janda and Nolan, 1979). Rapid tectonic uplift occuring within the last two million years has resulted in over 600 meters of stream incision along Redwood Creek (Kelsey, in press). The basin is underlain by highly sheared sandstones, mudstones and schists of the Franciscan assemblage (Harden and others, 1981). The deep incision combined with inherently unstable bedrock, seasonally high rainfall and extensive timber harvesting has resulted in abundant mass-movement activity. The dominate types of mass-movement are streamside landslides, debris slides, earthflows, blocksliding and soil creep (Harden and others, 1978; Swanston and others, 1983). Coleman (1973) reports that at least 36 percent of the Redwood Creek basin consists of landforms indicative of ancient or recent mass-movement activity.

Past work within the Redwood Creek basin indicates that landslide forms occupy three times as much area on sedimentary terrane as compared to areas underlain by schist, even though both rock types comprise equal portions of the catchment (Nolan and others, 1976; Harden and others, 1978). The dominant types of active or recently active landslides occurring within sedimentary terrane are earthflows, debris slides and streamside landslides. Although some streamside landslides and large debris slides are present in the schist (Kelsey and others, in press), previous investigators found few active, slow moving, deep-seated landslides (failure depths > 3m) equivalent to the earth flows on sedimentary terrane (Nolan and others, 1976). Instead, creep and blocksliding which occur over large, undefined portions of hillslopes and lack distinct boundaries, have been shown to be important mass-movement processes on areas underlain by schist bedrock (Swanston and others, 1983; Marron, 1982).

Estimated erosion rates from landslides and gullies can account for much of the sandstone-derived sediment in Redwood Creek, but available data concerning erosion rates for schist terrane cannot account for a substantial portion of the schist-derived sediment (Harden and others, 1978; M. Madej, personal communication, 1985). This discrepancy caused Harden and others (1978) to speculate that landsliding in schist terrane must be much more prevalent than was obvious on the aerial photographs used for the basin-wide landslide distribution analysis by Nolan and others (1976).

Studies now in progress within the lower Redwood Creek basin have documented two additional mechanisms of landsliding which may help account for more of the schist-derived sediment. LaHusen (1984), and LaHusen and Sonnevil (1984) documented an abundance of road-related debris flows occurring in schist terrain. Additionally, in our recent work in selected areas of the lower watershed, we have identified 33 active deep-seated translational landslides occurring on schist. Because they are forested, most of these slow moving landslides were not apparent on the small-scale aerial photographs used by previous workers. Preliminary results on the spatial distribution and movement characteristics of a sample of these 33 earth block slides (after Varnes, 1978), herein referred to as "block slides", is the subject of this report.

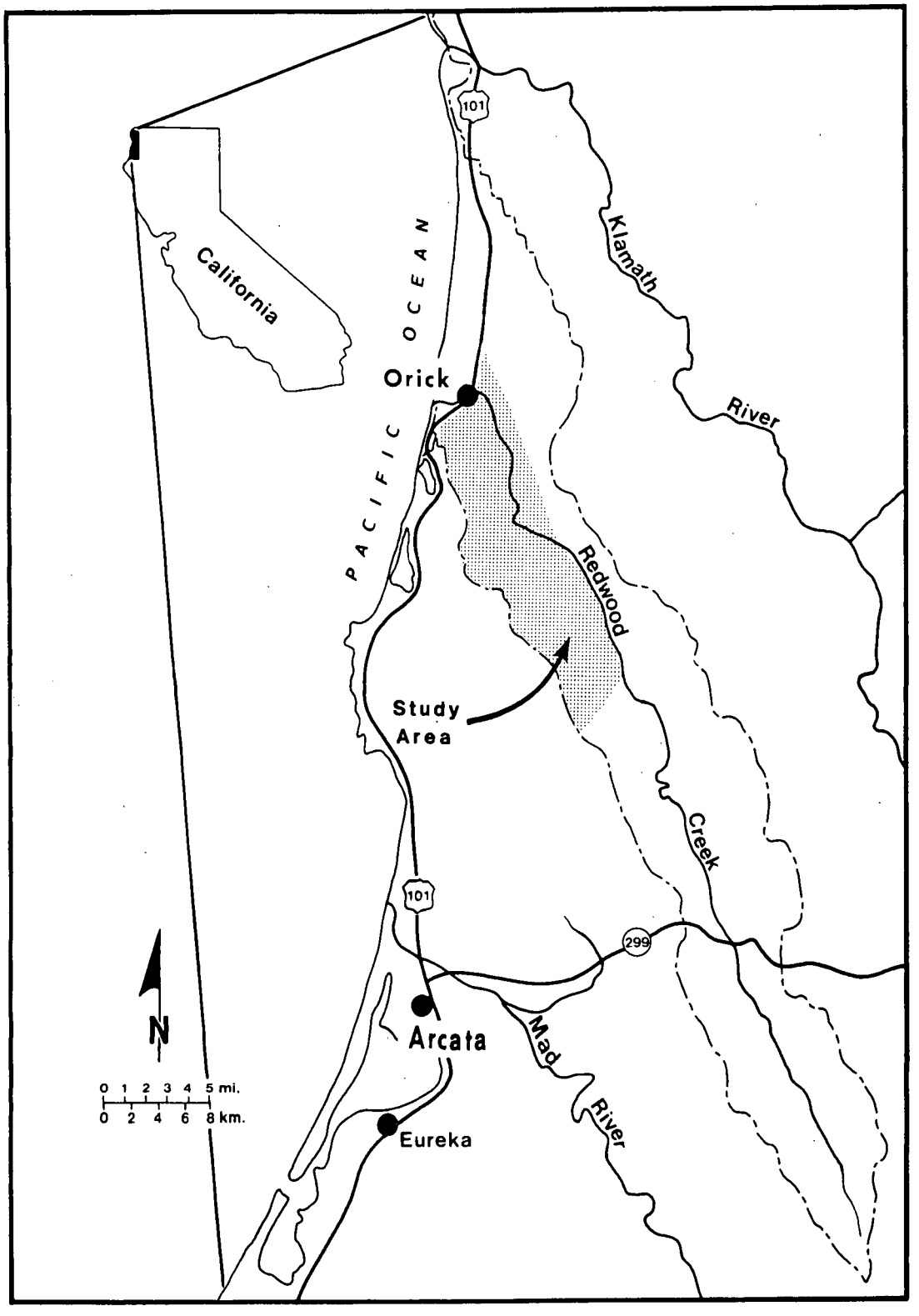

Figure 1. Map of the Redwood Creek basin showing location of study area.

CHARACTERISTICS OF BLOCK SLIDES

We have tentatively divided the block slides into two categories: 1) those comparatively small, discrete features with distinct lateral boundaries, and 2) larger features which do not have distinct lateral boundaries (Fig. 2). Most of the information for this preliminary report concerns the smaller discrete block slides.

Distribution

The study area (Fig. 1) includes that portion of the Redwood Creek basin, contained within Redwood National Park, which is underlain by the Schist of Redwood Creek. Figure 2 shows the distribution of known active block slides within the study area. Most of these landslides were discovered either by geomorphic field mapping (scale=1:1200) conducted prior to watershed rehabilitation projects or because they offset roads. A few of the landslides were identified during previous studies (Coleman, 1973; Nolan and others, 1976). Although some of the features shown in Figure 2 could be seen on aerial photographs or during low-altitude aerial reconnaissance, most were not identifiable due to the presence of trees. Additional features probably exist in non-roaded portions of the study area which have not yet been mapped.

Morphology

The discrete block slides investigated range in size from 0.5 to 2.0 hectares (Fig. 3). Widths of the landslides vary from 35 to 60 meters while slope lengths vary from 100 to 275 meters. Main scarp heights vary from 1 to 5 meters. Typically, lateral scarps are nearly vertical and range from less than 1 meter to over 3 meters in height. Gullies often form at one or both lateral scarps. Some of the landslides are flanked by less steep, vegetated, older lateral scarps which vary from one meter to over 10 meters high. Ground surface inclination on the landslides is commonly between 15 and 30 degrees.

The discrete block slides consist of one or more coherent blocks separated by minor scarps (Fig. 3). There is a tendency for those blocks farthest downslope to be more disrupted and exhibit characteristics indicative of internal deformation. Two of the block slides studied are highly disrupted and show evidence of a large component of flow in their movement. According to Varnes (1978), these complex slope movements, which appear to have a large component of flow, should be termed block slide - earth flows. However, for simplicity, all of the landslides shown in Figure 2 are referred to as block slides.

The larger, less discrete block slides involve up to 40 hectares of hillslope and are not bounded by well-defined lateral scarps. Ground surface inclination is more variable, ranging from 5 to 40 degrees. Although sometimes present, discrete blocks are not as common as on the smaller features.

All of the block slides are forested. Those which are in an old-growth redwood - Douglas-fir forest have fewer standing trees and more rotten downtimber on their lower portions than on their upper portions. Individual blocks can often be recognized by differences in the concentration of standing

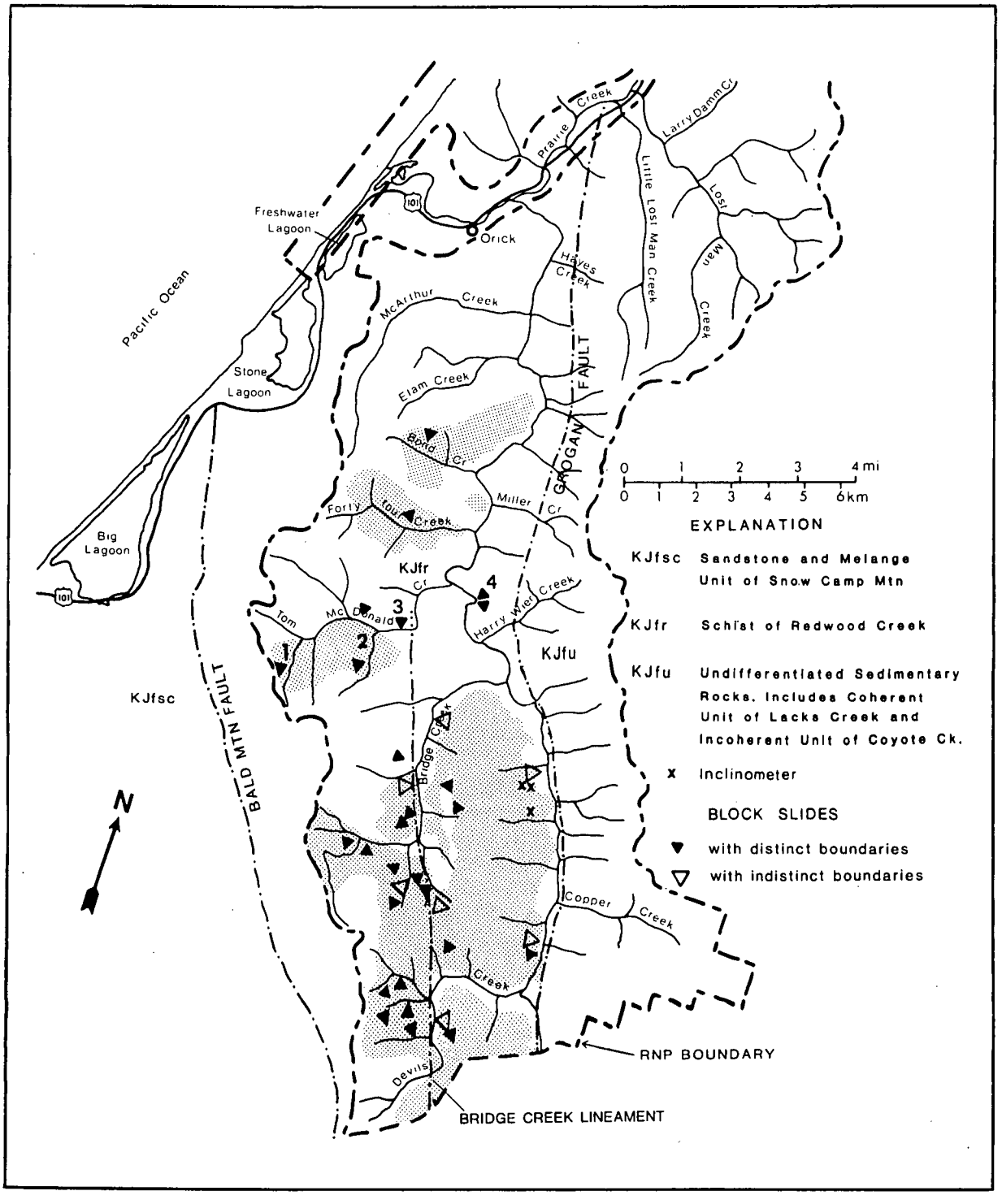

Figure 2. Generalized geologic map of the lower Redwood Creek basin (after Harden and others, 1981) showing known location of block slides. Stippled pattern shows those areas which have been field mapped at a scale of 1:1200. Numbered features are those referred to in text and Table 1: 1) Upper G-line Slide; 2) Lower G-line Slide; 3) Switchback Slide; and 4) Elbow Slide. Inclinometers shown are described by Swanston and others (1983).

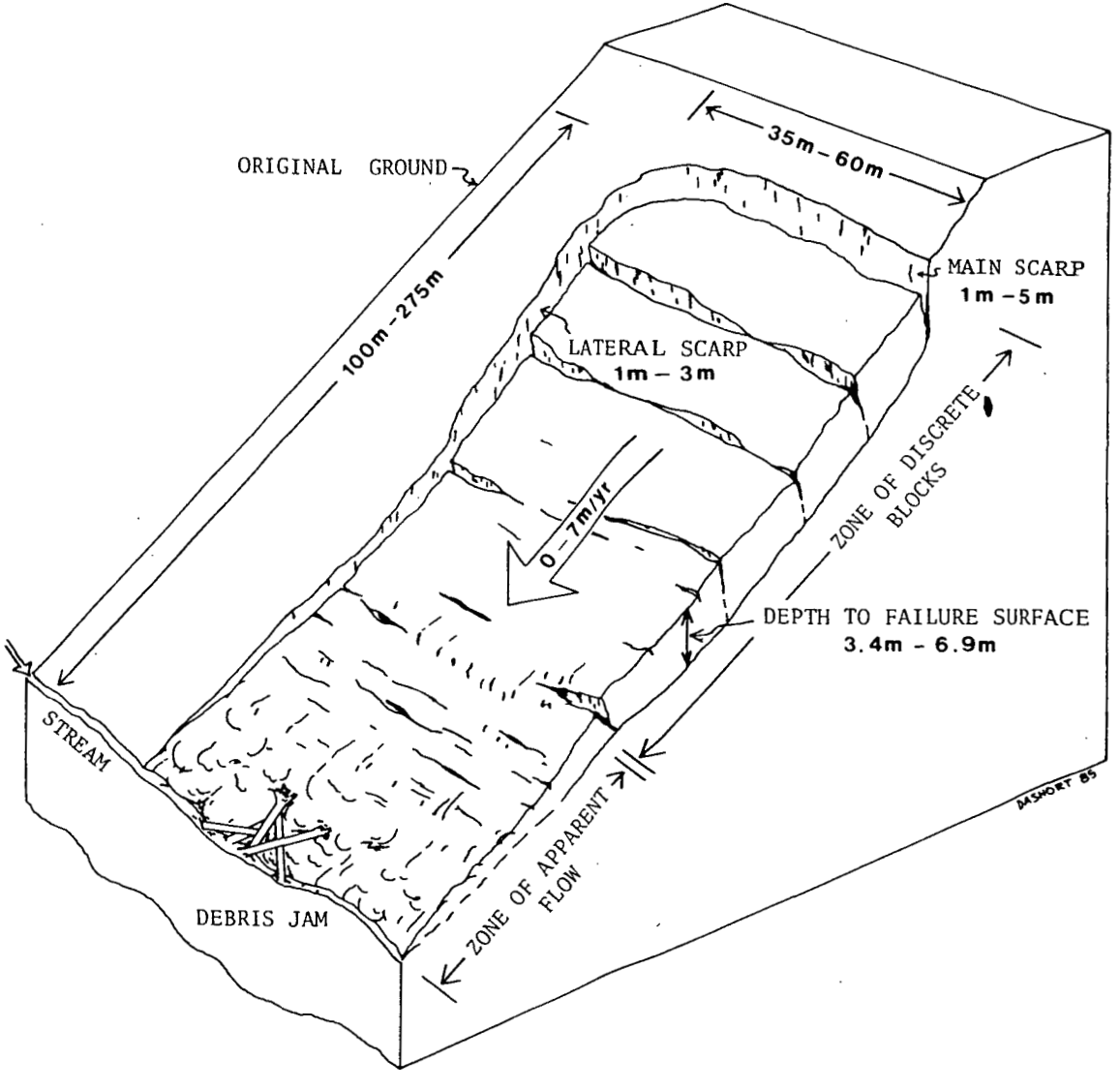

Figure 3. Schematic diagram showing salient features of a typical discrete block slide.

trees or rotten fallen trees. Evidently, landslide movement initiates low on the hillslope and progresses upslope in block-like fashion with time. On at least one of the features, progressive slope failure is expanding along lateral margins as well as upslope.

Where fallen timber has been introduced into a stream channel by block sliding, it may be transported away, as is the case with Redwood Creek's main channel. It may also result in debris jam formation if the stream power or channel width are insufficient to allow transport of this very large organic debris. Only one of the studied block slides has dammed a stream channel. Particle size analyses of soil and regolith samples suggest that about 40 percent of the sediment introduced into streams by block slides becomes bedload material (>2 mm diameter).

Lithologic Materials

Common to nearly all block slides is a highly sheared, black, albite-muscovite-chlorite-quartz schist with abundant carbonaceous material. More coherent, unsheared exposures of black schist are also common. This schist is a metamorphosed argillaceous rock. Although this material visually and tactually resembles a graphite schist, x-ray diffraction of six samples from different locations showed no graphite to be present. Similarly, Leathers (1978) did not find graphite in any samples collected from the Schist of Redwood Creek exposed along the Pacific coast between Big Lagoon and the mouth of Redwood Creek (Fig. 2). Overlying the sheared black schist is brownish-gray regolith containing abundant subangular clasts of a light-gray albite-muscovite-chlorite-quartz schist. Lenses of the sheared black schist are also present in this material, particularly near the basal contact. On the Switchback Slide (Table 1, Fig. 1), black schist material was not exposed at the ground surface but was discovered during drilling. The association of mass movement with sheared black schist is uncertain on a few of the block slides due to the absence of surface exposures and lack of subsurface drilling or trenching.

Failure Depths

Excessive episodic movement, limited funds, and poor accessibility to most of the block slides prohibits the use of conventional inclinometers to determine depths and styles of landslide movement. Alternately, depth-of-failure (DOF) indicators were installed with a portable drill rig. A DOF indicator (Fig. 4) consists of a 2.4 cm diameter PVC casing installed to a depth of seven to nine meters (the maximum depth attainable with the drill rig). A 20 cm length of steel rod attached to a stainless steel cable is lowered into the bottom of the hole. A similar size rod, attached to a measuring tape, is lowered from the top of the casing during periodic field inspections. If the bottom of the casing is below the failure surface and there has been sufficient movement and distortion of the casing to inhibit passage of the steel rods, the depths over which movement has occurred can be approximately determined (Fig. 4). The accuracy of determining failure zone thicknesses with DOF indicators is dependent upon the amount of movement which has occurred between installation and measurement, and dimensions (length and diameter) of the steel rod. The horizontal distance of movement which displaced the cased drill holes was not determined for this study.

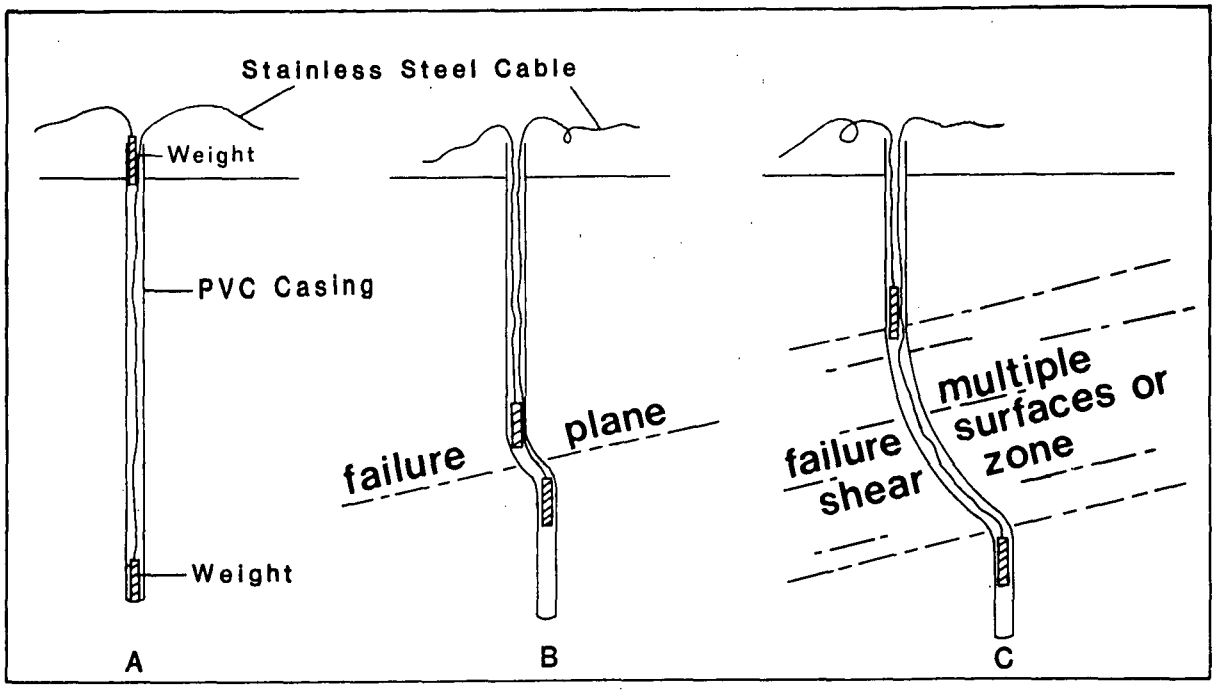

Figure 4. Schematic diagram showing depth-of-failure (DOF)indicator (A) before and (B or C) after movement.

Two DOF indicators were installed at separate locations on the Switchback and Lower G-line Slides (features 3 and 2, respectively, Fig. 2) in December, 1983. On the Upper G-line Slide (feature 1, Fig. 2), two separate pairs of DOF indicators were installed in November, 1983. One DOF indicator was displaced on the Switchback Slide and both pairs were displaced on the Upper G-line Slide during the 1983-84 winter (Table 1). At one of the locations on the Upper G-line Slide, the casings pinched during a two-week period between when the hole was drilled and when a rod was lowered into them, precluding an estimate of the failure zone thickness. The second (upper) pair of DOF indicators on the Upper G-line Slide showed inconsistent results. Although the lower constrictions in these two adjacent drill holes occurred at identical depths, the upper constrictions differed in elevation by 1.4 m, suggesting a wider zone of shear or multiple failure surfaces. These two upper G-line DOF indicators have since been obliterated by rehabilitation of the G-line road. The one DOF indicator which was displaced on the Switchback Slide suggested a narrow zone of shear. The remaining DOF indicator on the Switchback Slide and the two on the Lower G-line Slide were not offset enough to constrict the casing.

Black schist material was observed in the drilling effluent during installation of seven of the eight DOF indicators, however, it was impossible to tell if the schist bedrock was coherent or sheared. Table 1 lists the depths at which the marked color change from brown to black was observed in the drilling effluent. At two of the three locations with displaced

Feature Number	Name	Depth-of-Failure Indicator	Distance from Ground Surface to: Upper Constriction	Lower Constriction	Distance Between Constrictions	Depth to Black Schist
1	Upper G-line Slide	UGU20	6.76m	6.94m	0.18m	0
1	Upper G-line Slide	UGU25	5.39m	6.94m	1.55m	0
1	Upper G-line Slide	UGL20	3.41m	-	-	3.8m
1	Upper G-line Slide	UGL25	3.99m	-	-	4.0m
2	Lower G-line Slide	LGID25	-	-	-	0
2	Lower G-line Slide	LGDF25	-	-	-	5.2m
3	Switchback Slide	SWBUP25	-	-	-	-
3	Switchback Slide	SWBLO25	5.59m	≦5.67m	≦0.08m	5.9m

Table 1. Summary results from depth-of-failure (DOF) indicators. DOF indicators UGU 20 and UGU 25 were installed at similar elevations approximately 7 meters apart. UGL 20 and UGL 25 were installed 4 meters apart at similar elevations. All DOF indicators ranged from 7 to 8 meters deep.

DOF indicators, displacement was near the upper boundary of the black schist. Displacement at the third locality occurred within the black material.

Movement

Surface movement is being monitored on portions of three block slides by stakeline surveys or continuously recording slope-movement indicators. The Upper G-line Slide and Elbow Slide (Features 1 and 4, Fig. 2) have continuously recording slope-movement indicators across a lateral scarp (Fig. 5). One movement indicator utilizes a solid state data recorder and the other records movement on a strip chart. The solid state data recorder on the Elbow Slide is set to record a minimum of 7.5 mm of movement and the strip chart recorder (on the Upper G-line Slide) is sensitive to approximately 4 mm of movement. Since monitoring of Elbow Slide began in December, 1984, no movement has been recorded. However, a total of 45 mm of movement on the Upper G-line Slide was recorded during seven separate time periods between February 1984, and March 1985. All recorded movement occurred in response to individual storms or storm sequences.

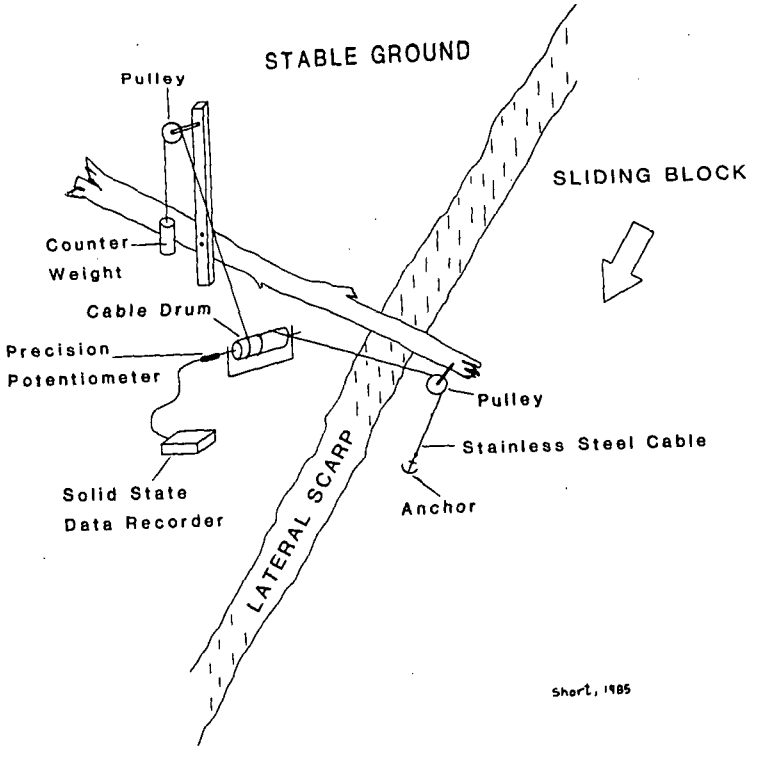

Figure 5. Diagram showing slope-movement-indicator installation on the Elbow Slide (feature 4, Fig. 2). On the Upper G-line Slide (feature 1) a strip chart recorder replaces the potentiometer and data recorder.

A stakeline was installed and measured with a theodolite and electronic distance meter on the Elbow and Switchback Slides in fall 1984, but neither have been remeasured yet. The stakeline across the Elbow Slide is located in the same area as a stakeline installed by the USGS in 1974 (Harden and others, 1978). They reported a maximum of 1.09 m of movement on the horizontal axis occurring between 1974 and 1976. Between 1976 and 1979, surveys showed an additional 0.55 m of movement (M. Nolan, written communication 1985). Our resurvey of the same stakeline in December 1984 indicates that at least 6.7 m of additional movement has occurred on the most active portion of the stakeline since 1979.

Other information concerning the timing and magnitude of movement for block slides is qualitative, consisting of field observations by National Park Service geologists. This information indicates that most movement occurs in direct response to prolonged, intense precipitation events or sequences of events. Movement of a very active, highly disrupted block slide was very responsive to rainfall during winter and spring 1983. Over seven meters of episodic movement occurred between late January and early April 1983 (Spreiter and Johnson, 1983). No movement has been observed on any of the block slides during the summer.

DISCUSSION

Controls on Block Slide Distribution and Depths of Movement

Although our investigation of block slides is at an early stage, some preliminary generalizations can be made concerning controls on their movement characteristics and spatial distribution. The most common characteristic of these features is the association with sheared black schist. On two block slides movement was detected near the boundary between the black schist and the overlying regolith with DOF indicators (Table 1). On a third block slide, the Elbow Slide, field observations indicate that movement is also occurring near or at this discontinuity in material types. Field observations suggest that cohesion is greater and permeability is less for the sheared black schist than in the overlying regolith. Presumably, the lower permeability impedes drainage into the sheared black schist, perching groundwater above it. The greater cohesion of the sheared black schist encourages failure surface development at this contact. Similar discontinuities in material properties occur at the boundary between coherent schist bedrock and overlying regolith on at least one block slide where sheared black schist was not found.

Most of the block slides identified occur in an elongate zone extending from Devils Creek to Tom McDonald Creek (Fig. 2). Within this zone, observations indicate that sheared and unsheared black schist comprises a greater proportion of the exposed bedrock than in schist terrane elsewhere in the park. This elongate zone (Fig. 2) is immediately to the west of the "Bridge Creek lineament", defined by Harden and others (1981) to coincide with aligned segments of Panther, Devils, Bridge and Tom McDonald Creeks. The lineament may be partially controlled by this concentration of highly sheared, easily eroded material. Future geologic mapping may show this black schist to be a distinct member of the Schist of Redwood Creek.

Comparison with Other Landslides

Swanston and others (1983) measured displacement along narrow shear zones at 5.5, 6.4 and 12.6 meter depths at three inclinometers located in schist terrane within Redwood National Park (Fig. 2). The two inclinometers which sheared at shallower depths are 10 m apart while the third inclinometer is 400 m to the south. The maximum movement they observed over a six-year period was small (16.4 mm/year). Their monitoring sites did not display scarps or other morphologic features typical of landslides, suggesting that the observed movement was of a more widespread, unconfined nature. We have observed much more rapid rates of movement (up to 7 m/year) occurring on block slides at depths comparable to one of the locations monitored by Swanston and others (1983). Perhaps the process is similar except that on block slides the blocks have detached from the hillslope and movement has accelerated substantially.

Large grassland-covered earth flows are a common type of mass-movement occurring in Franciscan sedimentary terrane in the Redwood Creek basin and elsewhere throughout northwest California (Nolan and others, 1976; Kelsey, 1978; Keefer and Johnson, 1983; Iverson, 1984). Characteristics of block slides which are also common to many earth flows include: 1) a predominately translational style of movement, 2) annual movement rates less than 10 m/year, 3) association with highly sheared argillaceous rock types (the black schist is metamorphosed mudstone), and 4) basal failure surfaces at approximately five meter depths.

Dissimilarities between earth flows and block slides also exist, and these are perhaps more important than their comparable characteristics. First, failure surfaces on block slides occur, at least locally, at lithologic boundaries (regolith/sheared black schist) whereas studies of earth flows have not identified lithologic contacts at basal shear zones (Keefer and Johnson, 1983; Iverson, 1984). Secondly, movement of block slides is episodic and appears to be uniquely associated with rainfall events whereas movement of some earth flows may persist from late fall to late spring and, in some instances, throughout summer (Iverson, 1984). Thirdly, although some earth flows are comparable in size to block slides, many earth flows are much larger, extending from major drainage divides to the valley bottom. Earth flows also commonly display more surficial evidence of slumping or internal deformation. Finally, most block slides lack the classic "teardrop" planimetric shape and sigmoidal profile characteristic of many earth flows.

Contrasts between movement of block slides and earth flows may be explained by differences in clay content of materials comprising the two types of failures. Particle size analyses indicate that block slides have an average of 14 percent clay in the <2 mm fraction (Sonnevil, unpublished data); about half the clay content of material comprising some earth flows on sedimentary terrane in the Redwood Creek basin (Iverson, 1984; J. Popenoe, personal communication, 1985). A higher clay content and associated lower permeability may increase retention of water and prolong the duration of movement.

Within schist terrane in the Redwood Creek basin, there are a large number of "trough-shaped" first-order drainages ranging in area from a few hectares to over a square kilometer. These have the appearance of having been formed by

mass-movement rather than fluvial processes. Nolan and others (1976) identified some of these features and many more have been located by National Park Service staff during detailed geomorphic mapping. Significantly, most of the block slides we have found incorporate or originate in these first-order drainage basins, suggesting that this process may represent an important mechanism for sculpting morphologically similar drainages common throughout the schist terrane of Redwood Creek.

Lithologic units similar to the Schist of Redwood Creek occur elsewhere. Kelsey and Hagans (1982) have correlated the Schist of Redwood Creek with the South Fork Mountain Schist in northwest California which, in turn, is lithologically similar to the Colebrooke Schist in southwest Oregon (Coleman, 1972) (Fig. 6). Literature concerning styles of landsliding on these lithologic units is sparse. Buer and James (1976) discuss landslides within the eastern half of the South Fork Mountain Schist which have similarities to the block slides. D. Haskins (personal communication, 1985) suggested that the block slides in Redwood Creek may be analagous to some active subsidiary landslides associated with ancient translational/rotational landslides in schist on the east side of South Fork Mountain. Landslides occurring on the western slopes of South Fork Mountain, particularly those underlain by metamorphosed argillaceous rocks, may also be block slides (R. Farrington, personal communication, 1985).

SUMMARY AND CONCLUSIONS

Slow moving, deep-seated landslides on schist terrane in the Redwood Creek basin are more common than is evident from aerial photographs. Detailed geomorphic mapping within the lower Redwood Creek basin has delineated 33 active block slides overlying schist bedrock. Characteristics common to inventoried features include: 1) predominately translational movement, 2) areal extent varying from 0.4 to 2.0 hectares, but occasionally ranging up to 40 hectares, 3) episodic, storm-dependent movement with observed total annual displacement up to seven meters, 4) observed depths to failure surfaces ranging between 3.4 and 6.9 meters, and 5) association with a highly sheared black schist, which is metamorphosed argillaceous rock.

Block slides differ from earth flows which are common on Franciscan sedimentary terrane in northwest California. Block slides are smaller than most earth flows and lack the "teardrop" planimetric shape and sigmoidal profile characteristic to many earth flows. Depths to failure surfaces on block slides can be lithologically controlled, but studies of earth flows have not demonstrated controls on failure surface locations. Monitored block-slide movement is more episodic than movement on monitored earth flows. Movement differences may result from the amount of clay in materials which comprise these two landslide types.

The number and distribution of block slides in the lower third of the Redwood Creek basin suggests that additional features exist upstream of Redwood National Park, particularly along the Bridge Creek lineament or other locations where sheared black schist is abundant. Block slides may be a common form of mass-movement outside of the Redwood Creek basin in terrane underlain by lithologic units similar to the Schist of Redwood Creek (for example, the South Fork Mountain Schist in northwest California and the

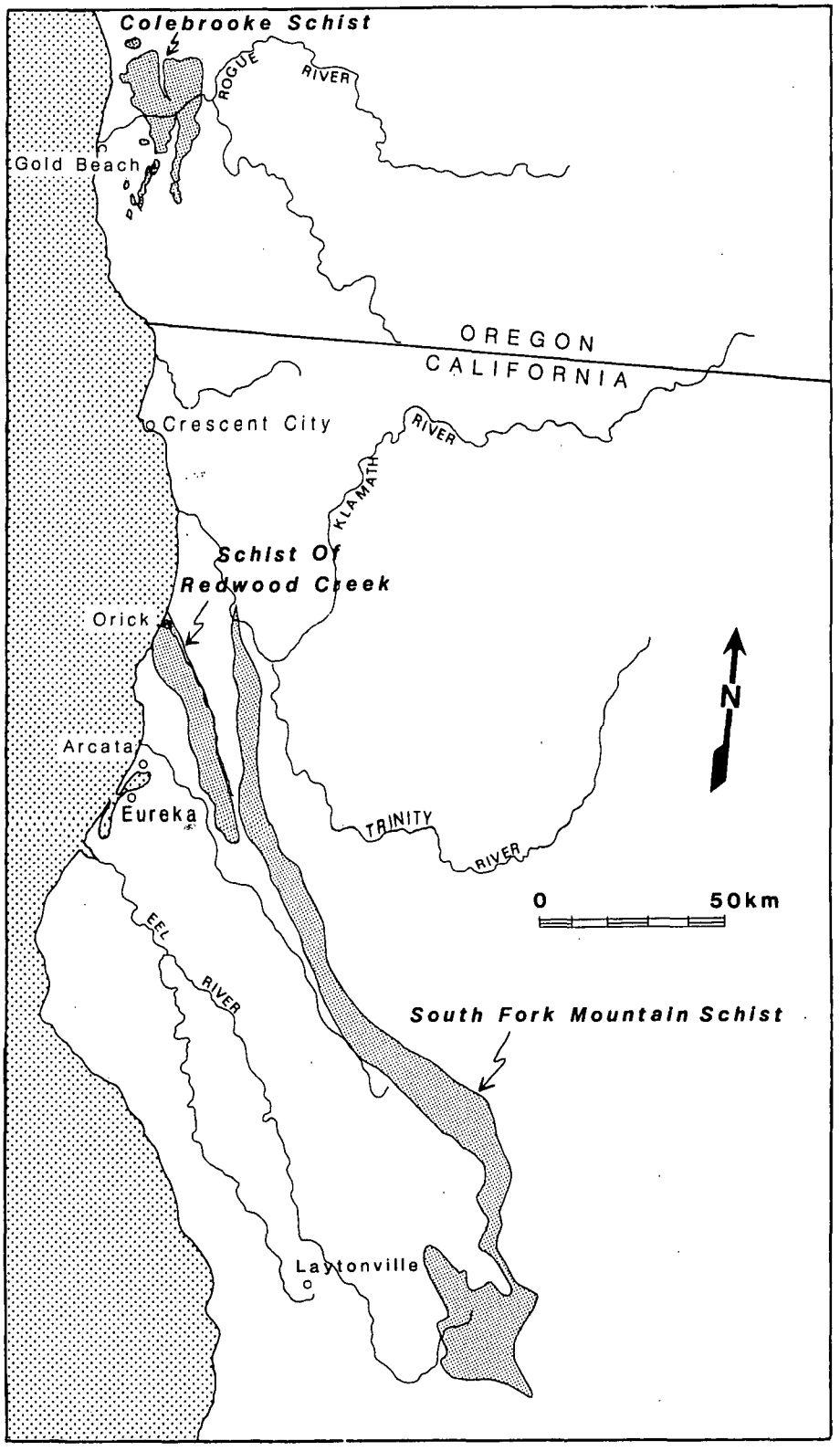

Figure 6. Map showing the distribution of the Schist of Redwood Creek, the South Fork Mountain Schist (Kelsey and Hagans, 1982) and the Colebrooke Schist (Coleman, 1972).

Colebrooke Schist in southwest Oregon). Because their movement occurs in small increments, block slides will not be major catastrophic sediment sources but, instead, represent a more persistent, long-term erosion process.

ACKNOWLEDGMENTS

We are indebted to the physical science staff of the watershed rehabilitation team at Redwood National Park whose mapping serves as a foundation for part of this study. Mike Nolan of the U.S. Geological Survey shared unpublished survey data from the Elbow Slide. Thoughtful reviews by Danny Hagans, Mary Ann Madej and Ken Utley clarified and improved the manuscript.

REFERENCES CITED

Buer, K., and James, S., 1979, South Fork Trinity River watershed erosion investigation: California Department of Water Resources, Northern District, Red Bluff, Ca., Reconnaissance Report, 83 p.

Coleman, R.G., 1972, The Colebrooke Schist of southwestern Oregon and its relation to the tectonic evolution of the region: U.S. Geological Survey Bulletin 1339, 61 p.

Colman, S.M., 1973, The history of mass movement processes in the Redwood Creek basin, Humboldt County, California: paper presented in lieu of M.S. thesis, University Park, Pennsylvania State University, Dept. of Geosciences, 180 p.

Harden, D.R., Janda, R.J., and Nolan, K.M., 1978, Mass movement and storms in the drainage basin of Redwood Creek, Humboldt County, California - A Progress Report: U.S. Geological Survey Open-File Report 78-468, 161 p.

Harden, D.R., Kelsey, H.M., Morrison, S.D. and Stephens, T.A., 1981, Geologic map of the Redwood Creek drainage basin, Humboldt County, California: Water Resources Investigations, Open-file report 81-496.

Iverson, R.M., 1984, Unsteady, nonuniform landslide motion: theory and measurement: Stanford, Ca, Stanford University, unpublished Ph.D. dissertation, 303 p.

Janda, R.J. and Nolan, K.M., 1979, Stream sediment discharge in northern California: in Guidebook for a Field Trip to Observe Natural and Resource-Management Related Erosion in Franciscan Terrane of Northern California: Geological Society of America, Cordilleran Section, p. IV1 - IV27.

Keefer, D.K., and Johnson, A.M., 1983, Earth flows: morphology, mobilization and movement: U.S. Geological Survey Professional Paper 1264, 56 p.

Kelsey, H.M., 1978, Earth flows in Franciscan melange, Van Duzen River basin, California: Geology, v.6, p. 361-364.

_____, in press, Tectonic and lithologic controls on the development of the inner gorge and erosion by streamside landsliding, Redwood Creek basin, northwestern California: Geological Society of America Bulletin.

Kelsey, H.M., and Hagans, D.K., 1982, Major right-lateral faulting in the Franciscan assemblage of northern California in late Tertiary time: Geology, v.10, p. 387-391.

Kelsey, H.M., Coghlan, M., Pitlick, J., and Best, D., in press, Geomorphic analysis of streamside landsliding in the Redwood Creek basin: in Geomorphic processes and aquatic habitat in the Redwood Creek basin, northwestern California: U.S. Geological Survey Professional Paper, M. Nolan, H. Kelsey, and D. Marron, eds.

LaHusen, R.G., 1984, Characteristics of management-related debris flows, northwestern California: in Proceedings of a symposium on the effects of forest land use on erosion and slope stability. May 7-11, 1984. Honolulu, Hawaii: International Union of Forestry Research Organizations, p. 139 - 145.

LaHusen, R.G., and Sonnevil, R.A., 1984, Accelerated incidence of debris flows, Redwood National Park, northwestern California [abs.]: Geological Society of America Abstracts with Programs, v.16, no.6, p. 567.

Leathers, S., 1978, Petrology, metamorphic grade, and structure of the Redwood Mountain outlier of the South Fork Mountain Schist on the coast of northern California: Arcata, Ca, Humboldt State University, unpublished B.S. thesis, 34 p.

Marron, D.C., 1982, Hillslope evolution and the genesis of colluvium in Redwood National Park, northwestern California; the use of soil development in their analysis: Berkeley, Ca, University of California, Berkeley, unpublished Ph.D. dissertation, 187 p.

Nolan, K.M., Harden, D.R. and Colman, S.M., 1976. Erosional landform map of the Redwood Creek basin, Humboldt County, California: U.S. Geological Survey Water Resources Investigation Open-File Map 76-42.

Spreiter, T., and Johnson, L., 1983, M-3-1 road and slope work and cost summary report, watershed rehabilitation unit 83-2: Orick, CA, National Park Service, unpublished report 74 p.

Swanston, D.N., Ziemer, R.R., and Janda, R.J., 1983, Influence of climate on progressive hillslope failure in Redwood Creek valley, northwest California: U.S. Geological Survey open-file report 83-259, 49 p.

Varnes, D.J., 1978, Slope movement types and processes, in Landslides: analysis and control: Transportation Research Board Special Report 176, Schuster, R., and Krizek, R., eds., p. 12-33.

QUATERNARY TECTONICS NORTH OF THE MENDOCINO TRIPLE JUNCTION THE MAD RIVER FAULT ZONE

Gary A. Carver, Department of Geology and Telonicher Marine Laboratory, Humboldt State University, Arcata, California

Introduction

Coastal California north of Cape Mendocino has been the locus of strong crustal compression during the Quaternary. Large northwest trending folds and parallel northeast dipping thrust and reverse faults have deformed Pleistocene deposits and influenced landforms throughout the region (Ogle, 1952, Woodward-Clyde Consultants, 1980, Carver et al., 1982). At the coast, localized uplift and subsidence associated with these structures is expressed as alternating reaches of emergent and submergent shoreline. Uplifted thrust blocks and large anticline crests form headlands sculpted by flights of raised glacio-eustatic marine terraces, while down-faulted blocks and synclinal troughs are occupied by lagoons, bays, and estuary-delta complexes. Steep youthful mountains, vigorous slope processes, deeply incised river valleys, and high fluvial sediment yields reflect the active tectonics of the northcoast region.

Regional Tectonic Setting

Although considerable information concerning tectonics of northwestern California has been developed in the past few years, a detailed regional tectonic model has not yet emerged. Throughout the late Tertiary the north coast region of California was situated along the Farallon-North American Plate boundary, a subduction margin (Atwater, 1970). Migration of the Mendocino Triple Junction into the north coast region occurred largely during the Quaternary.

The present tectonic setting of the northern California coast is strongly influenced by the triple junction and its northward movement. Quaternary structures resulting from thrust faulting and folding near the coast north of Cape Mendocino give way to high angle strike slip faults of the San Andreas system to the south and east (Herd, 1978, Kelsey and Allwardt, 1983) (Figure 1). Offshore Quaternary sediments of the continental shelf and slope are deformed by large youthful folds and faults (Fields et al. 1980, Silver, 1971); these structures are probably northern continuations of the onshore thrust faults and folds. Offshore of Oregon, these structures merge into the Juan de Fuca-Gorda subduction zone. Both the transform boundary south of the triple junction and the subduction margin to the north include broad complex systems of faults. The transition from transform to subduction tectonics, i.e., the triple junction, encompasses an equally broad and highly complex zone of transitional tectonics.

Compressional Tectonics North of the Mendocino Triple Junction

At least a dozen major Quaternary thrust faults or fault zones and several large youthful folds traverse the coastal region of California north of the triple junction (Ogle, 1952; Woodward-Clyde Consultants, 1980; Carver et al., 1982). Their cummulative Quaternary displacement represents at least 15 km of NE-SW crustal shortening. These northwest-trending northeast-dipping faults form a complex imbricate thrust belt within the overriding margin of the North American Plate along its boundary with the subducted southern portion of the Gorda Plate. The compression of the North American Plate margin may be the result of coupling between the accretionary wedge of the North America Plate and the underlying Gorda Plate, with outboard portions of the overriding wedge being rafted downward with the subducting plate. Internal deformation of the southern Gorda plate along northeast-trending left-lateral strike slip faults (Smith and Knapp, 1980; Smith, et. al. 1981), and the northward movement of the Pacific Plate result in a change in Gorda, North American convergence from east-west along the extreme northern California coast to nearly north-south near the triple junction. This change in convergence direction is reflected in compressional structures along the coast; principal folds and thrust faults strike nearly east-west at Cape Mendocino and gradually rotate to northwest-southeast further north (Figure 1). Magnetic anomalies on the Gorda plate show that this rotation in convergence was probably established during the Quaternary (Riddenhauf, 1984).

The Mad River Fault Zone

The Mad River Fault Zone (MRFZ), a prominent zone of imbricate thrust faults and associated folds, extends along the Mad River about 50 km from the coast inland to the vicinity of Maple Creek. The MRFZ is about 15 km wide and trends N35^{o}W. It contains 5 principal thrusts (Trinidad, Blue Lake, McKinleyville, Mad River, and Fickle Hill Faults) and numerous minor ones (Figure 2, 3). The Fickle Hill anticline, the Jacoby Creek syncline, and the Blue Lake anticline constitute major folds within the zone. At it's southeast end, near Maple Creek, compressional structures of the MRFZ merge with strike slip faults of the Eaton Roughs Fault Zone, a part of the San Andreas system (Kelsey and Allwardt, 1983). The dips of MRFZ faults range from 15^{o}-25^{o}NE at the coast to 35^{o}-45^{o}NE near Maple Creek. The folds are asymmetrical, with northern anticlinal limbs dipping northeast 20^{o}-30^{o}, and southern limbs near vertical and locally overturned. Their axis parallel the trend of the thrusts (N35W) and they plunge very gently NW. The fold limbs are cut by the thrust faults.

Stratigraphy

Assessment of the Quaternary tectonics of the Mad River Fault Zone is based on mapping and interpretation of several Quaternary stratigraphic datums. These include 1) the Klamath saprolite, 2) the Falor Formation, 3) the Patricks Point Terrace, and 4) fluvial terraces. These datums are widespread across the MRFZ, and were formed on nearly horizontal low relief

surfaces. Approximate ages of these datums have been determined. In addition, each of these stratigraphic features has tectonic significance relevant to the Quaternary development of the MRFZ. The MRFZ stratigraphy is summarized in Table 1.

The Klamath Saprolite

The Klamath saprolite is a very thick, very strongly developed weathering profile formed on pre-Quaternary rocks of north western California, especially the Franciscan Complex and Redwood Creek Schists. It mantles an extensive pre-Quaternary erosion surface of very low relief which Diller (1902) called the Klamath Peneplain. Locally the saprolite is many tens of meters thick, bright red, and clay-rich. It attests to a long period tectonic stability, low relief landscapes, little erosion, and prolonged chemical weathering. North of the MRFZ the saprolite is present on concordant flat topped ridges and mountains and extends into southwest Oregon. Within the MRFZ the saprolite is folded and displaced by faults. Early Quaternary marine and fluvial sediments of the Falor Formation lie depositionally on the saprolite limiting its age to late Tertiary. Preservation of the saprolite during the initial Falor transgression suggests tectonic processes in the region were relatively quiet at the end of the Tertiary.

Falor Formation

The Falor Formation (Manning and Ogle, 1950) includes locally thick sequences of poorly consolidated interbedded shallow marine sands and pebbly sands, estuarine and bay sands, silts, and clays, and fluvial gravels, sands, and silts. The deposits were laid down in a slowly subsiding depositional basin which extended across the MRFZ and was probably continuous with the Eel River basin to the south. Subsequent faulting has thrust Franciscan Complex rocks over the Falor deposits. In all measured stratigraphic sections of the Falor Formation, the top of the section has been removed by faulting, allowing determination only of minimum section thickness. Locally over 938 meters of Falor sediments are present in the MRFZ.

The age of the Falor Formation is constrained by a well-preserved volcanic ash layer present near its depositional base. This ash has been correlated on the basis of chemistry to the 1.8-2.0 m.a. Huckleberry Ridge Tuff from the Yellowstone caldera (A. Sarna-Wojcicki, pers. comm., 1983). The internal stratigraphy of the Falor Formation is complex and not well known. A widespread basal member composed of well-sorted quartz-rich sand containing well rounded silicous pebbles suggests open coastline conditions during initial Falor deposition. Higher in the section shallow open-marine sedimentation dominated in western portions of the MRFZ while estuarine and bay environments were present in the east. The entire section is punctuated by fluvial sand and gravel sequences, representing repeated transgression-regression cycles, possibly the result of early and mid Quaternary glacio-eustatic sea level fluctations. Representative stratigraphic sections of the Falor Formation in the eastern portion of the MRFZ are shown in Figure 4.

The lack of angular unconformities or disconformities with significant stratigraphic relief indicates MRFZ faulting and folding were not active during the deposition of the Falor sediments. About 1 km of subsidence at a rate slow enough to allow sedimentation in near sea level depositional settings is suggested by the formation's sedimentology and thickness. Development of fault and fold structures of the MRFZ probably terminated Falor deposition. Assuming sedimentation rates of 1 meter per 1000 years, tectonic activity in the MRFZ was initated no more than about 1 million years ago.

Patricks Point Terrace

Late Pleistocene marine terraces are present on headland sections of the coast in the vicinity of the MRFZ. Especially well developed is a sequence of at least six raised marine terraces at Trinidad (Stephens, 1982, Woodward-Clyde Consultants, 1980). The lowest of these, the Patricks Point Terrace, extends along the coast across the MRFZ. This terrace has been assigned an age of 85,000 years (isotope stage 5a) on the basis of soil development, stratigraphic position and comparison with worldwide sea level curves (Bloom et al., 1974). The terrace is displaced by each of the principal faults of the MRFZ. Prominent scarps and mole track ridges mark the fault traces, and the terrace surface is displaced vertically as much as 35 meters. These raised and deformed marine terraces indicate considerable tectonic activity in the MRFZ throughout the late Pleistocene.

Fluvial Terraces

Holocene and latest-Pleistocene fluvial terraces are present along the lower reaches of the Mad River and Jacoby Creek. The Holocene terraces are graded to modern sea level and lack of soil development; indicating they are less than 6000 years old. Raised fluvial terraces mantled with very weakly-developed soils represent latest Pleistocene river deposits. Locally, fault scarps up to 7 meters high cut these young fluvial terraces.

Activity of the MRFZ

Structural and stratigraphic reltionships indicate the MRFZ was initiated in the mid Pleistocene, perhaps about 1 million years ago. The existence of little-eroded saprolite beneath the Falor Formation and the lack of evidence of significant deformation during the deposition of the Falor Formation suggest the late Tertiary and early Quaternary landscape lacked relief associated with active folding and faulting.

Franciscan complex rocks have been thrust over Falor Formation sediments more than 1 km on each of the principal faults of the MRFZ. Minimum slip rates for these faults based on measured displacement of the base of the Falor Formation and the thickness of Falor sections beneath the overthrust Francisan range around 1 mm/year. Similar rates are derived from displacement of the late Pleistocene Patricks Point Terrace. Across the MRFZ cummulative displacement rates have been about 4 mm per year for the late

Quaternary. Fault displacements and slip rate determinations for the MRFZ are summarized in Table 2.

Conclusions

The MRFZ is a major northeast-dipping imbricate thrust fault and fold system of the mid and late Quaternary age in coastal northern California. It is a part of a broad region of compressional tectonic structures which define the Gorda-North American Plate Margin north of the Mendocino Triple Junction. To the south and east this system of compressional structures merges with the northern end of faults of the San Andreas Transform system. Thrust faulting and folding associated with the MRFZ was initated in the mid-Pleistocene after deposition of the Falor Formation. Prior to this thrusting, the tectonics of the area were relatively quiet. The onset of faulting in the MRFZ may represent the migration of the Mendocino Triple Junction northward into the northernwestern California region. Slip rates for principal faults within the MRFZ have been about 1 mm per year since the mid Pleistocene, and about 4 mm per year for the entire zone. Faulting, folding, and uplift associated with the mid and late Quaternary activity of the MRFZ and related compressional structures in the north coast region has generated the relief expressed by the present landscape and the structural complexity apparent in early and mid Quaternary deposits of coastal northern California.

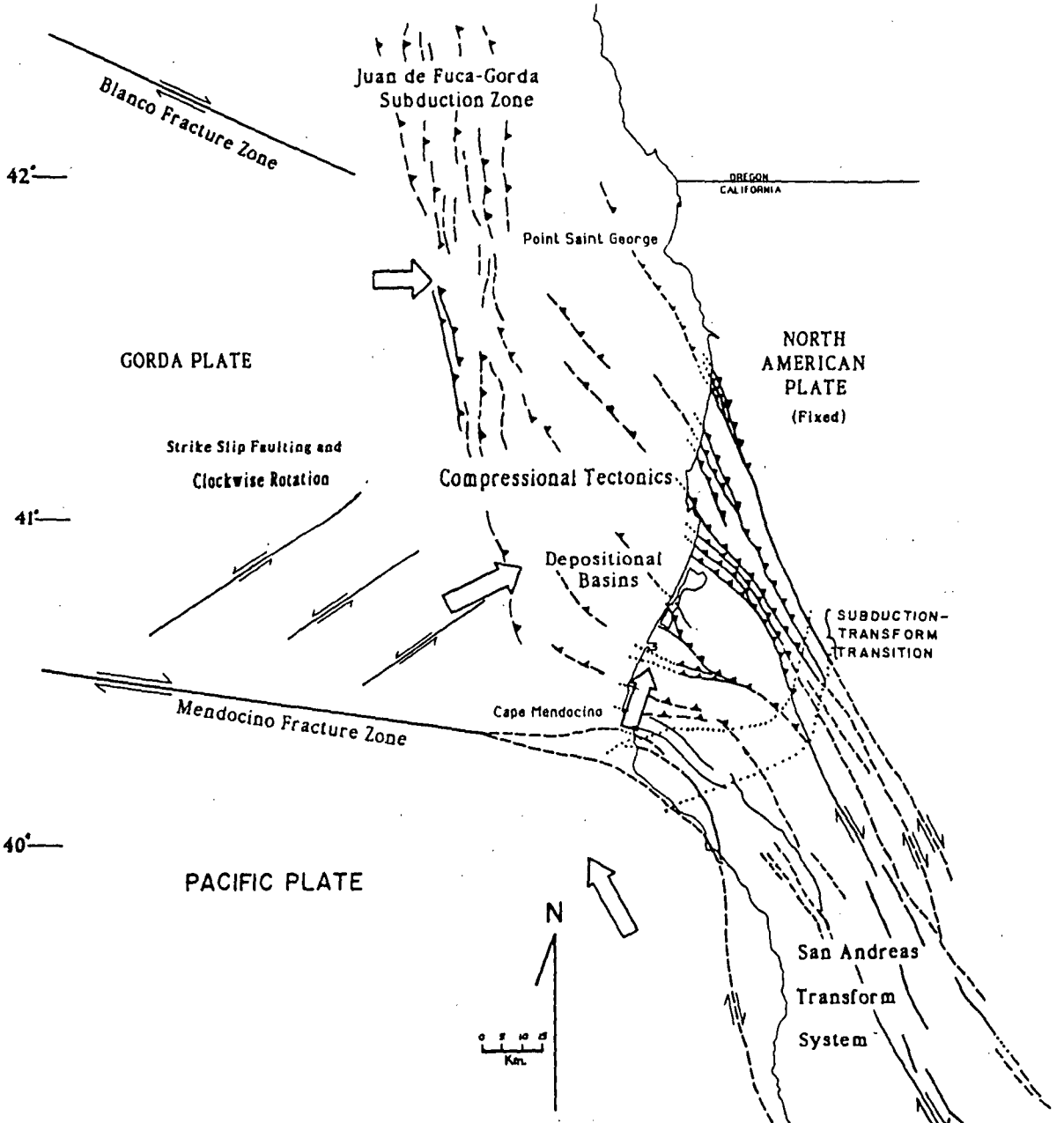

Figure 1. Regional tectonic setting of Northwest California in the vicinity of the Mendocino Triple Junction. Compressional structures of the Juan de Fuca-Gorda subduction zone trend onshore at their southern end and merge with strike slip faults of the San Andreas transform system. Large open arrows depict plate motion for the Pacific and Gorda Plates relative to a fixed North American Plate.

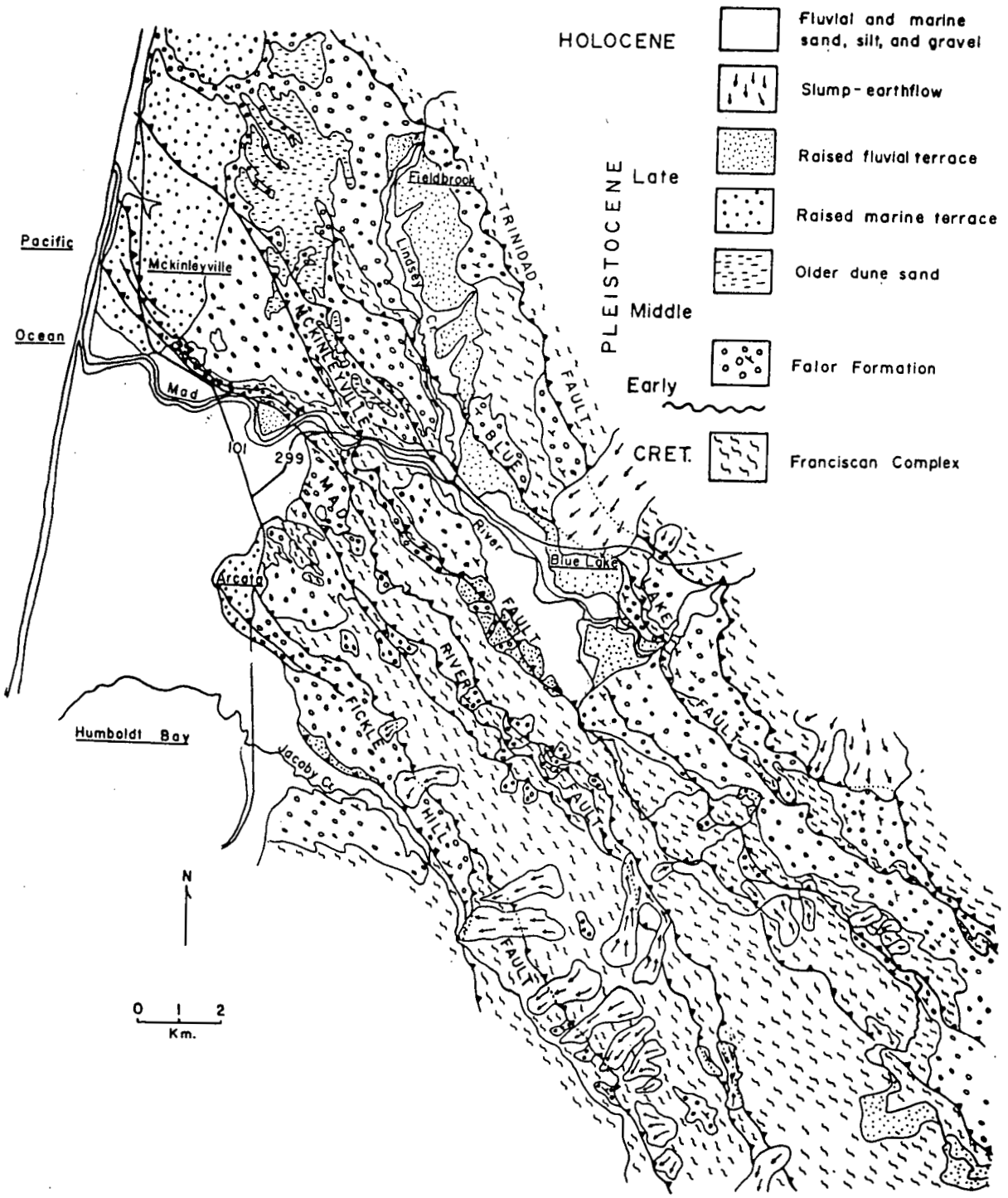

Figure 2. Quaternary Geologic Map of the Mad River Fault Zone.

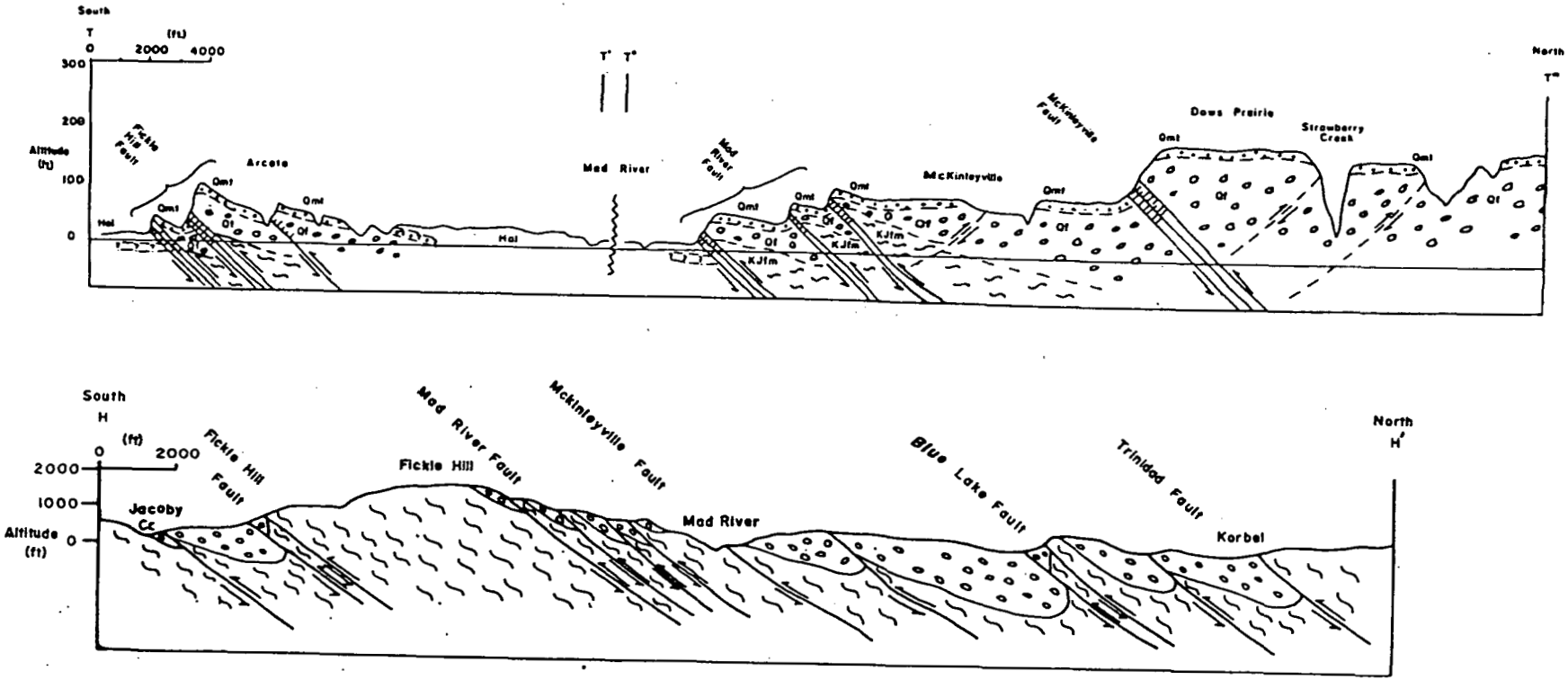

Figure 3. Geologic cross sections across the Mad River Fault Zone. Section T-T'-T'' is along the coast and illustrates the deformation of the late Pleistocene coastal terraces. Section H-H' is across the MRFZ near Korbel, and illustrates the deformation of the early Pleistocene Falor Formation.

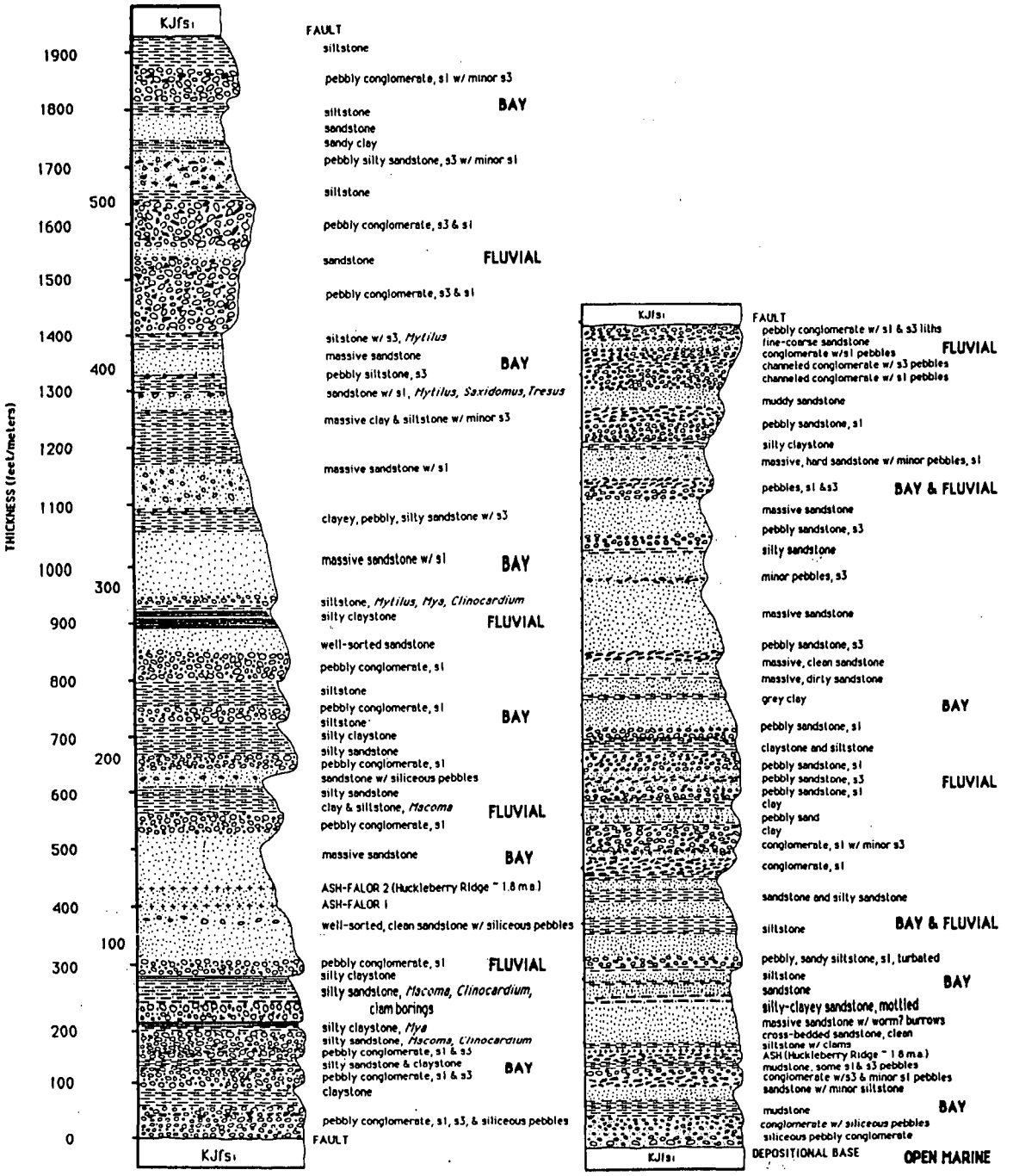

CANON CREEK SECTION HATFIELD PRAIRIE SECTION

Figure 4. Stratigraphic sections through the Falor Formation at Canon Creek and Hatfield Prairie. Above a basal sequence of shallow open marine deposits thick sequences of fluvial and bay sediments alternate. The Huckleberry Ridge ash (1.8-2.0 ma) lies in the lower portion of the bay facies just above the open marine sands. The sections lack angular unconformities or major disconformities and indicate slow continuous subsidence during deposition. The tops of the sections are terminated by thrust faults.

Age		Stratigraphic Unit		Tectonic/Sedimentologic
	MODERN	ACTIVE CHANNEL DEPOSITS		
	HOLOCENE	FLOOD PLAIN TERRACES		THRUST/REVERSE FAULTING--UPLIFT?
		FLUVIAL TERRACES		
		PATRICK'S PT.	65,000	THRUST/REVERSE FAULTING
	LATE PLEISTOCENE	TRINIDAD TERRACE SEQUENCE: WESTHAVEN	125,000	RAPID UPLIFT LOCALLY--GLACIO-EUSTATIC TERRACE CUTTING AND DEPOSITION
		SAVAGE CREEK		
		SKY HORSE		
		A-LINE		
		MAPLE STUMP		
	UNCONFORMITY			
QUATERNARY		MOONSTONE DEPOSITS	U SERIES DATE? >450,000	THRUST/REVERSE FAULTING-UPLIFT
		CRANNELL SANDS		
		*CRANNELL ASH?	>400,000	
	MIDDLE PLEISTOCENE	AGATE BEACH DEPOSITS		
		FALOR FM.		FLUVIAL AND SHALLOW MARINE DEPOSITION--MANY TRANSGRESSION AND REGRESSION CYCLES
	LOWER PLEISTOCENE			
		HATFIELD PRAIRIE ASH	1.8 M.a.	
			WEST ⟷ EAST	OPEN OCEAN ≷ ENCLOSED BASIN
				SLOW TECTONIC SUBSIDENCE--MARINE TRANSGRESSION AND DEPOSITION
	LOCAL UNCONFORMITY			
	LATE TERTIARY	SAPROLITE/HALTER RIDGE GRAVELS		-TECTONIC QUIESCENCE -EXTENSIVE WEATHERING -LOCAL FLUVIAL DEPOSITION?
TERTIARY	EARLY TERTIARY	UNCONFORMITY		REGIONAL UPLIFT AND EROSION
MESOZOIC		FRANCISCAN COMPLEX		SUBDUCTION ACCRETION
		KERR RANCH SCHIST		

Table 1. Stratigraphy of the Mad River Fault Zone and tectonic and sedimentologic interpretation of the development of the stratigraphic sequence.

Fault	Location	Datum	Age (m.a.)	Dip	Vertical Displacement (meters)	Dip Slip Displacement (meters)	Slip Rate (mm/yr)
Trinidad Fault	Anderson Ranch-Trinidad	Pat. Pt. Terrace	.85	25°	18	43	.50
Trinidad Fault	Jager Property-Trinidad	Pat. Pt. Terrace	.85	25°	14	33	.38
Trinidad Fault	Canon Creek	Falor Fm	1	40°	570	886	.88
Blue Lake Fault	Canon Creek	Falor Fm	1	40°	755	1174	1.11
Blue Lake Fault	Korbel	Falor Fm	1	35°	938	1631	1.64
McKinleyville Fault	Humboldt County Airport	Pat. Pt. Terrace	.85	25°	32	75	.64
McKinleyville Fault	Mad River Fish Hatchery	Fluvial Terrace	.02	30°	7	14	.70
McKinleyville Fault	Simpson Timber Co. Rd 4500	Falor Fm	1	35°	300	523	.52
Mad River Fault	School Road McKinleyville	Pat. Pt. Terrace	.85	25°	46	109	1.09
Mad River Fault	North Bank Road	Fluvial Terrace	.006	25°	3	7.1	.71
Mad River Fault	Simpson Timber Co. Rd 5400	Falor Fm	1	35°	330	575	.57
Fickle Hill Fault	Arcata	Older Marine Terrace	.2	25°	31	73	.36
Fickle Hill Fault	Jacoby Creek	Falor Fm	1	25°	350	828	.82
Mad River Fault Zone	Coastline	Pat. Pt. Terrace	.85	25°	127	300	3.53
Mad River Fault Zone	Jacoby Creek-Korbel Section	Falor Fm	1	35°	2305	4018	4.02

Table 2. Summary of displacement measurements and slip rates for faults in the MRFZ.

REFERENCES CITED

Atwater, T., 1970, Implications of plate tectonics for the Cenozoic tectonic evolution of western North America: Geol. Soc. Amer. Bull., v. 81, p. 3513-3536.

Bloom, A. L., Broecker, W. S., Chappell, J. M. A., Matthews, R. K., and Mesolella, 1974, Quaternary sea level fluctuations on a tectonic coast: new $^{230}Th/^{234}U$ dates from the Heon peninsula, New Guinea: Quaternary Research, v. 4, p. 185-205.

Carver, G. A., Stephens, T. A., and Young, J. C., (in preparation); Quaternary Geology Maps of Portions of the Arcata North, Arcata South, Korbel, and Blue Lake 7.5' Quadrangles, California Division of Mines and Geology Data Base Augmentation Program.

Carver, G. A., Stephens, T. A. and Young, J. C., 1983, Quaternary thrust and reverse faulting on the Mad River fault zone, coastal northern California, Geological Society of America abstracts with programs, v. 15, no. 5.

Carver, G. A., Stephens, T. A., and Young, J. C., 1982, Quaternary reverse and thrust faults, Mad River fault zone; in Late Cenozoic history and forest geomorphology of Humboldt County, California, Guidebook for Friends of the Pleistocene 1982 Pacific Cell Field Trip, p. 93-100.

Diller, J. S., 1902, Topographic development of the Klamath Mountains: U. S. Geological Survey Bulletin 196, 69 pp.

Field, M. E., Clark, S. H. and White, M. E., 1980, Geology and geologic hazards of the offshore Eel River basin, northern California continental margin; Open-File Report 80-1080, U.S. Geological Survey, Menlo Park, California, 80 p.

Herd, D. G., 1978, Intracontinental plate boundary east of Cape Mendocino, Geology, v. 6, p. 721-725

Kelsey, H. M. and Allwardt, A. O., 1983, Evidence for a major Quaternary fault zone in the Central Belt Franciscan melange, northern California; Geological Society of America abstracts with programs, v. 15, no. 5.

Manning, G. A., and Ogle, B. A., 1950, Geology of the Blue Lake Quadrangle, California; California Division of Mines and Geology Bulletin 148, 35 p.

Ogle, B. A., 1953, Geology of the Eel River Valley area, Humboldt County, California; California Division of Mines Bulletin 164, 128 p.

Riddihough, R., 1984, Recent Movements of the Juan de Fuca Plate System, Jour. Geophysical Res., v. 89, no. B8, p. 6980-6994

Silver, E. A., 1971, Transitional tectonics and late Cenozoic structure of the continental margin off northernmost California; Geological Society

of America Bulletin, v. 82, p. 1-22

Smith, S. W., and Knapp, J. A., 1980, The northern termination of the San Andreas Fault, in Studies of the San Andreas Fault Zone in northern California; California Division of Mines and Geology, Special Report 140.

Smith, S. W., McPherson, R. C., and Severy, N. I., 1981, The Eureka earthquake of 1980, breakup of the Gorda plate (abs), Earthquake Notes, 52, 44.

Stephens, T. A., 1982, Marine terrace sequence near Trinidad, California; in Late Cenozoic history and forest geomorphology of Humboldt County, California; guidebook for Friends of the Plesitocene 1982 Pacific Cell Field Trip, p. 100-105.

Woodward-Clyde Consultants, 1980, Evaluation of the potential for resolving the geologic and seismic issues at the Humboldt Bay Power Plant Unit No. 3, Appendixes, Woodward-Clyde Consultants, San Francisco, California.

THRUST FAULTING AND EARTHFLOWS: SPECULATIONS ON THE SEDIMENT BUDGET OF A TECTONICALLY ACTIVE DRAINAGE BASIN

by

Andre K. Lehre and Gary Carver
Department of Geology
Humboldt State University
Arcata, CA 95521

Introduction

In the last decade, considerable effort has been devoted to the definition and construction of sediment budgets in mountainous terrain, chiefly in Northern California, Oregon, and Washington (e.g., Dietrich and Dunne 1978; Dietrich and others 1982; Lehre, 1982a,b; Lehre, Collins, and Dunne 1983; Kelsey 1980, 1982; Kelsey and others 1981; Reid 1981). These studies have shown the utility of sediment budgets for predicting sediment yield and understanding process linkages; ultimately they should allow us to model landscape evolution. Although these studies were generally conducted in tectonically active areas (e.g., Kelsey 1980), none incorporated the possibility of direct tectonic transfer of material into the drainage basin. Many of these papers assume, in one sense or another, approximate long-term equilibrium between processes and products (e.g., in calculating soil residence time), but none considers the effect of tectonic input on equilibrium. Our objective in this paper is not to present finished research on the relations between tectonism and erosion in the Jacoby Creek basin --for that we have not got--but instead, to stimulate discussion as to what the relations are, how they might be modeled, what sorts of investigations/measurements might be useful in understanding them, and what their equilibrium implies. To this end we use a variety of crude mass-balance models, discussed below.

The Jacoby Creek Basin

The basin of Jacoby Creek above the gaging site is roughly rectangular, averaging 3.3 km wide and 11 km long (fig. 1). It is bounded on the north by Fickle Hill and on the south by Kneeland Ridge. Its vital statistics are summarized in Table 1. The creek heads at elevations of 550-650 m; the stream gage is at about 15 m (fig. 1). Average slope of the north side of the basin is 11°; that of the south side is 14°. The basin is covered chiefly by second-growth coniferous forest, parts of which are currently being logged.

The upper slopes of Fickle Hill consist largely of Franciscan melange and greywacke which have been thrust southward over Pleistocene shallow marine and continental sediments of the Falor Fm (Carver and others 1982; Carver and Stephens 1983; Carver, this volume). Falor sediments form much of the lower slopes of Fickle Hill. A small, nearly-horizontal patch of Falor sands lies in depositional contact with Franciscan melange on the crest of Fickle Hill (fig. 2 and Carver, this vol.) Kneeland Ridge consists chiefly of Franciscan rocks with a thin veneer of northeast-dipping Falor Fm --again in depositional contact with the Franciscan-- present locally near the creek.

Two major thrusts crop out on Fickle Hill about one third of the way between the creek and the divide (fig. 2). These faults, which are no older than about 1 m.y., have a total offset of around 1 km (Carver, this vol.) Estimates of faulting recurrence intervals, based on fault length-magnitude and magnitude-slip relations (e.g., Slemmons 1977), are on the order of

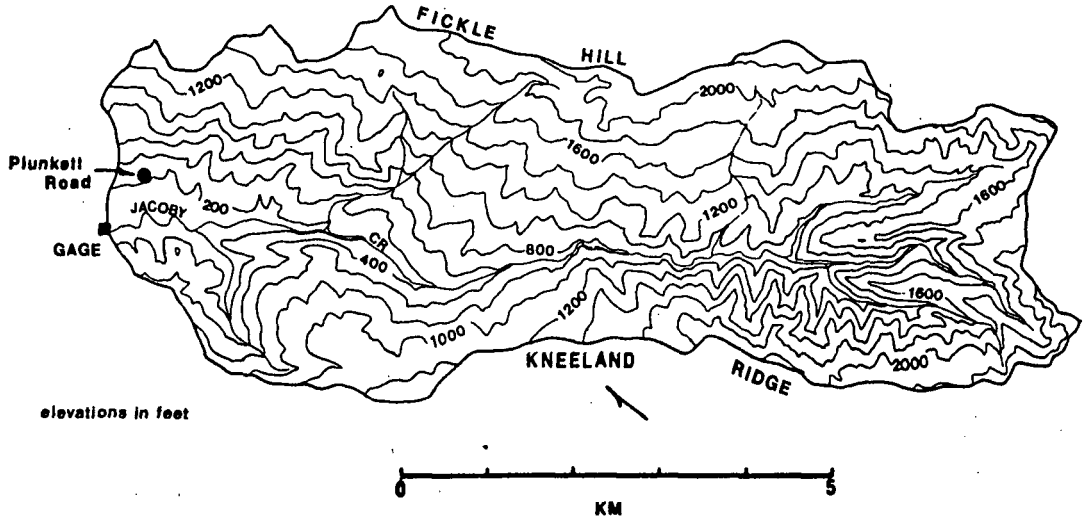

Figure 1. Topographic map of Jacoby Creek drainage basin above Tom Lisle's gage at covered bridge, compiled from Arcata South, Korbel, and Iaqua Buttes 7.5' quadrangles. Gage is located 4.7 km SE of Arcata, CA. Note that elevations are in feet.

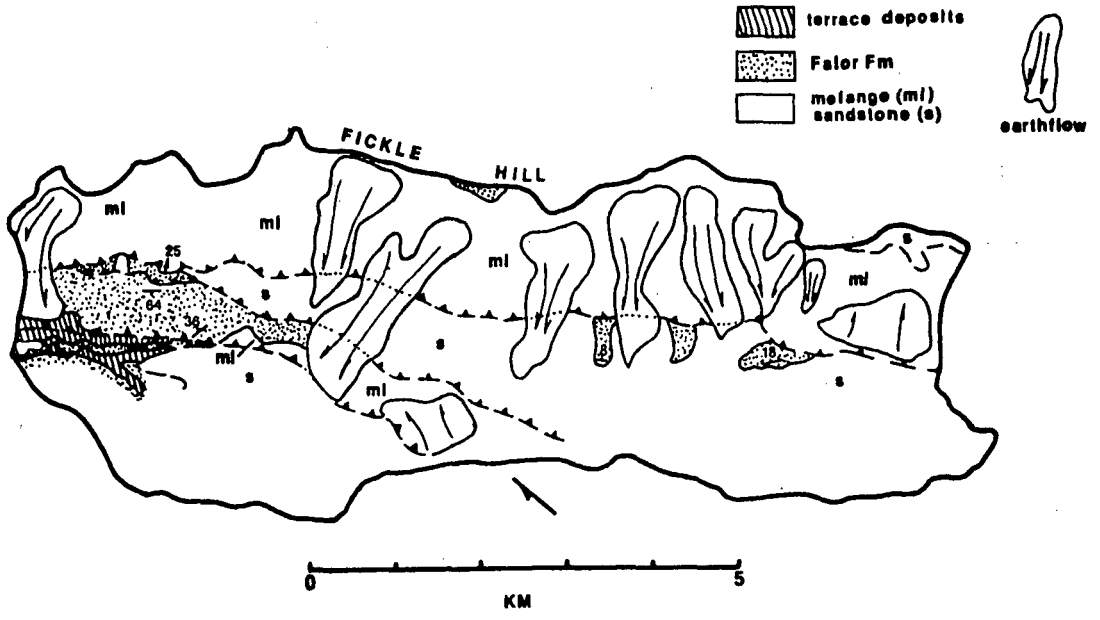

Figure 2. Geologic map of Jacoby Cr basin, simplified from mapping of Carver and Stephens (1985). Melange (ml) and greywacke sandstone (s) belong to the Franciscan group. Only active earthflows are indicated.

Table 1: Vital statistics of the Jacoby Creek basin

quantity	symbol	value	
drainage area	A	35.5	km^2
length of mainstem channel	L_{main}	12.5	km
total length of channels in basin	L_{tot}	160.5	km
drainage density	D_d	4.52	km/km^2
basin volume	V_{basin}	5.0	km^3
mean thickness of thrust sheet at divide	D_{thr}	0.84	km
relief ratio	R_r	64.2	m/km
mean annual discharge	Q_{mean}	0.85	m^3/s

5000-10,000 yr for offsets of 5-10 m/event. A reasonable estimate for mean rate of fault offset (Carver, this vol.) is 1mm/yr (1 m/1000 yr). This rate, which may be in error by 30%, is used throughout this paper.

The overall structure of Fickle Hill is an anticline cut by thrusts on its south flank. Jacoby Cr runs approximately along the axis of the adjacent syncline (fig 3). Structural relief due to folding is unknown, but is at least 200 m.

Erosional Processes in the Drainage Basin

Erosional processes active in the Jacoby Cr watershed are slump-earthflow, shallow debris slides, soil creep, sheet/rill erosion, and fluvial incision. Of these, large, active slump-earthflows originating in Franciscan melange appear the most important; they cover 20% of the drainage area of Jacoby Creek (from mapping of Carver and Stephens, 1985; see also fig. 2.) These earthflows typically head near the crest of Fickle Hill and extend down tributary valleys to Jacoby Creek. Old earthflow deposits and colluvium mantle interfluves between the mapped flows; these deposits (not shown on the geologic map) suggest more widespread earthflow activity in the past.

Shallow debris slides are restricted to colluvial hollows in Franciscan greywacke or are associated with roadcut and fill failures. Preliminary airphoto reconaissance suggests that these are quantitatively much less important than earthflows.

Seasonal and biogenic soil creep, as will be discussed later, are probably relatively unimportant. Sheet and rill erosion are important chiefly where vegetation has been removed by logging and roadbuilding; again, we suspect that they are quantitatively relatively unimportant.

Slopes in the Jacoby Cr drainage have obviously been dissected by streams. We have not yet been able to quantify their contribution to overall sediment yield, but they are clearly important in feeding earthflow debris and other slope-derived material to the main channel.

Sediment Yield of Jacoby Creek

The current sediment yield of Jacoby Creek at the gaging site, estimated by the duration curve - sediment rating curve method, is about 5500 t/yr. The sediment rating curve is based on 109 instantaneous water discharge and suspended-sediment concentration measurements taken during the period December 1978-December 1979 (Tom Lisle, unpub. data). We estimated the duration curve by prorating (by ratio to mean annual discharge) 1956-65 daily discharge data collected at a site 6.5 km upstream (Jorgensen and others, 1971). This technique has proved highly effective for regionalizing duration curves of North Coast streams (Lehre, unpub. data). The suspended load averages about 60% silt/clay and 40% sand (T. Lisle, pers. comm. 1985).

Bedload discharge in Northern California streams averages about 10-15% of suspended load discharge, although observed values range from 1-40% (see Lehre 1982a, Table 55). We have chosen 15% (825 t/yr) as a reasonable value for Jacoby Creek; bedload transport measurements at the site (Tom Lisle, pers. comm. 1985) confirm this. Bedload in Jacoby Cr is largely gravel.

We estimate total particulate load (bedload + suspended) for the creek at 6325 t/yr. Because we have no measurements of dissolved load, we ignore it below.

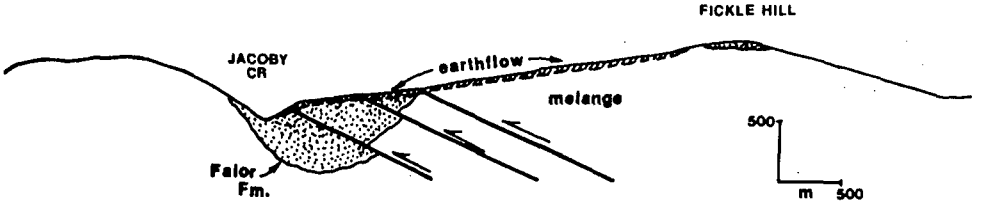

Figure 3. Structural cartoon of the Jacoby Cr basin based on mapping of Carver and Stephens (1985). Contact between Pleistocene Falor Fm. and Franciscan rocks (chiefly melange) is erosional unconformity, in part representing old abrasion platform. Thickness of Falor deposits in valley and amount of offset on individual faults are not known. Aggregate offset on faults in last 1 m.y. is about 1 km; north of Fickle Hill Falor Fm is 1 km thick. Thickness of earthflow deposits is exaggerated.

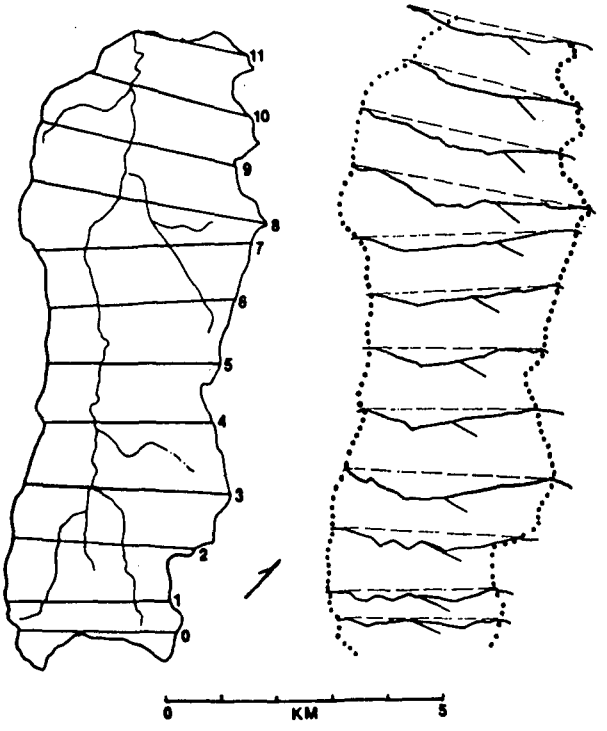

Figure 4. Cross-sections used to determine volume of Jacoby Cr basin. Dashed line is ridge-ridge tangent plane. Uppermost thrust is shown in each cross-section. No vertical exaggeration.

Denudation Rate and Soil Residence Time

Denudation rate for the drainage, assuming uniform lowering of the ground surface and no net storage of material in the basin, is given by a mass balance between sediment discharge and quantity eroded:

$$\text{denudation rate (m/yr)} = Q_s/AP_{rock} \quad (1)$$

For sediment discharge Q_s of 6325 t/yr (178 t/km^2/yr), A of 35.5 km^2, and P_{rock} of 2.5 t/m^3, the denudation rate (as rock) is 0.07 m/1000 y (.07 mm/yr). For soil with P_{soil} of 1.2 t/m^3, the denudation rate (as soil) is 0.15 m/1000 yr (0.15 mm/yr). In contrast, uplift rates computed from marine terraces in the Arcata-Trinidad area are 0.3-0.6 m/1000 yr (Carver and others 1982; Stephens 1982). Uplift is thus about four to eight times faster than denudation, implying 200 to 500 m of area-wide net uplift in the last 1 m.y. if the rates are valid over that time interval. A patch of shallow marine Falor Fm less than 2 m.y. old lying on top of Fickle Hill at 620 m (fig. 2, and Carver, this vol.) suggests the rates are reasonable.

Soil depth (pedogenic horizons) on hillslopes in the Jacoby Cr basin is on the order of 1.0 m. If we assume that soil thickness at any point stays constant with time (Dietrich and Dunne 1978), then a mass balance gives the number of years needed to erode the mean soil depth, z_{soil}:

$$\text{residence time (yr)} = (AP_{soil}\, z_{soil})/Q_s \quad (2)$$

This yields a residence time of 6700 yr, which seems exceptionally short for a forested basin. By contrast, Dietrich and Dunne (1978) estimated a 20,500 year residence time for soil in a forested basin in the Oregon Coast Range, and Kelsey (1982) estimated 15,000-50,000 yr of residence for surficial material in the Van Duzen River drainage. Residence times on the order of 12,000-20,000 yr thus seem more reasonable for Jacoby Cr soils. Possible causes of our seemingly low residence time are: 1) soils are at least twice as thick as we estimate, which does not seem reasonable; 2) current sediment yield is at least two times larger than the long term yield, which is possible, but has no supporting evidence; or 3) the assumptions of the residence time model do not apply because mass transport processes (such as earthflows) contribute significant volumes of saprolite, colluvium, and sheared rock as well as soil to the channel system. From fig. 2 this seems the most likely explanation.

Soil Creep vs. Earthflows

Several studies in the coastal mountains of northern California (Lehre 1982a,b), Oregon (Dietrich and Dunne 1978; Dietrich and others 1982), and Washington (Reid 1981) have proposed that sediment is transported from hillslope to stream chiefly by shallow debris slides and flows originating from colluvium-filled bedrock hollows (swales), which episodically fill and evacuate. These hollows fill by soil creep until sufficient material accumulates to allow sliding; thus creep rate, together with spatial frequency of hollows, ultimately determines denudation rate. This model appears generally applicable to steep slopes in weathered coherent rock (e.g., greywacke or volcanics); it is unlikely to be applicable where slope materials contain sufficient clay to allow flowage (e.g., Franciscan melange matrix).

A crude test as to whether soil creep could be responsible for most present-day denudation can be made by using a mass balance to compute the creep rate necessary to provide the observed sediment yield. Assuming a uniform creep rate supplying material to both banks of all channels in the basin:

$$\text{equilibrium creep rate (m/yr)} = Q_s/(2L_{tot}\, z_{cr}\, P_{soil}) \qquad (3)$$

where L_{tot} is the total length of channels in the basin and z_{cr} is mean thickness of the creeping material. Using L_{tot} = 160,500 m and assuming z_{cr} = 0.5 m, the required equilibrium creep rate is 0.033 m/yr (33 mm/yr). If the creeping layer is 1 m thick (which seems unreasonably large) the required creep rate is 0.016 m/yr (16 mm/yr). Since observed rates of seasonal or biogenic soil creep in such environments (Young 1972, Saunders and Young 1983) are on the order of 1-4 mm/yr, it appears unlikely that soil creep could be responsible for most current denudation of the basin. Assuming a 2 mm/yr creep rate over a 0.5 m depth, creep could directly supply only 385 t/yr (11 t/km^2/yr) or 6% of the observed sediment yield.

An analogous computation can be made for earthflows in the basin. Assuming a uniform rate of flowage supplying material to Jacoby Cr:

$$\text{equilibrium flow rate (m/yr)} = Q_s/(L_{ef}\, z_{ef}\, P_{rock}) \qquad (4)$$

where L_{ef} is total mean width of earthflows measured parallel to mainstem Jacoby Cr, and z_{ef} is mean earthflow thickness. For L_{ef} = 5500 m (calculated from fig. 2 by dividing earthflow area by mean length) and z_{ef} estimated at 10 m (c.f. earthflow thicknesses of 5-8 m in Iverson 1984, 10-30 m in Kelsey 1978, and 3-15 m in Swanston and Swanson 1976), the mean flowage rate required for equilibrium with current sediment yield is 0.046 m/yr (46 mm/yr). This rate is reasonable for forested earthflows (c.f. Swanston and Swanson 1976 table 2); but it is at least an order of magnitude less than those measured on grass-covered earthflows nearby (Kelsey 1978; Iversen 1984). The minimum rate of movement of the Plunkett Road earthflow at the west end of the basin (fig. 1), determined from damage to houses and roads, is 0.010-0.025 m/yr (10-25 mm/yr).

These simple calculations suggest that earthflows could easily supply most of the current sediment yield of the Jacoby Cr basin, but that it would be difficult for soil creep to do so. The predicted rate of earthflow movement is reasonable and similar to that actually observed.

Long-Term Erosion Rates

The long-term sediment yield of a drainage basin formed by simple incision of an originally planar surface, with no subsequent internal differential distortion (folding or faulting), is given by:

$$\text{long-term mean sediment yield (t/yr)} = (V_{basin}\, P_{rock})/T_o \qquad (5)$$

where V_{basin} is the volume of the basin below the original planar surface, and T_o is the time in years since incision began.

Although the Jacoby Cr basin has clearly undergone folding and faulting (figs. 2 and 3), it is instructive to apply this formula to it. Because the original Falor-Franciscan depositional surface --still horizontal-- is exposed on the top of Fickle Hill and, exhumed, forms the north slope of parts of Kneeland Ridge (Carver, this vol.), we approximated the original surface as a plane everywhere tangent to the crest of both ridges. (This is, of course, very crude: it neglects erosion of whatever Falor sediments lay above this surface, and ignores any contribution of tectonism to basin volume.) Basin volume (5.0×10^9 m^3) was calculated from 12 cross-sections spaced approximately 1 km apart (fig. 4).

Substituting present-day sediment discharge for the long-term value in (5) yields a basin age (To) of 1.98 m.y. This is too old: the Falor Fm, which is up to 1000 m thick north of Fickle Hill (Carver, this vol.), contains the 2.0 m.y. Huckleberry Ridge ash near its base (Andrei Sarna-Wojcicki, pers. comm 1985). Even if only 100-200 m of Falor sediments originally covered the top of Fickle Hill, any reasonable deposition rate suggests that a minimum of several hundred thousand years must have passed before erosion of the Jacoby Cr. basin could have begun.

If we assume basin development commenced about 1 m.y. ago (our best estimate), long-term sediment yield, computed from (5), is 12,500 t/yr, or approximately twice the current value. Perhaps this is real; Pleistocene climate changes may at times have produced sediment discharges well in excess of those presently observed. However, the value may be excessive for two reasons: 1) part of the measured basin volume is probably a result of tectonism, not erosion (see subsequent discussion); and 2) when basin relief was low (before appreciable incision or tectonism) erosion rates are likely to have been substantially smaller than current ones. Basin relief today is probably at a maximum. These results suggest that tectonic effects must be incorporated into any sediment budget model if we are to understand basin evolution.

A Simple Model of Basin Development under Thrusting

We propose a very simple-minded tectonic-erosional model as a first approximation for the development of the Jacoby Cr basin (fig. 5). In this model, an initially horizontal surface is thrust southward at a constant rate. The position of the creek is fixed; the divide is taken as a singular point which shifts upward and southward as thrusting continues. All relief between divide and creek is created by the thrusting; there is no differential erosional lowering of divide or creek. Material thrust into the basin (trapezoid ABDE in fig. 5) is regraded to form a slope of uniform angle (line DC) from divide to creek, thus increasing slope volume (triangle CDE); excess material (ABDE-CDE) is transported to the creek and removed. In this model, as thrusting continues, Fickle Hill grows in height and bulk, horizontal distance between creek and divide diminishes, and slope angle increases. Equations defining the model are given Appendix 1.

Figures 6-8 show the model predictions for a thrust fault dipping north at $\beta = 25°$ (the dip measured at the field trip stop) with initial (time-zero) creek-divide distance (L_0) of 3250 m, mean creek-fault distance (L_{cf}) of 900 m, and thrust rate of 1 mm/yr (0.001 m/yr). L_0 was determined from present day mean relief (R_{cd}) of 420 m and mean creek-divide distance (L_{cd}) of 2345 m by:

$$L_0 = L_{cd} + R_{cd} / \tan \beta \qquad (6)$$

This is the mathematical equivalent of sliding the divide back down to the level of the creek along a line parallel to the fault dip (see fig. 5).

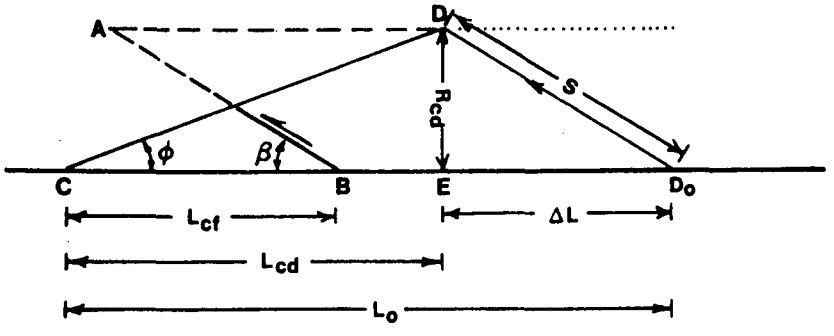

Figure 5. Definition sketch for model of basin development under thrusting. C is creek, D is divide, S is total slip, D_0 is position of divide before thrusting commenced. Initial topography is assumed flat (line C-D_0); dashed line A-D is imaginary position of that surface after slip S on fault has occurred. Line D_0-D shows path of divide as offset continues. Other symbols are discussed in text and appendix. Figure is schematic only.

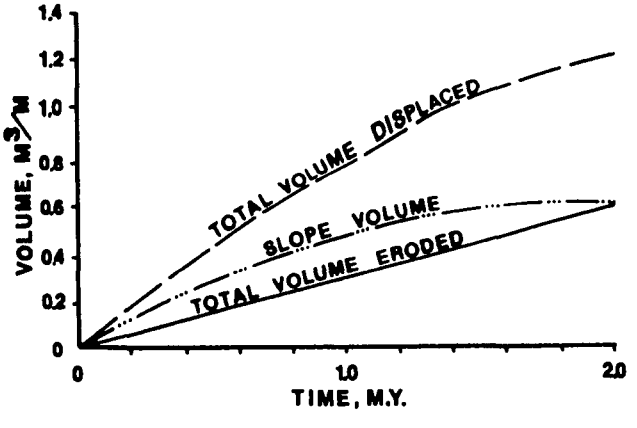

Figure 6. Total volume displaced, slope volume, and total volume eroded (difference between volume displaced and slope volume) as functions of time for model in fig. 5. Computed from eqs. A5-A7 in appendix. See text for discussion.

Total slip required to bring the divide from creek level to its current position is given by

$$S = R_{cd}/\sin \beta \qquad (7)$$

This amounts to 994 m, which, for a slip rate of 1mm/yr, implies a basin age of approximately 1 m.y.

The results of this simple model are illuminating. It suggests a reasonable age for the basin. It predicts a mean sediment yield of 7800 t/yr, only 25% larger than our estimated current yield of 6325 t/yr. If the basin is 1 m.y. old, the model predicts cumulative erosion of 3.1×10^9 m^3, only 11% less than our measured value of 3.4×10^9 m^3 for the volume beneath the ridge-ridge plane north of the creek. Our model thus seems to provide a reasonable first approximation of relations between tectonism and erosion in the basin.

Some Conclusions: Limitations and Implications of the Model

The proposed model has several defects. First, it predicts a uniform sediment yield which does not change with time (fig. 6). This is clearly unreasonable. In the early stages of basin formation, when relief (fig. 7) and slope (fig. 8) are very low, erosional processes should be less effective and sediment yield ought to be small; as relief and slope increase, we would expect increased sediment yield . This argument suggests that hillslope relief and volume initially grow more rapidly than the model predicts; perhaps at some point in slope development a threshold is then crossed which allows a more constant rate of erosion. This threshold might be that associated with the initiation of earthflows.

Second, the model does not explain how or why the slope is regraded to a constant angle. To achieve this, we need conveyor-belt like transport that effectively redistributes excess upper-slope material downslope. Earthflows are a likely candidate. At several sites (e.g., Plunkett Road), Franciscan melange debris has flowed downslope over Falor sediments. The south slope of Fickle Hill, though mantled by earthflows (fig. 2) appears surprisingly uniform in profile (fig. 4).

Third, thrust movement is unlikely to be uniform in time. While the mean slip rate may be 1mm/yr, actual displacement is most likely by increments of 5-10 m per event. We wonder if such sudden inputs of mass could trigger earthflow kinematic waves which would then lead to increased sedimentation in Jacoby Creek.

Fourth, the assumption that the divide and creek are fixed points which undergo no erosional lowering is unrealistic; both almost certainly do. However, the patch of Falor Fm on the crest of Fickle Hill suggests that this rate of lowering is small with respect to the rate of tectonism, and thus no great error is introduced. (We made this assumption because it greatly simplifies the geometry of the model; if we allow the divide to shift because of erosion the problem is much less tractable.)

Fifth, the model does not take into account structural deformation other than thrusting in development of the basin. Since the basin is in fact a syncline (figs. 2,3) a comprehensive model should include the effects of coseismic folding. Qualitatively, the effect of synclinal folding is to require a lower sediment yield than that predicted by our model, since some of the basin volume will be due to the downwarping.

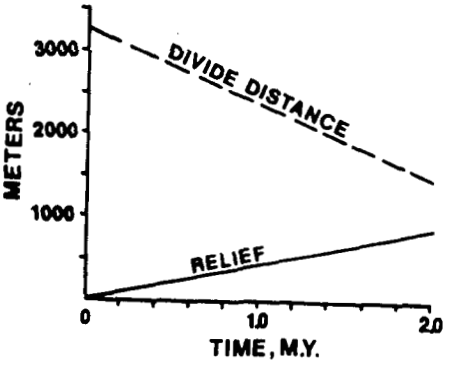

Figure 7. Creek-divide distance (L_{cd}) and relief (R_{cd}) as functions of time for model in fig. 5. Computed from eqs. A3 and A4 in appendix. See text for discussion.

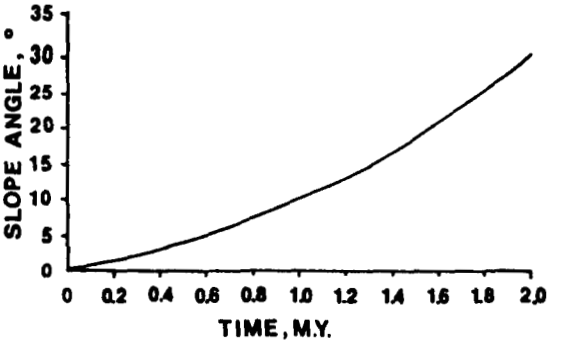

Figure 8. Increase in slope of south side of Fickle Hill with time for model in fig. 5. Computed from eq. A8 in appendix. See text for discussion.

Despite its limitations, the model strongly suggests that thrusting and erosion are not presently in equilibrium , i.e., that Fickle Hill is continuing to grow in relief and steepness. This hypothesis can be tested by a simple mass balance. The sediment yield required for equilibrium between thrusting and erosion is given by:

$$\text{equilibrium sediment yield (t/yr)} = r\, D_{thr}\, L_{thr}\, P_{rock} \qquad (8)$$

where r is thrust rate, D_{thr} is mean thrust plate thickness (measured from fault to divide along a line normal to the fault plane), and L_{thr} is fault length measured parallel to the valley axis. For r = 0.001 m/yr (1 mm/yr), D_{thr} = 840 m, and L_{thr} = 10,250 m, equilibrium sediment yield is 21,500 t/yr. This is approximately 3.5 times the current yield, supporting our contention that thrusting and erosion are <u>not</u> in equilibrium.

What does the future hold for the Jacoby Creek basin? According to our model, about 1 m.y. was needed for the south slope of Fickle Hill to attain its present mean gradient of 11°; fig. 8 indicates that it will grow to about 30° over the next million years. We do not believe this is likely; the materials are not strong enough. Instead, we propose that at some (unknown) future slope a threshold will be crossed and flowage rates will either increase greatly, or other processes (e.g., massive slumping or sliding) will take over to bring erosion and tectonism more nearly into equilibrium. We expect that such a transition would lead to major changes in Jacoby Creek. At least initially, the increased sediment input would lead to aggradation and the formation of fill terraces. Beyond this we have not ventured.

<u>Summary</u>

We have used simple mass balance calculations to investigate and model the relations between tectonism and sediment yield in a small basin undergoing active thrust faulting. Our results suggest that: 1) mass-balance approaches like ours can provide useful insight into basin development even if the input data and model are crude; 2) sediment budgets in tectonically active areas need to include explicitly a tectonic component if basin development is to be understood; and 3) "equilibrium" between erosion and tectonism can be best understood through sediment budget models, as these focus attention on the way dominant processes, process-linkages, and thresholds interact and change with time.

Our simple model suggests that tectonism and erosion in the Jacoby Cr drainage are <u>not</u> in equilibrium, and that Fickle Hill continues to grow in relief and bulk. Earthflows, originating in Franciscan melange of the upper thrust plate, redistribute thrust material downslope, and can account for the currently observed sediment yield of the basin.

<u>References Cited</u>

Carver, G.A., T.A. Stephens, and J. C. Young, 1982, Quaternary reverse and thrust faults, Mad River fault zone: *Friends of the Pleistocene 1982 Pacific Cell Field Trip Guidebook, August 5-8 1982*, p. 93-99.

Carver, G.A., and T.A. Stephens, 1983, Quaternary thrust and reverse faulting on the Mad River fault zone: *Geol. Soc. America Abstracts with Programs, 1983, v. 15 (5)*, p. 316.

Carver, G.A., and T.A. Stephens, 1985, Geologic maps of the Arcata South and Korbel quadrangles: *California Division of Mines and Geology Open-File Maps.*

Dietrich, W. and T. Dunne, 1978, Sediment budget for a small catchment in mountainous terrain: *Zeit. Geomorph. Supplbd. 29,* 191-206.

Dietrich, W.E., T. Dunne, N.F. Humphrey, and L. Reid, 1982, Construction of sediment budgets for drainage basins, *in* F.J. Swanson, R.J. Janda, T. Dunne, and D.N. Swanston eds., Sediment Budgets and Routing in Forested Drainage Basins: *U.S. Forest Service General Technical Report PNW-141*, p. 67-77.

Iverson, R.M., 1984, Unsteady nonuniform landslide motion: theory and measurement: unpub. Ph. D. thesis, Stanford University, Stanford, 302 p.

Jorgensen, L.N., M.A. Rose, R.D. Busch, and J.S. Bader, 1971, California streamflow characteristics (from records through 1968), v.1: *U.S. Geological Survey Water Resources Division Open-File Report 1004-05*, Menlo Park, 657 p.

Kelsey, H.M., 1978, Earthflows in Franciscan melange, Van Duzen River basin, California: *Geology, v. 6*, p. 361-364.

Kelsey, H.M., 1980, A sediment budget and analysis of geomorphic process in the Van Duzen River basin, north coastal California, 1941-1975: *Geol. Soc. America Bulletin, Part II, v. 91,* p. 1119-1216.

Kelsey, H.M., 1982, Hillslope evolution and sediment movement in a forested headwater basin, Van Duzen River, north coastal California: *in* F.J. Swanson, R.J. Janda, T. Dunne, and D.N. Swanston eds., Sediment Budgets and Routing in Forested Drainage Basins: *U.S. Forest Service General Technical Report PNW-141*, p. 86-96.

Kelsey, H.M., M.A. Madej, J. Pitlick, M. Coghlan, D. Best, R. Belding, and P. Stroud, 1981, Sediment sources and sediment transport in the Redwood Creek Basin: a progress report: *U.S. Nat. Park Service Redwood National Park Tech. Rept. 3*, 114 p.

Lehre, A.K., 1982a, Sediment mobilization and production from a small mountain catchment: Lone Tree Creek, Marin Co., California: unpub. Ph.D thesis, University of California Berkeley, 375 p.

Lehre, A.K., 1982b, Sediment budget of a small Coast Range drainage basin in north-central California, *in* F.J. Swanson, R.J. Janda, T. Dunne, and D.N. Swanston eds., Sediment Budgets and Routing in Forested Drainage Basins: *U.S. Forest Service General Technical Report PNW-141*, p. 67-77.

Lehre, A.K., B.D. Collins, and T. Dunne, 1983, Post-eruption sediment budget for the North Fork Toutle River drainage, June 1980-June 1981: *Zeit. Geomorph. Supplbd. 46*, p. 146-163.

Reid, L. M., 1981, Sediment production from gravel-surfaced forest roads, Clearwater Basin, Washington: *Univ. Washington Fisheries Research Inst. Report FRI-UW-8108*, Univ. Washington, Seattle, 247 p.

Saunders, I., and A. Young, 1983, Rates of surface processes on slopes, slope retreat, and denudation: *Earth Surface Processes and Landforms, v. 8*, p. 473-501.

Slemmons, D.B., 1977, State-of-the-art for assessing earthquake hazards in the United States; Report 6: Faults and earthquake magnitude: *U.S. Army Corps of Engineers Waterways Experiment Station*, Vicksburg, 166 p.

Stephens, T.A., 1982, Marine terrace sequence near Trinidad, Humboldt County, California, *Friends of the Pleistocene 1982 Pacific Cell Field Trip Guidebook, Aug. 5-8, 1982*, p. 100-105.

Swanston, D.N., and F. J. Swanson, 1976, Timber harvesting, mass erosion, and steepland forest geomorphology in the Pacific Northwest: *in* Coats, D.R., ed.: *Geomorphology and Engineering*, Dowden, Hutchinson & Ross, Stroudsburg, p. 199-221.

Young, A., 1972, Slopes: Oliver and Boyd, Edinburgh, 288 p.

APPENDIX: MODEL EQUATIONS

The quantities below are used in the equations defining the model of figure 5:

β: dip angle of thrust plane (°)

r: rate of thrusting (m/yr)

t: time since initiation of thrusting (yr)

S: total amount of slip on fault (m)

L_{cd}: distance from creek to divide, measured horizontally (m)

L_{cf}: distance from creek to fault trace, measured horizontally (m)

L_o: distance from creek to divide at $t = 0$ (m)

ΔL: total change in horizontal distance between creek and divide due to faulting (m)

R_{cd}: relief between creek and divide (m)

V_{trap}: total volume of material thrust into basin per unit length of fault; numerically equivalent to area of trapezoid ABDE ($m^3/m/yr$)

V_{tri}: total volume of hillslope per unit length of fault; numerically equivalent to area of triangle CDE ($m^3/m/yr$)

V_{eros}: total volume of material eroded per unit length of fault; numerically equivalent to ABDE-CDE ($m^3/m/yr$)

ϕ: angle of hillslope from crest to divide (°)

The equations which define the model are:

$$S = rt \tag{A1}$$

$$\Delta L = rt \cos\beta \tag{A2}$$

$$L_{cd} = L_o - \Delta L \tag{A3}$$

$$R_{cd} = rt \sin\beta \tag{A4}$$

$$V_{trap} = [L_o - L_{cf} - (\Delta L / 2)] R_{cd} \tag{A5}$$

$$V_{tri} = 0.5 R_{cd} [L_o - \Delta L] \tag{A6}$$

$$V_{eros} = V_{trap} - V_{tri} = 0.5 R_{cd} [L_o - 2L_{cf}] \tag{A7}$$

$$\phi = \tan^{-1}(R_{cd}/L_{cd}) \tag{A8}$$

PROGRAM OF TECHNICAL SESSIONS
KATE BUCHANAN ROOM, FOUNDERS HALL
HUMBOLDT STATE UNIVERSITY

0840 - 0900 WELCOME

0900 - 1000 ORAL SESSION #1

0900 - 0920 Dorothy J. Merritts: Use of the stream-gradient index to identify tectonic controls on fluvial systems, Cape Mendocino to Fort Bragg, northwestern California

0920 - 0940 Suzanne Hecker: Recurrence intervals and timing of Holocene faulting along a segment of the central Nevada seismic belt

0940 - 1000 William B. Bull and Peter L. K. Knuepfer: Impact of Pleistocene-Holocene climatic change on hillslopes in a humid, mesic watershed

1000 - 1040 COFFEE, TEA, COOKIE BREAK AND POSTER SESSION #1

1040 - 1140 ORAL SESSION #2

1040 - 1100 Steven L. Reneau, William E. Dietrich, Ronald I. Dorn, C. Rainer Berger, and Meyer Rubin: Landslides and climatic change in colluvium-mantled hollows, central California

1100 - 1120 Robert B. Jacobson: Magnitude and frequency of slope failures, Marion County, WV

1120 - 1140 Leslie M. Reid: Erosion and deposition in a discontinuous gully system

1140 - 1300 LUNCH IN COURTYARD

1300 - 1400 POSTER SESSION #2

1400 - 1500 ORAL SESSION #3

1400 - 1420 Lee E. Benda: Runout and deposits of debris flows in the Oregon Coast Range

1420 - 1440 Gordon Grant: The effect of timber harvest activities on the channel morphology of some western Cascade streams

1440 - 1500 Nick C. Varnum and Vicki L. Ozaki: Recent channel adjustments in Redwood Creek, CA

1500 - 1600 COFFEE, TEA, COOKIE BREAK AND POSTER SESSION #3

1600 - 1640 ORAL SESSION #4

1600 - 1620 Joan Florsheim: Hydraulic requirements for gravel bar formation, northwestern California

1620 - 1640 Randy D. Klein: The role of organic debris in channel erosion and armor development in disturbed headwater streams

POSTER SESSIONS:

NORTHWESTERN CALIFORNIA:

1) Donna C. Marron, K. Michael Nolan, and Harvey M. Kelsey: Progress Report on a compilation of research done in the Redwood Creek basin, California

2) James H. Popenoe: Soil-topography relationships on schist in Redwood National Park

3) Peter D. Bromirski: Seismic refraction investigation of two earthflows in Redwood Creek basin

4) Frank Bickner: Geology and alluvial history of the South Fork Eel River basin in Humboldt County, northern California

5) Dick LaVen and D. A. Short: Channel changes in the Bull Creek watershed: 1932 - 1984

ELSEWHERE:

6) K. Prestegaard, F. Van Ness, R. Henry, P. Goldschimdt, and M. Garbee: Movement of talus on rock hillslopes in Pennsylvania

7) Scott Lundstrom: Obsidian hydration dating applied to a faulted glacio-fluvial terrace in the upper Madison Valley, Montana

8) Kent E. Snyder and Ray B. Bryant: Slope processes and fragipan expression in soils of the Salamanca Re-entrant (New York).

RUNOUT AND DEPOSITS OF DEBRIS FLOWS IN THE OREGON COAST RANGE

Lee E. Benda

University of Washington

Runout and deposits of 46 debris flows were studied in Knowles Cr., a 52 km^2 basin underlain by uplifted marine sandstones of the Tyee/Flournoy formation located in the central Oregon Coast Range. Debris flows eroded to bedrock 1st- and 2nd- order channels with slopes greater than 10°. Deposition of debris flows resulted from reductions in slopes and increases in widths of channels and valley floors, conditions that were often encountered where 2nd- order channels intersected 3rd- and higher- order streams. In cases where debris flows entered and traveresed 3rd- order channels, deposition would occur along mid-reaches of channels at slopes of 4°.

Deposits of debris flows ranged from 2000-10,000 m^3 and contained large volumes of wood and up to 20% cobble and boulder sized sediments (160-3000 mm). Fluvial erosion of debris flow deposits increased with increasing drainage area above the point of deposition. Thus deposits of debris flows in upper basins can dominate local channel morphology for decades, whereas deposits of debris flows in lower areas of the basin can be severely eroded by floodwaters potentially generating debris floods.

Boulders contained in deposits of debris flows resist fluvial transport and remain at deposition sites. This results in distributions of boulders in channels that are related to patterns of debris flow activity. Second-order channels that intersect 4th- and 5th- order channels are sites of high densities of boulders because debris flows consistently deposit at these tributary junctions. Further, deposits of debris flows that occur at tributary junctions impinge on streams and induce channel meanders.

Recent debris flows in Knowles Cr. have deposited on fans of debris flow material that are at least 200 years old. Therefore, debris flows that occur consistently at the same locations within the basin develop depositional features that become an integral part of channel and valley floor morphology.

GEOLOGY AND ALLUVIAL HISTORY OF THE SOUTH FORK EEL RIVER BASIN IN HUMBOLDT COUNTY, NORTHERN CALIFORNIA

Bickner, Frank; Departments of Watershed Management and Geology, Humboldt State University, Arcata, California 95521

The landscape of the South Fork Eel River basin (1750km^2) of Northern California is dominated by the combined effects of rapid Quaternary tectonic uplift and climatic changes. The South Fork Eel River (SFER) between Garberville and the confluence with the main stem Eel River can be divided into three distinct basin/channel morphologic reaches. The reaches are defined by different terrace morphologies and stratigraphy, channel sinuosity, hillslope processes and channel processes.

Morphologic reach 1 is characterized by thirteen nested terrace surfaces 3m, 4m, 6m, 8m, 10m, 24m, 53m, 55m, 78, 108m, 259m, 270m, and 308m above the SFER in the Garberville area. These terraces were examined in detail. Tentative ages of the terraces are based on relative dating and on an over-simplified constant-incision-rate model. The model generally supports the terrace age groupings of (1) Holocene (2) 10-14,000 ybp (3) 24-76,000 ybp (4) 106-140,000 ybp and (5) greater than 300,000 ybp. Shallow bedrock sills influence gradient in this reach.

Morphologic reach 2 conspicuously lacks fluvial terraces. This is due, in part, to the high down slope movement rates of slump-earthflow complexes in the Franciscan Melange exceeding laterial river corrasion rates. Channel gradient in this reach is influenced by high sediment production and channel armoring by lag gravels and boulders.

In morphologic reach 3 the active channel widens and slope gradient decreases. The channel is bordered by a series of wide Holocene fill terraces composed of overbank and slack-water deposits. Strath terraces are restricted to large meander loop locations. The Holocene fill terraces become more extensive toward the confluence of the SFER and the main stem Eel River. Drill and seismic data indicate that channel fill in the lower 3.2km reach is approximately 10m deep increasing to 14m near the confluence with the main stem Eel River.

SEISMIC REFRACTION INVESTIGATION OF TWO EARTHFLOWS IN REDWOOD CREEK BASIN. BROMIRSKI, Peter D. Watershed Management Department, Humboldt State University, Arcata, CA. A seismic refraction investigation was conducted at earthflows located at Miner Creek and Counts Hill Prairie in the Redwood Creek basin. The purpose of this study was to determine the depth to the failure surface. Seismic results are compared with inclinometer data. Seismic lines of about 75m were run transverse to the slope. Travel time data was taken with a 12-channel seismograph using explosives as the source. A single channel instrument was used to determine surface velocity and depth. A surface layer and a deeper boundary were identified. At the Miner Creek site, surface layer thickness varied from 1-2.5m with a velocity range of 350-390m/s. The depth to the deeper boundary averaged about 10m while ranging from 6-15m. The average depth of 10m to the deeper boundary is consistent with the 8m plus inferred by Iverson (1984) from Miner Creek inclinometer data for shear zone depth in the center of the slide. The velocities for this zone varied from about 800-1100m/s, while basement velocities showed a variation of 1225-1700m/s. The shallow shear zone of about 5m observed by Iverson at the margin of the active portion of the slide may be associated with movement of the surface layer since the continuous failure boundary determined seismicly is about twice as deep. The water table, as inferred from piezometer data (Iverson, 1984), was not detected with the refraction technique, indicating a relatively diffuse boundary. Results from the Miner Creek and Counts Hill sites are compared and contrasted.

IMPACT OF PLEISTOCENE-HOLOCENE CLIMATIC CHANGE ON HILLSLOPES IN A HUMID, MESIC WATERSHED

William B. Bull, Geosciences Department, University of Arizona, Tucson, AZ 85721 and Peter L. K. Knuepfer, Department of Geological Sciences, Cornell University, Ithaca, NY 14853

Aggradation and degradation rates of late Quaternary streams are controlled by climate-change induced changes on watershed hillslopes. The rugged Charwell River drainage basin, South Island of New Zealand, is underlain by fractured graywacke, and ranges in altitude from 450 to 1600 m. Treeline is at 1200 m but may have been 1100 m lower during full-glacial climates (Soons, 1962; Stevens, 1974) when periglacial processes favored high sediment yields and valley-floor aggradation. For slopes lower than 1200 m, change to a warmer Holocene climate was associated with increases in stream power because of more storm runoff as the rainfall/snow ratio increased. Concurrent decreases in sediment yield occurred because of marked decreases in periglacial processes as alpine vegetation was replaced with rain forest. These changes in hillslope processes caused the stream subsystem to change modes of operation from aggradation to degradation. Variations in water and sediment yield resulted in 12 fill, cut, and strath terraces whose ages have been estimated by relative-absolute dating of cobble-weathering rinds and soil profiles. Latest Pleistocene valley aggradation was followed by an overall sequence of slow-rapid-slow channel downcutting. Holocene degradation rate probably varied as a function of how far removed the stream system was from threshold or equilibrium conditions.

HYDRAULIC REQUIREMENTS FOR GRAVEL BAR FORMATION NORTHWESTERN CALIFORNIA

Joan Florsheim, Dept. of Geology, U.C.S.B., Santa Barbara, CA 93106

Channel bar formation depends mainly on slope, particle size, and width to depth ratio. Based on field data for 15 north coastal gravel-bed stream reaches, no riffles or storage bars are present at slopes of 0.02 in reaches without obstacles. At slopes greater than 0.02, step-pool structure is common. Church and Jones' (1982) model, based on the relation of flow depth to particle size determines the maximum slope allowable for bar formation. The model agrees with our field data when Parker and Klingeman's (1982) value of $\tau^*=0.035$ for D50 is used. Furthermore, bar morphology is dependent on the relation between slope and bed material size.

The relationship between flow intensity and the product of channel slope and width to depth ratio denotes distinct fields for gravel bar morphology including: storage bars with riffles, storage bars only, and no bars (with step-pool morphology). Steep north coastal streams would probably form bars if mean particle sizes were smaller or width to depth ratios were larger.

THE EFFECT OF TIMBER HARVEST ACTIVITIES ON THE CHANNEL MORPHOLOGY OF SOME WESTERN CASCADE STREAMS

Gordon Grant
Graduate Research Assistant
Johns Hopkins University

This study was undertaken to determine whether channels with different management histories responded differently to a large storm event in December, 1964. Sequential aerial photographs were used to document channel response among a population of 38 fourth- and fifth-order channels located in the Oregon western Cascades. Analysis of 1959 and 1967 aerial photos revealed that channel response, as indicated by enlargement or opening of the riparain corridor, was not independent of management conditions in headwater areas; most of the riparian opening initiated at landslides out of clearcut or roaded areas. Detailed field measurements were made to determine 1) what specific processes were responsible for producing channel opening, 2) what were the effects of channel opening, as observed in the photos, in terms of channel and valley floor morphology, and 3) to what extent did local features, such as hillslope mass movements or bedrock outcrops, affect the degree to which channels opened.

In order to address these questions, channel and valley floor units were identified, mapped and measured in three channels with different response and management histories. Channel units were identified based on their slope, geometry, particle size distributions, and relative roughness; identified units included pools, rapids, boulder cascades, and bedrock and log falls. Valley floor units were identified by their heights above the low-water channel, stratigraphy; age of units was bracketed by tree-ring dating. Identified valley units included active channel surfaces, floodplains, debris flow deposits, and terraces. The distribution, frequency, sequence, and spacing of channel units were compared for open and unopened channel segments. While the frequency of pools was somewhat less in the open segments, this result was not statistically significant. Local valley wall constraints, such as bedrock outcrops and earthflows that impinged on channels, exerted stronger controls on the distribution of channel units than did opening. On the other hand, distribution of valley floor units was different between open and unopened segments with significantly greater percentages of the total valley area in floodplain or debris flow units along open segments. Valley wall constraints played an important role in determining where floodplain or debris flow units were located.

The implications of this study are: 1)Management activities in headwater areas can result in differential response of downstream channels to a large storm event; channel response consists of an apparent enlargement or opening of the riparian corridor and appears to be linked with pulse sediment delivery into channels from landslides; 2) Channel morphology, observed 20 years after the storm, does not appear to be significantly different between channels with different response histories, suggesting that channel recovery times are relatively rapid; 3) Large storms can produce significant changes in the distribution of valley floor surfaces which has implications for the dynamics of riparian zone ecosystems; the correlation between managment activities and storm effects suggest that these changes are more likely to be found in logged basins, and 4) Valley wall constraints, such as earthflows and bedrock outcrops strongly influence the location and distribution of channel and valley floor units in mountain streams.

RECURRENCE INTERVALS AND TIMING OF HOLOCENE FAULTING ALONG A SEGMENT OF THE CENTRAL NEVADA SEISMIC BELT

Hecker, Suzanne, Dept. of Geosciences, University of Arizona, Tucson, AZ 85721

Several lines of evidence indicate that the recurrence interval of large-magnitude faulting has varied temporally during the Holocene along a portion of the central Nevada seismic belt that spans historical (1954) ruptures and an adjacent portion of the Stillwater seismic gap. Alluvial fault scarps that offset a 12 ka shoreline evidence only one prehistoric offset and thus are amenable to morphologic age analysis. Diffusion equation modeling of scarp degradation, using the diffusion rate calculated for the Bonneville and Lahonton shorelines, indicates a probable age of 2.7-3.0 ka for the youngest prehistoric surface rupture in the area. Sedimentation rates in a graben formed during the event, calculated from a buried ash unit, constrain faulting to between about 2.0 and 5.0 ka and indicate a prefered age estimate of 3.2 ka. The faulting documented by the single-event scarps apparently was preceded by at least 8000 years of little or no activity along the front, as evidenced by similar displacement of early and mid-to-late Holocene fan surfaces. Estimates of surface age result from placing quantitative studies of soil-profile development ("Harden Indices") into an absolute age framework, using shorelines, evidence of Holocene salt accumulation, and several dated soils.

Recurrence intervals between major movements on individual fault zones during the Holocene evidently have varied from approximately 3000 to 8000+ years. Average long-term recurrence intervals of 7000-13,000 years and 6000-8000 years can be estimated for the late Quaternary and the last 10-13 m.y., respectively. In light of these results, average recurrence intervals should be used with caution when predicting shorter-term periods between events.

Given dating resolution, the timing of prehistoric Holocene faulting is essentially identical in the historically ruptured and unruptured sections of the study area, suggesting that the historical pattern of incremental filling of the central Nevada seismic belt with successive, large events may continue and eventually close the Stillwater seismic gap. Results of fault scarp modeling and numerical analysis of faulted and unfaulted soils show no distinction between the age of scarps studied in the seismic gap and those in the area of 1954 displacement.

MAGNITUDE AND FREQUENCY OF SLOPE FAILURES, MARION COUNTY, WV

Robert B. JACOBSON, Department of Geography and Environmental Engineering, The Johns Hopkins University, Baltimore, MD 21218

A 33 year record of slope failures constructed from tree ring dates of 197 failures in Marion County, WV, provides data for evaluation of the magnitude and frequency of these events. Allowing for a one to two year lag for tree colonization of failure scarps, peaks in the time series can be correlated with major runoff events. Peaks correlate well with the annual series of maximum 30 day and maximum 7 day runoff; the slope failure peaks do not correlate well with annual, maximum monthly, or maximum 24 hour precipitation. The greatest aggregate failure volume was produced in 1963; the greatest 30 day runoff on record, 20.32 cm, was recorded in spring of that year.

Correlation of failure volumes with specific annual 30 day runoff events allows estimation of the relationship between aggregate failure volume and recurrence interval of driving meteorological events. Percentage of the total landscape slope failure volume fits a power function: volume % = $.032(30 \text{ day runoff})^{1.9}$. The annual series of maximum 30 day runoff events fits a log-normal distribution. Multiplication of the runoff frequency distribution model by the volume percentage model gives the product of frequency and magnitude for a given amount of runoff, a measure of the cumulative geomorphic work done at different frequencies (Wolman and Miller, 1960). For this calibrated model the peak of the magnitude x frequency product curve occurs at 15.0 cm runoff, corresponding to approximately 4 year recurrence. Hence, on this landscape where slope failure is the dominant erosional and transport process, most geomorphic work occurs at moderate frequencies.

The Role of Organic Debris in Channel Erosion and Armor Development in Disturbed Headwater Streams

Randy D. Klein, Soil Conservationist, Redwood National Park, California

A major part of the watershed restoration program in Redwood National Park, Humboldt County, California, involves the excavation of fill material from stream crossings on former logging roads. The degree of channel erosion and armor development on 24 newly excavated stream crossings was measured following the 1982-83 winter runoff season. Other variables quantified related to channel morphometry, stream power, and abundance and arrangement of organic debris.

Drainage areas above the study reaches varied in size from 1.6 to 37.2 ha. Peak flow during the study period occurred during a rainfall event of three years recurrence interval.

Channel adjustments observed included: 1) downcutting, 2) lateral cutting, 3) armoring, 4) development of boulder/cobble cascades and organic knickpoints, and 5) changes in stream gradient. The magnitude of adjustments was largely dependent upon the adequacy of supply of channel-stabilizing materials relative to stream power. Organic debris and boulders accumulated in varying amounts and spatial distributions in the study reaches by either: 1) fluvial transport from upstream, or 2) exhumation during downward or lateral cutting.

Organic debris was found to be important in controlling channel scour and armoring requirements. Interlocking accumulations of organic debris evolved into stable (at least in the time scale of the study) knickpoints at variably spaced intervals. They function as local profile controls and sediment traps.

The proximity of organic debris jams to one another regulated the amount of scour occurring: the greater the distance between them, the greater the amount of intervening scour. In stream reaches where the organic debris supply was plentiful, profiles assumed stair-stepped configurations following minimal scour. Where these materials were less abundant, channel scour was more extensive and profiles assumed an exaggerated concave upward configuration.

Reaches which contained little or no organic debris experienced the greatest shift toward coarser channel bed sediments. Channel armoring materials, consisting chiefly of cobble-sized particles, were derived by lag accumulation from eroding bed and bank materials.

CHANNEL CHANGES IN THE BULL CREEK WATERSHED: 1932 - 1984

LaVen, Dick, Earth Sciences and Resources program, U.C. Davis, and D. A. Short, Watershed Management Department, Humboldt State University.

Channel changes in the Bull Creek Watershed (105 km^2), Humboldt County, California, have been documented through air photos and field survey data. Air photos taken periodically since 1932 show channel widening and the progradation of a delta at the confluence of Bull Creek with the South Fork Eel River since 1954. These channel changes either coincide with or follow closely behind widespread watershed disturbances; i.e., logging, roadbuilding, and fire.

Over 60% of the upper 67 km^2 of the Bull Creek watershed was logged between 1947 and 1965. Many tributaries responded to this widespread disturbance by channel widening and aggradation. The most pronounced of these was the 10.3 km^2 Cuneo Creek basin. Historic air and ground photos and on-site evidence indicate that a minimum of 6 m of aggradation and up to 100 m of channel widening occurred in the lower reaches of Cuneo Creek between 1953 and 1964.

Channel change was also evident in the lower watershed. Survey data from the lower reaches of Bull Creek (9,000 m) show aggradation in excess of 2 m following the 1955 flood and a net aggradation of up to 5 m for the period 1961 - 1983. The lower channel has been excavated twice (1956 - 1963 and 1965 - 1969) during this period of aggradation. Bull Creek has apparently lost the ability to transport coarse bedload since 1975. This is supported by plots of b, f, and m exponents of channel geometry using Rhodes' (1977) Triaxial method. Further verification is provided by regressions of y (cross-sectional area) and m exponents of channel geometry against time. In both cases, aggradation over time is statistically significant.

Low sediment discharge runs on a physical model of the Bull Creek-South Fork Eel River confluence replicate the channel bedforms shown in the 1932 air photos. High sediment discharge model runs suggest the Bull Creek delta to be the product of aggradation in both stream systems.

OBSIDIAN HYDRATION DATING APPLIED TO A FAULTED GLACIO-FLUVIAL TERRACE IN THE UPPER MADISON VALLEY, MONTANA

LUNDSTROM, Scott C., Department of Geology, Humboldt State University, Arcata, CA 95521

A key site to the interpretation of the Late Quaternary chronology of the Madison Range fault occurs where two fluvial terraces of the Madison River below Earthquake Lake are displaced. The lower terrace, at approximately 5m above present channel level on the upthrown side of the fault, is composed of coarse bouldery gravel with intermediate boulder diameters up to 3m and is considered to be a jokulhlaup type flood deposit related to upcanyon ice damming of the Madison River by the Beaver Creek glacier terminus. One exposure shows a possible buried soil manifested by an increase in fines and matrix carbonate at 2m depth, while at the surface is a weakly developed soil (A/Bw/C).

Obsidian granules (2-3mm), glacially and fluvially eroded and transported from the Yellowstone caldera, were found in the sandy matrix within and above the buried soil, and were examined in thin section to measure thickness of youngest hydration rinds on granule surfaces and cracks. Thin rinds above the buried soil average 9.3um in thickness (s.d.=1.0), whereas thin rinds within the buried soil average 9.8um (s.d.=1.2). Thicker rinds up to 40um are thought to represent previous abrasion events and remnants of original cooling cracks, and are excluded from calculations of means.

Use of the hydration rate curve developed by Pierce et al (1976), and adjustment of values for higher hydration rates at lower altitude and assumed warmer site temperature, allow correlation to an age assignment of approximately 30,000 yrs old for most recent abrasion of granules deposited at this study site. The possible buried soil with slightly thicker rinds suggests that some of the lower terrace gravel was deposited during an earlier stade of Pinedale time.

Progress report on a compilation of research done in the Redwood Creek basin, California

by Donna C. Marron, U.S. Geological Survey, Denver, Colorado
K. Michael Nolan, U.S. Geological Survey, Menlo Park, California
Harvey M. Kelsey, Western Washington University, Bellingham, Washington

Concern about the effects of timber harvest on resources of Redwood National Park stimulated extensive study of geomorphic processes and aquatic habitat in the Redwood Creek basin, California. Much of the research between 1973 and 1983 is summarized in "Geomorphic processes and aquatic habitat in the Redwood Creek basin, northwestern California," Nolan, K. M., Kelsey, H. M., and Marron, D. C., eds.: U.S. Geological Survey Professional Paper, in progress. The volume includes work by 31 investigators from the U.S. Geological Survey, the National Park Service, and several other institutions. Included are a summary paper; 3 papers on geology, storms, and land use; 13 papers on erosion and sediment transport; and 5 papers on aquatic habitat.

Papers examining erosion and sediment transport are grouped into 3 sections: hillslope processes, hillslope and channel processes, and channel processes. The hillslope-processes section examines major landslide types, creep, sheetwash, and rilling, and gullying. The hillslope-and-channel processes section examines relations between hillslope erosion, stream-sediment storage, and stream-sediment yields. Many of the channel processes examined in the third section caused severe geometry changes in response to a major storm in December 1964. Papers examining aquatic habitat describe the general aquatic biota and controls on habitat-related conditions, including water chemistry and temperature. Effects of timber harvest on naturally occurring conditions and processes are discussed in most papers in the volume.

The volume describes a delicate landscape that is sensitive to land use and major storms. The rapid rate at which processes operate in the basin facilitated frequent observations of change over a relatively short period of time, enabling researchers to base conclusions on an unusually large collection of data. Results presented are exceptional due to the intensity and interdisciplinary nature of the research effort.

USE OF THE STREAM-GRADIENT INDEX TO IDENTIFY TECTONIC CONTROLS ON FLUVIAL SYSTEMS, CAPE MENDOCINO TO FORT BRAGG, NORTHWESTERN CALIFORNIA

Dorothy J. Merritts, Department of Geosciences, University of Arizona, Tucson, AZ 85721

The influence of different rates of uplift on geomorphic processes and landscapes is best examined where uplift rates vary, but where climate, lithology, and geomorphic age are nearly constant. There are few areas in North America where these conditions are so closely met as in northwestern California, near the Mendocino triple junction. Late Quaternary uplift rates vary by an order of magnitude in 150 km, from 0.3 m/ka at Fort Bragg to about 4 m/ka near Cape Mendocino (Lajoie et al, 1982). Highest rates of uplift are probably spatially related to northward passage of the triple junction and its present geometrically unstable configuration. A highly seasonal humid, mesic climate prevails in this region. The lithologically similar King Range and Coastal terranes (Franciscan assemblage) consist of deformed and weakly metamorphosed argillites and sandstones of Upper Cretaceous to mid-Tertiary age.

A potentially powerful geomorphic tool, the stream gradient (SL) index, describes fluvial responses to different rates of uplift. SL values and longitudinal profile forms were compared for basins in areas with low, moderate, and high rates of uplift. Values of the SL index are products of gradient and stream length from the drainage divide. They are sensitive to changes in slope and therefore stream power. In low uplift areas, longitudinal profiles generally are concave, and SL values gradually decrease downstream (635-125). SL values are much higher for moderate uplift areas (796-431), and the profile form is very irregular, with alternating reaches of high and low SL values. SL values for streams in the highest uplift rate area are exceedingly high (2000-435). Profile form is typically convex and steep in upper reaches, and progressively more concave downstream. Significant and easily recognized differences in SL values and longitudinal stream profiles are useful for classifying tectonic activity in this region.

SOIL-TOPOGRAPHY RELATIONSHIPS ON SCHIST IN REDWOOD NATIONAL PARK

James H. Popenoe
Redwood National Park

Soil patterns on schist in Redwood National Park are correlated with overall slope position and, locally, with relief and bedrock competence. Degree of soil profile expression, measured by depth of horizonation, reddening and clay accumulation, is most obviously correlated with position in basins as a whole. Ultisols with reddish (5YR to 2.5YR) clay Bt horizons (Trailhead and Fortyfour series) are confined to higher, gentler slopes, where erosional activity has been low for a long time. Inceptisols with brownish (10YR to 7.5YR) clay loam B horizons (Ahpah, Coppercreek and Lackscreek series are the dominant soils on steep middle and lower slopes. Soils with gray or mottled C horizons (Devilscreek and Elfcreek series) occur along streams and in wet hollows underlain by failing, incompetent bedrock.

Kind and degree of soil development is determined by and closely correlated with rates, frequencies or types of naturally occurring hydrologic, geomorphic and pedogenic processes. Soils with little development occur both along stream channels, where there is the higher natural rate or frequency of movement, and on the highest peak where rates of erosion and pedogenesis may be low.

Depth of regolith is mostly a function of small scale relief and it is relatively insensitive to overall position in the watershed. Soils and regolith tend to deepen downslope from both main and spur ridges. The deeper soils (Coppercreek, Devilscreek and Trailhead) tend to be on relatively straight or concave topographic surfaces. The shallower soils (Ahpah, Fortyfour and Lackscreek) are on convex, relatively steep or high areas, usually associated with more competent bedrock. Depth of regolith can be interpreted as a function of local sediment availability.

Movement of talus on rock hillslopes in Pennslyvania

Prestegaard, K., Van Ness, F., Henry, R., Goldschmidt., P., and Garbee, M., Dept. of Geology, Franklin and Marshall College, Lancaster, PA 17604

The hill regions of southcentral Pennslyvania commonly contain areas with steep hillslopes covered by talus blocks. Recent research on similar hillslopes in Virginia has shown that many of these talus fields are active under present conditions, rather than vestiges of Pleistocene periglacial processes as was thought earlier.

We set up a study to monitor the rates of movement on two of these talus slopes near the Susquehanna River. Our goal was to determine rates of movement on two slopes with different slope angles, and to see if we could determine the main movement mechanisms or at least determine the major factors controlling rock movement on these hillslopes.

The first study area is an almost bare talus slope in a small watershed that is mainly covered by Eastern hemlock forest. On this slope, movement was monitored by surveying the location of marked surface particles, and by using the accumulation or removal of particles near trees to determine movement rates for the past 100 years. The surface surveys indicate that there has been no recent movement of the particles over a 6-month period. The vegetative evidence suggests that the average rate of movement of particles has been about 6 mm/year. In some locations, mainly in small swales or near stream channels, the rates of movement appear to be higher, averaging 10-35 mm/year. Vegetative evidence was not useful in determining particle movement rates on the second hillslope, so at the present, movement rates are available only for one hillslope.

The mechanisms of rock movement are not easily determined on these hillslopes. The particles are large, with an average b axis length of 50 cm and an average c axis length of 90 cm. The particles are elongated tabular blocks and their long axis is generally oriented in the mean downslope direction. On the first hillslope, the angle of internal friction of the material was determined by studying a small translational landslide that formed due to undercutting by an adjacent stream. The friction angle of the material appears to be about 35 degrees, which is quite close to the average 33 degree angle for the entire hillslope. Study of this small landslide also indicated that most of the blocks moved by sliding, with very little rotational movement of any given block. This suggested that the particles could potentially move down slope with the same surface exposed at all times. Lichen growth on the tabular blocks then would not be a good technique to use to determine particle movement rates.

In order to determine the possible role of subsurface water flow on the movement of these tabular blocks, we installed a grid of gypsum blocks at various depths within each talus field. The weight loss of each gypsum block should be a function of the flow velocity through the talus. Comparison of surface particle movement rates and water flow rates may give us a better picture of the movement processes as we monitor these hillslopes over the next few years.

Erosion and deposition in a discontinuous gully system

Leslie M. Reid
Geological Sciences, Univ. of Washington, Seattle

A recent episode of arroyo-cutting in northern Tanzania indicates that changes in hillslope conditions such as vegetation cover, infiltration rate, and microtopography can trigger profound changes in channel density and morphology. An understanding of the mechanisms by which such control is exerted would greatly aid both evaluation of the stability of channel networks subjected to changes in climate or land use, and interpretation of the climatic significance of valley fills and terraces.

Channel form reflects the balance between sediment transport capacity in a channel, sediment input to the channel, and erodibility of the channel bed and banks, and each of these factors is strongly influenced by hillslope conditions. In order to quantify these relations, discontinuous gully systems representing intermediate stages in the expansion of drainage networks have been monitored for 2 years with the intent of constructing sediment and water budgets for the gullies. Field measurements are being combined with analytic flow-routing models and shear stress measurements from a scale-model flume to construct a model capable of evaluating the stability of a channel network under given hillslope conditions.

The monitored sites are grazed, alluvium-filled, grassland valleys of the eastern San Francisco Bay area, where ephemeral quickflow is generated on cracking clay soils by overland flow. The discontinuous gullies form as a series of pits in unchannelled grassy swales. Comparison of maximum shear stress in the swales during extreme storms with minimum critical tractive force for those surfaces suggests that the pits must have formed at unvegetated sites; recently formed pits are associated with trail crossings, hoofprints, and ground-squirrel colonies. Pits enlarge and deepen by trampling, traction, dry ravel, and plunge-pool erosion, until the headcut and walls are high enough to induce toppling and slumping of crack-bound soil blocks during the wet season. Soil blocks deposited in the pool are broken down during the dry season by desiccation and trampling, producing a mantle of 1- to 32-mm clasts. Wet season flows then transport the clasts as rapidly disintegrating gravel and redeposit them on the downstream lip of the pool, while some finer-grained sediment is deposited in the vegetated swales between pools. Sequential air photos show that the headcut, pool, and lip migrate upstream as a unit, moving at a relatively uniform rate of 20 to 50 cm/yr; these migrating forms constitute the discontinuous gullies.

By 10 years after passage of the headcut the once-vertical walls have retreated to an angle of about 15° and are revegetated. The presence of hoofprints and associated terracette failures on the walls suggest that much of the retreat is due to trampling, and this effect is being evaluated by monitoring differences in morphology and process rates between grazed and exclosed gullies. Air photos spanning 45 years show little change in morphology of the channel despite the headward migration of the gullies, suggesting that under some conditions these discontinuous channels may be effectively stable. Observations in East Africa indeed show this to be the predominant channel form in some undisturbed grasslands.

LANDSLIDES AND CLIMATIC CHANGE IN COLLUVIUM-MANTLED HOLLOWS, CENTRAL CALIFORNIA

Steven L. Reneau, William E. Dietrich
University of California, Berkeley

Ronald I. Dorn, C. Rainer Berger
University of California, Los Angeles

Meyer Rubin
United States Geological Survey, Reston, Virginia

Bedrock hollows, mantled with thick deposits of colluvium, are abundant in many soil-mantled landscapes. The hollows lie upslope of drainage channels, have characteristic U- or V-shaped cross sections, and commonly contain 2-4 m of colluvium, although deposits may exceed 10 m in thickness. They have been recognized as the dominant source of shallow landslides in many regions, the landslides constituting a major source of sediment and a significant geologic hazard. Topographically-induced convergence of colluvial debris results in long-term deposition along the axes of the hollows, with recurrent but infrequent landslides eroding the stored debris. The landslides are generally triggered by relatively long duration-high intensity storms, such as the 1955, 1964, and 1982 storms in California. Field study of landslide scars indicates that landslides and subsequent erosion often expose large areas of the underlying bedrock, although frequently the colluvium in a hollow is only partially evacuated. Many landslides only remove upper horizons or do not extend the total length of the deposit, and the resulting depositional history in a hollow may be complex.

Charcoal collected from basal colluvium in hollows in the Coast Ranges of central California has yielded dates of 9000-21,000 yrs B.P., with a strong clustering from 11-14,500 B.P. The dates indicate that the last evacuation of colluvium down to bedrock at most of these sites was during the waning stages of the Late Wisconsin glacial period. We propose that the thick colluvial deposits record the effects of regional climatic change, specifically the frequency of long duration-high intensity storm events. The dates suggest that the latest-Pleistocene was characterized by a high frequency of these storms, resulting in frequent landslides and major erosion of colluvium from the hollows. A reduced frequency of storms in the early Holocene would have allowed thicker accumulations of colluvium to develop. This hypothesis is consistent with available paleoclimate reconstructions based on sea surface temperatures. It suggests that sediment flux through the hollows is sensitive to long-term climatic fluctuations, and that much of the colluvium stored in hollows accumulated during periods with a reduced frequency of storms capable of triggering landslides. The abundant modern landslides may partially reflect an increased storm frequency in the late Holocene, and a trend towards instability in some deposits due to pedogenically-controlled changes in soil properties.

Slope processes and fragipan expression in soils of the Salamanca Re-entrant (New York) by Kent E. Snyder and Ray B. Bryant, Cornell University, Ithaca, NY 14853

The relative importance of geologic vs pedogenic processes in the formation of fragipan horizons is a long standing question. The objective of this research was to evaluate the influence of slope processes and landscape evolution on the spatial distribution and expression of fragipans in the unglaciated Salamanca Re-entrant. Fieldwork and thermoluminescence dating suggest that the area has experienced substantial slope modification prior to and during the Late Wisconsinian (17,000 - 12,000 BP); evidence for this includes numerous large debris flows, buried/truncated rotational slumping, and at least two seperate periods of colluvial valley filling. Interpretations of local and regional pollen spectra suggest a tundra-like vegetation at that time. A series of excavations were made along a transect in a first-order stream headland. In the valley floor 2.5 to 3 meters of colluvium was present. The colluvial mantle thinned to less than 1 meter at the summit. All sites, except the shoulder and summit positions, had compact colluvial material similar to that characteristic of fragipan horizons. Colluvium in the footslope/upper toeslope showed the best fragipan character (i.e., well developed prismatic structure, brittle peds and firmness). Bulk density values of 1.8 to 1.9 g/cm^3 have been recorded in such material. Prismatic structure was better developed in the footslope and toeslope positions than the backslope. Overall, brittleness was best expressed in loam textures without regard for position. For comparison, several pits were dug in the footslope/toeslope position of a large (26 ha) debris flow down valley. The soils developed in this deposit were similar to those in footslope/upper toeslope positions in the transect. Although they had well expressed prisms and were firm, they lacked brittleness when moist. The flow material had bulk density values of 1.7 to 1.8 g/cm^3.

RECENT CHANNEL ADJUSTMENTS IN REDWOOD CREEK,CA

Varnum, Nick C. and Ozaki, Vicki L.,Redwood National Park, 791 - 8th St., Arcata, CA 95521

The channel configuration of Redwood Creek has changed dramatically since the early 1950's. Large sediment loads were introduced into the channel resulting from several large floods and associated streamside landsliding and gullying on cutover lands throughout the basin. Sedimentation during the 1964 flood (50 year recurrence interval (RI)) increased valley floor stored sediment by a factor of 1.5. Subsequent moderate to high flows have added and redistributed sediment in the channel. By 1980 there was little net change in the total volume. Since 1974, annual channel cross section surveys along 100 km of the channel and longitudinal profiles of the downstream 20 km document channel response to discharge and sediment load.

Surveys since 1974 verify that the upstream third of the channel has degraded substantially. In some reaches the streambed has downcut to near pre-1964 levels. Following a sedimentation pulse during the 1975 flood (RI=25 years) the middle third of the channel has continued to downcut in wide channel areas. In areas of narrow channels, cross sections have changed very little during the last 2-4 years.

Upstream reaches of the lower 20 km of the channel are continuing to degrade after a major pulse of aggradation in 1975. In 1977 the upstream, trailing edge of aggradation began to move downstream, and, by 1984 had moved 6 km from the top of the reach. As upstream areas of this reach degraded, a low flow channel has become vertically incised into adjacent gravel bars with relatively little lateral erosion. Degradation in this reach was accompanied by decreased channel gradients, increased pool and riffle development and increased streambed material sizes.

Aggradation has been occurring in the downstream sections of this reach since at least 1974 and probably since 1964. Low flow channels in aggraded reaches typically shift position annually. Present gravel bar surfaces above bankside vegetation lines indicate a new, higher bankfull elevation. Channel gradients have increased in the lower half of the aggraded reaches. Pool and riffle development and streambed material sizes have both increased since 1977, but less than in degrading sections of this reach. The downstream, leading edge of aggradation is less well defined than the upstream edge, but appears to have moved from 14 to 17 km from the top of this reach since 1975.

Gaging stations monitoring the upstream third of the channel and near the mouth indicate that present sediment transport has decreased about 40 percent from pre-1977 conditions at flows of RI=1.5 years. In addition, surveys indicate that during years with peak flows less than RI=1.5 years, the entire channel may show downcutting. Recovery of the lower Redwood Creek channel probably depends on further depletion of upstream sediment supply and continued years of moderate to low flows.